Interactions of cadmium, zinc, and phosphorus in marine *Synechococcus*: Field uptake, physiological and proteomic studies

By

Alysia Danielle Cox

B.S. *summa cum laude* in Geological Sciences
Arizona State University, Barrett Honors College, 2004

Submitted in partial fulfillment of the requirements for the degree of
Doctor of Philosophy

at the

MASSACHUSETTS INSTITUTE OF TECHNOLOGY

and the

WOODS HOLE OCEANOGRAPHIC INSTITUTION

June 2011

Signature of Author: _____

Joint Program in Chemical Oceanography
Massachusetts Institute of Technology
and Woods Hole Oceanographic Institution
May 3rd, 2011

Certified by: _____

Dr. Mak A. Saito
Thesis Supervisor

Accepted by: _____

Dr. Roger E. Summons
Professor of Earth, Atmospheric and Planetary Sciences
Chair, Joint Committee for Chemical Oceanography

Interactions of cadmium, zinc, and phosphorus in marine *Synechococcus*: Field uptake, physiological and proteomic studies

By

Alysia D. Cox

Submitted to the Department of Marine Chemistry and Geochemistry,
Massachusetts Institute of Technology-Woods Hole Oceanographic Institution,
Joint Program in Oceanography
on May 3rd, 2011, in partial fulfillment of the requirements for the degree of
Doctor of Philosophy

Abstract

A combination of uptake field studies on natural phytoplankton assemblages and laboratory proteomic and physiological experiments on cyanobacterial isolates were conducted investigating the interactions of cadmium (Cd), zinc (Zn), and phosphorus (P) in marine *Synechococcus*. Enriched stable isotope field uptake studies of ^{110}Cd in the Costa Rica Upwelling dome, a *Synechococcus* feature, showed that uptake of Cd occurs in waters shallower than 40 m, correlates positively with chlorophyll *a* concentrations and is roughly equivalent to the calculated upwelling flux of cadmium inside the dome. In laboratory experiments, *Synechococcus* WH5701 cells exposed to low picomolar quantities of free Cd under Zn deficiency show similar growth rates to no added Cd treatments during exponential growth phase, but show differences in relative abundances of many proteins involved in carbon and sulfur metabolism suggesting a great metabolic impact. During stationary phase, chronic Cd exposure in this coastal isolate causes an increase in relative chlorophyll *a* fluorescence and faster mortality rates. The interactions of acute Cd exposure at low picomolar levels with Zn and phosphate (PO_4^{3-}) were investigated in *Synechococcus* WH8102, an open ocean isolate. The presence of Zn appears vital to the response of the organism to different PO_4^{3-} concentrations. Comparisons with literature transcriptome analyses of PO_4^{3-} stress show similar increases in relative abundance of PO_4^{3-} stress response proteins including a PO_4^{3-} binding protein and a Zn-requiring alkaline phosphatase. A bacterial metallothionein, a Zn-associated protein, appears to be correlated with proteins present under low PO_4^{3-} conditions. Together, these experiments suggest that the interactions of Cd and Zn can affect *Synechococcus* and play a role in the acquisition of PO_4^{3-}.

Thesis Supervisor:
Mak A. Saito
Title: Associate Scientist, Marine Chemistry and Geochemistry Department,
Woods Hole Oceanographic Institution

Acknowledgements

There are many people that have helped me throughout the duration of this PhD work. I would especially like to thank my advisor, Mak Saito, for allowing me to work in his group, pursue my own ideas, and in general make my day-to-day research possible. I would like to thank my committee members Ed Boyle, Carl Lamborg, Nigel Robinson and Sonya Dyhrman for great discussion, suggestions whenever I needed them and willingness to be available for committee meetings. In particular, I thank Ed for his excellent inorganic perspective, especially his comments on Chapter 2; Carl for his discussion about many topics and in particular comments on Chapter 2; Nigel for his biological insight and advice on metallothioneins; and Sonya for her astute advice on culturing/analysis and helping me navigate the phosphorus literature.

I would like to thank the members of the Saito Laboratory, past and present; they are excellent people with whom to work and I cannot them enough for their positive attitudes and amazing work ethics: Erin Bertrand, Vladimir Bulygin, Tyler Goepfert, Dawn Moran, Abigail Noble, Daniel Tabersky and Anne Thompson. In particular, I thank Erin for keeping the mass spectrometry operational (Chapter 3 and 4), Vladimir for developing the extraction protocol that I used in Chapters 3 and 4 and help with protein chemistry, Tyler for fixing anything that broke and help with the color scheme in Chapter 4, Dawn for the starting recipe of the culture media, Abigail for dissolved cadmium measurements in Chapter 2, Daniel for help with experimental spectroscopic measurements, and Anne for flow cytometry cell numbers in Chapter 2.

I would also like to thank John Waterbury and Freddie Valois for the strains of *Synechococcus*, use of lab space, and discussion and Tristan Kading for low molecular weight thiol measurements in Chapter 3 and critical editing this thesis.

Thank you to Meg Tivey, former Marine Chemistry and Geochemistry Education Coordinator for much perspective over the years and for chairing my defense. I would also like to thank the Academic Programs Office for support on everyday details and travel to conferences especially Julia Westwater, Marsha Gomes, Jim Yoder, and also Ronni Schwartz (MIT JP Office). Thank you also to Mary Zawoysky, Susan Tomeo, and Shelia Clifford for assistance. Thank you to my officemates, who have always been up for poignant discussion: Abigail, Caitlin, and Tristan. I would also like to thank the Captains (Kent Sheasley and George Gunther), crews and chief scientists (Mak Saito and Joseph Montoya) of the RV Knorr and RV Seward Johnson for facilitating smooth research at sea. Thank you to Phil Gschwend and Everett Shock for inspiration.

Thanks to the Hyannis capoeristas: Anna, JP, Bernie, Verity, Santiago, Travis, Lauren, Dan, George, Caitlin, Liz, Tristan and Bethanie for keeping it real.

Thanks to all of my housemates (who also happen to be my friends) who made home a fun place to be: Ken Whelan, Abigail Noble, Cim Wortham, Luc Mehl, Andrew McDonnell, Kelton McMahon, Caitlin Frame, Marissa Black, Jason Black and John Jacob.

Thanks to my friends and fellow students, both near and far, for good times: Cara Fosdick, Brian Buczkowski, John Cartner, Verity Salmon, Michelle Bringer, Fern Gibbons, Nathaniel Green, Anne Rounds, Des Plata, Travis Meador, Taylor Crockford,

Li Ling Hamady, Alyson Santoro, Ben Hodges, Annette Hynes, Jessie Kneeland, Eoghan Reeves, and others among the JP students.

And finally, I would especially like to thank my family and cousins, because they are truly the best and I would not be here without them: cousins - Renee, Courtney, Ryan, and Jude and my family - Patrick, Gayla, Caitlin, and Alaina.

"We are the flow, we are the ebb, we are the weavers, we are the WEB"
- Shekhinah Mountainwater

To this incomplete WEB of people who have influenced my thoughts of science, thank you:

The work in this thesis was supported by a MIT Presidential Graduate Fellowship for one year, the Academic Programs Office for one semester, and awards to Mak Saito from the Office of Naval Research for three years. Funding awards to Mak Saito from NSF Chemical Oceanography, the Center for Microbial Oceanography Research and Education, and WHOI Ocean Life Institute also supported this research.

After the last river has been poisoned
Only after the last fish has been caught
Then you will find that money cannot be eaten.
-- Cree prophecy --

For those who come after

Table of Contents

List of Figures

List of Tables

Appendix II

Appendix III

Chapter 1: Introduction

Consider the earth, an approximately 4.5 billion year old differentiated planet with a radius of roughly 6,400 kilometers. The crustal thickness of earth is close to 40 kilometers and oceans cover around 70% of the earth's surface. Much of life on earth is driven by energy from the sun in the form of primary production as the base of the food chain. Primary productivity occurs on both land and the ocean. Marine primary productivity is thought to account for about 45% of total primary productivity (Falkowski, 1994; Field et al., 1998; Morel et al., 2003). Under the umbrella of marine primary productivity are dinoflagellates, diatoms, algae and cyanobacteria. Cyanobacteria are evolutionarily ancient and have persisted through many changes in ocean chemistry, including changing metal conditions. Marine *Synechococcus* have developed many adaptations to horizontal gradients in nutrients and light (Scanlan, 2003). This thesis explores the response of modern *Synechococcus* to changes in cadmium (Cd) and zinc (Zn) exposure with a focus on the interactions between these two elements and the effects of each on phosphorus (P) metabolism. Field experiments conducted in the Costa Rica Upwelling Dome, a *Synechococcus* feature, are presented in Chapter 2 and laboratory manipulations with axenic strains of *Synechococcus* are presented in Chapters 3 and 4.

Cyanobacteria

Cyanobacteria, especially marine cyanobacteria, are an integral part of the earth/life system as agents of carbon fixation and oxygen production. The marine cyanobacteria *Synechococcus* and *Prochlorococcus* contribute between 32 and 80% of the total primary productivity in oligotropic oceans (Rocap et al., 2002) and contribute about 50% of fixed carbon in some oceanic regions (Zwirglmaier et al., 2007). *Synechococcus* species alone are considered to be important contributors to global primary productivity and are thought to dominate phytoplankton populations throughout much of the world's oceans (Scanlan, 2003). In addition to their modern contribution to primary productivity, cyanobacteria are suspected to be responsible for the first biological oxygen generation starting around three billion years ago (Williams and Frausto da Silva,

2006) resulting in the oxygenation of the atmosphere 2.2-2.4 billion years ago (Catling et al., 2001; Catling and Claire, 2005) and thus have played a vital role in the chemistry and evolution of life on this planet.

Cyanobacteria are ubiquitous, versatile and have been found in diverse environments ranging from desert crusts, to freshwater and hot spring environments. Cyanobacteria are unique in that their cell walls have features of both gram negative and gram positive bacteria (Hoiczyk and Hansel, 2000). Cyanobacteria also contain phycobiliproteins, which enable them to adapt to their surrounding light environment, and among the cyanobacteria a great range of spectral variation in their antenna pigments can be found (Glazer, 1989). These phycobiliproteins have been used as fluorescence tags for cell surface markers (Kresage et al., 2009). Researchers have noted the aesthetic and chemical significance of the phycobiliproteins of cyanobacteria for over 130 years: " It would be difficult to find another series of colouring matters of greater beauty or with such remarkable and instructive chemical and physical peculiarities" (Sorby, 1877).

Evolution and zinc

The evolution of cyanobacteria is closely linked to the oxygenation status of the ocean, which directly affects the speciation of Zn and Cd. Zn is the cofactor for many proteases and vital in many enzymes. Zn was not as abundant during early evolution due to the formation of insoluble sulfide complexes (Canfield, 1998; Anbar and Knoll, 2002; Saito et al., 2003). Bacteria may have grown, operated and evolved with limited amounts of Zn. As the oceans changed, Zn became more bioavailable (Saito et al., 2003). The Zn requirements of many cyanobacteria are very low, which is consistent with the idea that cyanobacteria may have evolved in a sulfidic ancient ocean (Saito et al., 2003). Oxygen was toxic to many microorganisms early in their evolutionary history, which suggests the onset of higher levels of Zn may have been toxic prior to adaptation as well (former idea - Williams and Frausto da Silva, 2006). There was an explosion in the diversity of Zn-binding protein structures in eukaryotic organisms suggesting that the ocean was not anoxic or euxinic for this to occur (Dupont et al., 2006b). Because of compartmentalization, however, bacteria are able to cope with changing environmental

chemistry. Compartmentalization is thought to be important to the evolution of environmental chemistry and life (Williams and Frausto da Silva, 2006) and the study of metal ions in compartments can provide understanding of cell and environmental evolution that the organic chemistry of cells alone cannot provide (Williams, 2007). In the modern ocean, Zn availability may influence phytoplankton diversity in the Ross Sea (Saito et al., 2010). There are almost no studies of Zn handling mechanisms in marine cyanobacteria (Blindauer, 2008a). This thesis explores how the addition of Zn can decrease the toxicity of Cd in Chapter 3 and the interactions of Zn with Cd and P in Chapter 4.

Cadmium and zinc as trace metals

Cd and Zn are both group 12 elements in the periodic table, implying a certain degree of chemical similarity. In magmatic rocks, the ratio of Cd to Zn is about 1:500 (Goldschmidt, 1954). It has been known for over half a century that the concentration of Cd in seawater was less than 0.005 ppm (1 nM) (Noddack and Noddack, 1939), and geochemists noticed the accumulation of Cd in rocks of marine origin (Goldschmidt, 1954). Only in the 1970's were accurate measurements of Cd and Zn able to be made at the pM to nM levels found in surface seawater. Cd and Zn have nutrient-like profiles, meaning they are depleted in surface waters and increase with depth (Boyle, 1976; Bruland, 1980) (Figure 1.1). Cd correlates closely with dissolved phosphate, and Zn correlates with dissolved silicate concentrations throughout the oceans. This implies that like the major nutrients, Cd and Zn are taken up by microorganisms in the surface (as discussed in Chapter 2) and resolubilized at depth. These metals may have different roles in different environments. Zn is considered a micronutrient in the open ocean. Toxicity of Cd to a coastal cyanobacterium is presented in Chapter 3.

Like many other bioactive trace metals in surface waters, dissolved Cd and Zn in the ocean are complexed by strong organic ligands (Bruland, 1980; Bruland, 1992; Ellwood and van den Berg, 2000; Ellwood, 2004, and Morel et al., 2003). Whether or not Cd functions as a nutrient or toxin is likely to be controlled by its bioavailability. The bioavailability, in turn, is controlled by the speciation of trace metals (Hunter et al., 1997)

(Figure 1.2). In many studies, toxicity has been proportional to the summation of inorganic metal species added to the media (Sunda, 1988), although for copper and iron, organic ligands have been shown to be bioavailable (Hutchins et al., 1999; Maldonado et al., 1999; Quigg et al., 2006 and Semeniuk et al., 2009). Despite the fact that the speciation of bioactive trace metals directly influences bioavailability and bioavailability likely controls the status of a trace metal as a nutrient or a toxin, only a limited number of speciation measurements have been made in the ocean for Zn and Cd (Bruland, 1980; Bruland, 1992; Ellwood and van den Berg, 2000; Ellwood, 2004).

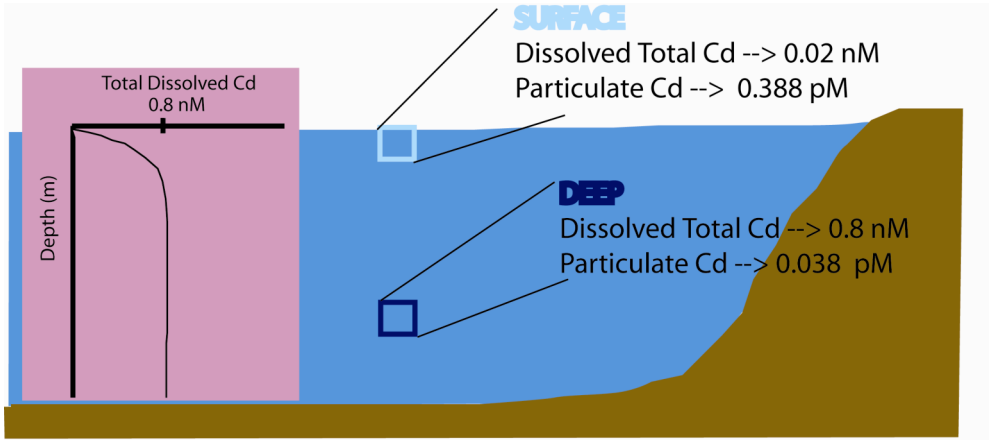

Figure 1.1: General Cd profile in the open ocean. Dissolved total Cd has a nutrient-like profile, closely correlated with phosphate, and reaches 0.8-1 nM concentrations at depth. Surface waters generally have low picomolar to undetectable dissolved total Cd. With the exception of iron, which has high particulate concentrations, particulate concentrations are usually an order of magnitude lower than dissolved concentrations and there are only a few high-quality data sets that exist (Sherrell and Boyle, 1992; Cullen et al., 2001). Dissolved total Cd numbers are from the central North Pacific (Bruland, 1992). Particulate Cd numbers are from the North Atlantic near Bermuda, 50 m and 1450 m (Sherrell and Boyle, 1992).

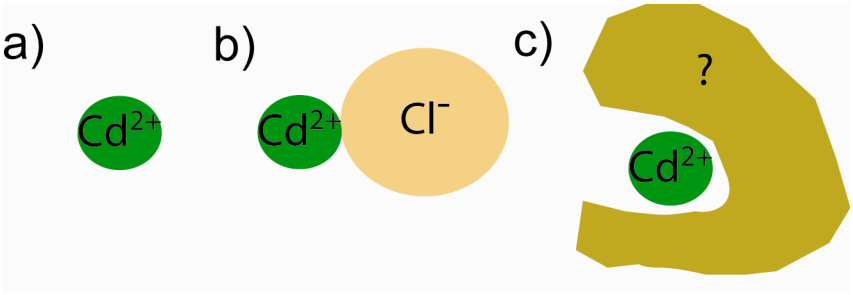

Figure 1.2: Cd^{2+} in the dissolved phase in seawater. a) Cd^{2+} as a free ion. b) Cd^{2+} complexed with Cl^- to form $CdCl^+$ (and other chlorocomplexes) c) Cd^{2+} bound to organic ligands of uncertain structure and origin. Inorganic Cd^{2+} is mostly present as $CdCl^+$ in seawater, although Cd^{2+} has been found to be 70% bound to organic ligands in some surface waters. Cd^{2+} and $CdCl^+$ are considered to be labile and bioavailable. Cd bound to organic ligands is not thought to be bioavailable.

There are only a few datasets which consider bioactive trace metals in the particulate fraction (Sherrell and Boyle, 1992; Cullen and Sherrell, 1999; Cullen et al., 2001). With the exception of iron, particulate concentrations tend to be an order of magnitude lower than dissolved concentrations (Cullen et al., 2001 and references therein). One can envision several mechanisms for the partitioning of metal ions within the particulate fraction. Metal ions can be taken up into microorganisms, adsorbed to the surface of microorganisms, adsorbed to particulate organic matter (POM), and adsorbed to mineral surfaces (Figure 1.3). Measuring the precise mechanism of partitioning within the particulate fraction is difficult. Uptake of Cd by microorganisms may be responsible for concentration of Cd in the particulate phase. Adsorption onto the cell surface is possible but not highly probable. Researchers have experimented with extracellular washes with varying degrees of success and found adsorption of Cd to be minor in low metal environments (Hudson and Morel, 1989; Tovar-Sanchez et al., 2003, 2004; Tang and Morel, 2006). The role of adsorption to inorganic mineral phases in the presence of particulate organic matter has not been determined. Cd uptake experiments conducted in the field are presented in Chapter 2.

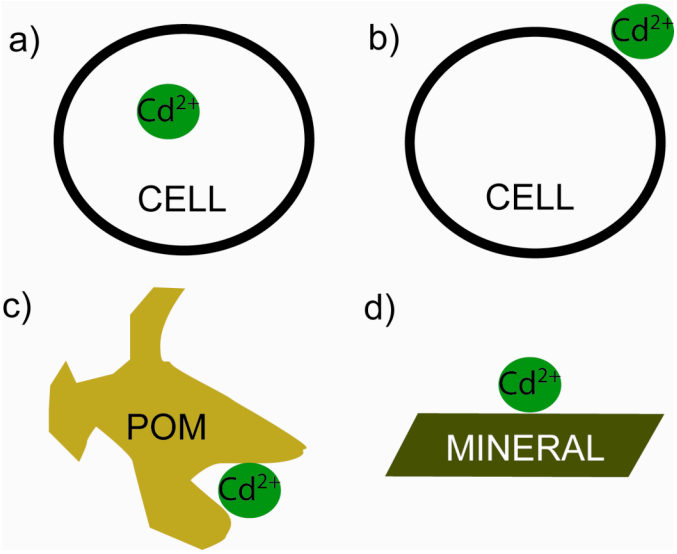

Figure 1.3: Cd^{2+} in the particulate phase of seawater. a) Uptake of Cd into microorganisms. b) Adsorption of Cd onto the surface of microorganisms. c) Adsorption of Cd^{2+} onto particulate organic matter (POM). d) Adsorption of Cd onto mineral surfaces. Intracellular cadmium (a) probably represents the largest fraction of Cd in the particulate phase. Adsorption onto the cell surface (b) is likely a small fraction. Adsorption to inorganic mineral phases (c) may play a minor role in particulate cadmium fractionation.

The interaction of cadmium and zinc and cellular uptake

Little is known about the intracellular partitioning of Cd and Zn following uptake in surface waters (Figure 1.3a). The question remains as to what the organisms are doing with Cd and Zn once inside the cell. This question was actively pursued in cyanobacteria using physiological and proteomic studies in Chapters 3 and 4. Zinc is vital to many enzymes. Of all enzymes with known structures, Zn is utilized in 9% of them (Waldron et al., 2009). This is second only to magnesium (16%) (Waldron et al., 2009). Cd, on the other hand, is only known in the structure of a single carbonic anhydrase (Xu et al., 2008). Some other possibilities for intracellular Cd include incorporation into calcium carbonate tests of foraminifera, binding by metallothionein, binding by low molecular weight thiols, sequestration in polyphosphates and possible use in other enzymes (Figure 1.4). Boyle 1976 posed the question to what part of the cell the Cd goes, either the soft part or the hard parts. The soft part is thought to dominate because the ratio of Cd:C in organic matter is 3.3×10^{-6} and Cd:C in carbonate minerals is less than 0.2×10^{-6} (Boyle, 1988). The carbonate phase, including foraminifera, is responsible for only 2% of

vertical cadmium transport (Boyle, 1988). This is important for the use of Cd:Ca as a paleoproxy for phosphate concentrations in foraminiferal calcite, through incorporation of Cd into foraminiferal tests (Boyle, 1988; Elderfield and Rickaby, 2000). Ho et al., 2003 did a study on the metal composition of fifteen marine eukaryotic plankton species. Their results corroborate that significant Cd may not be present in the hard parts. Cyanobacteria do not have hard parts, so Cd must be interacting with the cell, probably in the form of proteins or metabolites.

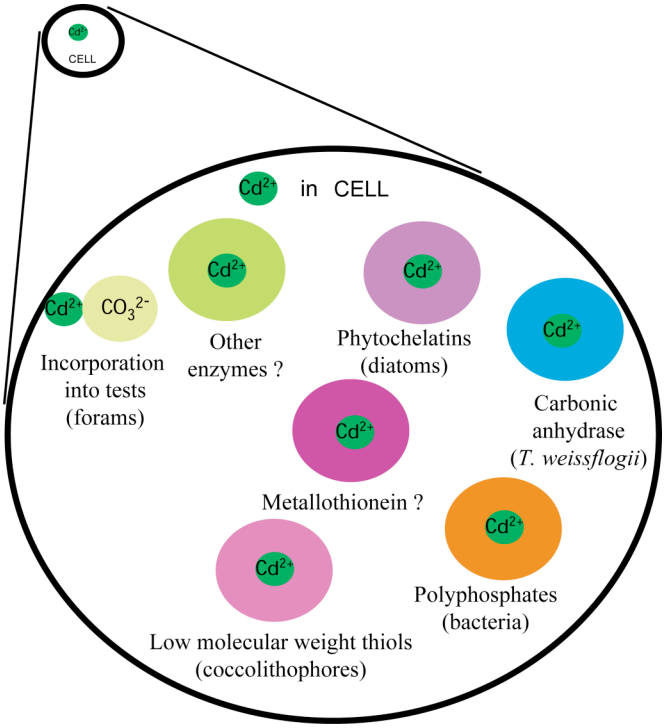

Figure 1.4: Cd inside a cell. The distribution of cadmium within the cell is unknown. Cd has been shown to replace Zn in the active site of carbonic anhydrase in the diatom, *T. weissflogii*. Incorporation into foraminiferal tests has been observed. Cd could possibly be used in other cellular enzymes.

The concept of Cd as a nutrient or a toxin has been investigated in cultures of cyanobacteria in Chapters 3 and 4. Cd has been shown to have toxic effects to eukaryotic organisms in culture (Lee and Morel, 1995), but in some instances of Zn limitation in the marine diatom *Thalassiosira weissflogii* and other species the addition of low levels of Cd restored the growth rate (Price and Morel, 1990; Lee and Morel, 1995; Sunda and Huntsman, 2000). It follows that Cd at low concentrations (pM) may act as a nutrient by

replacing Zn (Lee and Morel, 1995), with Cd replacing Zn in the active site of carbonic anhydrase (Morel et al., 1994; Lee et al., 1995; Lane and Morel, 2000 and Lane et al., 2005). Early work on this concept showed that in certain fungi Cd cannot physiologically replace Zn (Goldschmidt, 1954). However, *Synechococcus* species have been shown to have lower toxicity thresholds relative to eukaryotic organisms by approximately two orders of magnitude (Brand et al., 1986; Payne and Price, 1999; Saito et al., 2003). Carbonic anhydrase may not be the major sink for cellular Cd, given that the only known biological use of Cd is as a substitute for Zn in a Cd carbonic anhydrase (CdCA), and the gene for CdCA is not found in cyanobacterial genomes. A calculation and/or study demonstrating the fraction of cellular Cd in carbonic anhydrase has not been performed, although cadmium-containing carbonic anhydrases are a topic of active research (Lane et al., 2005; Park et al., 2007; Xu et al., 2008). The question of intracellular Cd partitioning is difficult to answer partially because the carbonic anhydrase content and subsequent Cd uptake of some cells has been suggested to change with pCO_2 (Cullen et al., 1999) and it is difficult to measure. The presence of Zn has been previously noted to have an effect on Cd toxicity (Saito et al., 2003) and Chapters 3 and 4 address this issue.

There is another possibility for the localization of intracellular Cd. Metallothionein, by binding metals, can act as an intracellular buffer (Figure 1.5). If the cell is not actively utilizing Cd, then perhaps it is being stored somewhere where it cannot affect the overall functionality of the cell. Metallothioneins have been observed to form clusters in cells with bound metals in mammalian systems. Synthesis of metallothioneins has been shown to be induced by increased metal and oxidative stress (Palmiter, 1998 and references therein).

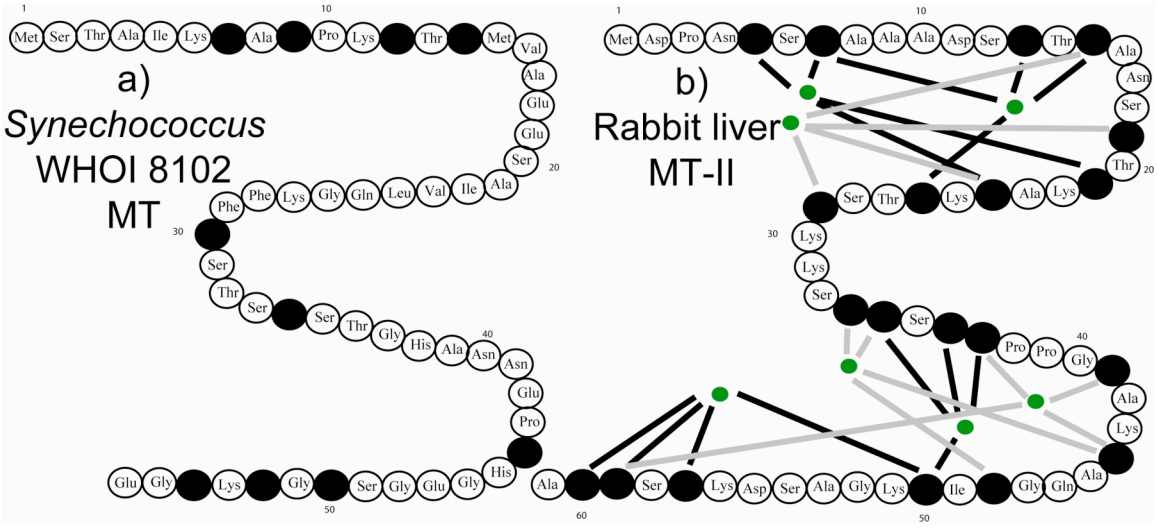

Figure 1.5: Metallothionein (MT) a) Metallothionein from the cyanobacterium, *Synechococcus* WH8102, 56 amino acid protein. b) MT-II from rabbit liver, 61 amino acid protein. MT-II binds seven Cd ions in two clusters. The number of metal ions bound and structure of metallothionein from WH8102 is unknown. Black depicts cysteine residues. Met = methionine, Ser = serine, Thr = threonine, Ala = alanine, Ile = isoleucine, Lys = lysine, Pro = proline, Val = valine, Glu = glutamic acid, Gly = glycine, Gln = glutamine, Phe = phenylalanine, His = histidine, Asn = asparagine, Asp = aspartic acid. Green spheres represent Cd^{2+} ions. Black and grey lines represent bonds from Cd^{2+} ions to cysteine residues.

Metallothioneins are found in organisms ranging from multicellular eukaryotes to bacteria and have been typically associated with the metals, zinc, copper, and cadmium, although they have also been observed to bind silver, mercury, and arsenic as well (Duncan et al., 2006). They belong to a super-family of intracellular metal-binding proteins (Coyle, 2002), although they have been reported extracellularly in eukaryotic organisms (Lynes, 2006). Metallothioneins are polypeptides that, based on equine renal metallothionein, have several of the following six features: 1) low molecular weight, approximately 56 amino acid residues, 2) high metal content, 3) a characteristic amino acid composition consisting of high cysteine content, and no aromatic amino acids (phenylalanine, tryptophan, and tyrosine) nor histidine, 4) unique amino acid sequence with a characteristic distribution of cysteine (cys) residues such as cys-X-cys, 5) spectroscopic features characteristic of metal thiolates (mercaptides), and 6) metal thiolate cluster (Kojima et al., 1999). Note that histidine has subsequently been found in

bacterial metallothioneins and can enhance the relative affinity for Zn in comparison to Cd (Blindauer, 2008b).

The precise function of eukaryotic metallothionein has eluded researchers ever since it was first isolated and identified in 1957 from horse kidney (Margoshes and Vallee, 1957). Metallothioneins may function as 1) metal resistance proteins for detoxifying zinc, cadmium, and copper; 2) reservoirs for the storage of excess Zn and/or copper that can be mobilized under metal limiting conditions; 3) metal chaperones that deliver Zn to Zn-dependent proteins; and 4) antioxidants that scavenge oxygen radicals (Palmiter, 1998). Bacterial metallothioneins have thus far been implicated in the cellular homeostasis of Zn through the binding, sequestering, and buffering of intracellular Zn (Robinson et al., 2001). In mammals, metallothioneins are thought to protect cells from oxidative damage (Cai and Cherian, 2003). Kang (2006) maintains that the redox cycle of metallothionein supports the use of metallothioneins in cell homeostasis, protection from oxidative stress, and metal detoxification. The role of metal detoxification has the most supporting evidence, although there also has been increasing evidence for the paramountcy of metallothionein to maintaining intracellular homeostasis of Zn and Cu, particularly the metal storage and chaperone roles of metallothionein (Suhy et al., 1999; Rae et al., 1999; O'Halloran and Culotta, 2000; and Outten and O'Halloran, 2001).

Turning to organisms relevant to the ocean and integral to global carbon cycling, metallothioneins have been found in the genomes of numerous *Synechococcus* strains, such as WH8102 (1), WH7803 (1), WH5701 (2), CC9311 (4) and CC9605 (3) (Palenik et al., 2003; Palenik et al., 2006). Protein database searches yield metallothionein proteins in eight *Synechococcus* species, three of them marine, two of them thermophiles, and none in *Prochlorococcus* species (twelve genomes searched). Amino acid alignments reveal on average 36% identity among these cyanobacterial metallothioneins. Palenik et al., 2003 suggest that *Synechococcus* seems to be more resistant to copper compared to *Prochlorococcus* and that the difference may be due to efflux pumps for metals present in *Synechococcus* that are not present in *Prochlorococcus*. Metallothionein may contribute to this difference. The role of metallothioneins and their relationship to metal

concentrations in the environment has been largely unexplored. The work involved in this thesis explored the possibility of metallothioneins being important for Zn homeostasis and the prevention of Cd toxicity and some data are shown in Chapter 4.

Metallothioneins are not the only compounds known to bind metals in cells (Figure 1.6). Other known metal binding ligands include phytochelatins, which were first isolated from plants and later observed to occur in ocean waters (Ahner et al., 1994, 1997). Phytochelatins were classified as a MT-III (Shaw et al., 1992). For phytochelatins to maintain a concentration of 20 pM in the water column they would need an extracellular turnover time of 100 days assuming an open ocean chlorophyll *a* concentration of 0.1 μg L^{-1}, a phytochelatin concentration of 2 μg per g chl *a*, and a phytoplankton turnover of 1 day (Ahner et al., 1994). The authors concluded that phytochelatins do not constitute a major fraction of the elusive metal ligands dissolved in seawater measured by electrochemists, because the thiols are subject to oxidation and the overall molecule subject to proteases. Protein database searches yield a putative phytochelatin synthase in *Prochlorococcus* and a phytochelatin synthase-like protein in *Synechococcus*, although it is said that phytochelatins have been extensively searched for and not found in many species of cyanobacteria (James Moffett, personal communication, 2007). Phytochelatins are comprised of a repeating peptide sequence of $(\gamma\text{-Glu-Cys})_n\text{-Gly}$, where n = 2-11 (Figure 1.6c).

Glutathione is a tripeptide of Glu-Cys-Gly, and a possible metal binding agent (Figure 1.6b). Low molecular weight thiols such as glutathione have been studied in marine phytoplankton and in the ocean (Tang et al., 2000; Dupont and Ahner, 2005; Dupont et al., 2006a). They are thought to be important to metal speciation (Dupont and Moffett et al., 2006). The vital amino acid for metal affinity in all of these compounds is cysteine (Figure 1.6a). Particulate and dissolved total and reduced thiols were made in collaboration with Tristan Kading in a repeat experiment of the Zn-deprived chronic Cd experiment discussed in Chapter 3, and the preliminary results show that these metabolites are an important response to Cd exposure in *Synechococcus* WH5701.

Metallothionein is just one of several possible biomolecules to be involved in metal homeostasis, and the least studied in marine environments.

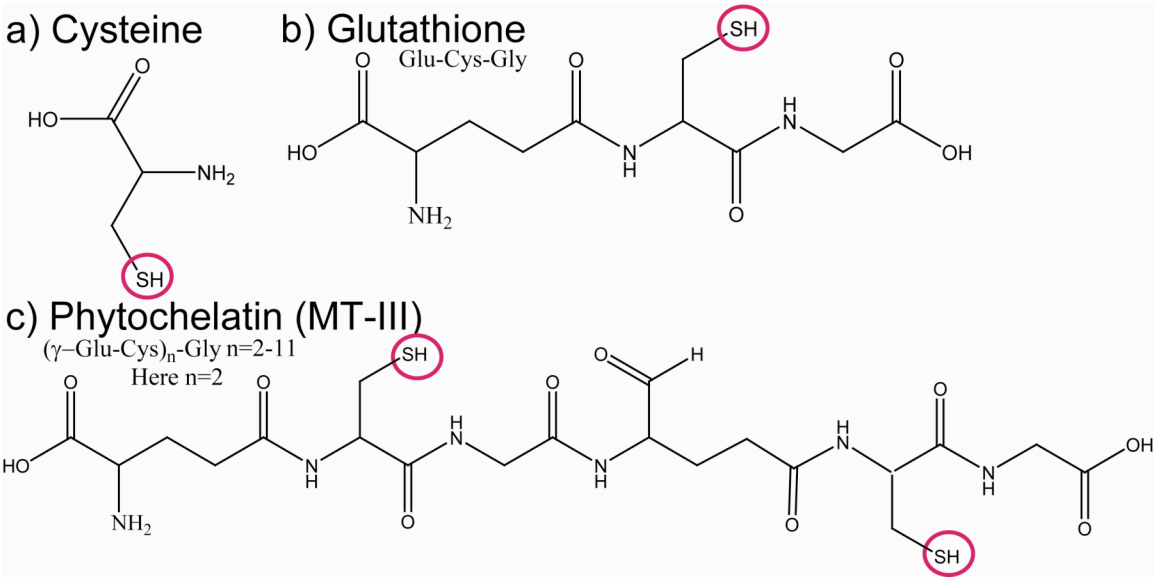

Figure 1.6: Possible metal binding moieties in cells. a) the amino acid cysteine. b) glutathione. c) phytochelatin, classified as a MT-III.

In a recent EXAFS study of Cd binding to the surfaces of *Bacillus subtilis* and *Shewanella oneidensis*, sulfhydryl sites on the surface of cells may be important for environmental metal binding (Mishra et al., 2010). Loadings varied from 1-200 ppm and phosphoryl sites were more important than carboxyl ligands for Cd binding at high Cd loadings, carboxyl sites were important at intermediate Cd loadings and sulfhydryl sites were dominant at low Cd loadings (Mishra et al., 2010). These loadings are many orders of magnitude greater than any loadings one might expect in the marine environment, nevertheless, this is related evidence for the importance of sulfhydryl-metal binding.

Interaction of zinc and phosphorus

As Zn and Cd are known to interact, and Cd and phosphate are observed to be correlated in the ocean, so do Zn and P have an observed relationship. Zn and P are thought to be an example of Type III biochemically dependent colimitation, where the uptake of one nutrient, P, is dependent upon adequate nutrition with regard to the other, Zn (Saito et al, 2008). Alkaline phosphatase may be at the root of this; it is in many cases a Zn-requiring enzyme (Morel et al., 2003) and is used to access organic phosphonates,

often during times of low phosphate availability. Based on extrapolation of experimentation with the coccolithophore *Emiliania huxleyi*, Zn and P colimitation could occur in highly oligotrophic regions such as the Sargasso Sea (Shaked et al., 2006). The interactions of Zn and P are addressed in Chapter 4.

Environmental Gradient Culture Studies

During the course of this thesis work, five strains of marine *Synechococcus* WH5701, WH8109, WH7803, WH7805 and WH8102 with sequenced genomes (or sequencing in progress as in the case of WH8109) were used as representatives of organisms adapted to a varying natural oceanic chemical gradient due to their original isolation location from Long Island Sound (WH5701) out to the Sargasso Sea (WH8102) (Figure 1.7). The coastal side of the environmental gradient is expected to have higher trace metal availability and experience increased variability in irradiance due to mixing relative to the open ocean. Researchers have long been interested in the interaction and interdependence between microorganisms and their environmental milleux. Strains with genomic information were chosen so that proteomic analyses could be performed. All strains were maintained over the course of two-plus years in a modified EDTA-buffered PRO-TM media both with and without the addition of Zn. Most of my experiments were done with the cultures maintained without Zn in the media. The physiological (in all cases) and proteomic responses (in some cases) to varying metal manipulations of cadmium, zinc, copper and iron as well as macronutrient manipulations with phosphate and nitrate were investigated in order to elucidate the interactions of these metals with each other and the respective strains of cyanobacteria. Two of these experiments are presented in Chapters 3 and 4.

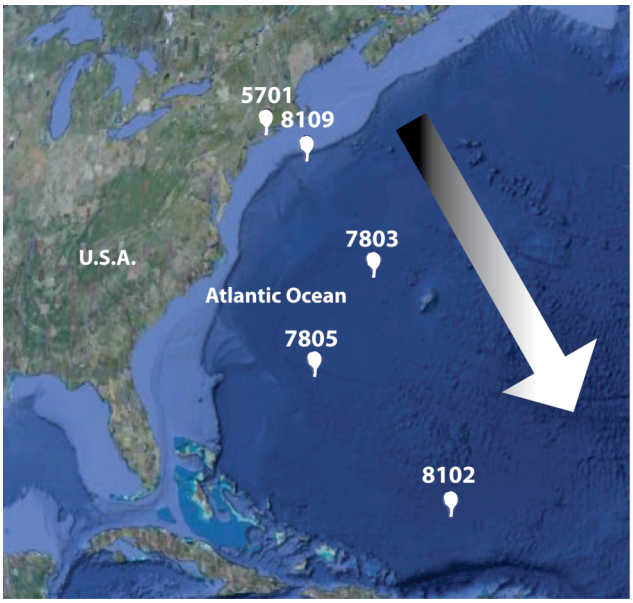

Figure 1.7: Original isolation locations of *Synechococcus* WH strains. Arrow symbolizes an environmental gradient.

At the beginning of the culture experimentation during this thesis work, the hypothesis was that the more coastally proximal strains would be better able to deal with Cd and Zn stress because of their origin, thus inheriting a greater genetic capability to deal with environmental stressors. The role of Cd as nutrient or toxin was queried under this hypothesis because of the fine line between toxin and nutrient that has been noted in the literature for this element, the oceanographic relationship observed between cadmium and phosphate, and the uptake of Cd observed in the field described in Chapter 2. Strains were deprived of Zn in order to find the limits of Cd toxicity, it was noted in earlier studies that the presence of Zn decreased the toxicity of Cd (Saito et al., 2003). Preliminary studies (data not shown) led to the studies that are presented here in Chapters 3 and 4.

Metals and proteins in cells interact in many ways. Many proteins directly require metals as cofactors in order to properly function. In this thesis, the different exposures of cyanobacterial cells to Cd and Zn were shown to affect relative protein abundances and by inference the overall functionality of a cell. This global proteomics approach provides a relative quantification of changes in protein abundance between samples in a given experiment and may be considered systems biology. Examining these data may indicate potential mechanisms of action with regard to the effects of metals and macronutrients

inside a cell and is the first level of investigation. The data sets produced in Chapters 3 and 4 provide some insights to potential mechanisms of metal homeostasis and toxicity in cyanobacterial cells, but inevitably provoke more questions providing an excellent base from which to launch future research, be it absolute quantification of proteins using the same samples using triple quadrupole mass spectrometry, detailed biochemical investigations, more culture studies, or interactions in the environment. In the future, as proteomic methods are applied to environmental samples and combined with particulate and dissolved metal and metabolite measurements as well as parallel laboratory investigations into mechanisms, perhaps the interactions of Cd, Zn and P in the ocean will become clear. As for this thesis, it represents a first step into understanding Cd uptake in the ocean and the interactions of Cd, Zn, and P in marine cyanobacteria.

References

Ahner, B.A., Price, N.M. and Morel, F.M.M. 1994. Phytochelatin production by marine phytoplankton at low free metal ion concentrations: laboratory studies and field data from Massachusetts Bay. *PNAS* 91: 8433-8436.

Ahner, B.A., Morel, F.M.M. and Moffett, J.W. 1997. Trace metal control of phytochelatin production in coastal waters. *Limnology and Oceanography* 42(3): 601-608.

Anbar, A.D. and Knoll, A.H. 2002. Proterozoic ocean chemistry and evolution: a bioinorganic bridge? *Science* 297: 1137-1142.

Blindauer, C.A. 2008a. Zinc-handling in cyanobacteria: An Update. *Chemistry and Biodiversity* 5: 1990- 2013.

Blindauer, C.A. 2008b. Metallothioneins with unusual residues: Histidines as modulators of zinc affinity and reactivity. *Journal of Inorganic Biochemistry* 102: 507-521.

Brand, L.E., Sunda, W.G. and Guillard, R.R.L. 1986. Reduction of marine phytoplankton reproduction rates by copper and cadmium. *Journal of Experimental Marine Biology and Ecology* 96: 225-250.

Boyle, E.A., Sclater, F. and Edmond, J.M. 1976. On the marine geochemistry of cadmium. *Nature* 263: 42-44.

Boyle, E.A. 1988. Cadmium: chemical tracer of deepwater paleoceanography. *Paleoceanography* 3: 471-489.

Bruland, K. W. 1980. Oceanographic distributions of cadmium, zinc, nickel, and copper in the North Pacific. *Earth and Planetary Science Letters* 47: 176-198.

Bruland, K.W. 1992. Complexation of cadmium by natural organic ligands in the central North Pacific. *Limnology and Oceanography* 37(5): 1008-1017.

Cai, L. and Cherian, M.G. 2003. Zinc-metallothionein protects from DNA damage induced by radiation better than glutathione and copper- or cadmium metallothioneins. *Toxicology Letters* 136: 193-198.

Canfield, D.E. 1998. A new model for Proterozoic ocean chemistry. *Nature* 396: 450-453.

Catling, D. C., Zahnle, K. J. and McKay, C.P. 2001. Biogenic methane, hydrogen escape, and the irreversible oxidation of early Earth. *Science* 293: 839-843.

Catling, D.C. and Claire, M.W. 2005. How Earth's atmosphere evolved to an oxic state: a status report. *Earth and Planetary Science Letters* 237: 1-20.

Coyle, P., Philcox, J.C., Carey, L.C. and Rofe, A.M. 2002. Metallothionein: The multipurpose protein. *Cellular and Molecular Life Sciences* 59: 627-647.

Cullen, J.T., Field, M.P. and Sherrell, R.M. 2001. Determination of trace elements in filtered suspended marine particulate material by sector field HR-ICP-MS. *Journal of Analytical Atomic Spectrometry* 16 (11): 1307-1312.

Cullen, J. T., Lane, T. W., Morel, F. M. M. and Sherrell, R. M. 1999. Modulation of cadmium utilization in phytoplankton by seawater concentration. *Nature* 402: 165-167.

Cullen, J.T. and Sherrell, R.M. 1999. Techniques for determination of trace metals in small samples of size-fractioned particulate matter: phytoplankton metals off central California. *Marine Chemistry* 67: 233-247.

Duncan, K.E.R., Ngu, T.T., Chan, J., Salgado, M.T., Merrifield, M.E. and Stillman, M.J. 2006. Peptide folding, metal-binding mechanisms, and binding site structures in metallothioneins. *Experimental Biology and Medicine* 231: 1488-1499.

Dupont, C.L. and Ahner, B. 2005. Effects of copper, cadmium, and zinc on the production and exudation of thiols by *Emiliania huxleyi*. *Limnology and Oceanography* 50(2): 508-515.

Dupont, C.L., Moffett, J.W., Bidigare, R.R. and Ahner, B.A. 2006a. Distributions of dissolved and particulate biogenic thiols in the subartic Pacific Ocean. *Deep Sea Research Part I: Oceanographic Research Papers* 53(12): 1961-1974.

Dupont, C.L., Yang S., Palenik B., and Bourne, P.E. 2006b. Modern proteomes contain putative imprints of ancient shifts in trace metal geochemistry. *Proceedings of the National Academy of Sciences* 103 (47): 17822-17827.

Elderfield, H. and Rickaby, R.E.M. 2000. Oceanic Cd/P ratio and nutrient utilization in the glacial Southern Ocean. *Nature* 405: 305-310.

Ellwood, M.J. and Van den Berg, C.M.G. 2000. Zinc speciation in the Northeastern Atlantic Ocean. *Marine Chemistry* 68: 295-306.

Ellwood, M.J. 2004. Zinc and cadmium speciation in subantarctic waters east of New Zealand. *Marine Chemistry* 87: 37-58.

Falkowski, P. G. 1994. The role of phytoplankton photosynthesis in global biogeochemical cycles. *Photosynthesis Research* 39 (3): 235-258.

Field, C.B., Behrenfeld, M.J., Randerson, J.T. and Falkowski P. 1998. Primary production of the biosphere: Integrating terrestrial and oceanic components. *Science* 281: 237-240.

Glazer, A. N. 1989. Directional energy transfer in a photosynthetic antenna. *The Journal of Biological Chemistry* 264: 1-4.

Goldschmidt, V.M. 1954. edited by Alex Muir. Geochemistry. Oxford at Clarendon Press.

Ho, T.Y., Quigg, A., Finkel, Z.V., Milligan, A.J., Wyman, K., Falkowski, P.G., and Morel, F.M.M. 2003. The elemental composition of some marine phytoplankton. *Journal of Phycology* 39: 1145-1159.

Hoiczyk, E. and Hansel, A. 2000. Cyanobacterial cell walls: News from an unusual prokaryotic envelope. *Journal of Bacteriology* 182(5): 1191–1199.

Hudson, R.J.M. and Morel, F.M.M. 1989. Distinguishing between extra- and intracellular iron uptake in marine phytoplankton. *Limnology and Oceanography* 34: 1113-1120.

Hunter, K.A., Kim, J.P., and Croot, P.L.1997. Biological roles of trace metals in natural waters. *Environmental Monitoring and Assessment* 44: 103-147.

Hutchins, D.A., Witter, A. E., Butler, A. and Luther, G.W. 1999. Competition among marine phytoplankton for different chelated iron species. *Nature* 400: 858–861.

Kang, Y.J. 2006. Metallothionein redox cycle and function. *Experimental Biology and Medicine* 231: 1459-1467.

Kojima, Y., Binz, P.A., and Kaegi J.H.R. 1999. Nomenclature of metallothionein: Proposal for a revision. In *Metallothionein IV* ed. Klaassen, C. pgs. 3-5.

Kresage, N., Simoni, R.D., Hill, R. L. 2009. Phycobilisome architecture: the work of Alexander N. Glazer. *The Journal of Biological Chemistry* 284 (36): e12-e14.

Lane, E.S., Semeniuk, D. M., Strzepek, R. F., Cullen, J.T. and Maldonado, M. T. 2009. Effects of iron limitation on intracellular cadmium of cultured phytoplankton: Implications for surface dissolved cadmium to phosphate ratios. *Marine Chemistry* 115: 55-162.

Lane, T.W. and Morel, F.M.M. 2000. A biological function for cadmium in marine diatoms. *Proceedings of the National Academy of Sciences* 97: 4627-4631.

Lane, T.W., Saito, M.A., George, G.N., Pickering, I.J. and Prince, R.C. 2005. A cadmium enzyme from a marine diatom. *Nature* 435: 42.

Lee, J.G. and Morel, F.M.M. 1995. Replacement of zinc by cadmium in marine phytoplankton. *Marine Ecology Progress Series* 127: 305-309.

Lee, JG., Roberts, S.B. and Morel, F.M.M. 1995. Cadmium: a nutrient for the marine diatom *Thalassioria weissflogii*. *Limnology and Oceanography* 40: 1056-1063.

Lynes, M.A., Zaffuto K., Unfricht, D.W., Marusov, G., Samson, J.S. and Yin, X. 2006. The physiological roles of extracellular metallothionein. *Experimental Biology and Medicine* 231: 1548-1554.

Maldonado, M. T. and Price, N. M. 1999. Utilization of iron bound to strong organic ligands by plankton communities in the subarctic Pacific Ocean. *Deep Sea Research Part II* 46: 2447–2473.

Marchant, R., Banat, I. M., Rahman, T. J. S. and Berzano, M. 2002. What are high-temperature bacteria doing in cold environments? *Trends in Microbiology* 10(3): 120-121.

Margoshes, M. and Vallee, B.L. 1957. A cadmium protein from equine kidney cortex. *Journal of the American Chemical Society* 79: 4813-4814.

Mishra, B., Boyanov, M.I., Bunker, B. A., Kelly, S.D., Kemner, K.M., Nerenberg, R., Read-Daily, B.L. and Fein, J.B. 2009. An X-ray absorption spectroscopy study of Cd binding onto bacterial consortia. *Geochimica et Cosmochimica Acta* 73 (15): 4311-4325.

Morel, F.M.M., Milligan, A.J. and Saito, M.A. 2003. Marine bioinorganic chemistry: The role of trace metals in the oceanic cycles of major nutrients. Treatise on Geochemistry Volume 6 The Oceans and Marine Geochemistry. eds. Henry Elderfield. H.D. Holland and K.K. Turekian. 6.05: 113-143.

Noddack, I. and Noddack, W. 1939. Die Häufigkeiten der Schwermetalle in Meerestieren. *Arkiv för zoology* 32A(4) Stockholm: Almqvist & Wiksell.

O'Halloran, T.V., and Culotta, V.C. 2000. Metallochaperones, an intracellular shuttle service for metal ions. *The Journal of Biological Chemistry* 275(33): 25057-25060.

Outten, C.E. and O'Halloran, T.V. 2001. Femtomolar sensitivity of metalloregulatory proteins controlling zinc homeostasis. *Science* 292: 2488-2492.

Palenik, B., Ren, Q., Dupont, C.L., Myers, G.S., Heidelberg, J.F., Badger, J.H., Madupu, R., Nelson, W.C., Brinkac, L.M., Dodson, R.J., Durkin, A.S., Daugherty, S.C., Sullivan, S.A., Khouri, H., Mohamoud, Y., Halpin, R., Paulsen, I.T. 2006. Genome sequence of *Synechococcus* CC9311: Insights into adaptation to a coastal environment. *PNAS*: 103(36): 13555-13559.

Palenik, B., Brahamsha, B., Larimer, F.W., Land, M., Hauser, L., Chain, P., Lamerdin, J., Regala, W., Allen, E.E., McCarren, J., Paulsen, I., Dufresne, A., Partensky, F., Webb, E.A., and Waterbury, J. 2003. The genome of a motile marine *Synechococcus*. *Nature* 424: 1037-1042.

Palmiter, R.D. 1998. The elusive function of metallothioneins. *PNAS* 95: 8428-8430.

Park, H., Song, B. and Morel, F. M. M. 2007. Diversity of the cadmium-containing carbonic anhydrase in marine diatoms and natural waters. *Environmental Microbiology* 9(2): 403-413.

Payne, C.D. and Price, N.M 1999. Effects of cadmium toxicity on growth and elemental composition of marine phytoplankton. *Journal of Phycology* 35: 293-302.

Price, N.M. and Morel, F.M.M. 1990. Cadmium and cobalt substitution for zinc in a marine diatom. *Nature* 344: 658-660.

Quigg, A., Reinfelder, J. R. and Fisher, N.S. 2006. Copper uptake kinetics in diverse marine phytoplankton. *Limnology and Oceanography* 51: 893–899.

Rae, T.D., Schmidt, P.J., Pufahl, R.A., Culotta, V.C. and O'Halloran, T.V.1999. Undetectable intracellular free copper: the requirement of a copper chaperone for superoxide dismutase. *Science* 284: 805-808.

Robinson, N. J., Whitehall, S.K., and Cavet, J.S. 2001. Microbial metallothioneins. *Advances in Microbial Physiology* 44: 183-213.

Rocap, G., Distel, D.L., Waterbury, J.B., and Chisholm, S.W. 2002. Resolution of *Prochlorococcus* and *Synechococcus* ecotypes by using 16S-23S ribosomal DNA internal transcribed spacer sequences. *Applied and Environmental Microbiology* 68(3): 1180-1191.

Saito, M.A., Sigman, D.M. and Morel, F.M.M. 2003. The bioinorganic chemistry of the ancient ocean: the co-evolution of cyanobacterial metal requirements and biogeochemical cycles at the Archean-Proterozoic boundary? *Inorganica Chimica Acta* 356: 308-318.

Saito, M.A, Goepfert, T.J. and Ritt, J. 2008. Some thoughts on the concept of colimitation: Three definitions and the importance of bioavailability. *Limnology and Oceanography* 53(1): 276–290.

Saito, M. A., Goepfert, T. J., Noble, A. E., Bertrand, E. M., Sedwick, P. N. and DiTullio, G. R. 2010. A seasonal study of dissolved cobalt in the Ross Sea, Antarctica: micronutrient behavior, absence of scavenging, and relationships with Zn, Cd, and P. *Biogeosciences* 7: 4059-4082.

Semeniuk, D.M., Cullen, J.T., Johnson, W.K., Gagnon, K., Ruth, T.J. and Maldonado, M.T., 2009. Plankton copper requirements and uptake in the subarctic Northeast Pacific Ocean. *Deep Sea Research I* 56: 1130-1142.

Shaked, Y., Xu, K., Leblanc, K. and Morel, F. M. M. 2006. Zinc availability and alkaline phosphatase activity in *Emiliania huxleyi*: Implications for Zn-P co-limitation in the ocean. *Limnology and Oceanography* 51: 299–309.

Shaw, C.F. III., Stillman, M.J. and Suzuki, K.T. Metallothioneins: An overview of metal-thiolate complex formation in metallothioneins. In Stillman, M.J., Shaw, C.F. III., and Suzuki, K.T. (eds.) 1992. Metallothioneins. VCH Publishers 1-13.

Sherrell, R.M. and Boyle, E. A. 1992. The trace metal composition of suspended particles in the oceanic water column near Bermuda. *Earth and Planetary Science Letters* 111: 155-174.

Scanlan, D.J. 2003. Physiological diversity and niche adaptation in marine *Synechococcus*. *Advances in Microbial Physiology* 47: 1-64.

Sorby, H.C. 1877. On the characteristic colouring-matters of the red groups of algae. *Journal of the Linnean Society of London: Botany* 15: 34-40.

Suhy, D.A., Simom, K.D., Linzert, D.I.H. and O'Halloran, T.V. 1999. Metallothionein is part of a zinc-scavenging mechanism for cell survival under conditions of extreme deprivation. *The Journal of Biological Chemistry* 274(14): 9183-9192.

Sunda, W.G. 1988. Trace metal interactions with marine phytoplankton. *Biology and Oceanography* 6: 411-442.

Sunda, W.G. and Huntsman, S.A. 2000. Effect of Zn, Mn, and Fe on Cd accumulation in phytoplankton: Implications for oceanic Cd cycling. *Limnology and Oceanography* 45(7): 1501-1516.

Tang, D., Hung, C., Warnken, K. W. and Santschi, P. H. 2000. The distribution of biogenic thiols in surface waters of Galveston Bay. *Limnology and Oceanography* 45(6): 1289–1297.

Tang, D. and Morel, F.M.M. 2006. Distinguishing between cellular and Fe-oxide-associated trace elements in phytoplankton. *Marine Chemistry* 98(1): 18-30.

Tovar-Sanchez, A., Sañudo-Wilhelmy, S.A., Garcia-Vargas, M. Weaver, R.S., Popels, L.C. and Hutchins, D.A. 2003. A trace metal clean reagent to remove surface-bound iron from marine phytoplankton. *Marine Chemistry* 82: 91-99.

Tovar-Sanchez, A., Sañudo-Wilhelmy, S.A., Garcia-Vargas, M., Weaver, R.S., Popels, L.C. and Hutchins, D.A. 2004. Corrigendum to "A trace metal clean reagent to remove surface-bound iron from marine phytoplankton". [*Marine Chemistry* 82 (2003) 91–99] *Marine Chemistry* 85: 191.

Williams, R. J. P. 2007. Systems biology of evolution: the involvement of metal ions. *Biometals* 20: 107–112.

Williams, R. J. P. and Frausto da Silva, J.J.R. 2006. The Chemistry of Evolution: The Development of our Ecosystem. Elsevier.

Xu, Y., Feng, L., Jeffrey, P. D., Shi, Y. and Morel, F. M. M. 2008. Structure and metal exchange in the cadmium carbonic anhydrase of marine diatoms. *Nature* 452: 56-61.

Zwirglmaier, K., Heywood, J. L., Chamberlain, K., Woodward, E. M., Zubkov, M. V. and Scanlan, D. J. 2007. Basin-scale distribution patterns of picocyanobacterial lineages in the Atlantic Ocean. *Environmental Microbiology* 9(5): 1278-90.

Chapter 2

Enriched Stable Isotope Uptake and Cadmium Addition Experiments with Natural Picophytoplankton Assemblages in the Costa Rica Upwelling Dome

Abstract

Cadmium (Cd) can function as either a nutrient or toxin in the marine environment. This duality has been demonstrated in phytoplankton cultures where Cd has been shown to have toxic effects to cyanobacteria, but acts as a nutrient in the marine diatom *Thalassiosira weissflogii* by biochemically replacing zinc (Zn). Whether or not Cd functions as a nutrient or toxin is likely to be controlled by its bioavailability to organisms, detoxification mechanisms the organisms may possess that give a toxicity threshold or sensitivity, and exposure or dosage. Like many other trace metals in surface waters, Cd is complexed by strong organic ligands, which are thought to be produced by marine phytoplankton, particularly the cyanobacteria, *Synechococcus*.

In the summer of 2005, the bioavailability and uptake of Cd in the Costa Rica Upwelling Dome was examined using Cd addition and enriched stable isotope uptake experiments. The Costa Rica Dome is a tropical thermocline dome in the Eastern Pacific fed uniquely by a coastal wind jet that produces a habitat with high phytoplankton biomass relative to surrounding waters. This dome supports some of the highest cell densities of the cyanobacterium, *Synechococcus*, reported in nature, making it an ideal place to observe microbial processes that may be affected by the higher abundance of *Synechococcus*. The greater hypothesis was that greater ligand production inside the dome might prevent Cd toxicity, but as a first step in this manuscript we tested whether or not communities inside the dome were less vulnerable to Cd toxicity than those outside the dome.

Higher quantities of biomass, higher toxicity thresholds of the microbial communities, and perhaps greater ligand production inside the dome, may prevent toxicity to upwelled Cd in this region, relative to the oligotrophic waters. Bottle incubation experiments with Cd additions ranging from 0.5 to 5 nM resulted in reduced chlorophyll *a* outside of the dome relative to control treatments, but showed no reduction in chlorophyll *a* inside the dome, consistent with this hypothesis. Moreover, tracer uptake experiments were conducted with the intermediate-abundance stable isotope ^{110}Cd at stations within and without the dome, in which variations with depth and time were examined. Cd totals were measured shipboard and in the lab using anodic stripping voltammetry, showing depletion of total Cd in the surface waters and increased concentrations with depth. Cd uptake was greatest within the upper 40 m of water inside the dome, decreased with depth and increased with time. Uptake correlated positively with chlorophyll *a* concentrations. Together, these experiments suggest uptake of Cd into the microbial loop in the upper water column both in and out of the Costa Rica Dome, but show that Cd toxicity was not induced within the dome (presumably due to a higher amount of biomass in that region) and that perhaps *Synechococcus* has a lower sensitivity to Cd relative to *Prochlorococcus* outside of the dome.

INTRODUCTION

Phytoplankton and Cadmium in the Marine Environment

Marine phytoplankton are important contributors to primary productivity and have been a vital part of the ecosystem for billions of years (see page 11 in Chapter 1 for a more detailed discussion). Cadmium (Cd) is biogeochemical enigma, toxic but with a nutrient-like distribution in the ocean, implying biological uptake and regeneration at depth. The details of the relationship between marine phytoplankton and Cd are still not well understood.

Cd is a trace metal with concentrations ranging from 1 to 1,100 pM in the open ocean (Bruland, 1980). Cd profiles are nutrient-like, resembling phosphorus profiles; concentrations are depleted in surface waters, increase with depth, and are fairly constant in deep waters (Boyle et al., 1976; Bruland, 1980; Boyle, 1988). The 'kink' noticed in plots of dissolved Cd:PO_4^{3-} ratios has been the topic of much discussion in the literature. Some conclude it is an artifact of fitting straight lines to seawater data caused by preferential extraction of Cd relative to P in those waters, without providing a mechanism (Elderfield and Rickaby, 2000). One mechanism is a slightly deeper regeneration cycle for Cd than for P (Boyle, 1988). Others propose that the injection of Cd-depleted high latitude Southern Ocean waters into intermediate depths of the global ocean may be the mechanism (Frew and Hunter, 1992). Further Southern Ocean data drew these authors to add formation of high-Cd Antarctic bottom waters near the Antarctic continent and remineralization of low-Cd-P detritus from biota produced in waters formed at the subtropical convergence as two additional mechanisms (Frew and Hunter, 1995). Others have proposed that the low Cd: PO_4^{3-} ratios in the iron-depleted waters of the Southern Ocean and subarctic Pacific are caused by high levels of Zn depletion, which induce high levels of Cd uptake by phytoplankton (Sunda and Huntsman, 2000). Yet others have proposed the preferential removal of Cd relative to PO_4^{3-} in Fe-limited waters is the result of chronic Fe limitation reducing phytoplankton growth rates relative to non-Fe limited phytoplankton, while not affecting Cd uptake rates, thereby causing the kink (Cullen, 2006; Lane et al., 2009).

Like most other trace metals in surface waters, Cd is complexed by strong organic ligands as mentioned in Chapter 1 (Bruland, 1980; Bruland, 1992; Morel et al., 2003; Ellwood, 2004). The speciation of Cd and other trace metals determines their bioavailability (Hunter et al., 1997). Bioavailability refers to the ability of a substance to be taken up into a cell. If a molecule is not bioavailable then it cannot act as either a nutrient or a toxin. Due to the dissociation of trace-metal complexes, however, bioavailability may ultimately become a kinetic concept as discussed by Morel et al. (2003).

For a detailed discussion of the toxic effects of Cd to organisms in culture, relationship to Zn and a nutritive use of cadmium in a carbonic anhydrase of a eukaryotic diatom see pages 19-20 in Chapter 1. In work studying toxicity of copper to cyanobacteria, *Prochlorococcus* were inhibited at free Cu^{2+} that did not affect *Synechococcus*, although high-light adapted *Prochlorococcus* were more copper resistant than low-light adapted *Prochlorococcus* (Mann et al., 2002). In addition, *Prochlorococcus* has less genes annotated that cope with metal stress than *Synechococcus*, including less metal efflux pumps (Palenik et al., 2003) and no genes for metallothionein.

The Costa Rica Upwelling Dome

The Costa Rica Upwelling dome is a tropical thermocline dome located near 9^{o}N 90^{o}W, with a diameter ranging from 100 to 1000 km. Uniquely fed by a coastal wind jet, it is seasonably predictable, characterized by a shoaling of the thermocline by local cyclonic wind stress curl off of the coast during February and March. It separates from the coast during May-June and expands to the west during July-November. The dome produces a habitat with high phytoplankton and zooplankton biomass relative to that of surrounding tropical waters (Fiedler, 2002) (Figure 2.1). Interest in the dome began with observation of the physical oceanography by Wyrtki 1964, nutrient distributions by Broenkow in 1965, wind generation of the dome by Hofmann et al. 1981, and turned to the consideration of autotrophic picoplankton by Li et al. 1983. The increased primary productivity, biological effects, and phytoplankton assemblages of this feature continue

to intrigue scientists (Fiedler, 2002; Franck et al., 2003; Saito et al., 2005). The highest cell reported cell densities of *Synechococcus* have been recorded in the dome, varying from 1.2 x 10^6 and 3.7 x 10^6 cells mL^{-1} (Saito et al., 2005). These high cell densities make the dome an ideal place to observe microbial community processes dominated by *Synechococcus*.

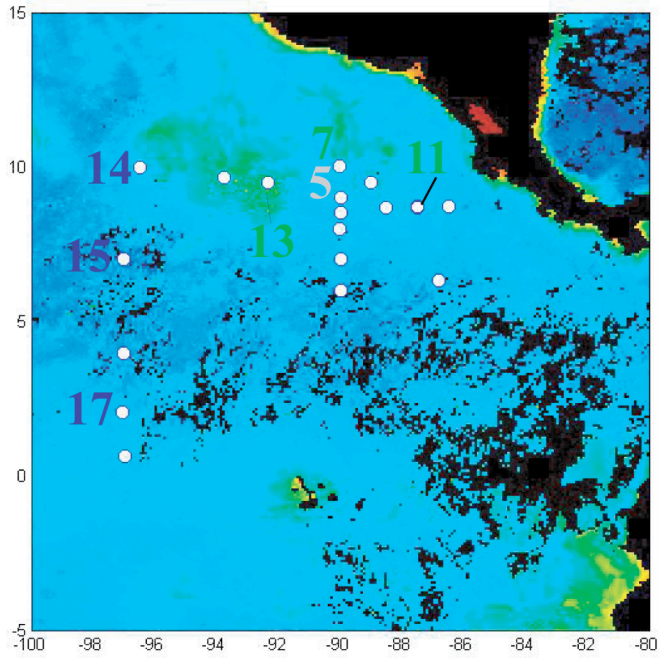

Figure 2.1: Costa Rica Upwelling Dome Stations, July-August 2005. Stations superimposed by Nathan Ahlgren on time-averaged chlorophyll data from the Ocean Color home page. See Appendix I, Table I.1. Green- inside the dome, blue- outside the dome, grey- intermediate.

7, 11, 13
5
14, 15, 17

^{110}Cd Enriched Stable Isotopes and Incubation Techniques to Examine Bioavailability

The eight stable isotopes of Cd range in natural abundance from 0.89 (^{108}Cd) to 28.73% (^{114}Cd) (Figure 2.2). In this study, ^{110}Cd, with a natural abundance of 12.49%, was used as a tracer of Cd uptake into the particulate fraction (> 0.2 μm). ^{110}Cd can be traced by an increase in concentration and deviation of samples from natural isotope abundance ratios (Table 2.1). Previously, uptake experiments have involved radiotracers such as ^{65}Zn, ^{55}Fe, ^{59}Fe or ^{109}Cd (Morel et al., 1994; Sunda and Huntsman, 1995; Cullen et al., 1999; Hutchins et al., 1999). Recently, low abundance stable isotopes of other elements have been used as tracers to study processes such as adsorption/desorption of particulate Cu, Zn, and Ni in estuaries (Gee and Bruland, 2002), bioaccumulation of Hg

in lakes (Pickhardt et al., 2002), exchange of Fe and Zn between soluble, colloidal, and particulate size-fractions in shelf waters (Hurst and Bruland, 2007), and Cd and Cu uptake in a freshwater snail (Croteau and Luoma, 2007). Using stable isotopes over radiotracers affords many advantages including increased safety, ease of shipboard use clearance, and relatively felicitous waste disposal. This is the first reported study to use stable isotopes of Cd as a tracer of uptake in oceanic environments.

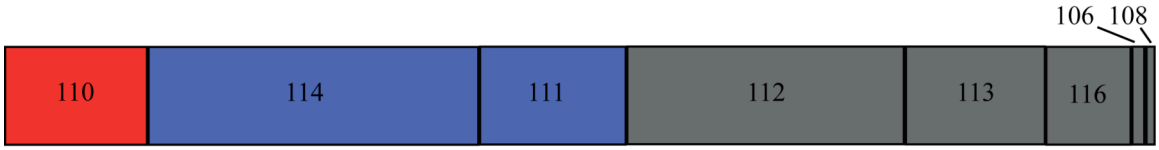

Figure 2.2: Relative abundances of stable cadmium isotopes. Red - ^{110}Cd, tracer in this study. Blue -^{111}Cd and ^{114}Cd, measured isotopes in this study. Grey - other cadmium isotopes. Based on IUPAC values.

Table 2.1: Cadmium natural isotope abundance and isotope ratios

Isotope	IUPAC value
^{106}Cd	0.0125(6)
^{108}Cd	0.0089(3)
^{110}Cd	0.1249(18)
^{111}Cd	0.1280(12)
^{112}Cd	0.2413(21)
^{113}Cd	0.1222(12)
^{114}Cd	0.2873(42)
^{116}Cd	0.0749(18)
Isotope ratios	
^{114}Cd/^{110}Cd	2.300
^{114}Cd/^{111}Cd	2.245
^{111}Cd/^{110}Cd	1.025

Natural cadmium isotope abundances and ratios of the three isotopes measured in this study, based on IUPAC values. See Figure 2.2.

One goal of this study was to demonstrate that ^{110}Cd can be used to trace the movement of dissolved $^{110}Cd^{2+}$ to the particulate phase. Ideally, this transfer would represent biological uptake of bioavailable Cd. There are limitations in terms of

measuring biological uptake of Cd into cells. One must consider the definition of uptake and what it means to measure uptake in an environmental sample. The word "uptake" refers to the act of absorption, more specifically in biological terms, into a living organism. From the present field study, no distinction can be made between i) Cd absorption into cells, ii) Cd adsorption to the surface of cells, iii) Cd adsorption to non-living particulate organic matter, and iv) Cd adsorption to particulate inorganic matter. In this study, the word "uptake" refers to the absorption of dissolved Cd into the particulate fraction, presumably into the cells of the phytoplankton community (i). Biological uptake (i) is likely to dominate the signal (due to the abundance of actively growing autotrophic cells in the photic zone); however, the methods of this study do not allow for the distinction between these four options. One disadvantage of this method is that if the cells are Zn or Cd limited, the addition may stimulate growth. To our knowledge, Cd limitation has never been shown in any organism. It is also notoriously difficult to limit cyanobacteria for Zn, although it can be easily achieved with diatoms. Another goal of this study is to show that one 24-hr timepoint can be adequately used to measure Cd uptake as opposed to a time course or shorter-term experiment. Because casts at sea can occur around the clock, uptake rates may be affected by whether or not it is daylight when the incubation starts. In the microbial community different microorganisms may be actively taking up molecules at different points in a diel cycle. Allowing the sample to incubate with Cd over one diel cycle removes some of the concern of differential uptake due to time of day.

The disparity in toxicity thresholds between eukaryotic diatoms and among cyanobacteria, the reported nutritive use of Cd in a eukaryotic marine carbonic anhydrase, and the reports of organic ligands being produced in the Costa Rica Dome microbial community led to the investigation of Cd toxicity to natural phytoplankton assemblages. This location allowed a comparison between communities dominated by *Synechococcus* and *Prochlorococcus*. Observed toxicity to Cd treatments suggests that added Cd is bioavailable and entering cells, whereas no toxic effects suggest that added

Cd is either perhaps less bioavailable, that is bioavailable yet taken up and detoxified, or that the same dosage affected different subsets of the microbial community differently.

Bioavailable refers to the ability of a chemical species to be absorbed into a cell and can be thought of as a spectrum ranging from more to less bioavailable. Some chemical species may be more bioavailable; for example, inorganic Cd may be more bioavailable than organically complexed Cd, although the bioavailability of organically complexed Cd is not known. In addition, the dissociation of trace-metal complexes over time can affect bioavailability (Morel et al., 2003). Also, different chemical species can be more or less bioavailable to different microorganisms. As mentioned in Chapter 1, toxic effects in culture have been observed to be proportional to the summation of inorganic species (Sunda, 1988), although for copper and iron, organic ligands have been shown to be bioavailable (Hutchins et al., 1999; Maldonado et al., 1999; Quigg et al., 2006 and Semeniuk et al., 2009).

Toxicity is another biological term with a plurality of meanings. Toxicity can be considered the deleterious effects of a substance to an organism. Toxicity itself refers to the degree of being poisonous, or degree of harmful effects produced by a substance in an organism. Toxic effects can range from decreased performance to death. In general, even a metal that at normal levels has nutritive properties in large enough quantities can cause toxicity. In this chapter, the word "toxicity" will be used to indicate decreased performance of bottled phytoplankton assemblages in terms of decreased chlorophyll *a* concentrations relative to a control treatment with no added Cd.

There is also another, less well known toxicological dose response model called hormeisis. The hormetic dose-response curves can be considered in two ways, the first is a low-dose stimulatory and high-dose inhibitory response to physiological processes such as growth and the second is a low-dose reduction and high-dose enhancement of adverse effects such as carcinogenesis (Calabrese, 2005). The concept of hormeisis is especially relevant to both the study of Cd and of cyanobacteria in particular because Cd may be a nutrient at low concentrations and is also known to be toxic at higher concentrations and

because cyanobacteria show responses at low dosages. In the case of Cd, the hormetic response may be due to a pulse of cellular Zn release due to Cd exposure.

Cell size and natural vs. laboratory conditions can make a difference in the sensitivity of organisms to toxic substances. *Prochlorococcus* cells are smaller than *Synechococcus* cells. In considering sensitivity of organisms to toxic substances, a recent study by Echeveste et al. (2010) showed that smaller phytoplankton cells were more sensitive to exposure of polycyclic aromatic hydrocarbons (PAHs) than larger ones, particularly *Synechococcus* and *Prochlorococcus* and that natural communities were more sensitive to PAHs than cultures of phytoplankton.

The Costa Rica Upwelling dome in the summer of 2005 provided an ideal natural laboratory in which to compare a unique, *Synechococcus*-dominated environment to an oligotrophic, *Prochlorococcus*-dominated one. The cruise track included stations inside and outside the dome, allowing for comparisons between different phytoplankton assemblages. This study aims to address the duality of Cd as a nutrient or toxin in the marine environment by considering Cd bioavailability from multiple angles, using the tools of ^{110}Cd uptake experiments, toxicity studies, biological parameters and natural total dissolved and labile Cd measurements.

METHODS

Preparation of Plasticware

All sampling bottles and materials were rigorously cleaned to avoid metal contamination. All cleaning took place in a Class 100 clean room. Bottles were rinsed with 18.2 mΩ Milli-Q (Millipore) water soaked overnight in 1% citranox, rotated, soaked overnight, then rinsed seven times with Milli-Q water. The bottles were filled with 10% HCl (Baker instra-analyzed) by volume and soaked for a minimum of a week, rotated, and soaked for another week. Bottles were rinsed seven times with pH 2 HCl (Baker instra-analyzed) and stored double-bagged in plastic zip bags. Preparation of acid-clean tubes for holding water for nutrient analysis progressed the same as the trace-metal clean ones with the following exception. Instead of individually filling each tube, tubes were

soaked in a 10% HCl (Baker instra-analyzed) by volume bath for a week with stirring to ensure exposure of every surface to acid.

Sample Collection

Collection occurred during Cruise KN 182-05 aboard the R/V Knorr, July 17-29, 2005 from the Costa Rica Upwelling Dome (Figure 2.1, Table I.1). Water samples were collected using modified 10 L Go-Flo bottles (General Oceanics) suspended on a Kevlar line triggered with a Teflon messenger. Teflon coated O-rings replaced the standard O-rings and Teflon plug valves replaced the standard stopcocks in the modified Go-Flo sampling devices (Bruland et al., 1979). Samples for electrochemical analysis of Cd totals were pressure-filtered through 142 mm, 0.4 μm polycarbonate Nuclepore filters housed in a polycarbonate "filter sandwich" and stored in trace-metal clean polyethylene bottles. Samples for nutrient analysis were stored frozen in acid-cleaned 50 mL centrifuge tubes until analysis by Paul Henderson of the Nutrient Facility at WHOI. Water samples for time course stable isotope uptake experiments and toxicity experiments were collected using a trace-metal clean diaphragm pump that fed into a fifty-liter carboy in a positive pressure clean room environment made of laminar flow hoods and plastic sheeting.

Chlorophyll* a *Estimation

Shipboard chlorophyll *a* measurements were made following the JGOFS procedure involving filtration onto 47 mm GF/F filters (Whatman), acetone extraction, acidification, and measurement on a fluorometer (JGOFS, 1994). Size-fractionated measurements were made using 2 and 10 μm filters. A Picofluor hand-held fluorometer was used. GF/F filters slated for analysis in the lab were folded in half, wrapped in aluminum foil and frozen until analysis. A TD 7000 fluorometer was used and was calibrated using an Ultrospec 2100 pro and a chlorophyll *a* standard (Sigma). Calibration of lab to shipboard chlorophyll data was performed in triplicate samples analyzed both shipboard and in the lab.

Flow Cytometry

Flow cytometry samples were collected and preserved in 0.125% glutaraldehyde (Tousmis) incubated for 10 minutes in darkness and flash-frozen in liquid nitrogen. Samples were thawed in a water bath at 22°C for 5 minutes before analysis on an Influx cell sorter (Cytopeia) using 2 μm fluorescent beads as an internal standard.

Cd^{2+} Addition Experiments

Bottle incubation experiments were performed with 0, 0.5, 1, 1.5, and 5 nM total Cd^{2+} treatments in 1 L polycarbonate bottles with water from 8 or 15 m depth. These concentrations are the total concentration of Cd^{2+} added and should be roughly equivalent to the final concentration assuming the original water was devoid of Cd, no sorption to the walls of the bottle, and relatively little total incorporation into particles. Cd stocks were prepared from $3CdSO_4 \cdot 8H_2O$ and diluted with Milli-Q and 10% HCl (Seastar) to pH 2 in polymethylpentene volumetric flasks. Bottles were cleaned between stations by rinsing, shaking and briefly soaking in 10% HCl, followed by five rinses of pH 2 HCl (Baker instra-analyzed). Cd^{2+} additions were not pre-equilibrated with existing seawater, so the labile Cd could vary depending upon the amount of natural ligands that may have been present in the seawater previous to addition. Each treatment was done in triplicate and carried out in a positive pressure clean room environment. Bottles were incubated in an on-deck seawater flow-through incubator made with blue Plexiglass (35% transmittance), the same light level for all depths. The Station 5 experiment incubated for four days, whereas experiments performed at Stations 11, 14, and 17 incubated for three days. Time zero chlorophyll *a* measurements for Station 5 and 11, as well as final chlorophyll *a* for Station 5 were performed shipboard. Time zero samples for Stations 14 and 17 as well as time final samples from Stations 11, 14, and 17 were frozen and analyzed in the laboratory on land.

^{110}Cd Stable Isotope Uptake Experiments

When choosing a tracer, the relative abundance as well as ease of measurement need be considered. ^{110}Cd is intermediate in abundance and has a small potential for interference. ^{106}Cd, ^{108}Cd, and ^{116}Cd have isobaric interferences from major Pd (^{106}Pd:

~27%) or Sn (^{116}Sn: ~14%) isotopes. ^{112}Cd and ^{114}Cd have isobaric interference with minor Sn nuclides with less than 1% relative abundances. ^{110}Cd and ^{113}Cd may have potential interferences with Pd and In, respectively (Ripperger and Rehkämper, 2007). ^{111}Cd has no isobaric interferences and would be a more ideal tracer, but ^{110}Cd was readily available and thus used. The Cd isotope spike was prepared by dissolving $^{110}CdO_2$ (Oak Ridge National Laboratory) in 5% HNO_3 (Seastar Baseline). Dilutions were made using Milli-Q. The spike was analyzed by ICP-MS to comprise 0.1 nM ^{110}Cd, 0.0019 nM ^{111}Cd, and 0.001 nM ^{114}Cd. When added to filled 250 mL bottles, the added concentrations were 120 pM ^{110}Cd, 1.9 pM ^{111}Cd, and 0.73 pM ^{114}Cd.

An overall schematic for analyses associated with ^{110}Cd stable isotope uptake experiments is displayed in Figure 2.3. Samples for dissolved Cd analyses were filtered through a 0.4 μm polycarbonate Nuclepore filter and stored in trace-metal clean polyethylene bottles until analysis by anodic stripping voltammetry (ASV). Experiments to discern ^{110}Cd particulate uptake were performed at depths varying from 8-600 m. Bottles were incubated for 24 hours. Time course ^{110}Cd uptake experiments involved bottles being harvested after a combination of 3, 6, 12, 18, 24, 36 and 48 hours. All spike additions and consequent filtrations were carried out in a positive pressure clean room environment. Bottles were incubated in the on-deck incubator. The 120 pM $^{110}Cd^{2+}$ spike was added to 250 mL polycarbonate bottles filled with unfiltered seawater and sealed tightly. Bottles were immediately transferred to the incubator.

Collection of biomass occurred by filtration of 200 mL of water at 5 psi onto acid-cleaned 0.2 μm polycarbonate GE Osmonics filters. The use of a 1 mL seawater rinse was implemented from Station 11 onwards (this did not appear to affect the results), and appropriate blanks were collected. Filters were stored frozen in trace-metal clean 1 mL tubes until lab analyses. Filter towers were rinsed with pH 2 HCl between samples and with 10% HCl (Baker instra-analyzed) at the end of each day. Filter blanks, filter tower blanks (placing the filter onto a cleaned tower) and seawater rinse blanks were collected periodically throughout the cruise. Polycarbonate bottles were cleaned between experiments with a rinse, shaking and a brief soak in 10% HCl, followed by a pH 2 HCl

rinse (Baker instra-analyzed). ^{67}Zn additions were also performed. These data are not discussed here, but the ^{67}Zn particulate results at each depth were used as the preexisting particulate Cd for calculating uptake in the ^{110}Cd-spiked sample.

^{110}Cd Sample Acid Digestion and Inductively Coupled Plasma Mass Spectrometry Analysis

All work was performed in a Class 100 clean room under a laminar flow hood. Acid digestion methodologies were developed after protocols reported in the literature (Cullen and Sherrell, 1999; Ellwood and Hunter, 1999, 2000; Hurst and Bruland, 2008).

Filters were removed from the freezer and transferred to trace metal clean Teflon or polypropylene vials. The filters were digested for 4 hours at 120^{o}C in 50% HNO_3 (Seastar Baseline) and 2.5% HF (Seastar Baseline) and the filters removed. After evaporation just to dryness, the residue was resuspended in 5% HNO_3 (Seastar Baseline) with a 1 ppb indium internal standard and run on an Element II ICP-MS in low resolution mode, using an Aridus desolvator system.

Standards consisting of 1, 2, 3, and 4 ppb total Cd and Zn (8.9-35.6 nM) with a 1.6 ppb In internal standard were made and used to calculate Cd concentrations after ICP-MS analysis. Natural Cd isotope abundances of the standards were assumed to calculate concentrations of ^{110}Cd, ^{111}Cd and ^{114}Cd. Note that this method uses an overabundance of ^{110}Cd and should greatly outweigh any natural fractionation signals. It is not comparable to recent studies of natural Cd isotope fractionation using multi-collector ICP-MS, which can detect deviations in the ratio of ^{114}Cd/^{110}Cd with the precision of 2-6 parts per 10,000 (Ripperger and Rehkämper, 2007). Note also that there are response biases in ICP-MS that can cause a slight deviation of the measured isotopic ratio to deviate from the natural abundance isotope ratio. These deviations were not corrected for in these data and may be a few percent.

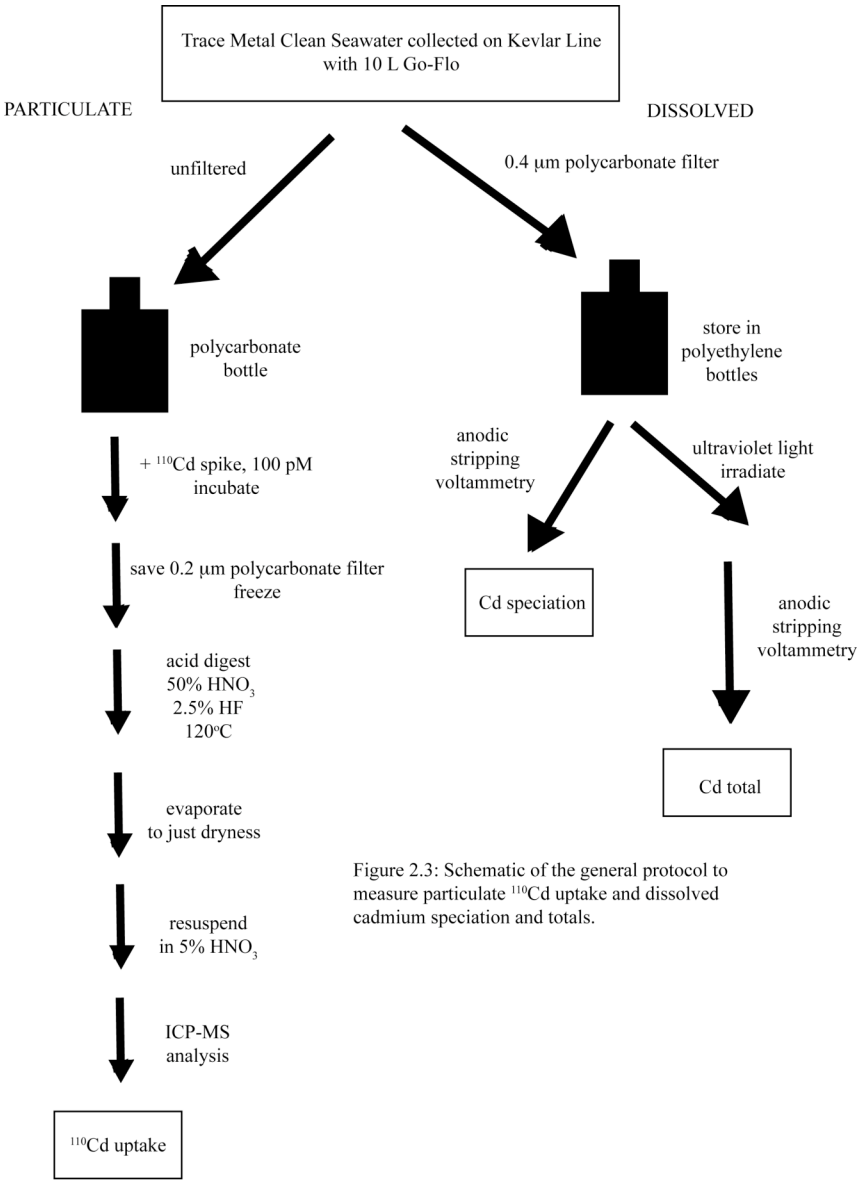

Figure 2.3: Schematic of the general protocol to measure particulate ^{110}Cd uptake and dissolved cadmium speciation and totals.

Anodic Stripping Voltammetry Analyses of Total Dissolved Cadmium

Total Cd measurements were performed using a mercury-plated rotating disc electrode (RDE). Protocols were based after Fischer et al., 1999 and Ellwood, 2004. At the beginning of each day, the RDE was polished with AlO_2 and plated with Hg. Plating occurred in a solution of 10 mL Milli-Q water, 50 μL thiocyanate, 33 μL 3 M KCl (Fluka puriss), and 1 mL 1000 ppm Hg reference solution (Fisher). The solution was purged for 10 minutes and plated at a current of -1.5 V for 10 minutes. Total Cd concentrations were determined from samples that were UV irradiated for 2 hours by standard additions

of 250 pM Cd prepared from Fisher certified stock solutions diluted in pH 2 Milli-Q water and polymethylpentene volumetric flasks. A step potential of 9 mV, deposition potential of -1.5 V, and scan time of 3 minutes were used during the analyses. The detection limit is approximately 15 pM.

RESULTS

Defining Inside and Outside the Dome

The dome is biologically defined in this study as having an order of magnitude or greater *Synechococcus* cell numbers than outside the dome, in addition to the physical oceanographic context of a shoaled thermocline. Stations inside the dome had *Synechococcus* cell numbers equal to or greater than 2×10^5 cells mL^{-1} and an abundance of *Synechococcus* relative to *Prochlorococcus* by at least a factor of three to one. Stations outside the dome are dominated by *Prochlorococcus* by at least a factor of 3 and have *Synechococcus* cell numbers on order of 3.5×10^4 or less, almost an order of magnitude less than inside the dome. Stations 7, 11, 13 were considered to be inside the dome, Station 5 was intermediate and Stations 14, 15 and 17 were outside the dome. Station 5 is considered intermediate because it has *Synechococcus* cell numbers on order of 1×10^5, and almost equal cell numbers of *Synechococcus* and *Prochlorococcus*. *Prochlorococcus* dominates *Synechococcus* at Stations 14, 15, and 17.

Calculating Cadmium Uptake Using ^{110}Cd

Total Cd uptake was calculated using the following equation, assuming that the spike was as available as the existing Cd:

$$\frac{[^{110}Cd_{sample}\ (pmol\ L^{-1}\ d^{-1}) - {}^{110}Cd_{blank}\ (pmol\ L^{-1}\ d^{-1})]}{[^{110}Cd_{spike}\ (pM) + {}^{110}Cd_{natural}\ (pM)]} \times Cd_{total}\ (pM) = Cd_{total}\ \text{Uptake Rate}\ (pmol\ L^{-1}\ d^{-1})$$

$^{110}Cd_{sample}$ (in units of pmol L^{-1} d^{-1}) is the particulate ^{110}Cd measured using ICP-MS of the filter, normalized to volume of seawater and one day of incubation. A difference between radiotracers such as ^{57}Co is that there may be $^{110}Cd_{sample}$ already in the particulate fraction. This was accounted for by subtracting the particulate blank, $^{110}Cd_{blank}$. Particulate $^{110}Cd_{blank}$ will hereafter be referred to as preexisting particulate

^{110}Cd. The particulate blank bottle in these experiments had ^{67}Zn added, but no Cd spike. The ^{67}Zn spike was confirmed to contain virtually no ^{110}Cd, ^{111}Cd, or ^{114}Cd. The ^{67}Zn added to this bottle should not affect the preexisting Cd. Preexisting Cd is measured in units of pmol L^{-1} d^{-1}. It is assumed that the particulate blank is in steady state, i.e. it represents the Cd already in the particulate fraction and any possible natural uptake that could occur during incubation for twenty-four hours is negligible. Dividing the particulate ^{110}Cd by the total dissolved ^{110}Cd yields the fraction of ^{110}Cd that has moved from the dissolved pool to the particulate pool per day. The total dissolved ^{110}Cd is comprised of the dissolved ^{110}Cd added as a spike plus any natural, preexisting dissolved ^{110}Cd (Figure 2.4c). The natural preexisting ^{110}Cd was calculated by multiplying the total dissolved Cd measured by ASV (Figure 2.4a) by the natural abundance of ^{110}Cd, 0.1249 (Figure 2.4b).

When there is very little natural total dissolved Cd, as occurs in the surface waters, $^{110}Cd_{natural}$ approaches zero, Cd_{total} approaches $^{110}Cd_{spike}$ and they cancel out of the equation. Total Cd uptake is then represented entirely by ^{110}Cd uptake. One could then consider this a sort of potential uptake, since the natural dissolved Cd $<<$ $^{110}Cd_{spike}$ at these depths. As natural total dissolved Cd increases with depth, the uptake of the tracer is diluted (Figure 2.4c). Using one group of procedural blanks measured using ICP-MS (n = 4), the detection limit for particulate Cd uptake rate with one standard deviation error is 0.021 ± 0.007 pmol L^{-1} d^{-1}.

Depth profiles of ^{110}Cd uptake rate, total dissolved Cd, total and size-fractioned chlorophyll *a*, and *Prochlorococcus* and *Synechococcus* cell numbers at Station 11, inside the dome are shown in Figure 2.4, data in Appendix I (Table I.2). The dissolved ^{110}Cd spike added to the bottle from each depth (120 pM) is shown in Figures 2.4a, b, and c. The dissolved ^{110}Cd spike is greater than the natural, total dissolved Cd at depths shallower than 40 m (Figure 2.4a). The spike is greater than the natural dissolved ^{110}Cd at every depth (Figure 2.4b). When the spike is added, it contributes a significant amount of the total dissolved Cd at shallow depth, but the contribution decreases with depth as total dissolved Cd increases. ^{110}Cd particulate uptake rates are detectable shallower than

40 m (Figure 2.4d), consistent with total dissolved Cd depletion (Figure 2.4a) and higher biomass in surface waters (Figure 2.4d, e).

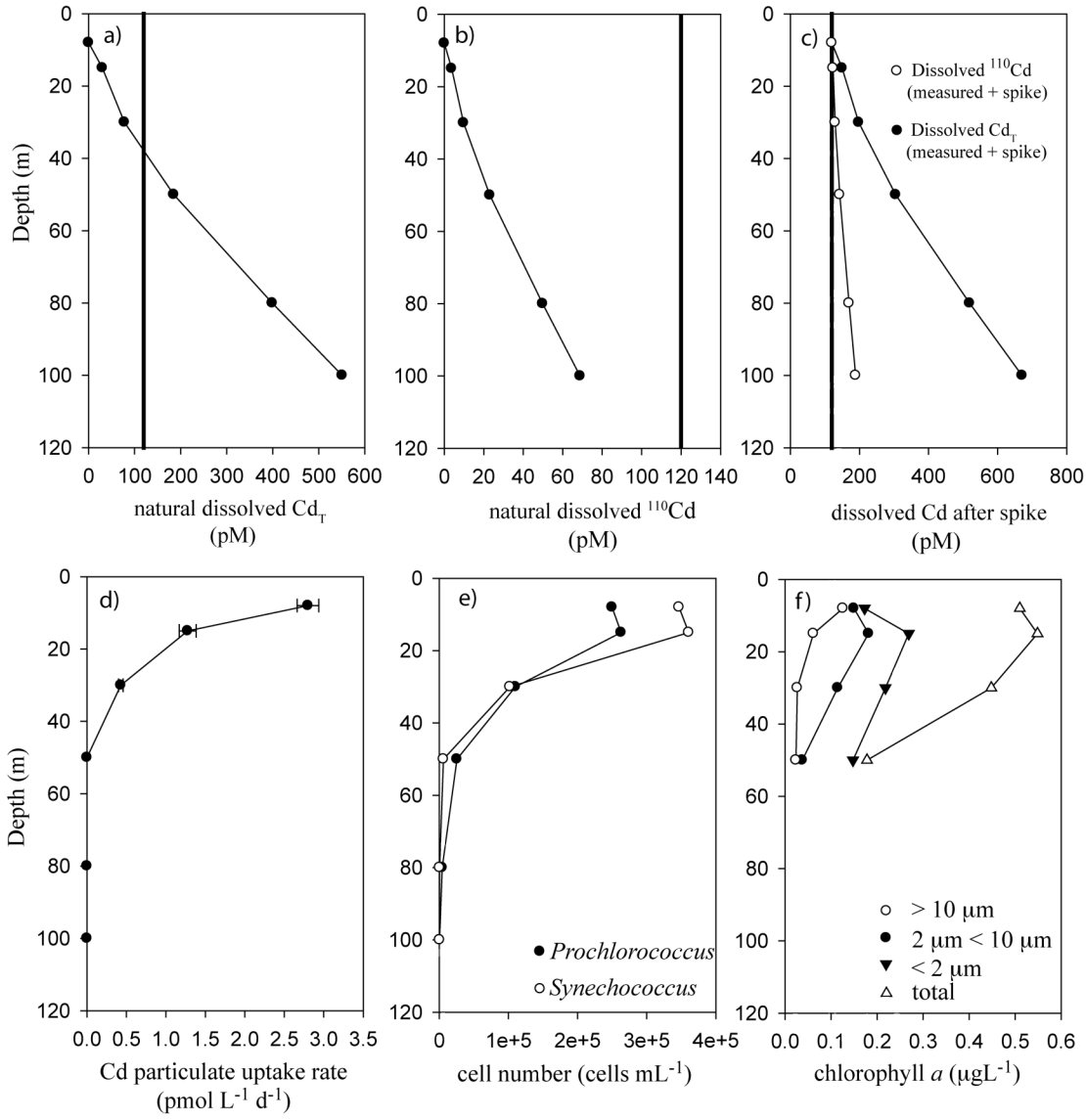

Figure 2.4: Station 11, inside the dome. Depth profiles of natural total dissolved Cd, total dissolved Cd after adding ^{110}Cd spike, particulate Cd uptake rate, *Synechococcus* and *Prochlorococcus* cell numbers, and total and size-fractionated chlorophyll *a*. a) Natural, total dissolved Cd. b) Natural, total dissolved ^{110}Cd. c) Total dissolved Cd and ^{110}Cd in each bottle with spike added. d) Cd particulate uptake rates relative to control. Error bars indicate counting error of a single measurement. e) *Synechococcus* and *Prochlorococcus* cell numbers, f) Size-fractionated chlorophyll *a*. Solid lines in a), b) and c) represent 120 pM of ^{110}Cd spike added, total dissolved Cd added is 122.5 pM. Data in Appendix I, Table I.2.

Isotope ratios can also be examined to track uptake of the spike, in addition to increased amounts of ^{110}Cd in the particulate phase. A depth profile of particulate isotope ratios from Station 11, inside the dome, is shown in Figure 2.5, data in Appendix I (Table I.4). Particulate isotope ratios of $^{114}Cd/^{110}Cd$ and $^{111}Cd/^{110}Cd$ are lower relative to natural abundance (Figure 2.5a), whereas in the preexisting particulate Cd samples, isotope ratios are relatively consistent with natural abundance ratios (Figure 2.5b). Error bars represent propagation of root mean square deviation of one measurement, instrument counting error. Similarly, in the ^{110}Cd time course experiment for Station 11, $^{114}Cd/^{110}Cd$ and $^{111}Cd/^{110}Cd$ particulate ratios are lower than natural abundance and decrease with time (Figure 2.6, Table 2.5).

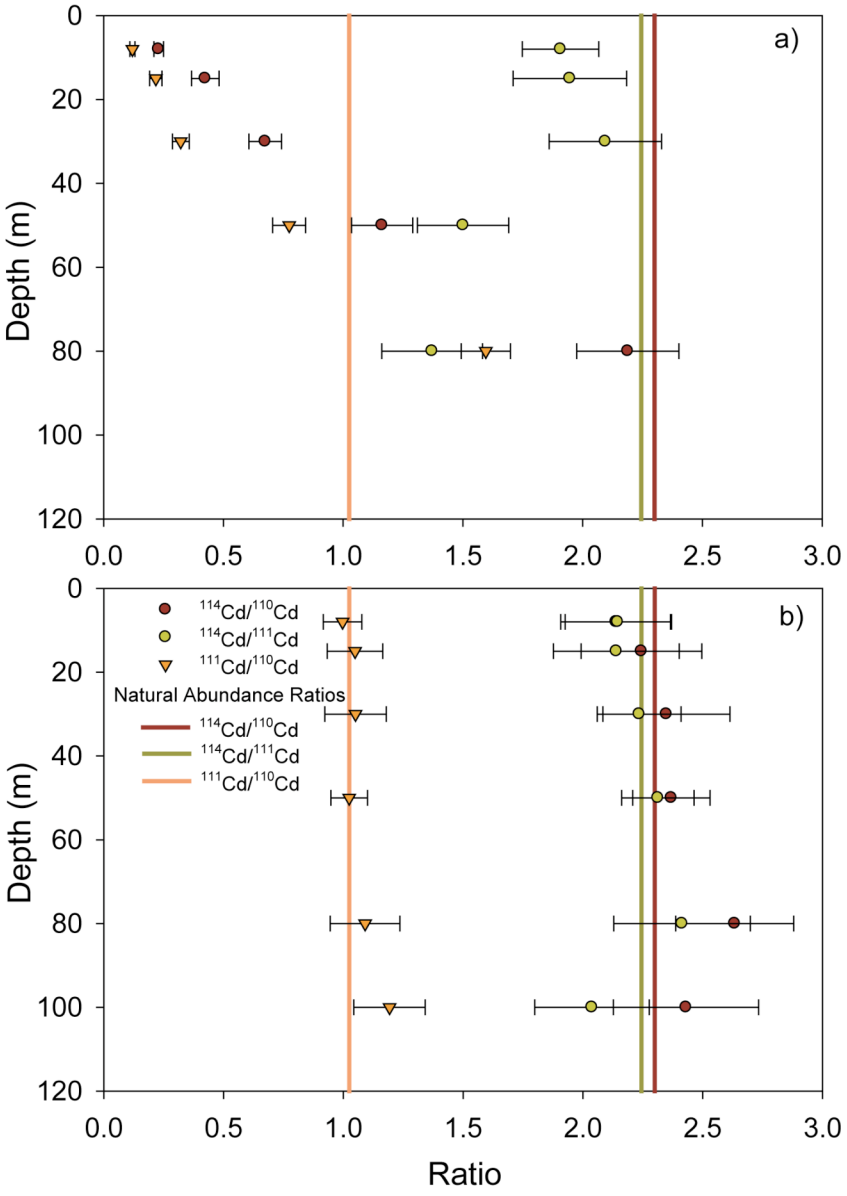

Figure 2.5: Depth profiles of particulate cadmium isotope ratios, Station 11. a) Samples spiked with ^{110}Cd. b) Samples with no ^{110}Cd spike. The negative offset of $^{114}Cd/^{110}Cd$, $^{111}Cd/^{110}Cd$ ratios from natural abundance in shallow waters indicates ^{110}Cd uptake. Error bars are counting error of one ICP-MS measurement. See Table I.4.

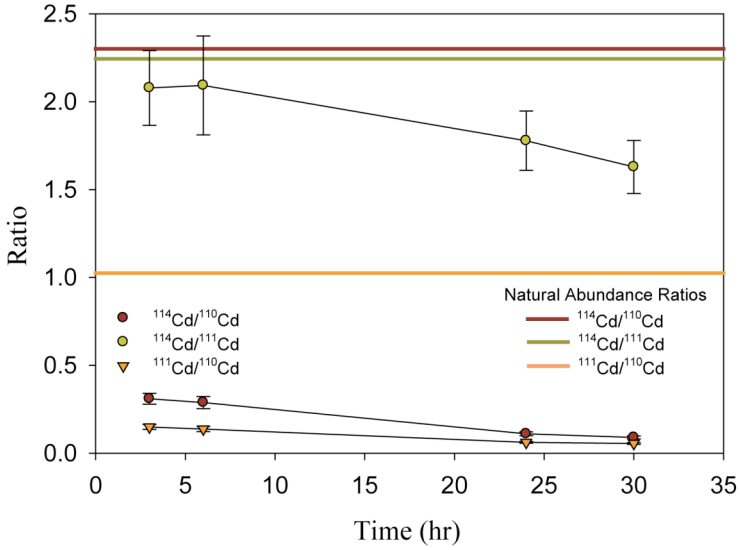

Figure 2.6: $^{114}Cd/^{110}Cd$, $^{111}Cd/^{110}Cd$ and $^{114}Cd/^{111}Cd$ particulate cadmium ratios with time for Station 11 samples spiked with ^{110}Cd. The negative offset of $^{114}Cd/^{110}Cd$, $^{111}Cd/^{110}Cd$ ratios from natural abundance and decrease of these ratios with time indicate uptake of the spike, ^{110}Cd. See Table I.5.

Outside the dome, a similar phenomenon is observed. Depth profiles of ^{110}Cd uptake, total dissolved Cd, total and size-fractioned chlorophyll *a* and *Prochlorococcus* and *Synechococcus* cell numbers at Station 17, outside the dome are shown in Figure 2.7, data in Table I.3. ^{110}Cd particulate uptake rates are detectable shallower than 40 m (Figure 2.7a, d), consistent with total dissolved Cd depletion (Figure 2.7b) and higher biomass in surface waters (Figure 2.7c, e, f).

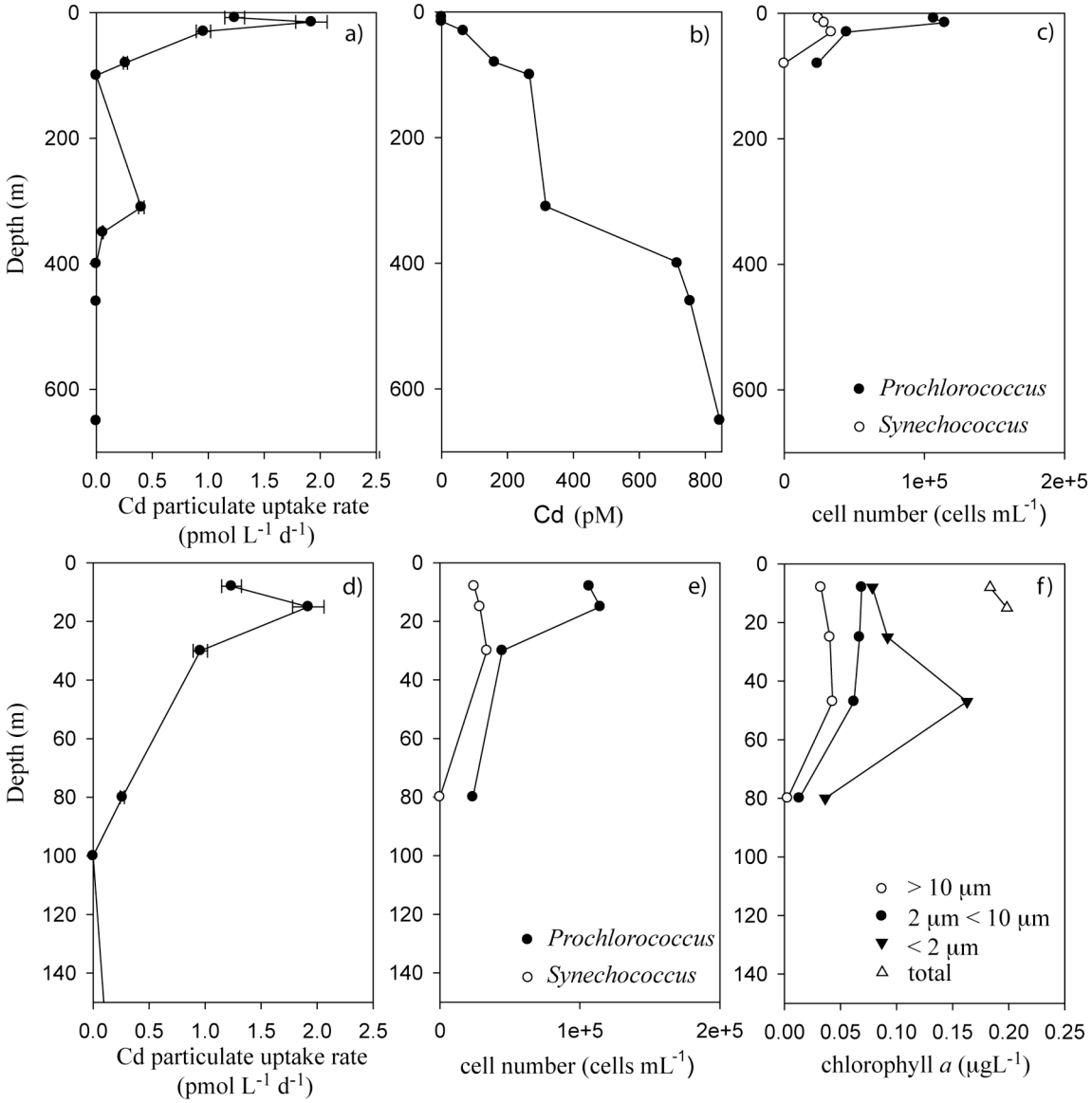

Figure 2.7: Station 17, outside the dome. Depth profiles of particulate Cd uptake, total dissolved cadmium, *Synechococcus* and *Prochlorococcus* cell numbers, and total and size-fractionated chlorophyll *a*. a) Cd particulate uptake rates. b) Total dissolved cadmium. c) *Synechococcus* and *Prochlorococcus* cell numbers. d) Particulate Cd uptake rates. e) *Synechococcus* and *Prochlorococcus* cell numbers. f) Size-fractionated chlorophyll *a*. Note difference in depth scale for d), e), and f). Note that two sets of the size-fractionated chlorophyll *a* measurements were not at the exact depths as the other measurements, the alternate depths are 25 and 47 m. See Table I.3.

Particulate Cd uptake in pmol L^{-1} vs. time is plotted in Figure 2.8 for time course experiments at Stations 5, 7, 11, 13, 15, and 17. Slope of the line yields a Cd uptake rate in pmol L^{-1} d^{-1}. These calculations yield similar uptake rates to those calculated using a single 24-hour time point (Table 2.2), suggesting that using one 24-hour time point at a

given station and depth is an adequate estimate of total Cd uptake. These samples are not corrected for natural dissolved Cd because it was not measured at three of the stations (Stations 7, 13, and 15) and total dissolved Cd was undetectable at the other three stations (Stations 5, 11, and 17). Because total dissolved Cd was undetectable, ^{110}Cd uptake is equal to total Cd uptake and this assumption is extended to the other three stations. These samples are also not corrected for preexisting particulate Cd. See Figure 2.9 for a brief discussion on the need to correct for preexisting particulate Cd.

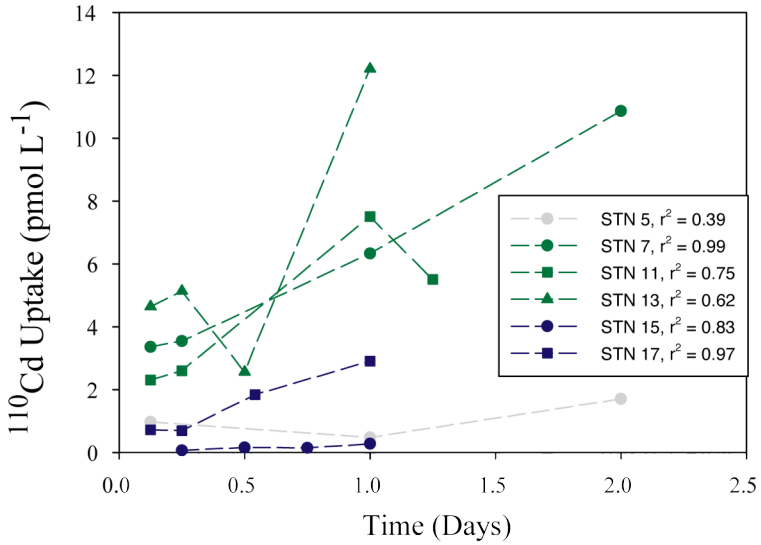

Figure 2.8: ^{110}Cd particulate uptake vs. time. Time course uptake experimental results at Stations 5, 7, 11, 13, 15, and 17 from 15 m depth. Slopes of lines yield Cd uptake rates in pmol L^{-1}d^{-1}. See Table 2.2 and I.6.

Table 2.2: Calculated particulate ^{110}Cd uptake rates from time course experiments and one 24 -hour point

Station	Cd Uptake Rate (pmol L^{-1} d^{-1}) from slope	r^2	Cd Uptake Rate (pmol L^{-1} d^{-1}) from 24 hour	Cd Uptake Rate (pmol L^{-1} d^{-1}) 24 hour difference
5	0.42	0.39	0.47	0.05
7	4.05	0.99	6.33	0.53
11	3.89	0.75	7.5	0.55
13	8.56	0.62	12.2	1.31
15	0.24	0.83	0.27	0.02
17	2.7	0.97	2.9	0.22

See Figure 2.12. Particulate Cd uptake rate calculated from slope of ^{110}Cd uptake vs. time. Particulate Cd uptake rate calculated from ^{110}Cd concentration at a time of 24 hours divided by one day. Errors on particulate Cd uptake rate are counting errors from a single ICP-MS measurement.

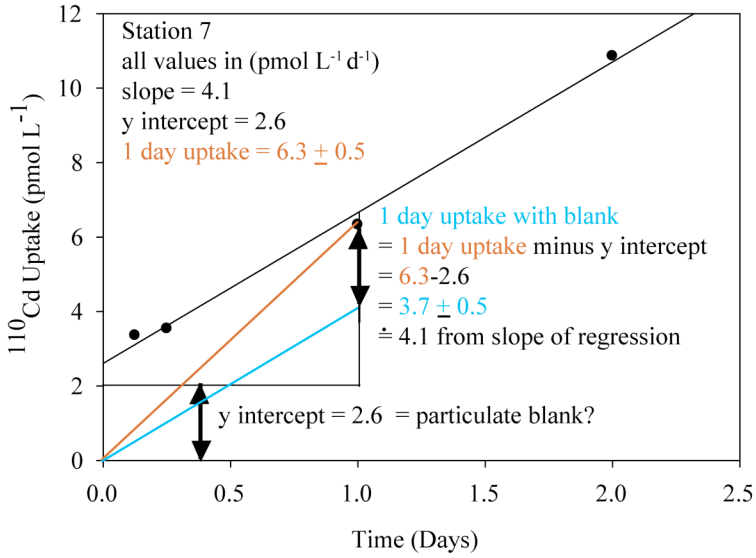

Figure 2.9: Argument for a particulate blank correction, more necessary with increasing inital biomass. Time course uptake points from Station 7. When the y-intercept from the slope of regression line is subtracted from the 1 day time point, an uptake rate is obtained that is within error of the uptake rate obtained from the slope of the regresson line. Red and blue colors indicate non-corrected and corrected values, respectively.

Cadmium Addition Experiments

At the initial time of Cd addition, Station 11, inside the dome, had three times more total chlorophyll *a* than the other stations; the total concentration was 366 ng L^{-1}. Stations 5, 14, and 17 had relatively similar initial chlorophyll *a* concentrations of 115, 78 and 124 ng L^{-1} respectively (Figure 2.10a, Table 2.3). Stations 5 and 11, intermediate and inside the dome have higher *Synechococcus* cell numbers, 1.3 x 10^5 and 3.6 x 10^5 cells mL^{-1}, relative to Stations 14 and 17, which are outside the dome and have approximately an order of magnitude less *Synechococcus* cells, 3.5 x 10^4 and 2.9 x 10^4 cells mL^{-1}, respectively (Figure 2.10b, Table 2.3). *Prochlorococcus* cell numbers are on the order 10^5 cells mL^{-1} at all four stations, so Stations 14 and 17 have an order of magnitude more *Prochlorococcus* than *Synechococcus* (Figure 2.10b, Table 2.3).

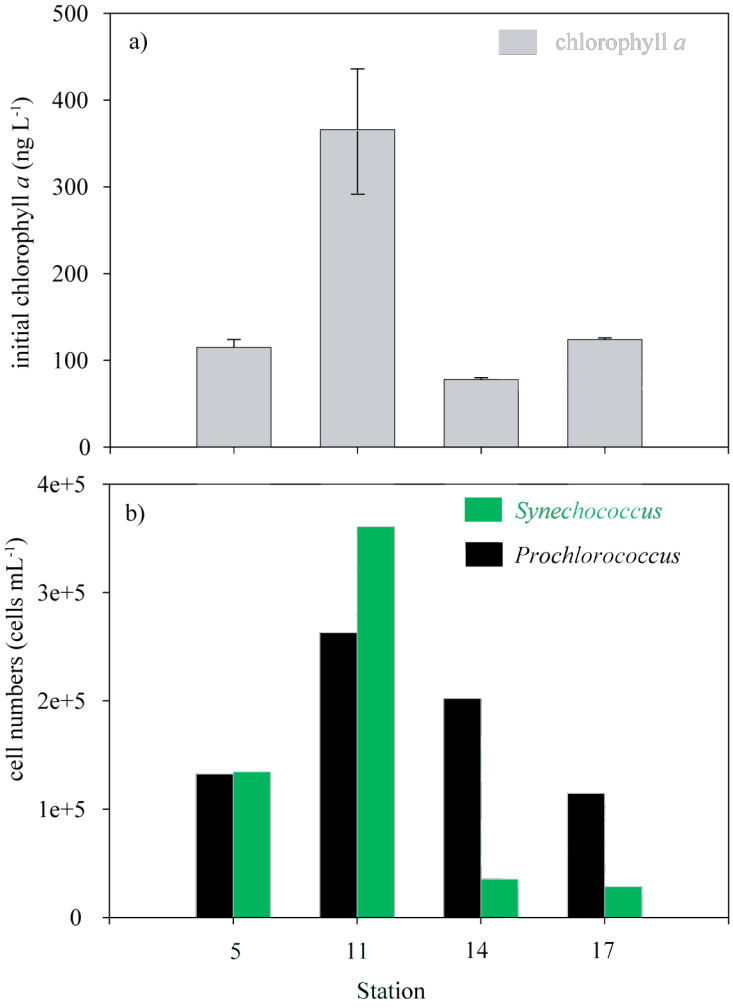

Figure 2.10: Initial chlorophyll *a* and cyanobacterial cell numbers for cadmium addition experiments. a) Initial chlorophyll *a* concentrations. Error bars represent one standard deviation of triplicate measurements. b) Inital *Synechococcus* and *Prochlorococcus* cell numbers. Note that Station 5 (intermediate in terms of the dome) had low initial chlorophyll *a* concentrations, comparable to Stations 14 and 17 (outside the dome), but like Station 11, a greater abundance of *Synechococcus* cells. See Table 2.3.

The control treatments in all stations increased in chlorophyll *a* concentration relative to initial conditions by 13%, 105%, 88% and 247% for Stations 5, 11, 14, and 17 respectively (Figure 2.11, compare solid to dashed lines). Note that Station 5 effectively did not grow, the initial and final chlorophyll *a* concentrations are within error. Other incubations performed on this same cruise at this station investigating the effects of cobalt, iron and DFB (desferrioxamine B) showed an approximately two-fold decrease in *Synechococcus* cell abundance in the control treatment at harvest compared to initial abundance, with an approximately two-fold increase in *Prochlorococcus* cell abundances in the control (Thompson, 2009). When Cd concentrations were artificially enhanced by 0.5 to 5 nM in three to four day bottle incubations, chlorophyll *a* was reduced relative to the control by 10% for at least three of the Cd treatments at all four stations (Figure 2.11,

Table 2.3). At Station 5, chlorophyll *a* was reduced by 10% under 0.5, 1.5, and 5 nM Cd^{2+} additions (Figure 2.11a, Table 2.3). At Station 11, chlorophyll *a* was reduced by 10% under 0.5, 1, 1.5, and 5 nM Cd^{2+} additions (Figure 2.11b, Table 2.3). At Station 14, chlorophyll *a* was reduced by 10% under 1, 1.5, and 5 nM Cd^{2+} additions (Figure 2.11c, Table 2.3). At Station 17, chlorophyll *a* was reduced by 10% under 0.5, 1, 1.5, and 5 nM Cd^{2+} additions (Figure 2.11d, Table 2.3). Chlorophyll *a* was reduced relative to the control by 50% under 5 nM Cd^{2+} addition at Station 17 (Figure 2.11d, Table 2.3). A greater decrease in chlorophyll *a* with increasing Cd^{2+} additions was observed at Stations 14 and 17 (Figure 2.11c and 2.11d).

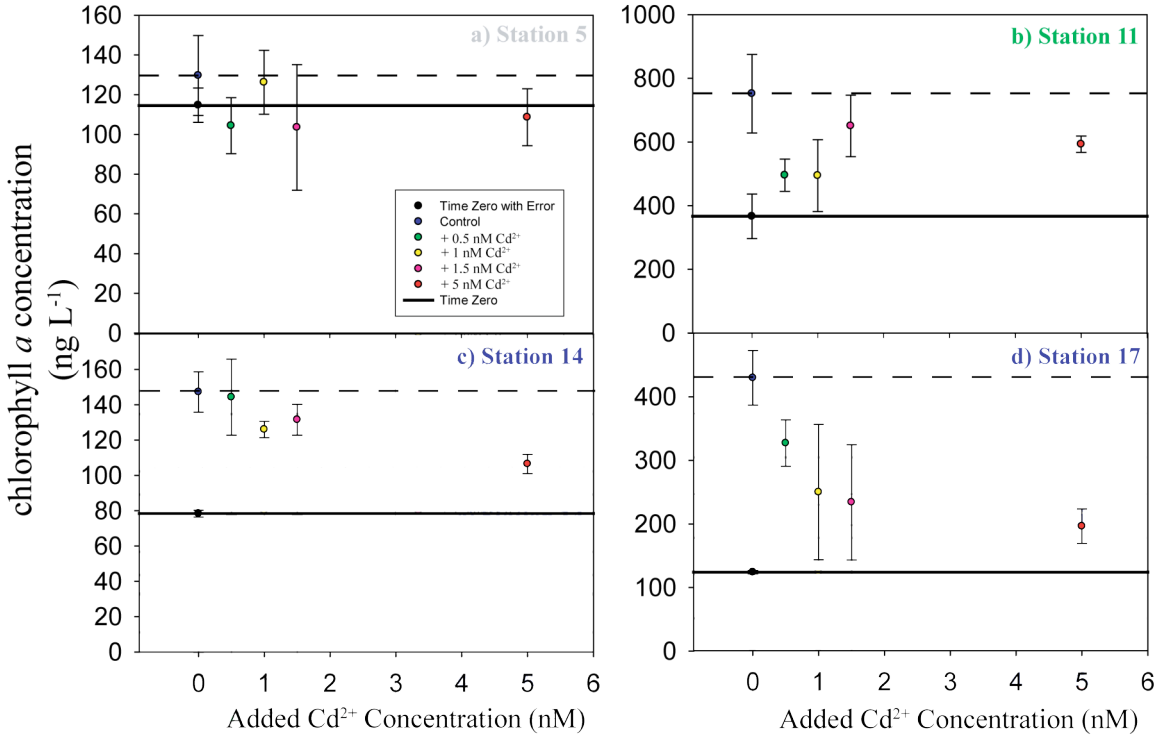

Figure 2.11: Chlorophyll *a* in ng L^{-1} with range of Cd^{2+} treatments for four stations after three days. a) Station 5, intermediate in terms of the dome. b) Station 11, inside the dome. c) Station 14, outside the dome. d) Station 17, outside the dome. Error bars are standard deviations of triplicate bottles. Solid line indicates time zero chlorophyll *a* concentration. Dotted line indicates time final chlorophyll *a* concentration in the no added Cd^{2+}. Note that the incubation at Station 5 ran for four days. See Table 2.3.

Table 2.3: Initial conditions and chlorophyll *a* results, Cd^{2+} addition experiments

Station Depth Inital Cd_T	Total Cd Added (nM)	chlorophyll *a* (ng L^{-1})	*Prochlorococcus* (cells mL^{-1})	*Synechococcus* (cells mL^{-1})
Station 5	Time Zero	115±20	$1.32x10^5$	$1.34x10^5$
15 m	0	130±20		
nd	0.5*	104±14		
	1	126±16		
	1.5*	104±32		
	5*	109±14		
Station 11	Time Zero	366±70	$2.63x10^5$	$3.61x10^5$
15 m	0	752±124		
nd	0.5*	495±51		
	1*	494±113		
	1.5*	650±97		
	5*	593±26		
Station 14	Time Zero	78±2	$2.02x10^5$	$3.54x10^4$
8 m	0	147±11		
57pM	0.5	144±21		
	1*	126±5		
	1.5*	132±9		
	5*	106±5		
Station 17	Time Zero	124±2	$1.14x10^5$	$2.85x10^4$
15 m	0	430±43		
nd	0.5*	327±36		
	1*	250±106		
	1.5*	234±91		
	5**	196±27		

See Figures 2.10 and 2.11. Depths water was collected for bottle incubation and initial dissolved total cadmium concentrations are listed under the station. Errors on chl *a* standard deviation are from three replicate bottles. * = decrease of 10% in chlorophyll *a* concentration relative to control at time final. ** = decrease of 50% in chlorophyll a concentration relative to control at time final.

^{110}Cd Uptake at Seven Stations Compared to Biological Parameters

As shown in Figure 2.12a, c, higher uptake rates occurred at Stations 7, 11 and 13, 6.1, 2.8 and 2.8 pmol L^{-1} d^{-1}, respectively, inside the dome than at intermediate Station 5, 1.3 pmol L^{-1} d^{-1} and the stations outside the dome, 14, 15, and 17, 0.2, 0.96, and 1.9 pmol L^{-1} d^{-1}, respectively (Table 2.4). Linear regressions of particulate ^{110}Cd uptake vs. biological measurements of *Synechococcus* and *Prochlorococcus* cell abundances and total chlorophyll *a* for maximum particulate ^{110}Cd uptake depth at these seven stations yielded weak to moderate correlations. The highest correlation was with total chlorophyll *a*, having an r^2 value of 0.75.

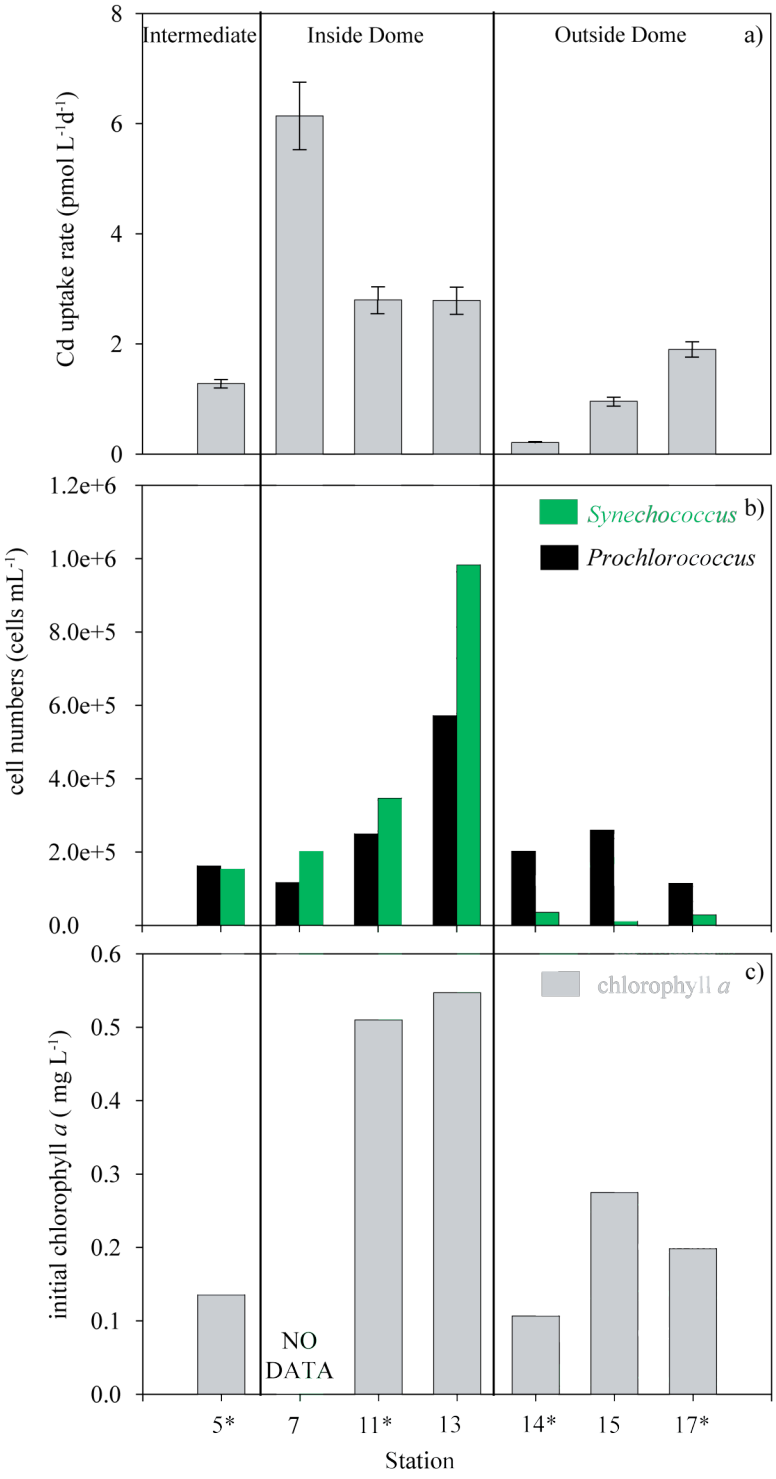

Figure 2.12: Maximum Cd uptake rates, *Synechococcus* and *Prochlorococcus* cell numbers per mL, and chlorophyll *a* concentrations at a depth of 15 m for stations discussed in this paper. a) Maximum Cd uptake rates. Error bars represent counting error of a single ICP-MS measurement. b) Cyanobacteial cell numbers. c) Chlorphyll *a* concentrations. * = Cd additon experiment performed. Notice that Stations 7, 11 and 13 have higher *Synechococcus* counts (inside the dome) relative to Stations 14, 15 and 17 (outside the dome). Station 5 has approximately equal counts (intermediate). *Prochlorococcus* dominates *Synechococcus* at Stations 14, 15, and 17. Note that higher uptake rates tend to occur in stations inside the dome and with higher chlorophyll *a*. Note that data for Station 14 are from a depth of 8 m and uptake rate for Station 7 was measured using surface pump water and not a Go-flo bottle. See Table 2.4.

Table 2.4: Maximum particulate Cd uptake rates, cyanobacterial cell numbers and chlorophyll *a* concentrations

Station	Depth (m)	Cd Uptake Rate (pmol L^{-1} d^{-1})	*Prochlorococcus* (cells mL^{-1})	*Synechococcus* (cells mL^{-1})	chl a (ng L^{-1})
5	8	1.28±0.07	$1.62x10^5$	$1.54x10^5$	0.135
7	15	6.14±0.61	$1.17x10^5$	$2.01x10^5$	nm
11	8	2.8±0.24	$2.50x10^5$	$3.47x10^5$	0.510
13	8	2.79±0.24	$5.72x10^5$	$9.84x10^5$	0.547
14	8	0.21±0.01	$2.02x10^5$	$3.54x10^4$	0.107
15	15	0.96±0.07	$2.60x10^5$	$1.11x10^4$	0.275
17	15	1.9±0.14	$1.15x10^5$	$2.85x10^4$	0.198

nm = not measured. Note that Station 7 uptake rate was measured from a surface pump sample, unlike the other stations, at which the water came from Go-flo bottles. See Figure 2.12.

DISCUSSION

Utility of ^{110}Cd Uptake Method

The results of this study suggest that ^{110}Cd can be successfully used as a stable isotope tracer in marine environments. The ^{110}Cd uptake data suggest that at least a small fraction of ^{110}Cd is bioavailable when a 120 pM spike is added to seawater and incubated for 24 hours, assuming that this method measures actual biological uptake into a cell.

Cadmium Addition Experiments

Cd ligand concentrations measured previously in the North Pacific had a concentration of 0.1 nM (Bruland 1992); the only other Cd ligand data published are from off the coast of New Zealand, with ligand concentrations of 1-2 nM (Ellwood, 2004). Toxicity was thus expected to be observed at 5 nM total Cd in experiments at all stations. Concentrations of total Cd added were chosen in search of a toxicity threshold. Cd addition experiments were run longer (multiple days) than uptake experiments (one day) to allow multiple day/night cycles and chance for growth of the bottled organisms over time.

Of the four stations at which Cd addition experiments were performed, Station 11 stands out in terms of having the highest initial chlorophyll *a* concentration of the four stations by a factor of three. When considering this variability in terms of toxicity

experiments, one may expect Station 11 to show a different result than the other three stations due a higher biomass taking up Cd and reducing the toxic effect. This however, is not the case- Station 11 shows a result different from Stations 14 and 17 (Figure 2.11). Results from Stations 14 and 17 show a reduction in chlorophyll *a* with increasing Cd concentrations, a toxicity effect. Stations 11 and also 5 show relatively constant chlorophyll *a* concentrations with increasing Cd concentrations, or at least no clear toxicity effect. If not chlorophyll *a*, perhaps the fact that Station 5 did not grow in the control relative to initial conditions explains the deviation from expectation, or perhaps the presence of *Synechococcus* prevented toxicity at this station.

Stations 5 and 14 had relatively similar initial conditions, although Station 14 grew and Station 15 did not. There are five noted differences: 1) Station 5 incubated for four days whereas the other stations incubated for three days, 2) Station 5 had about a factor of 1.5 less *Prochlorococcus* than Station 14, 3) Station 5 had a factor of 3.8 times more *Synechococcus* than Station 14, 4) Station 5 had undetectable Cd initially compared to 57 pM Cd^{2+} at Station 14, and 5) Station 5 water was collected from 15 m depth compared to 8 m for Station 14. Considering these possibilities, an incubation difference of 3 or 4 days (1) is probably not going to affect growth or no growth of an experiment. The collection of water from different depths (5) would arguably affect the microbial community composition initially and also the affinity of that community for a particular light environment. Bottles collected at 8 and 15 m were both incubated at the same percentage of ambient light in the on-deck incubator. The differing initial concentrations of total dissolved Cd (4) is probably not the reason because Stations 11 and 17 experiments showed growth and they also had initial concentrations that were below the detection limit. This leaves differences in cyanobacterial cell numbers (2 and 3).

A disparity in *Synechococcus* cell numbers is observed. Although cell numbers are higher at Station 11 than at Station 5 by a factor of 2.8, 3.6×10^6 cells mL^{-1} and 1.3×10^6 cells mL^{-1} respectively, both Stations 5 and 11 have significantly higher cell numbers than either of Stations 14 and 17 (Figure 2.11). Station 5 and Station 11 have *Synechococcus* cell numbers greater than the oligotrophic stations by a factor of four and

eight respectively. These data are consistent with the hypothesis that *Synechococcus* could be producing an organic ligand that binds the added Cd, making it less bioavailable and thus preventing toxicity. *Prochlorococcus* dominates *Synechococcus* at Stations 14, 15 and 17, and Stations 14 and 17 do show a toxic effect suggesting that *Prochlorococcus* may be more sensitive to Cd concentrations and/or may not be contributing an organic ligand to bind Cd. Speciation measurements would help by directly measuring the concentration of organic Cd-ligand complexes. Comparing inside and outside the dome toxicity results do suggest that the prevention of Cd toxicity to the phytoplankton community inside the dome is related to the increased presence of *Synechococcus*. One explanation is the production of organic ligands by *Synechococcus* that result in a greater degree of complexation of Cd relative to outside the dome and another is that more phytoplankton biomass reduces the dosage that each cell would receive. Both of these hypotheses are consistent with the data, although cannot be proven.

The combination of ^{110}Cd uptake experiments, Cd addition experiments, biological parameters, and natural total dissolved Cd measurements leaves us with some unanswered, tantalizing questions for the future: 1) What is the total microbial community at the different stations? 2) Is the Cd all taken up inside the cell? 3) Does a higher abundance of *Synechococcus* cells in the microbial community help prevent toxicity?

Do kinetics affect uptake?

The rate of Cd uptake can be considered in terms of Michaelis-Menten kinetics. Put simply, the total uptake rate is directly proportional to a kinetic rate constant, the bioavailable Cd and the quantity of microorganisms. Inorganic species of trace metals are typically bioavailable, as well as some organic forms. This means speciation is crucial when contemplating bioavailability. In this study, as the biological community and the ^{110}Cd uptake rate decreased, the total dissolved Cd (and thus probably the bioavailable Cd) increased with depth. This suggests that uptake was related to the presence of organisms. The Cd addition experiments had a longer exposure to Cd at higher concentrations than uptake experiments. If cyanobacteria, as hypothesized, were

producing ligands, stations with low cyanobacterial biomass (outside the dome) would likely be unable to produce ligands at a fast enough rate to bind Cd and reduce toxicity and so high Cd treatments at these stations would show toxic effects.

Microbial community composition

The entire microbial community composition is not known. Chlorophyll *a* concentrations (a surrogate for total phytoplankton community) and size-fractionated chlorophyll *a* concentrations (gives an idea of diatoms vs. the smaller picocyanobacteria) were estimated. The picophytoplankton, *Prochlorococcus* and *Synechococcus*, were counted using microscopy and flow cytometry. Other members of the microbial community such as diatoms, bacteria, and Archaea were not enumerated and could potentially be contributors to Cd cycling processes. A study by Franck et al., 2003 found that diatom abundances in the controls of three-day bottle incubation experiments in the Costa Rica Upwelling Dome were an order of magnitude lower than experiments conducted off the coast of central California. The total number of diatoms and flagellates in the controls were around 450 cells per mL (Franck et al., 2003). These low diatom abundances are consistent with the size-fractioned chlorophyll *a* data in this study, which show that the ≤ 2 μm size fraction at Stations 11 and 17 is the greatest component of total chlorophyll *a* (Figures 2.4f, 2.6f; Tables I.2, I.3). Diatoms could be responsible for some of the Cd uptake, but our data do not allow us to determine this.

Cadmium flux - The supply of upwelled cadmium approximately equals uptake rate

The Cd supply at Station 11 from upwelling was estimated using a rate of 10^{-4} cm s^{-1} measured in this region by Wyrtki (1964), multiplied by the concentration difference between the total dissolved Cd measured at 100 m and the surface (Figure 2.13a). The estimated uptake flux of dissolved Cd was estimated by calculating a depth integrated dissolved Cd consumption using measured Cd uptake rates (Figure 2.13b). These two fluxes were each estimated to be on order of 5×10^4 pmol m^{-2} d^{-1}. This implies that the upwelled Cd is taken up into the particulate fraction, depicted as a green circle in Figure 2.14. Fluxes out of the surface box would be advection and export to both the mid- and deep ocean. These processes were not investigated in this study.

a) Estimated upwelling flux

$X_{Cd}=w\ (C_D-C_S)$

$=(10^{-4}\ cm\ s^{-1})\ (551-0)\ (pmol\ L^{-1})$
$(8.64 \times 10^4\ s\ d^{-1})\ (10^4\ cm^2\ m^{-2})$
$(10^{-3}\ L\ mL^{-1})\ (mL\ cm^{-3})$
$= 5 \times 10^4\ pmol\ m^{-2}\ d^{-1}$

Upwelling

X_{Cd} = supply of Cd from upwelling
w = upwelling (Wyrtki, 1964)
C_D = dissolved Cd concentration deep
C_S = dissolved Cd concentration surface

b) Estimated uptake flux

$Z_{Cd}= 0.5\ (U_S+U_D)\ (D_D-D_S)$ depth integrated

$=\ (2800)\ (pmol\ m^{-3}\ d^{-1})\ (8)\ (m)$
$+0.5\ (2800+1300)\ (pmol\ m^{-3}\ d^{-1})\ (15-8)\ (m)$
$+\ 0.5\ (1300+430)\ (pmol\ m^{-3}\ d^{-1})\ (30-15)\ (m)$
$+0.5\ (430+0)\ (pmol\ m^{-3}\ d^{-1})\ (50-30)\ (m)$
$= 5 \times 10^4\ pmol\ m^{-2}\ d^{-1}$

Uptake

Z_{Cd} = consumption of Cd by uptake
U = uptake rate
U_S = uptake rate, shallow
U_D = uptake rate, deep
D_S = depth, shallow
D_D = depth, deep

Figure 2.13. Equations, calculations and variables for estimating a) upwelled and b) taken up cadmium fluxes at Station 11, inside the dome. Assuming upwelling from 100m and depth integrated upwelling calculated from the surface 100m.

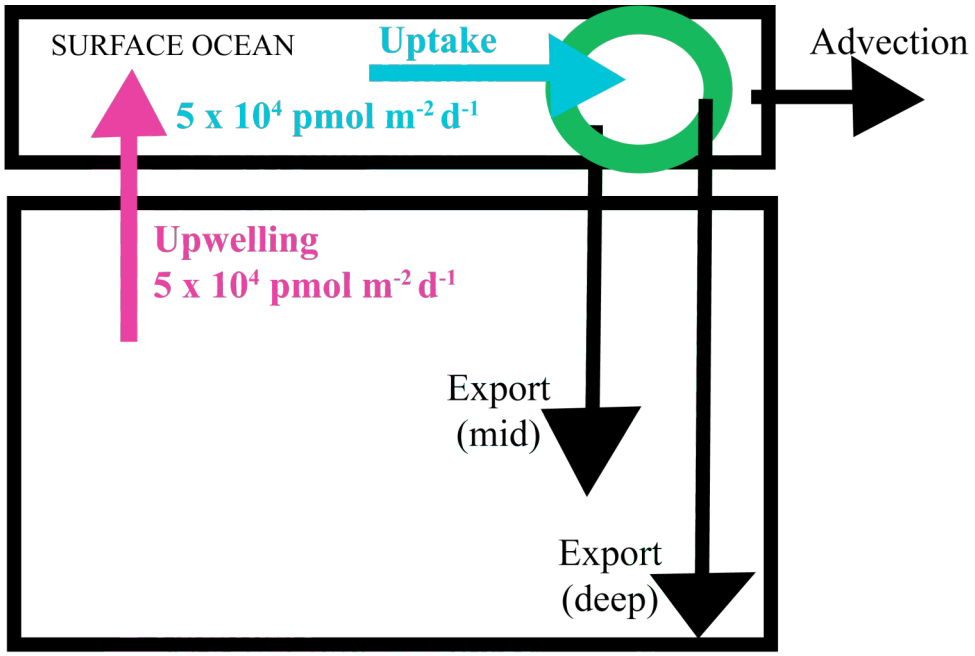

Figure 2.14: Two-box model of Cd biogeochemistry in the Costa Rica upwelling dome. Calculated upwelling flux of Cd is estimated to be approximately equal to that of Cd that is taken up into the particulate fraction. Pink arrow - upwelling flux of Cd. Blue arrow - uptake flux of Cd into particulate fraction. Green circle - particulate fraction in the surface ocean. Black arrows - fluxes out of the surface ocean and particulate fraction not estimated in this study - advection and export both mid and deep.

CONCLUSIONS

In conclusion, results of 24-hour uptake studies suggest that ^{110}Cd as a spike can successfully be used as an intermediate abundance, stable isotope tracer. An increase in particulate ^{110}Cd concentration in spiked samples relative to preexisting Cd and a decrease in $^{114}Cd/^{110}Cd$ and $^{111}Cd/^{110}Cd$ isotope ratios indicated the uptake of ^{110}Cd in waters shallower than 40 m. The uptake rate of Cd correlated positively with chlorophyll *a* concentrations. Results of time course ^{110}Cd uptake studies indicate uptake with time in spiked samples because the ^{110}Cd concentrations increase and the $^{114}Cd/^{110}Cd$ and $^{111}Cd/^{110}Cd$ isotope ratios decrease with time. Linear regression analyses of concentration versus time in these studies also suggest that a 24-hour time point is an adequate measurement of uptake and demonstrate that considering preexisting particulate Cd in the form of a particulate blank in high biomass regions is necessary. Depth integrated uptake estimates of total Cd consumption compared to estimated upwelling flux of Cd suggest that the dissolved upwelled Cd in the dome is taken up into the particulate fraction. Cd addition experiments suggest that higher cell numbers of *Synechococcus* are related to prevention of Cd toxicity in the dome, but outside the dome with lower cell numbers of *Synechococcus*, in the cyanobacterial community dominated by *Prochlorococcus*, toxic effects are observed. This suggests that the greater biomass and microbial community prevent toxicity of added Cd, perhaps by diluting the Cd throughout the community in the dome. Outside the dome, *Prochlorococcus* is the numerically dominant member of the cyanobacterial community and may be more sensitive to Cd and the Cd is diluted less over the overall community. Electrochemical measurements of total dissolved Cd demonstrate a nutrient-like profile and correlation with nutrients, as expected. Together, these experiments suggest that uptake of Cd into the microbial loop occurs in the upper water column both in and out of the Costa Rica Dome, but show that Cd toxicity is not induced within the dome presumably due to a greater amount of biomass in that region and less sensitivity of that biomass to Cd.

Acknowledgements

I would like to thank the captain, crew, and science party of the R/V Knorr 185-2. Thank you to Abigail Noble for total dissolved Cd measurements, Anne Thompson for *Synechococcus* and *Prochlorococcus* cell numbers, Lisa Moore and lab for size fractionated chlorophyll measurements, Eric Webb for shipboard cell numbers, Nathan Ahlgren for figure of stations, Matthew Hurst and Seth John for discussion and Dave Schneider for assistance on the ICP-MS. Thanks to members of the Saito and Moffett labs - Jim Moffett, Andrew Rose, Chad Hammerschmidt, Rachel Wisniewski (now Jakuba), Tyler Goepfert, Dreux Chappell, Michelle Bringer and Erin Bertrand. Thank you to Ed Boyle, Carl Lamborg and Ben Van Mooy for helpful review. This work was funded by NSF Chemical Oceanography (OCE-0327225 and OCE-0452883) and supported by a MIT/WHOI Joint Program Summer Research Fellowship and MIT Presidential Scholar Fellowship.

References

Boyle, E.A., Sclater, F. and Edmond, J.M. 1976. On the marine geochemistry of cadmium. *Nature* 263: 42-44.

Boyle, E.A. 1988. Cadmium: chemical tracer of deepwater paleoceanography. *Paleoceanography* 3: 471-489.

Broenkow, W. W. 1965. The distribution of nutrients in the Costa Rica Dome in the Eastern Tropical Pacific Ocean. *Limnology and Oceanography* 10(1): 40-52.

Bruland, K.W., Franks, R.P., Knauer, G.A., and Martin, J.H. 1979. Sampling and analytical methods for the determination of copper, cadmium, zinc, and nickel at the nanogram per liter level in sea water. *Analytica Chimica Acta* 105: 233-245.

Bruland, K. W. 1980. Oceanographic distributions of cadmium, zinc, nickel, and copper in the North Pacific. *Earth and Planetary Science Letters* 47: 176-198.

Bruland, K.W. 1992. Complexation of cadmium by natural organic ligands in the central North Pacific. *Limnology and Oceanography* 37(5): 1008-1017.

Calabrese, E.J. 2005. Toxicological awakenings: the rebirth of hormesis as a central pillar of toxicology. *Toxicology and Applied Pharmacology* 204: 1- 8.

Croteau, M.N., Luoma, S.N. and Pellet, B. 2007. Determining metal assimilation efficiency in aquatic invertebrates using enriched stable metal isotope tracers. *Aquatic Toxicology* 83: 116-125.

Cullen, J. T., Lane, T. W., Morel, F. M. M. and Sherrell, R. M. 1999. Modulation of cadmium utilization in phytoplankton by seawater concentration. *Nature* 402: 165-167.

Cullen, J.T. and Sherrell, R.M. 1999. Techniques for determination of trace metals in small samples of size-fractioned particulate matter: phytoplankton metals off central California. *Marine Chemistry* 67: 233-247.

Elderfield, H. and Rickaby, R.E.M. 2000. Oceanic Cd/P ratio and nutrient utilization in the glacial Southern Ocean. *Nature* 405: 305-310.

Ellwood, M.J. and Hunter, K.A. 1999. The determination of the Zn/Si ratio in diatom opal: a method for the separation, cleaning and dissolution of diatoms. *Marine Chemistry* 66: 149-160.

Ellwood, M.J. and Hunter, K.A. 2000. The incorporation of zinc and iron into the frustule of the marine diatom *Thalassoiosira pseudonana*. *Limnology and Oceanography* 45(7): 1517-1524.

Ellwood, M.J. 2004. Zinc and cadmium speciation in subantarctic waters east of New Zealand. *Marine Chemistry* 87: 37-58.

Echeveste, P., Agusti, S. and Dachs, J. 2010. Cell size dependent toxicity thresholds of polycyclic aromatic hydrocarbons to natural and cultured phytoplankton populations. *Environmental Pollution* 158(1): 299-307.

Fiedler, P.C. 2002. The annual cycle and biological effects of the Costa Rica Dome. *Deep-Sea Research I* 49: 321-338.

Fischer, E. and van den Berg, C.M.G. 1999. Anodic stripping voltammetry of lead and cadmium using a mercury film electrode and thiocyanate. *Analytica Chimica Acta* 385: 273-280.

Franck, V.M., Bruland, K.W., Hutchins, D. A. and Brzezinski, M.A. 2003. Iron and zinc effects on silicic acid and nitrate uptake kinetics in three high-nutrient, low-chlorophyll (HNLC) regions. *Marine Ecolgy Progress Series* 252: 15–33.

Gee, A.K. and Bruland, K.W. 2002. Tracing Ni, Cu, and Zn kinetics and equilibrium partitioning between dissolved and particulate phases in South San Francisco Bay, California, using stable isotopes and high-resolution inductively coupled plasma mass spectrometry, *Geochimica et Cosmochimica Acta* 66: 3063-3083.

Hofmann, E.E., Busalacchi, A.J. and O'Brien, J.J. 1981. Wind Generation of the Costa Rica Dome. *Science* 214: 552-554.

Hunter, K.A., Kim, J.P. and Croot, P.L.1997. Biological roles of trace metals in natural waters. *Environmental Monitoring and Assessment* 44: 103-147.

Hurst, M.P. and Bruland, K.W. 2007. An investigation into the exchange of iron and zinc between soluble, colloidal, and particulate size-fractions in shelf waters using low-abundance isotopes as tracers in shipboard incubation experiments. *Marine Chemistry* 103: 211-226.

Hurst, M.P. and Bruland, K.W. 2008. The effects of the San Francisco Bay plume on trace metal nutrient and nutrient distributions in the Gulf of the Farallones. *Geochimica et Cosmochimica Acta* 72: 395-411.

Hutchins, D.A., Wang, W.X., Schmidt, M.A. and Fisher, N.S 1999. Dual-labeling techniques for trace metal biogeochemical investigations in aquatic plankton communities. *Aquatic Microbial Ecology* 19: 129-138.

Hutchins, D.A., Witter, A. E., Butler, A. and Luther, G.W. 1999. Competition among marine phytoplankton for different chelated iron species. *Nature* 400: 858–861.

JGOFS (Joint Global Ocean Flux Study) Protocols (1994) Protocols for the Joint Global Ocean Flux Study (JGOFS). Core Meas, Manual Guides 29: 119-122.

Li, W.K.W., Subba Rao, D.V., Harrison, W.G., Smith, J.C., Cullen, J.J., Irwin, B. and Platt, T. 1983. Autotrophic picoplankton in the tropical ocean. *Science* 219: 292-295.

Maldonado, M. T. and Price, N. M. 1999. Utilization of iron bound to strong organic ligands by plankton communities in the subarctic Pacific Ocean. *Deep Sea Research Part II* 46: 2447–2473.

Mann, E. L., Ahlgren, N., Moffett, J.W. and Chisholm, S. W. 2002. Copper toxicity and cyanobacteria ecology in the Sargasso Sea. *Limnology and Oceanography* 47: 976-988.

Morel, F.M.M., Milligan, A.J. and Saito, M.A. 2003. Marine bioinorganic chemistry: The role of trace metals in the oceanic cycles of major nutrients. Treatise on Geochemistry Volume 6 The Oceans and Marine Geochemistry. eds. Henry Elderfield. H.D. Holland and K.K. Turekian. 6.05: 113-143.

Morel, F.M.M., Reinfelder, J.R., Roberts, S.B., Chamberlain, C.P., Lee, J.G. and Yee, D. 1994. Zinc and carbon co-limitation of marine phytoplankton. *Nature* 369: 740-742.

Pickhardt, P.C., Folt, C.L., Chen, C.Y., Klaue, B. and Blum, J.D. 2002. Algal blooms reduce the uptake of toxic methylmercury in freshwater food webs. *Proceedings of the National Academy of Sciences of the United States of America*: 99: 4419-4423.

Quigg, A., Reinfelder, J. R. and Fisher, N.S. 2006. Copper uptake kinetics in diverse marine phytoplankton. *Limnology and Oceanography* 51: 893–899.

Ripperger, S. and Rehkämper, M. 2007. Precise determination of cadmium isotope fractionation in seawater by double spike MC-ICPMS. *Geochimica et Cosmochimica Acta* 71: 631-642.

Saito, M.A., Rocap, G. and Moffett, J.W. 2005. Production of cobalt binding ligands in a *Synechococcus* feature at the Costa Rica upwelling dome. *Limnology and Oceanography* 50(1): 279-290.

Semeniuk, D.M., Cullen, J.T., Johnson, W.K., Gagnon, K., Ruth, T.J. and Maldonado, M.T. 2009. Plankton copper requirements and uptake in the subarctic Northeast Pacific Ocean. *Deep Sea Res. I* 56: 1130-1142.

Sunda, W.G. 1988. Trace metal interactions with marine phytoplankton. *Biology and Oceanography* 6: 411-442.

Sunda, W.G. and Huntsman, S.A. 1995. Iron uptake and growth limitation in oceanic and coastal phytoplankton. *Marine Chemistry* 50: 189-206.

Sunda, W.G. and Huntsman, S.A. 2000. Effect of Zn, Mn, and Fe on Cd accumulation in phytoplankton: Implications for oceanic Cd cycling. *Limnology and Oceanography* 45(7): 1501-1516.

Thompson, A.W. 2009. Iron and *Prochlorococcus*. Ph. D. Thesis. Joint Program in Biological Oceanography, Massachusetts Institute of Technology, Dept. of Biology and the Woods Hole Oceanographic Institution.

Wyrtki, K. 1964. Upwelling in the Costa Rica Dome. *U.S. Fish Wildlife Service Fishery Bulletin* 63: 355-372.

Chapter 3

Zinc-deprived coastal *Synechococcus* WH5701 show physiological and strong proteomic response to chronic cadmium stress

Abstract

Synechococcus sp. WH 5701 is a euryhaline, phycocyanin-rich, phycoerythrin lacking marine cyanobacterium. It was isolated originally from Long Island Sound, a coastal environment with high trace metal availability and variable irradiance due to mixing. To test the response of this organism to free cadmium (Cd), generally considered a toxin with one known nutritive use in a marine diatom, cultures were exposed to 4.4 and 44 pM free Cd^{2+}. Physiological measurements of cell counts, chlorophyll *a* and phycoerythrin fluorescence throughout growth, stationary and death phases show Cd had little effect on growth rates, but higher Cd concentrations caused an increase in mortality rates and maximum chlorophyll *a* fluorescence. Global proteomic analysis of relative protein abundance at five time points throughout the entire growth curve revealed a greater abundance of ribosomal and photosystem I proteins during exponential growth relative to stationary phase. Cd caused a two-fold or more increase in relative abundance of ribosomal proteins, arylsulfatases, cysteine metabolism and chlorophyll *a* biosynthesis proteins, among others, and a two-fold or more decrease in the relative abundance of core photosystem I, carboxysome-associated and hypothetical proteins during exponential growth, suggesting chronic Cd exposure had a great metabolic impact.

INTRODUCTION

Marine cyanobacteria play an important role in primary productivity and the evolution of the environment on earth as discussed on pages 13-14 of Chapter 1. Cadmium (Cd) and zinc (Zn) are trace elements with nutrient distributions in the ocean (discussed on pages 15-16 of Chapter 1) and have shown to have interactions in culture (discussed on pages 18-20 of Chapter 1).

Synechococcus WH5701 is a marine subcluster 5.2, MC-B (Scanlan, 2003) cyanobacteria, originally isolated from Long Island Sound. It is euryhaline, phycocyanin-rich, and lacks phycoerythrin II. Not much culture work exists in the literature concerning WH5701 thus far and although the MC-A group is thought to be the dominant *Synechococcus* group within the euphotic zone of open ocean and coastal waters (Fuller et al., 2003 and references therein), recent studies on the diversity of *Synechococcus* strains isolated from the Baltic Sea show picocyanobacteria, very similar to WH5701 by 16S rRNA-ITS (Haverkamp et al., 2009). WH5701 is a good coastal environmental model because of the original isolation location and it may have arguably already been affected by increased anthropogenic inputs before isolation.

Cells are known to take up Cd even though it is not required for growth. If cells do not require Cd, the destination of Cd inside a cell is of interest. Metals are tightly regulated in cells and metal sensing is important (Waldron et al., 2009). Cd can interfere with the metals calcium, zinc, and iron (Martelli et al., 2006). In diatoms, Cd can be taken up through manganese and zinc transporters (Sunda and Huntsman, 2000). Experimental support in animal cells for Cd substituting for native metals is scarce at best, despite this being often proposed as the leading mechanism of Cd toxicity (Martelli et al, 2006). Mechanisms of toxicity in photosynthetic organisms range from Cd replacing magnesium in chlorophyll in plants (Küpper et al., 1998) to Cd^{2+} binding reaction centers in *Rhodobacter sphaeroides* thereby reducing rates of electron transfer from photosystem II to Q_B (Okamura et al., 2000 and reference therein).

Metallothioneins and low molecular weight thiols are a possibility for intracellular Zn storage and Cd detoxification are discussed on pages 20-24 of Chapter 1. Low

molecular weight thiols have been produced by cultures of *Emiliania huxleyi* upon exposure to cadmium, zinc, and copper (Dupont and Ahner, 2005) and measured in the Galveston Bay (Tang et al., 2000) and the subarctic Pacific Ocean (Dupont and Moffett et al., 2006). The possibility of low molecular weight thiols as a response to Cd is considered in this chapter

In this chapter, the physiological and proteomic responses of the coastal *Synechococcus* WH5701 to chronic Cd stress under Zn deficient conditions will be presented, a condition not often encountered in the environment due to the greater relative abundance of Zn. The biological function of an element can only be assessed properly against a background of deficiency state (Vallee and Ulmer, 1972). It is notoriously difficult to limit cyanobacteria for Zn. If Cd is interfering with Zn metabolism, these experimental conditions would be likely to reveal that situation. Our physiological and proteomic data show that this coastal cyanobacterium does not appear much affected by the addition of Cd^{2+} during growth phase due to the similar growth rates of the Cd treatments to the no added Cd, but the change in relative abundance of proteins show that the exposure to Cd has a major impact on photosynthesis, protein synthesis, carbon fixation, and sulfur metabolism. The physiological effects of Cd surface during stationary phase with an increase in maximum chlorophyll *a* fluorescence with the Cd treatments relative to the control and faster mortality rates. This paper also provides a comprehensive view of the change in relative protein abundance throughout the growth curve of *Synechococcus* WH5701.

METHODS

Culturing and protein extraction

Axenic cultures of *Synechococcus* sp. WH 5701 obtained from J. Waterbury (Woods Hole Oceanographic Institution) were maintained in a PRO-TM media (modified from Saito et al., 2002) made with 75% oligotrophic seawater obtained from the oligotrophic South Atlantic ocean and prepared by microwave sterilization and the addition of chelexed and filtered nutrients (1.1 mM NO_3^- and 65 µM PO_4^{3-}) and EDTA-

complexed metals (22.2 μM EDTA, 171 nM $MnCl_2$, 5.7 nM Na_2MoO_4, 19 nM Na_2SeO_3, 2.22 μM $FeCl_3$, 19 nM $CoCl_2$, 19 nM $NiCl_2$). Chronic Cd treatments had Cd added to a total concentration of 10 and 100 nM $CdCl_2$, with the free concentrations estimated to be 4.4 pM Cd^{2+} and 44 pM Cd^{2+}, respectively, using thermodynamic data from EDTA stability constant data from Martell and Smith, 1993. The ratio of Cd^{2+}: Cd_{TOT} was calculated to be 1:2267. This ratio in a PRO-TM media with 11.7 μM EDTA (Saito et al., 2002) was calculated to be 1:1216 (Saito et al., unpublished data) and 1:6026 in a media with 100 μM EDTA (Sunda and Huntsman, 1998). The ratio of Cd^{2+} to the total of major inorganic species in a PRO-TM media with 11.7 μM EDTA (Saito et al., 2002) was calculated to be 1:36 (Saito et al., unpublished data). The blank of the medium was not determined. Previous researchers doing similar trace metal culture studies have assumed background metal concentrations of 100 pM for cobalt (Sunda and Huntsman, 1995; Sunda and Huntsman, 1998; Saito et al., 2002), 900 pM for Zn (Sunda and Huntsman, 1995; Sunda and Huntsman, 1998) and 100 pM for cadmium (Sunda and Huntsman, 1998). Cultures were grown in either 28 mL polycarbonate tubes or 1 L polycarbonate bottles under 30 μmol photons (μEinstein) $m^{-2}s^{-1}$ continuous white light. All plasticware was soaked for two days in a detergent, then two weeks in 10% HCl (Fisher, trace metal grade), rinsed with pH 2 HCl and then microwave sterilized. Culture growth was monitored by a combination of chlorophyll *a* and phycoerythrin fluorescence and cell counting by microscopy. Growth rates were calculated from the natural log of *in vivo* relative chlorophyll *a* fluorescence (n = 5). Mortality rates were calculated from the natural log of *in vivo* relative chlorophyll *a* fluorescence ($n \geq 4$). For protein samples, approximately 150 mL of culture were harvested by centrifugation in a Beckman J2-21M centrifuge at 18,566 g for 30 min at 4°C, decanted, transferred into a microtube and centrifuged again at 14,000 g for 15 min at room temperature, decanted, and frozen at -80°C.

Protein was extracted from the digestion of frozen whole cell pellets. Sample tubes were kept on ice throughout the extraction process, unless otherwise noted. Cell pellets were resuspended in 500 μL of 100 μM ammonium bicarbonate buffer solution,

pH 8.0, (AMBIC) ice cold. Using a Branson sonifier 450, samples were sonicated on ice for 4 min at 70% duty with an output of 3. After a 5 min pause, samples were sonicated for another 4 min. Samples were centrifuged at 4°C at 14,000 g for 35 min. 200 µL of supernatant was precipitated overnight with 800 µL of -20°C acetone.

Acetone-precipitated samples were centrifuged at 4°C at 14,000 g for 30 min and decanted. One hundred µL of freshly made 7.5 M urea in AMBIC and 25 µL of AMBIC were added to the acetone-precipitated pellet. Samples were incubated for approximately 15 min at room temperature with periodic vortexing then resuspended by incubation for 5 min at 95°C. A 100 µL aliquot was removed and 5 µL of 200 mM dithiothreitol (DTT) in AMBIC was added and incubated for 1 hr at 56°C, shaken at 400 rpm. The sample was vortexed and centrifuged at 14,000 g for 2 min. Twenty µL of 200 mM iodacetamide in AMBIC was added and incubated for 1 hr at room temperature in the dark, shaken at 400 rpm. 20 µL of 200 mM DTT in AMBIC was added, mixed, centrifuged for 2 min as above, and incubated for 1 hr at room temperature, shaken at 400 rpm. After incubation, the sample was centrifuged for 2 min as above. Total protein yield was assayed using the Biorad DC Protein Assay. Trypsin (Promega) was reconstituted in 500 µL of 50 mM acetic acid and added in a trypsin to protein ratio of 1:50. The sample was mixed, vortexed, centrifuged for 2 min as above, and incubated for approximately 16 hours at 37°C, shaken at 400 rpm.

After trypsin digestion, the sample was vortexed, centrifuged for 2 min, and 20 µL of LC-MS grade glacial acetic acid added. Sample was evaporated by speed vacuum for approximately 3 h to a final volume of approximately 600 µL. Sample was centrifuged at 14,000 g for 30 minutes and the supernatants collected. Four µg of protein was added per injection.

Liquid Chromatography-Mass Spectrometry (LC-MS)

The digests were analyzed by LC-MS using a Paradigm MS4 HPLC system with reverse phase chromatography, Thermo LTQ ion trap mass spectrometer and Microhm ADVANCE source (2 µL/min flow rate, 345 min runs, 150 mm column, 40 µL injections, water ACN gradient). Each digest was injected three times for a total of 45

mass spectrometry runs. Mass spectra were processed by SEQUEST and PeptideProphet with a fragment tolerance of 1.0 Da (monoisotopic), parent tolerance of 2.0 Da (monoisotopic), fixed modification of +57 on C (carbamidomethyl), variable modification of +16 on M (oxidation) and a maximum of 2 missed trypsin cleavages using a database including reversed proteins and common contaminants. Spectral counts of 45 files were compiled in Scaffold 3 with a peptide false discovery rate of 1.7%, minimum peptide and protein confidence levels of 95 and 99%, respectively with a minimum of 2 peptides. (Peng et al., 2003; Zhang et al., 2006). A spectral count is the number of times a particular peptide from a protein is sampled during an MS/MS experiment and is indicative of protein relative abundance. Graphs are made with spectral counts of proteins that have a minimum of four identified peptides and the function assigned by using the Kyoto Encyclopedia of Genes and Genomes (KEGG). Tables are made by ratios of average spectral counts with at least one value greater than or equal to 5 spectral counts.

RESULTS AND DISCUSSION

This section begins with physiological and then moves to proteomic data. The physiological data from three experiments is presented and discussed (28 mL reconnaissance experiment, 1 L experiment with protein data, and 28 mL repeat and addition of Zn experiment). Any low molecular weight thiol data discussed were from a fourth experiment in 500 mL cultures performed concurrently with the 28 mL repeat and Zn addition experiment. The complex proteomic dataset is presented in terms of cluster analysis, then pairwise-comparison of Cd treatments to the control at each timepoint throughout the experiment and ties the protein data back to the physiological observations by discussion of functional groups of proteins affected by Cd.

Physiological Data

The growth of WH5701 under chronic Cd concentrations ranging from no added Cd^{2+} to 44 pM free Cd^{2+} in duplicate 28 mL tubes as monitored by the relative fluorescence of chlorophyll *a* in vivo measured over approximately 30 days yielded three salient observations (Figure 3.1). First, despite differing Cd concentrations, growth rates of all treatments were similar throughout five days of exponential growth (Figures 3.1, 3.2a). Growth rates (n = 5) were calculated from the average of duplicate tubes. Second, the addition of Cd resulted in an increase in the maximal chlorophyll *a* fluorescence that was the most pronounced in the highest Cd addition, 44 pM Cd^{2+} (Figures 3.1, 3.2b). And third, the addition of Cd increased the mortality rates of the 4.4 (n = 14) and 44 pM Cd^{2+} (n = 9) relative to the control (n = 16) by a factor of 1.8 and four, respectively (Figures 3.1, 3.2c). Mortality rates once the cultures began to die were 1.3 and 2.5 times greater than the control (n = 8) for 4.4 (n = 11) and 44 pM Cd^{2+} (n = 9) treatments, respectively (Figure 3.2d). In a repeat experiment in 28 mL tubes, extended to include the presence of tens of picomolar Zn^{2+} in the media, growth rates were again similar, however the addition of Cd did not result in an increase in chlorophyll *a* fluorescence or increased mortality rates (Figure 3.3).

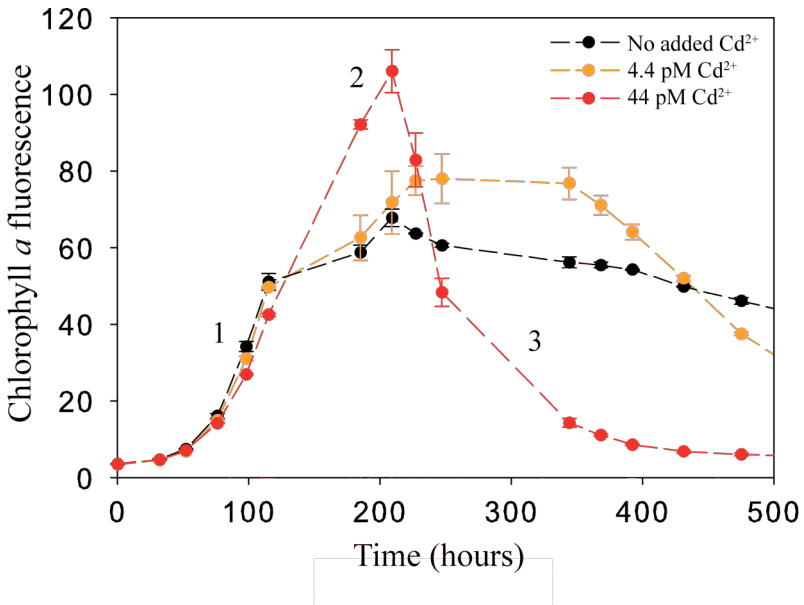

Figure 3.1: Growth of WH5701 under chronic Cd^{2+} stress as measured by relative chlorophyll *a* fluorescence, points are averages of duplicates. This was a reconaissance experiment in 28 mL tubes. Error bars represent range of duplicate measurements. Note 1) similar growth rate through exponential phase 2) increased maximum chlorophyll *a* fluorescence with added Cd^{2+} and 3) increased mortality rates with added Cd^{2+}. These are physiological effects.

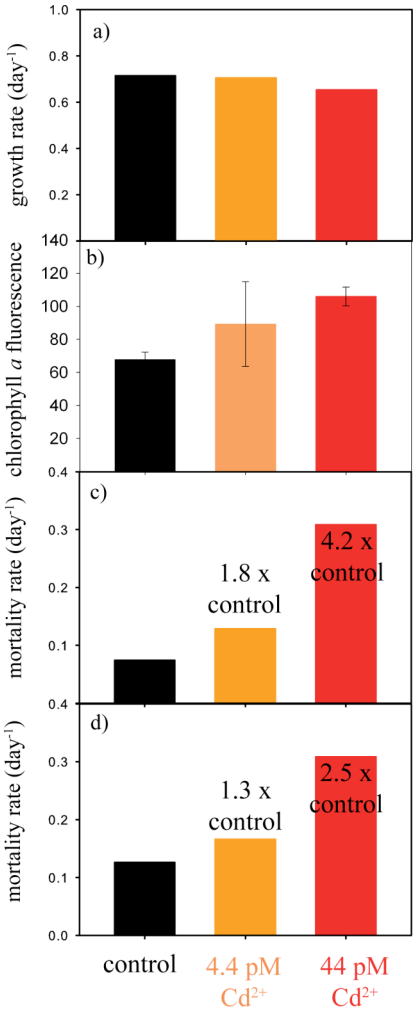

Figure 3.2: a) Growth rates, b) maximum chlorophyll *a* fluorescence, c) mortality rates and d) mortality rates once dying calculated from Figure 3.1. Error bars represent range of duplicate measurements.

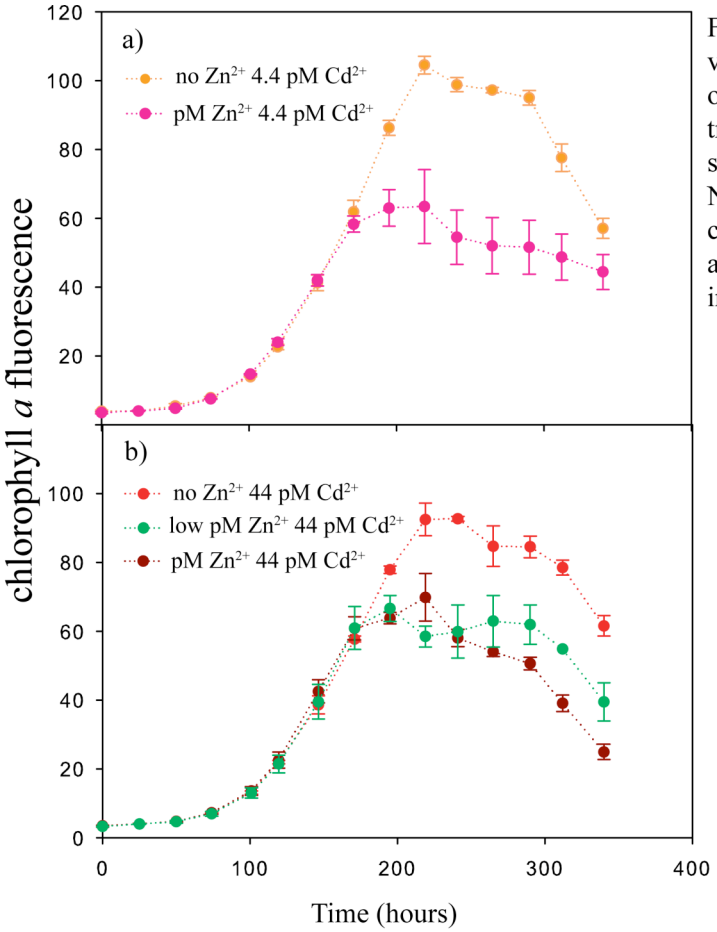

Figure 3.3: Chlorophyll *a* fluorescence vs. time, 28 mL tubes. Error bars are one standard deviation of biological triplicates. This is a repeat and extension of the reconaissance experiment. Note lack of Cd^{2+}-caused increased chlrophyll *a* maxium fluorescence around 200 h with the presence of Zn^{2+} in the media.

Similar physiological results were obtained upon repetition of the reconnaissance experiment with singlicate 1 L cultures, with cell numbers monitored and samples collected for global proteomic analysis at five time points throughout the growth curve (Figure 3.4). Again, growth rates among the three treatments were similar when calculated using chlorophyll *a* and phycoerythrin (data not shown). According to cell number, the cells entered stationary phase around 120 hours. Cell numbers revealed similar growth rates and showed that the loss of chlorophyll *a* fluorescence during death phase was due to a decrease in cell numbers (compare Figure 3.4a, b and c). The chlorophyll *a*/phycoerythrin fluorescence ratio increases steadily through growth and early stationary phase across all treatments. The Cd treatments continue to increase through stationary phase, however, while the control does not. Instead, the Cd treatments diverge from each other and the control (Figure 3.4d).

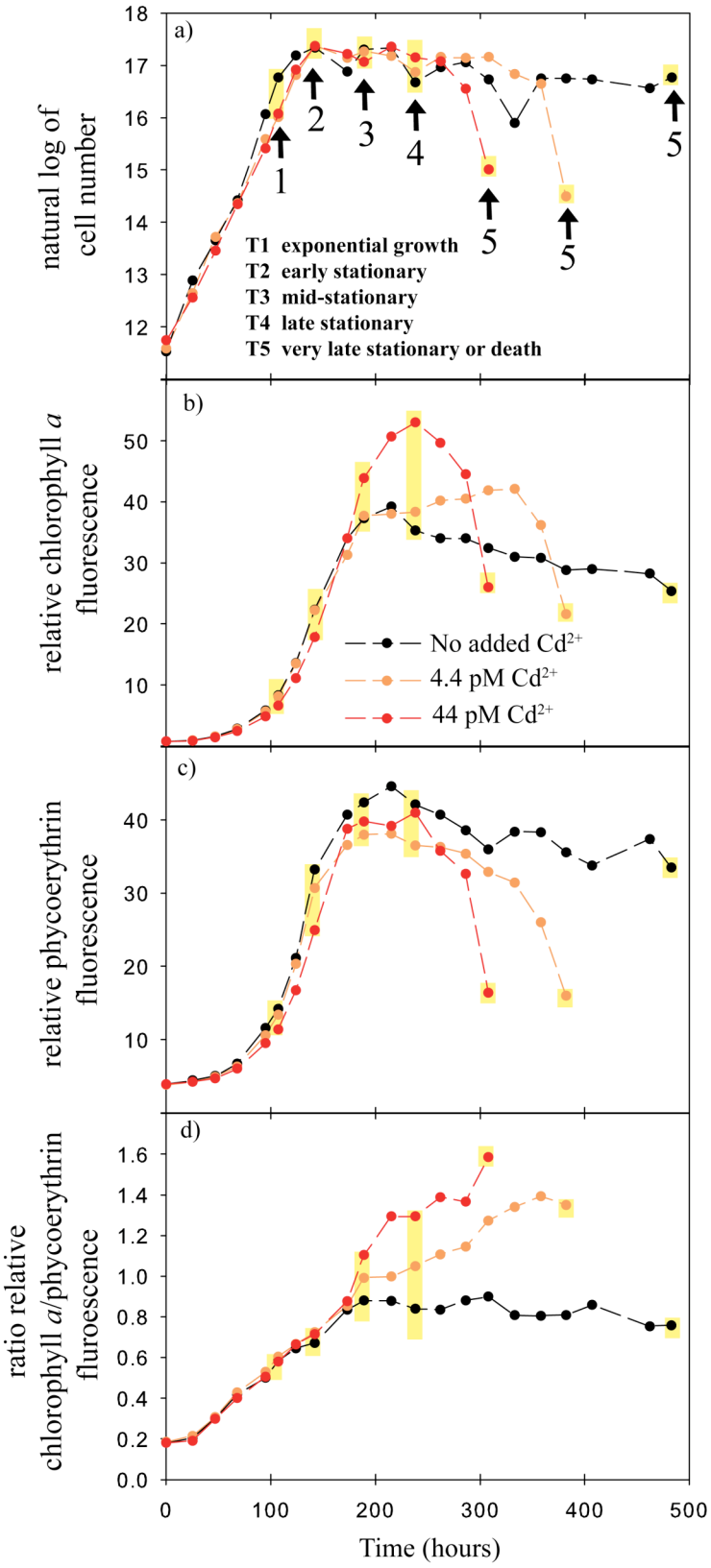

Figure 3.4: Physiological factors with time in a 1 L chronic Cd^{2+} experiment with WH5701. a) Natural log of cell number, b) relative chlorophyll *a* fluorescence, c) relative phycoerythrin fluorescence, and d) ratio of relative chlorophyll *a* to phycoerythrin fluorescence. Samples were taken for global proteomic analysis at five timepoints throughout the life of the culture, highlighted in yellow. Growth effects observed in Figures 3.1 and 3.2 were reproduced in this experiment. Each treatment was one bottle. Cells entered stationary phase at about 120 h. The ratio of chlorophyll *a* to phyocerythrin increases throughout stationary phase with the higher cadmium treatments.

Since Cd is generally considered a toxic metal, with only one known nutritive use in a marine diatom carbonic anhydrase, one might expect the diminishment of growth rates upon chronic exposure to Cd. In these experiments with *Synechococcus* WH5701, this was not the case. With the physiological monitors of relative chlorophyll *a* and phycoerythrin fluorescence and cell number, no difference among the treatments could be detected during exponential growth. Physiological toxicity in the form of cellular death arresting stationary phase in Cd treatments in this experiment implies cellular uptake of Cd and makes one wonder about the cellular destination of Cd upon entry to the cell and mechanism of toxicity. Differences can be observed in the global proteomic data from exponential growth that could begin to answer this question. Various hypotheses exist for mechanisms of Cd toxicity or detoxification including the replacement of native metals with Cd, induction of metallothioneins, induction of phytochelatins, and/or binding by smaller ligands such as glutathione. Experimental evidence for the replacement of native metals with Cd is scarce in animal cells (Martelli et al., 2006) and could only be hinted at with the global proteomic data obtained in this study. To show the replacement of native metals, detailed biochemical work would be required beyond the scope of this study. The induction of metallothioneins by Cd exposure has been observed at many levels of life from cyanobacteria to mammals (Margoshes and Vallee, 1957; Palmiter, 1998; Duncan et al., 2006) and also recently from the marine cyanobacterium WH8102 (Cox and Saito, unpublished data). Lowering peptide tolerances in the analysis of WH5701 yields the presence of this small protein, although not enough to quantify relative abundances. In this case, lack of presence does not imply absence.

Physiologically (cell number, chlorophyll *a* fluorescence and phycoerythrin fluorescence), there is no observable effect of chronic Cd stress during exponential growth. Chronic Cd stress does affect the cells, however, giving the Cd cultures a much faster mortality rate, 1.8 x and 4 x that of the control for 4.4 pM Cd^{2+} and 44 pM Cd^{2+} treatments, respectively. Other researchers have found that Cd interferes with photosynthesis in an unicellular algae, *Chlamydomonas reinhardtii* (Gillet et al., 2006).

Our data show that Cd is interfering with photosynthesis even though there are no observed physiological effects during growth. There is also the question of bioavailability. The cultures are buffered with EDTA, theoretically providing constant picomolar free concentrations of Cd^{2+}. As the cells grow and produce ligands that bind the metals, they could become more (or less) bioavailable. A recent study has suggested that the uptake of copper by field populations of phytoplankton in the subarctic Northeast Pacific Ocean from organic copper complexes is important (Semeniuk et al., 2009). Uptake rates of copper bound to oxidized glutathione in the 0.2 -2 μM fraction were similar to those of natural ligands (Semeniuk et al., 2009). It is interesting to note that measurements of dissolved and particulate thiols in a repeat experiment show a large pool of intracellular oxidized glutathione in the 44 pM Cd^{2+} treatment that is not present in the no added Cd treatment and also less cysteine in the media of the 44 pM Cd^{2+} treatment than the no added Cd treatment. These data are consistent with the concept of organically bound Cd uptake, but also consistent with the idea of uptake of inorganic Cd with consequent intracellular binding. We cannot at present distinguish between these two processes. Increasing bioavailability of Cd throughout the progression of the experiment would not fully explain the lack of physiological effects observed during growth phase. There could be differences in metal sensing among the treatments (Waldron et al., 2009), which would be difficult to specifically detect in these data.

Global Proteomic Data - Cluster analysis

Analysis resulted in the identification of 747 proteins from 153,721 mass spectra over 45 injections (3 treatments at 5 time points injected in triplicate) with a 1.7% peptide false discovery rate using 95% peptide minimum confidence level, 99.9% protein minimum confidence level and a minimum of 2 peptides. This experiment identified 22.3% of the 3346 possible proteins present in the genome of WH5701. Graphs are constructed from an analysis resulting in the identification of 432 proteins from 141,210 mass spectra with a 0.3% peptide false discovery rate using 95% peptide minimum confidence level, 99.9% protein minimum confidence level and a minimum of 4 peptides. Using these more stringent conditions, 12.9% of the 3346 possible proteins present in the

genome of WH5701 were identified.

Considering all treatments across time, 152 proteins were above a threshold count average signal of greater than or equal to 5 spectral counts and a minimum difference of 10 counts. Cluster analysis of these 152 proteins (Eisen et al., 1998) reveals changes in protein abundance that appear related to growth phase, but also Cd^{2+} effects (Figure 3.5). The proteins cluster into six groups, labeled by the growth phase (exponential-death) in which proteins are present and most abundant (Figure 3.5). The order of the treatments on the x-axis in Figure 3.5 is T1-T5 from left to right with the treatments in each time point ordered from no Cd to 44 pM Cd^{2+}. Group 1 consists of 21 proteins that are most present in exponential growth and early stationary phase (T1 and T2) and not present by mid-stationary phase, 11 of which are ribosomal proteins (Figure 3.5). Twenty-three Group 2 proteins are present in exponential growth, early and mid-stationary phases (T1, T2, T3) and not present in late stationary or death phases, many of which are involved in metabolism (Figure 3.5). Forty-two proteins that are present in mid-and late stationary phase (T3, T4) but not in very late stationary/death phase are considered Group 3 (Figure 3.5). Many are involved in metabolism and regulation, and a few proteases. A small group of 11 proteins comprises Group 4; they are most abundant in early or mid-stationary to late stationary (Figure 3.5). Four of them are hypothetical proteins, and another is involved in nitrogen metabolism regulation. Group 5 consists of 25 proteins present in mid-stationary to very late stationary/death phase and 14 of them are hypothetical (Figure 3.5). Others are involved in protein folding, iron transport, cell wall degradation, oxidative stress and two in photosystem II. Group 6 can best be described as less abundant in high Cd treatment during exponential growth but present during both Cd treatments during death phase and consists of 29 proteins. Many of these proteins are involved in photosynthesis, carbon fixation, ATP synthesis and the ABC transport of nitrogen and phosphorus.

Allowing the treatments (x-axis) to cluster in addition to the proteins (y-axis) groups the treatments into five clusters (a-e) from left to right (data not shown): a) T1 control and T1 4.4 pM Cd^{2+}; b) T2 control, T1 44 pM Cd^{2+}, T2 4.4 pM Cd^{2+}, and T2 44

pM Cd^{2+}; c) T3 control, T3 4.4 pM Cd^{2+}, and T3 44 pM Cd^{2+}; d) T4 4.4 pM Cd^{2+}, T4 44 pM Cd^{2+}, and T5 control; and e) T4 control, T5 4.4 pM Cd^{2+}, and T5 44 pM Cd^{2+}. This clustering suggests that exponential growth phase (T1) relative protein abundances 44 pM Cd^{2+} are similar to early exponential phase (T2) relative protein abundances in all treatments and that late stationary phase (T4) no added Cd^{2+} relative protein abundances are similar to the death phase (T5) Cd^{2+} relative protein abundances. The latter observation is correlated with an approximate factor of two drop in cell number in the no added Cd^{2+} treatment from T3 to T4. By comparison, cell numbers in the Cd^{2+} treatments drop about two orders of magnitude from T4 to T5. Together, these observations suggest that the no added Cd^{2+} treatment underwent a minor episode of cell death from T3 to T4 that was reflected in the proteome.

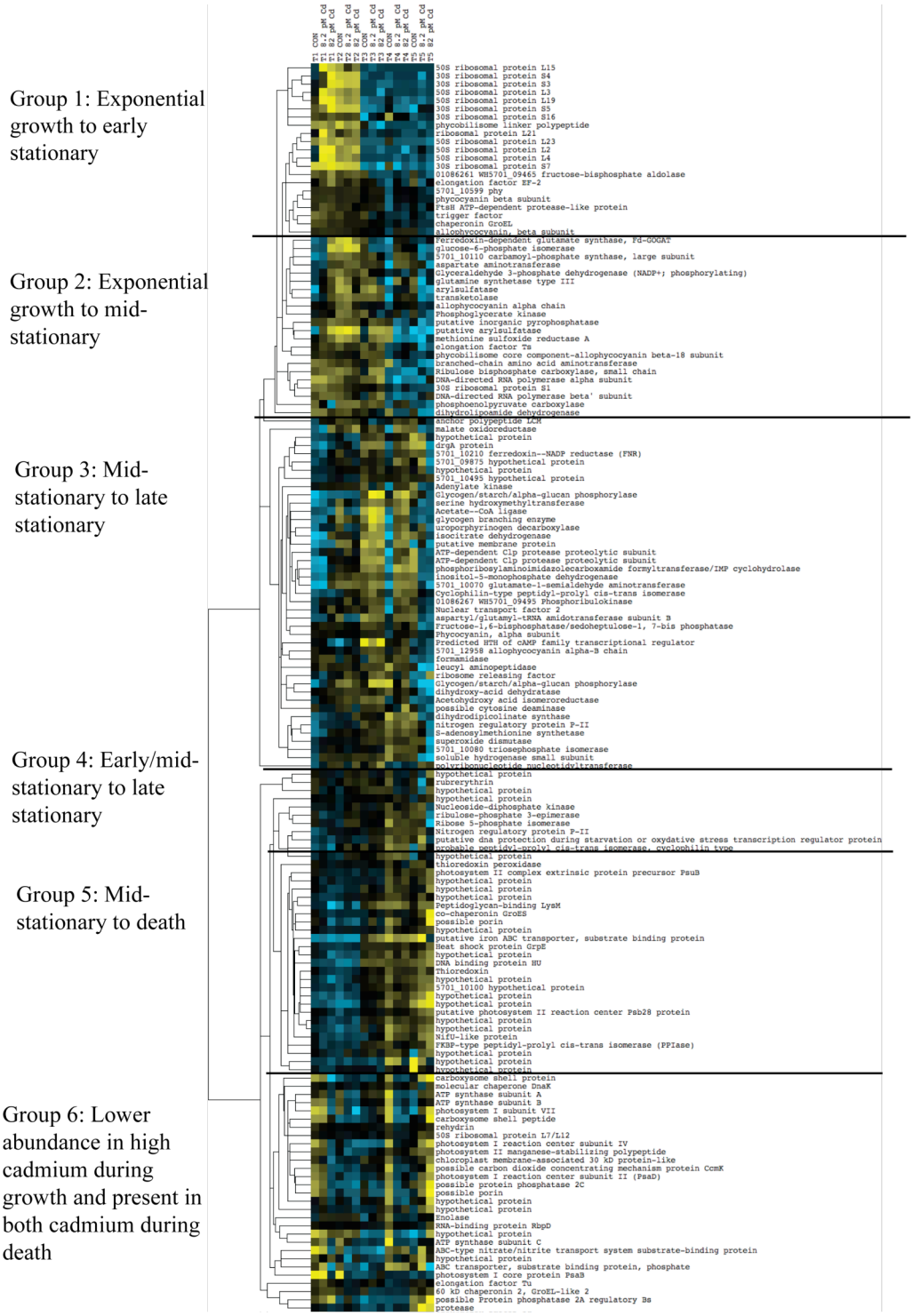

Figure 3.5: Cluster analysis of relative protein abundance. Yellow is higher and blue is lower relative abundance compared to black, the centered mean value. T1 to T5 from left to right. Order at each time point is control, 4.4 pM Cd^{2+} and 44 pM Cd^{2+}. 152 proteins with at least 5 counts and different by a value of 10 averaged spectral counts from triplicate injections are included here. Data are log transformed, centered and clustered by Kendall's Tau, centroid linkage.

Global Proteomic Data - Pairwise comparisons by phase of growth

In addition to cluster analysis, which gave a global view of changes in the entire detected proteome under these specific conditions and revealed very clearly changes in relative protein abundance with growth phase as well as some Cd effects, pairwise analyses of relative protein abundance in one Cd treatment compared to the control at each timepoint directly addresses changes caused by the addition of Cd. Figure 3.6 is a summary of this pairwise analysis. It depicts the number of proteins that are more abundant by greater than or equal to two-fold in a Cd treatment compared to the control (red) and the control compared to Cd (black). Overall, the number of proteins that were more than two-fold differentially abundant was the greatest during late stationary (T4) and very late stationary/death phase (T5) compared to growth through mid-stationary phases (T1-T3) (Figure 3.6). Tables of the actual proteins that changed at each timepoint, as well as their respective KEGG functions will be found under their respective timepoint.

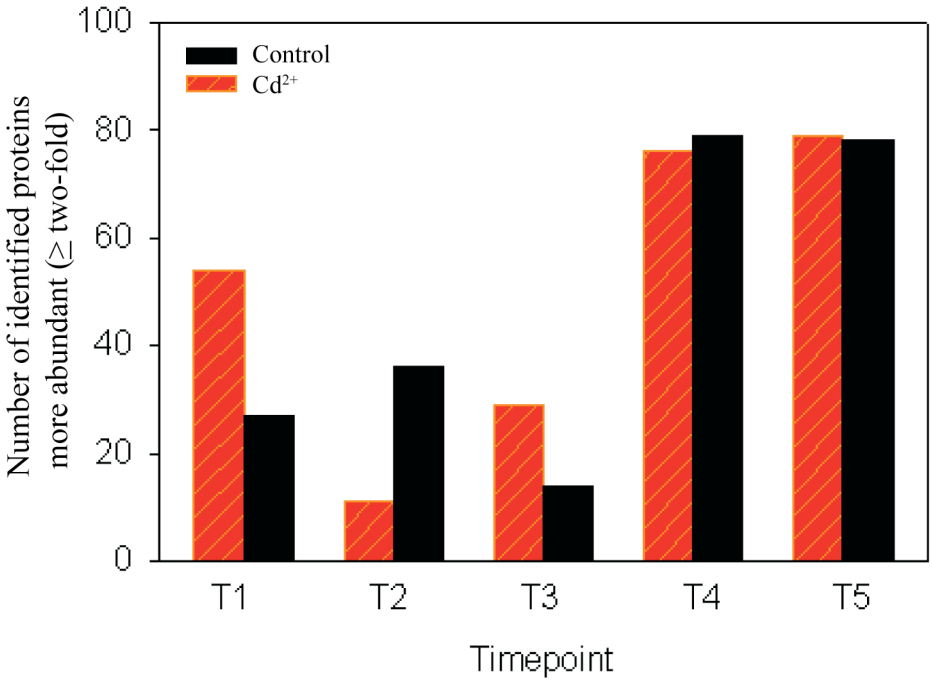

Figure 3.6: Number of identified proteins more abundant (≥ two-fold) in the control (black) and cadmium treatments (red) by time point. Proteins have an average spectral count of at least 5.

Exponential Growth Phase (T1)

During exponential growth phase, 54 proteins were above a threshold count signal of greater than or equal to 5 spectral counts and were more abundant by $\geq$ two-fold in at least one of the Cd treatments compared to the control (Figure 3.7, Table 3.1). Twenty-seven proteins by the same stringencies were more abundant in the control compared to at least one of the Cd treatments (Table 3.2). 4.4 and 44 pM Cd^{2+} treatments have an overabundance of many ribosomal proteins, arylsulfatases, an isocitrate dehydrogenase, proteins involved in chlorophyll biosynthesis, and cysteine metabolism, among others compared to the control (Table 3.1). The hypothetical protein WH5701_01855, 16 times more abundant in the high Cd treatment compared to the control, showed nucleotide BLAST alignment with a query of length 1521 to a putative uroporphyrinogen decarboxylase with a score of 316 bits, 70% identity of 763 and E-value of $2e^{-44}$ (Altschul et al., 1997), another protein involved in chlorophyll biosynthesis. The Cd treatments have an underabundance of photosystem I, carboxysome and hypothetical proteins relative to the control (Table 3.2). Eight times less abundant in the high Cd treatment than the control is a WH5701_09565 hypothetical protein that showed nucleotide BLAST alignment with a query of length 594 to an uncharacterized conserved secreted protein in *Synechococcus* WH7803 with a score of 131 bits, 71% identity of 304 and E-value of $7e^{-27}$ (Altschul et al., 1997).

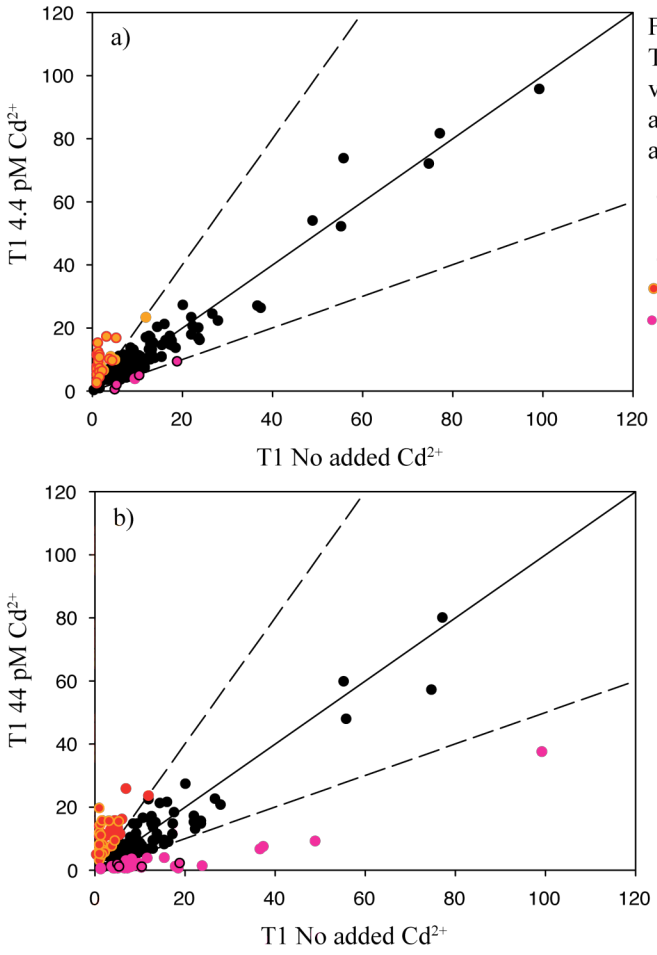

Figure 3.7: Relative abundance of proteins, T1 exponential growth phase. a) 4.4 pM Cd^{2+} vs. No added Cd^{2+} b) 44 pM Cd^{2+} vs. No added Cd^{2+} . Solid line is 1:1. Dashed lines are 1:2 and 2:1.

- less than two-fold abundant
- more abundant in 4.4 pM Cd^{2+} ($\geq$ two-fold)
- more abundant in 44 Cd^{2+} ($\geq$ two-fold)
- more abundant in both Cd^{2+} ($\geq$ two-fold)
- more abundant in no added Cd^{2+} ($\geq$ two-fold)

Table 3.1: WH5701 proteins during exponential growth phase (T1) that are more abundant in the Cd^{2+} treatments than the control by ≥ two-fold.

WH5701 ID	KEGG Function	Protein	4.4 pM Cd^{2+} abundance relative to control	44 pM Cd^{2+} abundance relative to control
02239	St,L	putative arylsulfatase	+7.4	+20.9
01855	Ukn	hypothetical protein	+1.1	+16.4
01780	TCA	isocitrate dehydrogenase	+1.4	+14.0
12014	M,Nu,PB	adenylosuccinate synthetase	0	+13.2
07436	GI,T	30S ribosomal protein S4	+2.5	+11.9
05660	GI,T	50S ribosomal protein L2	+12.3	+11.7
13125	Gly	glucose-6-phosphate isomerase	+1.1	+11.3
05540	GI,T	30S ribosomal protein S9	+2.6	+11.2
04620	St,L	arylsulfatase	+6.8	+10.0
10070	Po,Chl	glutamate-1-semialdehyde aminotransferase	-1.1	+9.5
05570	GI,T	30S ribosomal protein S13	+3.9	+9.5
05670	GI,T	50S ribosomal protein L4	+9.9	+8.8
09740	Ukn	hypothetical protein	+3.2	+8.5
10110	M,A,Nu	carbamoyl-phosphate synthase large subunit	+1.5	+8.3
01005	M,N	ferredoxin-dependent glutamate synthase, Fd-GOGAT	+1.5	+8.3
05590	GI,T	50S ribosomal protein L15	+1.4	+8.3
05645	GI,T	30S ribosomal protein S3	+1.8	+7.3
05605	GI,T	50S ribosomal protein L6	+7.9	+6.6
13665	GI,T	30S ribosomal protein S2	+2.9	+6.4
01045	GI,T	30S ribosomal protein S10	+2.1	+6.1
09149	C	malate oxidoreductase	-1.9	+5.9
05615	GI,T	50S ribosomal protein L5	+7.5	+5.7
15591	M, V,Po,Chl	δ-aminolevulinic acid dehydratase	+1.5	+5.5
03654	M	glycogen/starch/alpha-glucan phosphorylase	+2.7	+5.3
05640	GI,T	50S ribosomal protein L16	+4.6	+5.2
05675	GI,T	50S ribosomal protein L3	+7.3	+5.1
13900	GI,T	50S ribosomal protein L19	+5.5	+5.0
14966	GI,T	50S ribosomal protein L27	+3.9	+4.2
05595	GI,T	30S ribosomal protein S5	+1.5	+4.0
05975	Cy, Met,Se	S-adenosylmethionine synthetase	+1.4	+3.9
05565	GI,T	30S ribosomal protein S11	+1.8	+3.9
01600	M,E,C,An	transketolase	+1.7	+3.8
02844	M,E,C	glyceraldehyde 3-phosphate dehydrogenase (NADP+; phosphorylating)	+1.5	+3.7
08064	M,Nu,PB	inositol-5-monophosphate dehydrogenase	-1.2	+3.6
06556	M, Nu,GI	polyribonucleotide nucleotidyltransferase	+1.8	+3.4

Table 3.1 (continued):

WH5701 ID	KEGG Function	Protein	4.4 pM Cd^{2+} abundance relative to control	44 pM Cd^{2+} abundance relative to control
04010	U,Si	nuclear transport factor 2	+1.8	+3.1
02259	GI	possible protein phosphatase 2A regulatory Bs	+1.5	+2.9
02929	U,M	soluble hydrogenase small subunit (DHSS)	+3.2	+2.9
08944	M,N,A,S	glutamine synthetase type III	+1.7	+2.7
01030	GI,T	elongation factor EF-2	+1.5	+2.7
01085	M,C,A,Cy	aspartate aminotransferase	-1.1	+2.6
05625	GI,T	50S ribosomal protein L14	+2.9	+2.6
05655	GI,T	30S ribosomal protein S19	+1.1	+2.4
15281	PS	anchor polypeptide L_{CM}	+2.2	+2.1
11829	(N)	nitrogen regulatory protein P-II	+1.4	+2.0
10080	C	triose phosphate isomerase	+1.5	+2.0
05545	GI,T	50S ribosomal protein L13	+2.7	+2.0
14961	GI,T	50S ribosomal protein L21	+8.8	+3.2
02989	GI,T	50S ribosomal protein L20	+5.4	+3.3
01770	M,V	heme oxygenase	+4.9	+2.9
11799	En,Tr	polar amino acid transport system substrate-binding protein	+4.3	+2.1
02614	ABC, P	ABC transporter, phosphate	+2.7	-6.6
02994	GI,T	50S ribosomal protein L35	+2.6	+1.8
07346	GI,Rr,D	cell division protein (ftsZ)	+2.2	-1.0

Arranged in highest to lowest fold change, 44 pM Cd^{2+}, then 4.4 pM Cd^{2+}. + = fold greater than control, - = fold less than control, St = steriod hormone synthesis, L = lipid biosynthesis, Ukn = unknown, TCA = TCA cycle, M = metabolism, Nu = nucleic acid metabolism, PB = purine biosynthesis, GI = genetic information processing, T = translation, Gly = glycolosis, Po = porphryn biosynthesis, Chl = chlorophyll biosynthesis, Met = methionine synthesis, Se = selenoaminoacid synthesis, E = energy metabolism, An = ansamycin metabolism, U = unclassified, Si = signalling, N = nitrogen, A = amino acid metabolism, S = sulfur metabolism, C = CO_2 fixation, Cy = cysteine metabolism, PS = photosynthesis, V = vitamin metabolism, En = environmental sensing, Tr = transport, ABC = ABC-type membrane transport, Rr = replication and repair, D = cell division

Table 3.2: WH5701 proteins during exponential growth phase (T1) that are two-fold or more less abundant in the Cd^{2+} treatments compared to the control.

WH5701 ID	KEGG Function	Protein	4.4 pM Cd^{2+} abundance relative to control	44 pM Cd^{2+} abundance relative to control
11339	C	carboxysome shell protein	-1.4	-28
01585	PS	photosystem I subunit VII (psaC)	-1.2	-14.4
05480	PS	photosystem I core protein (psaB)	+1.1	-11.3
07859	M,E,PS	apocytochrome f precursor (petA)	-1.6	-10.8
05475	PS	photosystem I core protein (psaA)	+1.1	-9.9
05780	M,E,C,Cb	phosphoenolpyruvate carboxylase	+1.1	-9.9
06176	PS	photosystem I reaction center subunit IV (psaE)	-2.0	-8.4
09565	Ukn	hypothetical protein	-1.3	-8.2
15251	PS	ATP synthase subunit B	-1.4	-7.8
00710	U,Om	possible porin (som)	-1.8	-7.5
15961	U	possible protein phosphatase2C	-1.6	-6.4
07894	PS	photosystem I reaction center subunit III (psaF)	+1.2	-6.3
06000	PS	photosystem II chlorophyll-binding protein	+1.4	-5.4
05795	PS	photosystem I reaction center subunit II (psaD)	-1.4	-5.4
15121	PS	ATP synthase subunit B	+1.1	-5.3
11319	C	possible carbon dioxide concentrating mechanism (CcmK)	-1.4	-5.0
00840	Ukn	hypothetical protein	-1.2	-4.8
13795	Ukn	hypothetical protein	-2.7	-4.6
02604	Ukn	hypothetical protein	-1.2	-4.5
07651	PS	chloroplast membrane-associated 30 kD protein-like	-1.6	-4.5
01150	PS	photosystem II manganese-stabilizing polypeptide	-1.1	-3.9
13075	Ukn	hypothetical protein	-1.5	-3.0
11354	C	carboxysome shell peptide	-1.1	-2.6
15156	Ukn	hypothetical protein	-8.8	-2.5
11984	PS	possible ferredoxin (2Fe-2S)	-1.1	-2.3
13850	Ukn	hypothetical protein	-1.7	-2.3
13745	M,E,C	ribulose-phosphate 3-epimerase	-2.5	-1.8

Arranged in highest to lowest fold change, 44 pM Cd^{2+}, then 4.4 pM Cd^{2+}. + = fold greater than control, - = fold less than control, * = also in Table 3.1, C=CO_2 fixation; PS = photosynthesis, M = metabolism, E = energy metabolism, Cb = carbohydrate metabolism, Ukn = unknown, U = unclassified, Om = outer membrane protein

Early Stationary Phase (T2)

During early stationary phase, 11 proteins were above a threshold count signal of greater than or equal to 5 spectral counts and were more abundant by ≥ two-fold in at least one of the Cd treatments compared to the control (Table II.1). Thirty-six proteins by the same stringencies were more abundant in the control compared to at least one of the Cd treatments (Table II.2). 4.4 and 44 pM Cd^{2+} treatments have an overabundance of 4 hypothetical proteins, and an extra cellular solute-binding protein family 3, among others, compared to the control (Table II.1). The Cd treatments have an underabundance of photosystem I, ATP synthase, arylsulfatase and six ribosomal proteins relative to the control (Table II.2).

Mid-Stationary Phase (T3)

During mid-stationary phase, 24 proteins were above a threshold count signal of greater than or equal to 5 spectral counts and were more abundant by ≥ two-fold in at least one of the Cd treatments compared to the control (Table II.3). Fourteen proteins by the same stringencies were more abundant in the control compared to at least one of the Cd treatments (Table II.4). 4.4 and 44 pM Cd^{2+} treatments have an overabundance of two proteins involved in chlorophyll biosynthesis, coproporphyrinogen III oxidase and uroporphyrinogen decarboxylase, a stationary phase survival protein (SurE), the extracellular solute-binding protein family 3, and the putative arylsulfatase among others, compared to the control (Table II.3). The Cd treatments have an underabundance of a few purine biosynthesis proteins and two phycobilisome proteins, among others relative to the control (Table II.4).

Late Stationary Phase (T4)

During late stationary phase, 76 proteins were above a threshold count signal of greater than or equal to 5 spectral counts and were more abundant by ≥ two-fold in at least one of the Cd treatments compared to the control (Table II.5). Seventy-nine proteins by the same stringencies were more abundant in the control compared to at least one of the Cd treatments (Table II.6). 4.4 and 44 pM Cd^{2+} treatments have an overabundance of three proteins involved in chlorophyll biosynthesis, two proteins

involved in cysteine and sulfur metabolism, 16 hypothetical proteins, and phycobilisome-associated pigments, among others, compared to the control (Table II.5). The Cd treatments have an underabundance of ATP synthase, three carboxysome-related proteins, and 25 hypothetical proteins, among others relative to the control (Table II.6).

Very Late Stationary or Death Phase (T5)

During very late stationary phase for the control and death phase for the Cd treatments, 79 proteins were above a threshold count signal of greater than or equal to five spectral counts and were more abundant by $\geq$ two-fold in at least one of the Cd treatments compared to the control (Table 3.3). Seventy-eight proteins by the same stringencies were more abundant in the control compared to the Cd treatments (Table 3.4). 4.4 and 44 pM Cd^{2+} treatments have an overabundance of 36 hypothetical proteins, photosystem I proteins, carboxysome proteins, and ATP synthase, among others, compared to the control (Table 3.3). The Cd treatments have an underabundance of 12 hypothetical proteins, phycobilisome-related pigments, a protein involved in chlorophyll biosynthesis, among others relative to the control (Table 3.4).

Table 3.3: WH5701 proteins during very late stationary or death phase (T5) that are more abundant in the Cd^{2+} treatments than the control by ≥ two-fold.

WH5701 ID	KEGG Function	Protein	4.4 pM Cd^{2+} abundance relative to control	44 pM Cd^{2+} abundance relative to control
01585	PS	photosystem I subunit VII	+8.1	+27.2
13075	Ukn	hypothetical protein	+2.6	+24.9
13725	Ukn	hypothetical protein	+6.0	+14.5
00710	Mp	possible porin	+3.4	+14.5
04880	Ukn	hypothetical protein	+8.9	+11.4
11924	U, T	ribosome releasing factor	+1.1	+10.8
15671	U	methionine sulfoxide reductase B	+3.0	+8.8
02979	Ukn	hypothetical protein	+1.0	+8.4
11339	C	carboxysome shell protein	+4.8	+8.1
00705	Mp	possible porin	+1.2	+7.7
14306	Ukn	hypothetical protein	+2.5	+7.1
14296	Ukn	hypothetical protein	+3.5	+6.6
15116	GI, F	co-chaperonin GroES	+1.6	+6.5
11354	C	carboxysome shell peptide	-1.3	+6.4
07276	Ukn	hypothetical protein	+2.3	+6.3
14301	Ukn	hypothetical protein	+2.5	+5.9
05795	PS	photosystem I reaction center subunit II (psaD)	+3.1	+5.6
11319	C	possible carbon dioxide concentrating mechanism protein (Ccmk)	+1.2	+5.5
06176	PS	photosystem I reaction center subunit IV	+2.9	+5.3
02634	GI,T	30S ribosomal protein S6	+1.3	+5.2
05845	Ukn	hypothetical protein	+1.5	+5.1
15071	U, GI	DNA-directed RNA polymerase omega subunit	+1.3	+5.0
10230	U,M,Nu	possible cAMP phosphodiesterase class-II	+3.3	+5.0
15241	PS	ATP synthase subunit A	+4.1	+4.8
12273	Ukn	hypothetical protein	+4.3	+4.6
15886	Ukn	hypothetical protein	-1.1	+4.5
01175	Ukn	hypothetical protein	+1.4	+4.4
15441	U, GI	DNA-directed RNA polymerase beta' subunit	+2.3	+4.1
15961	GI	possible protein phosphatase 2C	+1.4	+4.1
05950	Ukn	hypothetical protein	+4.1	+4.1
05560	U, GI	DNA-directed RNA polymerase alpha subunit	-1.4	+4.0
16056	M,GI,F,EnPd	possible serine protease	+3.3	+3.8
12638	Ukn	hypothetical protein	+1.4	+3.8
15121	PS	ATP synthase subunit B	+2.6	+3.2
05925	Ukn	hypothetical protein	-1.1	+3.1
07396	Ukn	hypothetical protein	+1.5	+3.0
02259	GI	possible protein phosphatase 2A regulatory Bs	-1.3	+2.9

Table 3.3 (continued, page 2 of 3)

WH5701 ID	KEGG Function	Protein	4.4 pM Cd^{2+} abundance relative to control	44 pM Cd^{2+} abundance relative to control
09099	Ukn	hypothetical protein	+3.2	+2.9
07651	PS	chloroplast membrane-associated 30kD protein-like	+1.5	+2.9
11349	U	methionine sulfoxide reductase A	-2.2	+2.7
16031	Ukn	hypothetical protein	+2.4	+2.7
06581	U,N	NifU-like protein	+2.1	+2.7
10549	Ukn	hypothetical protein	-2.1	+2.7
05815	Chl	coproporphyrinogen III oxidase	+1.4	+2.7
02030	GI,T	50S ribosomal protein L9		
08194	Ukn	hypothetical protein	+1.2	+2.5
02664	Ukn	hypothetical protein	-1.6	+2.5
14786	GI,F	FKBP-type peptidyl-prolyl cis-trans isomerase (PPIase)	+1.1	+2.4
12034	Ukn	hypothetical protein	+1.5	+2.4
06691	Pp,Pd	protease	+4.0	+2.4
02829	Ukn	hypothetical protein	+1.6	+2.4
06556	M,Nu,GI	polyribonucleotide nucleotidyl-transferase	+3.0	+2.4
00770	GI,Rr,Ra	DNA repair protein (radA)	+1.2	+2.4
08389	Ukn	hypothetical protein	+2.0	+2.4
14806	Ukn	hypothetical protein	-2.0	+2.2
05140	M,Cb,Gly E,C	phosphoglycerate kinase	-1.0	+2.2
13085	Ukn	hypothetical protein	+1.8	+2.1
02654	Ukn	hypothetical protein	+2.4	+2.1
06191	Cw	peptidoglycan binding (LysM)	+2.0	+2.0
11644	Ukn	hypothetical protein	+8.6	+5.9
14406	GI,F,En,Ca	probable peptidyl-prolyl cis-trans isomerase, cyclophilin type	+7.7	+3.3
04715	N,ABC	ABC-type nitrate/nitrite transport system	+7.4	+2.0
11799	En,Tr	polar amino acid transport system substrate binding protein	+6.6	+2.4
02409	Ukn	hypothetical protein	+6.2	+2.1
15736	Ukn	hypothetical protein	+5.9	+2.1
15626	U	putative membrane protein	+5.7	+1.1
04975	Ukn	hypothetical protein	+5.6	-1.5
11524	Cy,Se	cysteine synthase A	+4.8	-3.3
02614	P,ABC	ABC transporter, substrate binding protein, phosphate	+4.1	-8.5
11729	Ukn	hypothetical protein	+3.7	-1.5
09875	Ukn	hypothetical protein	+3.5	-4.7
02904	Ukn	hypothetical protein	+3.3	+2.5
03890	U, O	putative DNA protection during starvation or oxidative stress transcription regulator protein	+3.0	-2.2*

Table 3.3 (continued, page 3 of 3)

WH5701 ID	KEGG Function	Protein	4.4 pM Cd^{2+} abundance relative to control	44 pM Cd^{2+} abundance relative to control
15926	M,Cb,Nu	phosphoglucomutase (pgm)	+2.6	-2.7
02264	Ukn	hypothetical protein	+2.4	-1.3
12533	Chl	uroporphyrinogen decarboxylase	+2.4	-2.5
08984	M,V,B6	pyridoxal phosphate biosynthetic protein	+2.2	-4.4
12134	U,Fe,ABC En	putative iron ABC transporter, substrate binding protein	+2.1	-4.4
12543	Ukn	hypothetical protein	+2.1	-2.2*

Arranged in highest to lowest fold change, 44 pM Cd^{2+}, then 4.4 pM Cd^{2+}. + = fold greater than control, - = fold less than control, * = also in Table 3.4, PS = photosynthesis, Ukn = unknown, Mp = membrane protein, U = unclassified, T = translation, C = CO_2 fixation, GI = genetic information processing, F = protein folding, M = metabolism, Nu = nucleic acid metabolism, En = environmental sensing, Pd = progein degradation, N = nitrogen metabolism, Chl = chlorophyll biosynthesis, Pp = peptidase, Rr = replication and repair, Ra = radiation sensitivity (cyanobase), Cb = carbohydrate metabolism, Gly = glycolosis, E = energy metabolism, Cw = cell wall membrane biosynthesis (cyanobase), Ca = calcium signaling pathway, ABC = ABC-type membrane transport, Tr = transport, Cy = cysteine metabolism, Se = selenoaminoacid synthesis, P = phosphate metabolism, O = oxidative stress, V = vitamin metabolism, B6 = vitamin B6 metabolism, Fe = iron metabolism.

Table 3.4: WH5701 proteins during very late stationary or death phase (T5) that are two-fold or more less abundant in the Cd^{2+} than the control treatments.

WH5701 ID	KEGG Function	Protein	4.4 pM Cd^{2+} abundance relative to control	44 pM Cd^{2+} abundance relative to control
08594	Ukn	hypothetical protein	-7.5	-32
01860	Ukn	hypothetical protein	-7.6	-22.7
07171	U,N	drgA protein	+1.0	-17.2
05830	U,GI	putative ribonuclease D	-1.4	-15.1
10240	M	probable aminopeptidase N	-7.6	-14
10070	Po, Chl	glutamate-1-semialdehyde aminotransferase	-3.6	-13.3
02929	U,M	soluble hydrogenase small subunit (DHSS)	-7.7	-13.2
14571	C	ribose 5-phosphate isomerase	-1.0	-13.1
11489	M,G	probable glutathione reductase	-5.0	-13
11104	Ukn	hypothetical protein	-8.7	-12
14791	U,O	superoxide dismutase	-1.0	-11
07321	M,pp	ATP-dependent Clp protease proteolytic subunit	-8.3	-10.4
04620	St,L	arylsulfatase	-7.4	-10.2
01595	M,L	3-oxacyl-(acyl-carrier protein) synthase II	-14.2	-9.5
01520	M,Nu, V	phosphoribosylaminoimidazole carboxamide formyltransferase/ IMP cyclohydrolase	-8.7	-9.1
03684	M,A	putative agmatine ureohydrolase	-11	-8.6
07326	M,pp	ATP-dependent Clp protease proteolytic subunit	-8.2	-7.7
14881	M,G	leucyl aminopeptidase	-15.7	-7.6
15331	(N)	nitrogen regulatory protein P-II	-1.7	-7.2
13785	M,A,V	dihydroxy-acid dehydratase (ilvD)	-3.2	-7.2
03624	M	GDP-mannose pyrophosphorylase	-2.9	-7.0
10080	M,C	triosephosphate isomerase	-1.8	-7.0
04930	GI,T	aspartyl/glutamyl-tRNA amido-transferase subunit B	-4.3	-6.9
07426	M,Cb,Gly TCA,A	dihydrolipoamide dehydrogenase	-6.3	-6.7
01085	M,C,A	aspartate aminotransferase	-1.1	-6.7
04640	M,Cb	phosphoglucomutase/phospho-mannomutase family protein	-5.4	-6.5
01940	Ukn	hypothetical protein	-1.6	-6.2
12134	En,ABC	putative iron ABC transporter substrate binding protein	+2.1	-6.0
08064	PB	inositol-5-monophosphate dehydrogenase	-6.3	-6.0
13745	M,E,C	ribulose-phosphate 3-epimerase	+1.1	-5.9
08459	GI,T	glutamyl-tRNA (Gln) amido-transferase subunit A	-(0,8.7)	-5.9
02854	GI,D	putative cyclophilin-type peptidyl-prolyl cis-trans isomerase	-18.4	-5.8

Table 3.4 (continued, pg 2 of 3):

WH5701 ID	KEGG Function	Protein	4.4 pM Cd^{2+} abundance relative to control	44 pM Cd^{2+} abundance relative to control
03039	M,A,Ly	dihydrodipicolinate synthase	-8.5	-5.5
13760	M,Cb	glucose-1-phosphate adenyl-transferase (glgC)	-11.5	-5.5
10210	PS	ferredoxin--NADP reductase (FNR)	-1.1	-5.4
10355	M,A,Ly	diaminopimelate decarboxylase (lysA)	-2.5	-5.4
15771	GI,T	translation initiation factor IF-2B subunit alpha (elF2B)	-1.2	-5.4
05975	Cy,Met,Se	S-adenosylmethionine synthetase	-1.5	-5.1
05860	Ukn	hypothetical protein	-4.1	-5.1
05580	M,Nu,PB	adenylate kinase	-6.4	-5.0
03604	M	glycogen/starch/alpha-glucan phosphorylase	-1.7	-4.8
10200	M,Cb,A,G	putative glucose 6-phosphate dehydrogenase	-3.7	-4.8
09875	Ukn	hypothetical protein	+3.5	-4.7
05145	M,Cb,E,C	phosphoglycerate kinase	-2.3	-4.4
01780	TCA	isocitrate dehydrogenase	-1.5	-4.3
05930	PS	phycobilisome linker polypeptide	-1.9	-4.2
04010	U,S	nuclear transport factor 2	-2.5	-4.2
09149	C	malate oxidoreductase	-6.5	-4.0
13750	M,Cb,Glypp,E,C	fructose-1,6-bisphosphatase/sedo-heptulose-1,7-bisphosphatase (glpx-SEBP)	-5.8	-4.0
01600	M,E,C,An	transketolase	-5.4	-3.5
04910	M,Nu	nucleoside-diphosphate kinase (ndk)	+1.2	-3.1
15281	PS	anchor polypeptide L_{CM}	-1.9	-2.9
15291	PS	allophycocyanin, beta subunit	-2.2	-2.9
08944	M,N,A,S	glutamine synthetase type III	-14.8	-2.8
01470	M,A,V	serine hydroxymethyltransferase	-3.7	-2.7
13670	GI,T	elongation factor Ts (tsf)	-5.8	-2.7
00775	En	two-component resonse regulator	-5.7	-2.7
05150	U,Si	universal stress protein (Usp)	-4.4	-2.6
15881	PS	phycobilisome rod-core linker polypeptide cpcG (L-RC 28.5)	-1.3	-2.5
12094	M,E,Op	putative inorganic pyrophosphatase	-4.9	-2.5
13170	GI,D	cyclophilin-type peptidyl-prolyl cis-trans isomerase	-1.9	-2.4
10110	M,A,Nu	carbamoyl-phosphate synthase, large subunit	-4.4	-2.4
05910	PS	phycobilisome linker polypeptide	-5.6	-2.3
03890	U,O	putative dna protection during starvation or oxidative stress transcription regulator protein	+3.0	-2.2*
12543	Ukn	hypothetical protein	+2.1	-2.2*
12958	PS	allophycocyanin alpha-B chain	-1.3	-2.1
01965	U	ruberythrin	-7.7	-1.1

Table 3.4 (continued, pg 3 of 3):

WH5701 ID	KEGG Function	Protein	4.4 pM Cd^{2+} abundance relative to control	44 pM Cd^{2+} abundance relative to control
13345	M,pp	ATP-dependent Clp protease proteolytic subunit	-5.5	-1.9
01030	GI,T	elongation factor EF-2	-5.1	-2.0
14771	Ukn	hypothetical protein	-3.7	-2.0
02844	M,E,C,Chl	glyceraldehyde 3-phosphate dehydrogenase (NADP+; phosphorylating)	-3.7	-1.5
00735	Ukn	hypothetical protein	-3.4	+1.6
09565	Ukn	hypothetical protein	-3.3	+1.5
00840	Ukn	hypothetical protein	-2.9	+1.4
02619	GI,F	molecular chaperone DnaK	-2.5	+1.2
02005	U,A	glycine cleavage system H protein	-2.4	+1.9
15476	U,Pd	serine protease, trypsin family: chemotrypsin serine protease	-2.2	+1.1
14806	Ukn	hypothetical protein	-2.0	+2.3

Arranged in highest to lowest fold change, 44 pM Cd^{2+}, then 4.4 pM Cd^{2+}. + = fold greater than control, - = fold less than control, * = also in Table 3.3, T = translation, GI = genetic information processing, C = CO_2 fixation, PB = purine biosynthesis, St = steroid hormone synthesis, L= lipid biosynthesis, Cy = cysteine metabolism, Met = methionine synthesis, Se = selenoaminoacid synthesis, TCA = TCA Cycle, Po = porphyrin biosynthesis, Chl = chlorophyll biosynthesis, Gly = glycolosis, N = nitrogen, PS = photosynthesis, P=phosphate metabolism, M = metabolism, A = amino acid metabolism, V = vitamin metabolism, Nu = nucleic acid metabolsim, E = energy metabolism, An = ansamycin metabolism, Si = signaling, U = unclassified, ABC = membrane transport ABC type, S = sulfur metabolism, Pp = peptidase, Mp = membrane protein, F = protein folding, Fe = iron metabolism, Tr=transport, En = environmental sensing, Cb = carbohydrate metabolism, Ly = lysine synthesis, Op = oxidative phosphorylation, Pd = protein degradation.

Global Proteomic Data - Pairwise by function and physiological effects

When grouped by function, the proteomic response at different growth stages showed noticeable trends. This next section of the results and discussion groups proteins by function. All proteins discussed were differentially abundant between a Cd treatment and the control by $\geq$ two-fold. This section begins with the biosynthesis of chlorophyll, follows the energy path through photosynthesis and carbon fixation and then other metabolic processes. These functions are placed in the greater context of the three physiological observations: 1) similar growth rates among treatments despite Cd^{2+} addition (Figures 3.1 and 3.2a), 2) increased maximal chlorophyll *a* fluorescence with Cd^{2+} addition (Figures 3.1 and 3.2b), and 3) increased mortality rates with Cd^{2+} addition

(Figures 3.1 and 3.2c).

Chlorophyll biosynthesis

Five proteins involved in the biosynthesis of chlorophyll, a 17 step enzymatic process, were $\geq$ two-fold differentially abundant between the control and at least one of the Cd treatments during at least one of the growth phases (Figure 3.8). These five proteins are glutamate-1-semialdehyde transferase (Step 3), δ-aminolevulinic acid dehydratase, also known as porphobilinogen synthase (Step 4), uroporphyrinogen decarboxylase (Step 7), coproporphyrinogen III oxidase (Step 8), and protochlorophyllide oxidoreductase (Step 16) (Figure 3.8).

Glutamate-1-semialdehyde transferase, which catalyzes the reaction of L-glutamic acid 1-semialdehyde to δ-aminolevulinic acid in the presence of pyridoxal phosphate, was more abundant in the 44 pM Cd^{2+} treatment relative to the control during exponential growth (T1) and late stationary (T4) (Figure 3.8, Tables 3.1, II.5) and more abundant in the 4.4 pM Cd^{2+} treatment relative to the control during late stationary (T4) (Figure 3.8, Table II.5). Glutamate-1-semialdehyde transferase was more abundant in the control than both of the Cd treatments during very late stationary and death phase (Figure 3.8, Table 3.4).

δ-aminolevulinic acid dehydratase, also known as porphobilinogen synthase, a Zn-requiring enzyme which catalyzes the reaction of δ-aminolevulinic acid to porphobilinogen, was more abundant in the 44 pM Cd^{2+} treatment relative to the control during exponential growth (T1) (Figure 3.8, Tables 3.1) and more abundant in the control than both of the Cd treatments during late stationary (Figure 3.8, Table II.6).

Uroporphyrinogen decarboxylase, which catalyzes the reaction of uroporphyrinogen III to coproporphyrinogen III, was more abundant in the 44 pM Cd^{2+} treatment relative to the control during late stationary (T4) (Figure 3.8, Table II.5) and more abundant in the 4.4 pM Cd^{2+} treatment relative to the control during mid- and late stationary (T3 and T4) (Figure 3.8, Tables II.3, II.5). Uroporphyrinogen decarboxylase was more abundant in the control than both of the Cd treatments during early stationary (T2) (Figure 3.8, Table II.2).

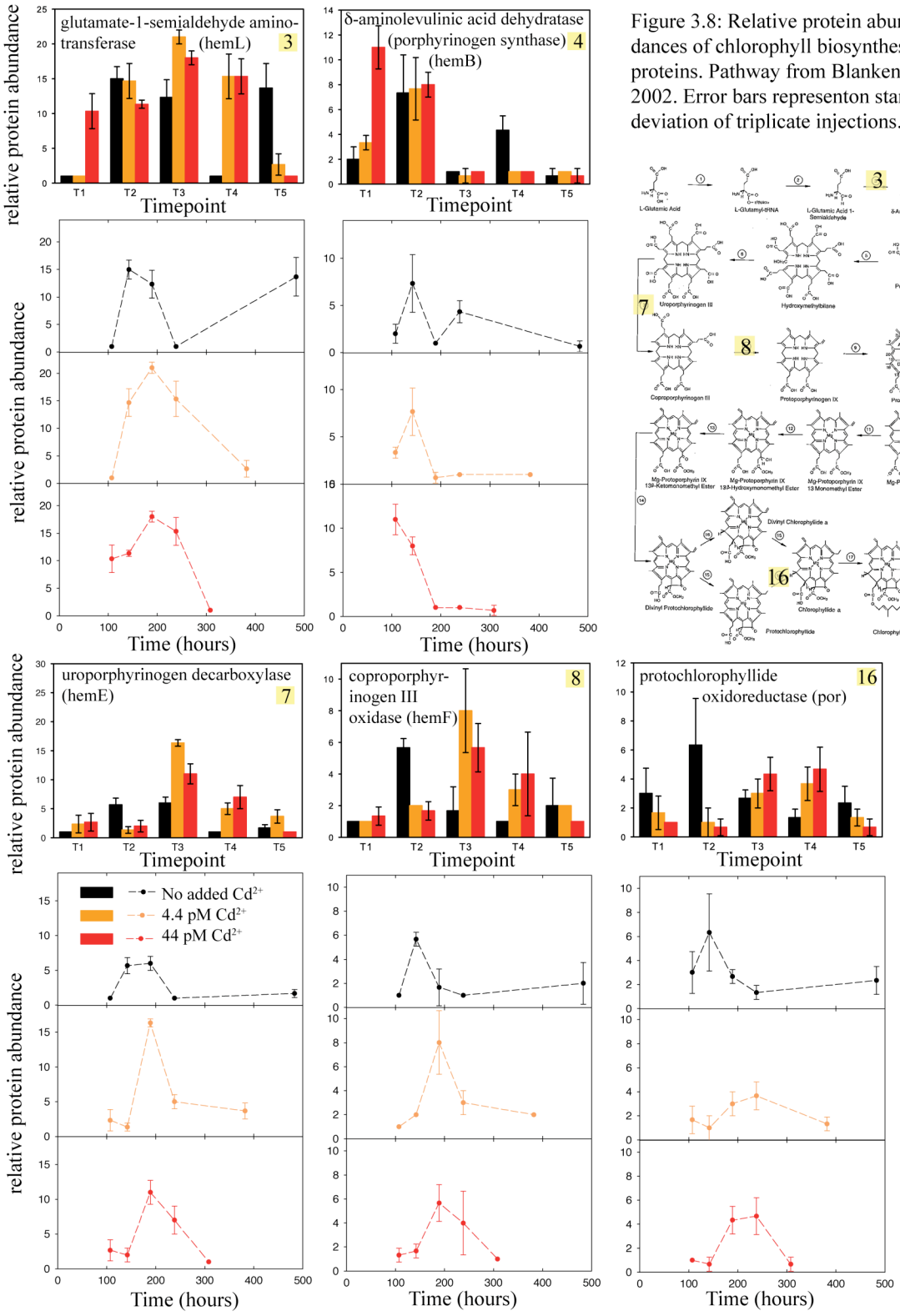

Figure 3.8: Relative protein abundances of chlorophyll biosynthesis proteins. Pathway from Blankenship 2002. Error bars represenon standard deviation of triplicate injections.

Coproporphyrinogen III oxidase, which catalyzes the reaction of coproporphyrinogen III to protoporphyrinogen IX, was more abundant in both the 4.4 and 44 pM Cd^{2+} treatment relative to the control during mid- and late stationary (T3 and T4) (Figure 3.8, Tables II.3, II.5). Uroporphyrinogen decarboxylase was more abundant in the control than both of the Cd treatments during early stationary (T2) (Figure 3.8, Table II.1).

Protochlorophyllide oxidoreductase, which catalyzes the reaction of protochlorophyllide to chlorophyllide a, was more abundant in both the 4.4 and 44 pM Cd^{2+} treatment relative to the control late stationary (T4) (Figure 3.8, Table II.5). Protochlorophyllide oxidoreductase was more abundant in the control than both of the Cd treatments during early stationary (T2) (Figure 3.8, Table II.2).

The dramatic physiological effects with chronic Cd exposure observed in this experiment (increased chlorophyll *a* maximum and faster death rate in the Cd treatments) are not observed when Zn is added to the media (Figure 3.3). This may imply that the presence of Zn is integral to the photosynthetic functionality, perhaps by Cd disrupting a Zn regulatory system causing an induction of the chlorophyll biosynthesis pathway resulting in overproduction of chlorophyll. If this is true, we still do not know the exact mechanism or the site of this influence. The lack of dramatic physiological effects with Cd in the media when Zn is also present implies that the ratio of Cd/Zn matters for toxicity of Cd to cyanobacteria in culture and consequently could play a role in the environment.

The origin of a physiological maximum in chlorophyll *a* fluorescence at T4 (Figure 3.4a), late stationary phase, for the 44 pM Cd^{2+} treatment, because of an increased quantity of chlorophyll *a* is supported by a greater than two-fold increase in relative abundance of glutamate-1-semialdehyde transferase, uroporphyrinogen decarboxylase and coporphyrinogen III oxidase, three enzymes in the chlorophyll *a* biosynthesis pathway at T3 and T4 (Figures 3.4, 3.8, Tables II.3, II.5). The 4.4 pM Cd^{2+} treatment also reached a similar maximum fluorescence in-between protein sampling points T4 and T5 and has the same more than two-fold relative increase in these three

enzymes. This hypothesis is not supported in that the chlorophyll *a* fluorescence per cell with time (a proxy for chlorophyll *a* per cell) does not show much difference between the control and Cd treatments (plot not shown).

Two similar alternative hypotheses hinge on the fact that a change in chlorophyll *a* fluorescence directly reflects photosystem II, as expected in most photosynthetic organisms (Campbell et al., 1998). However, due to the ability of cyanobacteria to adapt chromically (Everroad et al., 2006), the slight contribution of phycobiliproteins to the chlorophyll emission spectrum (Campbell et al., 1998), and the possible slight contribution of photosystem I chlorophyll (Campbell et al. 1998 and reference therein), one cannot always assume this direct correlation of chlorophyll *a* fluorescence with photosystem II. Although chromic adaptation of many strains of marine *Synechococcus* has been investigated by Palenik (2001), whether or not WH5701 is capable of chromic adaptation is as of yet unknown. The first hypothesis is that Cd directly binds to photosystem II centers causing an increase in chlorophyll *a* fluorescence. Addition of 3-(3,4-dichlorophenyl)-1,1-dimethylurea (DCMU) to cyanobacteria causes the closing of photosystem II centers, resulting in a rapid rise in fluorescence (Campbell et al., 1998). This hypothesis cannot be tested by this global proteomic dataset. The second hypothesis is that Cd disrupts or reduces electron transport, based on the pot model of Beutler 2003 and related evidence of Zn^{2+} and Cd^{2+} binding to the bacterial reaction center in *Rhodobacter sphaeroides* thereby reducing rates of electron transfer from photosystem II to Q_B (Okamura et al., 2000 and reference therein). In the pot model, excitons with a particular intensity produced by absorbed light energy strike photosystem II. There are three subsequent means of deexcitation: photochemical quenching, fluorescence, and thermal deexcitation. If an increase in fluorescence is observed, assuming a constant input and no change in photosystem II, then photochemical quenching leading to the electron transport train or thermal deexcitation must be reduced. This could be tested by global proteomics by comparing the relative abundances if the cytochrome b_6f complex or enzymes involved in the synthesis of quinone were detected, but these enzymes were not observed.

Alternatively, the *in vivo* substitution of the Mg^{2+} binding in chlorophyll by heavy metals (mercury, copper, cadmium, nickel, zinc, and lead), leading to the breakdown of photosynthesis in plants, has been shown to be an important damage mechanism (Küpper et al., 1998). The substitution of Cd or Zn for magnesium in chlorophyll destabilizes the first excitation state, as deduced by lowered *in vitro* fluorescence quantum yield of heavy metal substituted chlorophylls compared to magnesium chlorophyll (Küpper et al., 1998). There has been one known photosynthetically active Zn-bacteriochlorophyll in *Acidiphilium rubrum* (Wakao et al., 1996). The substitution of the magnesium in chlorophyll with Cd is probably not what is happening in this experiment because we would expect the chlorophyll *a* fluorescence to decrease, due to the instability of Cd chlorophyll (Küpper et al., 1996), not increase as we observed. Or because the heavy metal substitution rate in plants is only about 2% for the total chlorophyll, albeit this substitution rate still produces a massive breakdown in photosynthesis (Küpper et al., 1998), substitution could be happening in this experiment and it would undetected.

Cd caused some changes in chlorophyll *a* biosynthesis proteins in this experiment, but we have not shown this to be directly linked to an increase in chlorophyll *a* itself. The chlorophyll *a* maximum is probably related to Cd interfering with Zn because we do not see the chlorophyll *a* maximum when Zn is added to the media (Figure 3.3). Cd could be interfering with Zn regulation. Zn could be involved in photosynthetic regulation and Cd is interfering. Oxidative stress is known to modulate apoptosis. Apoptosis is the process of programmed cell death in animal systems and apoptotic processes have begun to be considered in phytoplankton (Vardi et al., 2007). If Zn is modulating oxidative stress and the cells are Zn deficient, Cd can be affecting oxidative stress, which may cause cell death. There is also a dosage of Cd and time effect. Cells exposed to an order of magnitude more Cd, 44 pM Cd^{2+} show the effects first and cell numbers dramatically decrease and then the cells exposed to 4.4 pM Cd^{2+} show similar effects later in the experiment and then cell numbers decrease dramatically (Figure 3.4a,b).

Phycobilisome

Phycobilisomes gather excitation energy from incoming photons. The proteins that comprise phycobilisomes comprise a large percentage of the total protein mass in a cyanobacterial cell, and indeed we see phycocyanin and allophycocyanin as the most abundant proteins in our global proteomic data. In phycobilisomes, phycobiliproteins bind phycobilins (chromophores) by covalent thioether bonds to cysteinyl residues (MacColl, 1998; Everroad et al., 2006). Phycobilisomes are thought to be able to transfer excitation energy to both photosystem II and I (Mullineaux, 1999). Four phycobilisome-associated proteins: the α subunit of phycocyanin, β subunit of allophycocyanin, anchor polypeptide L_{CM} and phycobilisome linker polypeptide were more than two-fold differentially abundant between the control and at least one of the Cd treatments at one of the time points (Figure 3.9).

The α subunit of phycocyanin, the outer rod in the phycobilisome, was overall the most abundant protein identified in this experiment. The β subunit of allophycocyanin, a core component in the phycobilisome, was the third most abundant protein identified. During late stationary phase (T4), these two pigments were more abundant in the two Cd treatments than the control (Figure 3.9, Table II.5). During very late stationary/death phase, phycocyanin and allophycocyanin were more abundant in the control than the two Cd treatments (Figure 3.9, Table 3.4).

The anchor polypeptide L_{CM}, another core component of the phycobilisome, was more abundant in both of the Cd treatments during exponential growth (T1) and more abundant in the control than the two Cd treatments during very late stationary/death phase (T5) (Figure 3.9, Tables 3.1, 3.4).

The phycobilisome linker polypeptide, peptides that link together the discs of pigments, is more abundant in the control than the 44 pM Cd^{2+} treatment during early and mid-stationary and very late stationary/death (T2, T3, T5) (Figure 3.9, Tables II.3, II.4, 3.4). The linker polypeptide is more abundant in the control than the 4.4 pM Cd^{2+} during very late stationary/death (T5) (Figure 3.9, Table 3.4).

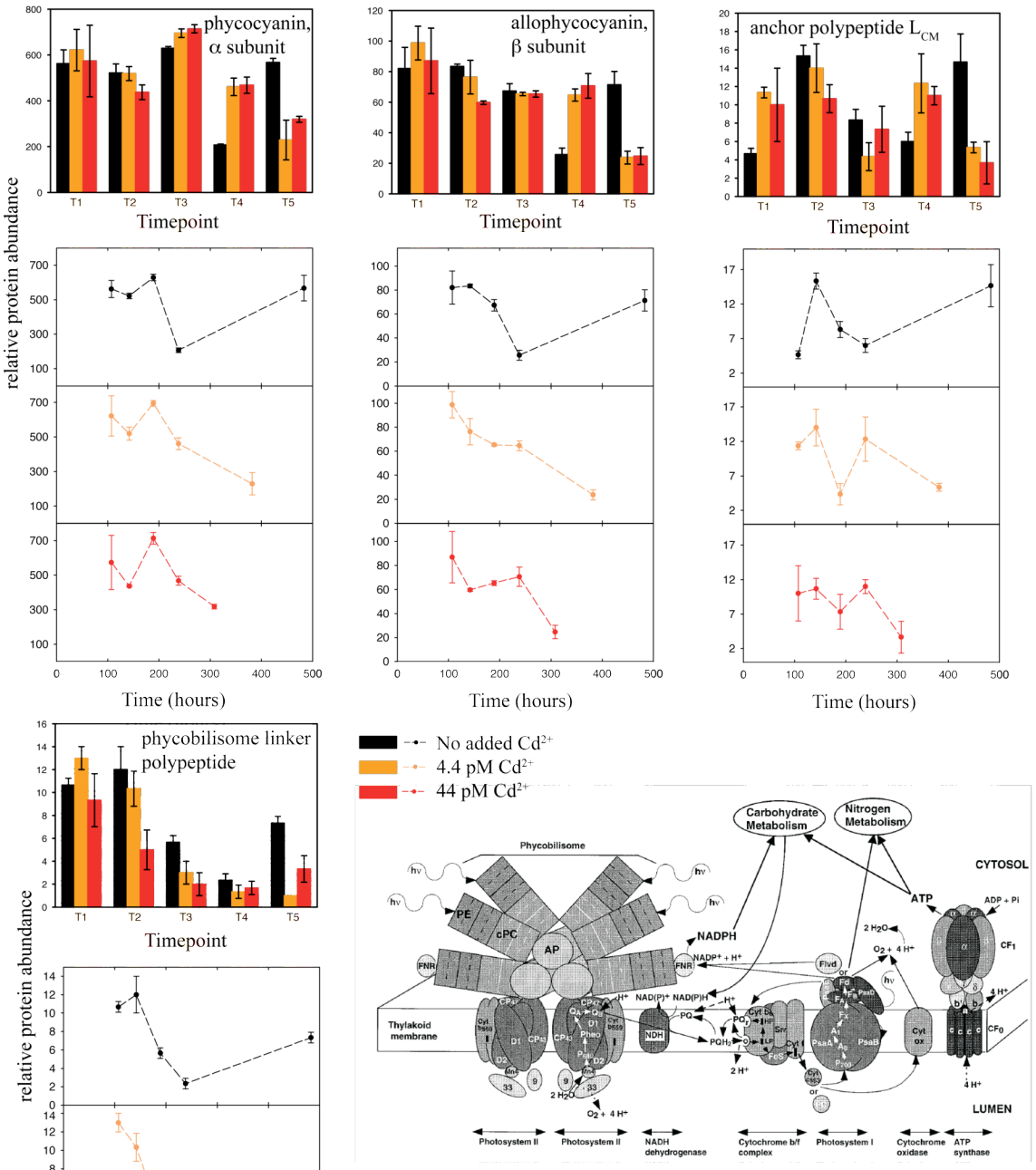

Figure 3.9: Relative protein abundances of photosynthesis proteins located in the phycobilisome that have a greater than two-fold differential abundance between a Cd^{2+} and the no added Cd^{2+} treatment at at least one timepoint. Error bars represent one standard deviation of triplicate injections. Schematic of cyanobacterial photosynthetic machinery from Campbell et al., 1998.

Chronic Cd exposure in both the 4.4 pM Cd^{2+} and 44 pM Cd^{2+} treatments caused a three-fold increase in the rate of the degradation of pigments in the phycobilisome relative to the control as calculated by the decrease in spectral counts of phycocyanin β subunit (calculated from Figure 3.9). The mechanism causing the faster degradation of pigments in the Cd treatments is unknown. One possibility is the direct binding of Cd to the covalent thioether bonds to cysteinyl residues that link phycobiliproteins to phycobilins (Everroad et al., 2006) causing degradation of the protein, another possibility assumes phycobiliproteins are continually made, but allocation of sulfur to other processes in the cell, such as production of low molecular weight thiols or metallothioneins, would make sulfur unavailable for use in synthesis of phycobiliproteins. This suggestion of lack of accessible sulfur combined with the observed increase in relative abundance of arylsulfatases, enzymes that scavenge sulfur from organo-sulfur compounds in times of low sulfate abundance, could be taken to imply that the cells are experiencing sulfur starvation. In this instance, however, sulfur starvation would have to be a result of phosphate limitation, because there is mM sulfate in the media. Sulfate uptake transport systems tend to require ATP (Silver and Walderhaug, 1992). In addition, the loss of pigmentation, as evidenced by the lower abundance of phycocyanin and allophycocyanin in Cd treatments compared to the control during very late stationary/death phase, (T5) agrees well with the lower cell counts attributable to cell death in the cultures.

Photosystem II

Phycobilisomes are thought to transfer excitation energy to photosystem II (PSII), but also photosystem I (Mullineaux, 1999). Three PSII proteins: PSII protein (PsbC), PSII Mn-stabilizing polypeptide, PSII chlorophyll binding protein, and a protein annotated as "chloroplast membrane associated protein 30kD protein-like" were more than two-fold differentially abundant between the control and at least one of the Cd treatments at one of the timepoints (Figure 3.10).

PSII protein (PsbC) and the PSII chlorophyll binding protein were more abundant in the control and 4.4 pM Cd^{2+} than the 44 pM Cd^{2+} during exponential growth (T1) (Figure 3.10, Table 3.2) and more abundant in the control than the Cd treatments during early stationary (T2) (Figure 3.10, Table 3.2). The PSII Mn-stabilizing polypeptide, involved in PSII water oxidation, was more abundant in the control and 4.4 pM Cd^{2+} than the 44 pM Cd^{2+} during T1 (Figure 3.10, Table 3.2). The protein annotated as "chloroplast membrane associated 30kD protein-like" was more abundant in the control than the 44 pM Cd^{2+} treatment during T1 (Figure 3.10, Table 3.2) and more abundant in the control than both Cd treatments during late stationary (T4) (Figure 3.10, Table II.6). During very late stationary/death (T5), however, it is more abundant in the 44 pM Cd^{2+} treatment than both the control and the 4.4 pM Cd^{2+} treatment (Figure 3.10, Table 3.3).

Besides the aforementioned PSII Mn-stabilizing protein, chlorophyll-binding protein and PsbC, which were lower in abundance in the Cd treatments compared to the control during growth, three other components of PSII were detected whose relative abundances either were too low or did not change dramatically between the control and Cd treatments. The fact that the PSII proteins with greater than 5 spectral counts have similar relative abundances in the Cd treatments compared to the control throughout the experiment implies that a portion of the core part of PSII does not appear to be affected by Cd. This is consistent with the reduced electron transport causing the increase in chlorophyll fluorescence. Studies have shown the direct binding of Cd^{2+} to core proteins of PSII thereby reducing electron transport (Okamura et al., 2000). PSII is comprised of D1 and D2 reaction center core proteins, CP43 (a chlorophyll *a* binding core antenna

protein associated with the reaction center), an oxygen-evolving complex and cytochrome b559. Under acclimation to low growth light, functional PSII content is approximately equal to the D1 protein content (Six et al., 2007) from (Burns et al., 2006). D1 was not observed, but core protein D2 was detected with at most three spectral counts, the fact that it is detected means this protein could be quantified using labeled peptides using a triple quadrupole mass spectrometer, which can target a specific mass range. The other two proteins had similar relative abundances among Cd treatments compared to the control: PSII complex extrinsic protein precursor (PsuB) and a putative PSII reaction center Psb28 with counts up to 42 and 19 respectively.

The PSII Mn-stabilizing polypeptide, involved in PSII water oxidation, was more abundant in the control and 4.4 pM Cd^{2+} than the 44 pM Cd^{2+} during T1 (Figure 3.10, Table 3.2). Because this protein is less abundant in the 44 pM Cd^{2+} treatment, Cd could be interfering with the stabilization of Mn. Perhaps the evolution of oxygen is similar or decreased in the 44 pM Cd^{2+} treatment compared to the control and 4.4 pM Cd^{2+} treatments, which could help to explain why an increase in oxidative stress related proteins with chronic Cd was not observed, as previously noted in *Chlamydomonas reinhardtii* (Gillett et al., 2006), until stationary phase if at all.

Similar to some carboxysome-associated proteins, like the possible carbon concentrating mechanism, the carboxysome shell peptide, and the carboxysome shell protein, the protein annotated as "chloroplast membrane associated 30kD protein-like" is more abundant in the control than the 44 pM Cd^{2+} treatment during T1 (Figure 3.13, Table 3.2) and more abundant in the 44 pM Cd^{2+} treatment than both the control and the 4.4 pM Cd^{2+} treatment during T5 (Figure 3.13, Table 3.3). This could imply some sort attempt at carbon fixation in the 44 pM Cd^{2+} treatment while the cells are lysing or perhaps the production of these proteins is upregulated by the combination of Cd exposure and cell death. In addition, many PSII proteins can be removed and yet render PSII still functional (Blankenship, 2002). Knowing this, the lack of PsbC and the PSII chlorophyll binding protein in the 44 pM Cd^{2+} treatment does not mean that PSII is nonoperational, perhaps merely less effective.

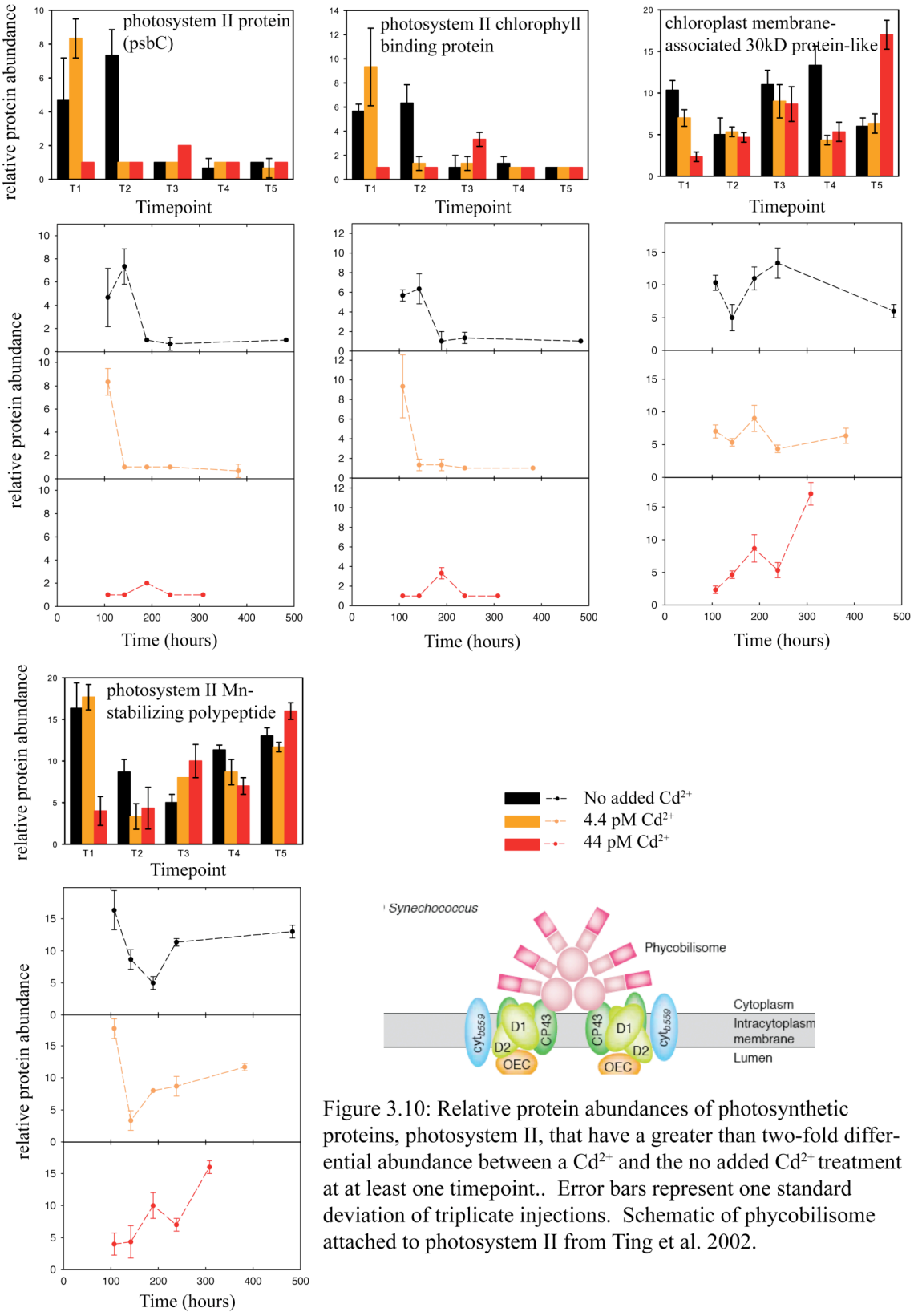

Figure 3.10: Relative protein abundances of photosynthetic proteins, photosystem II, that have a greater than two-fold differential abundance between a Cd^{2+} and the no added Cd^{2+} treatment at at least one timepoint.. Error bars represent one standard deviation of triplicate injections. Schematic of phycobilisome attached to photosystem II from Ting et al. 2002.

Photosystem I

Electrons are transferred from PSII to photosystem I (PSI). The cyclic flow of electrons through PSI generates a H^+ gradient across the thylakoid membrane, which is used to generate ATP using ATP synthase. Some of the most dramatic differences in relative protein abundance between the treatments are observed in PSI proteins. Five PSI proteins: core protein (PsaB), subunit III (PsaF), reaction center subunit II (PsaD), reaction center subunit IV (PsaE), and reaction center subunit VII (PsaC), were more than two-fold differentially abundant between the control and at least one of the Cd treatments at one of the timepoints (Figure 3.11).

PSI proteins, core protein PsaB and subunit III (PsaF) are more abundant in the control and 4.4 pM Cd^{2+} than the 44 pM Cd^{2+} treatment during exponential growth (T1) (Figure 3.11, Table 3.2). They are more abundant in the control than both Cd treatments during early stationary (T2) (Figure 3.11, Table II.2). They are similarly not abundant among all treatments throughout the remainder of stationary phase T3, T4, and T5 (Figure 3.11).

PSI reaction centers subunits II (PsaD) and IV (PsaE) are more abundant in the control and 4.4 pM Cd^{2+} than the 44 pM Cd^{2+} treatment during exponential growth (T1) (Figure 3.11, Table 3.2). They are more abundant in the control than both Cd treatments during late stationary (T4) (Figure 3.11, Table II.6). During very late stationary/death (T5), however, they are more abundant in the 44 pM Cd^{2+} treatment than both the control and the 4.4 pM Cd^{2+} treatment (Figure 3.11, Table 3.3).

PSI reaction center subunit VII (PsaC) is more abundant in the control and 4.4 pM Cd^{2+} than the 44 pM Cd^{2+} treatment during exponential growth (T1) (Figure 3.11, Table 3.2). It is more abundant in the control than both Cd treatments during early and late stationary (T2 and T4) (Figure 3.11, Tables II.2, II.6). During very late stationary/death (T5), however, it is more abundant in the 44 pM Cd^{2+} treatment than both the control and the 4.4 pM Cd^{2+} treatment (Figure 3.11, Table 3.3).

The lower relative abundance of five PSI proteins during exponential growth phase in the 44 pM Cd^{2+} treatment than both the control and the 4.4 pM Cd^{2+} treatment

(Figure 3.11, Table 3.2) suggests that there is a threshold between 4.4 and 44 pM Cd^{2+} that affects the presence of PSI proteins. More Cd may be taken up faster because it is more abundant. For example, at T1, there is less of PsaB and PsaF in 44 pM Cd^{2+} treatment, whereas at T2 there is more of PsaB and PsaF in the control than both of the Cd treatments. This suggests that the threshold was reached in the 4.4 pM Cd^{2+} treatment by T2.

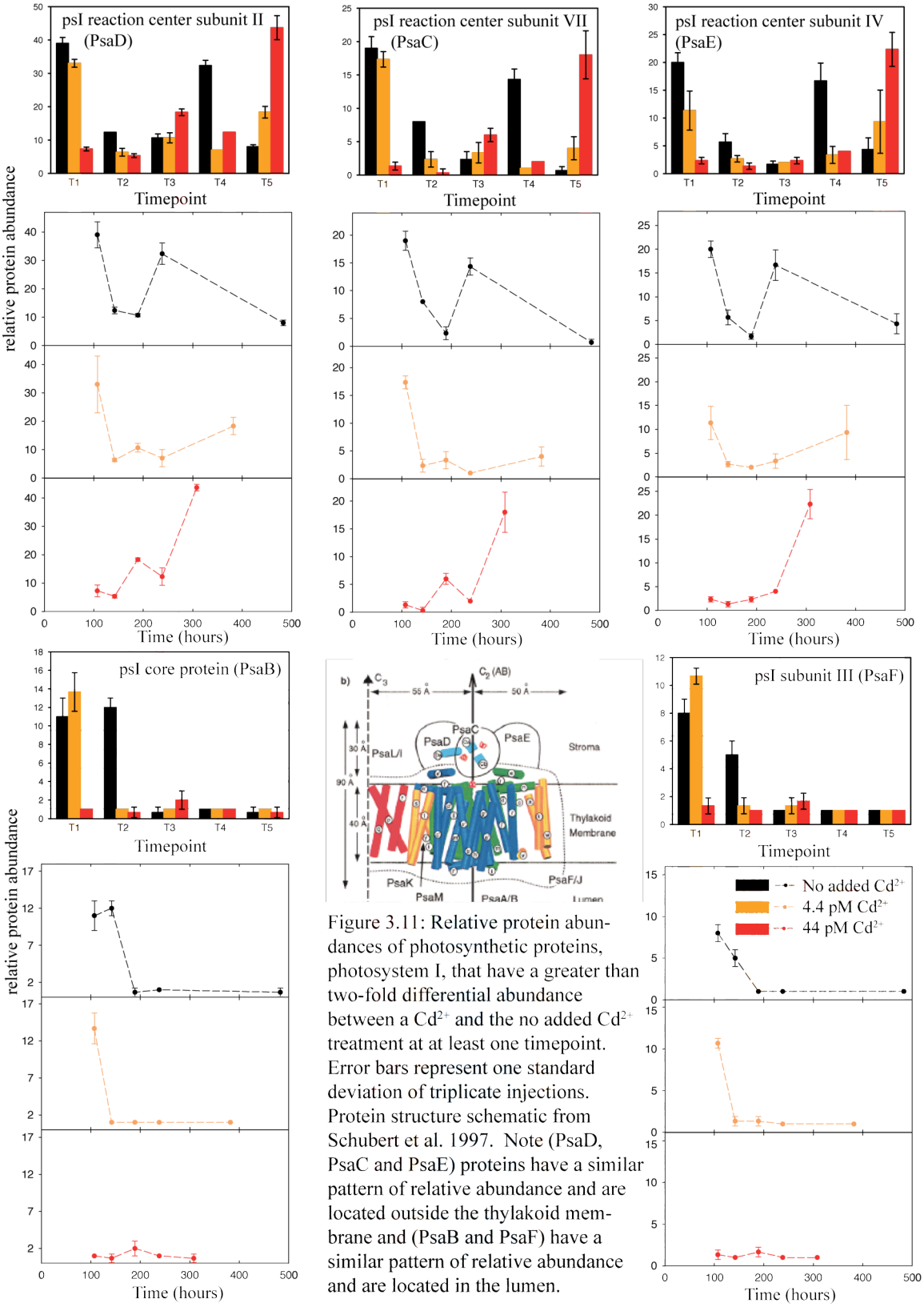

Figure 3.11: Relative protein abundances of photosynthetic proteins, photosystem I, that have a greater than two-fold differential abundance between a Cd^{2+} and the no added Cd^{2+} treatment at at least one timepoint. Error bars represent one standard deviation of triplicate injections. Protein structure schematic from Schubert et al. 1997. Note (PsaD, PsaC and PsaE) proteins have a similar pattern of relative abundance and are located outside the thylakoid membrane and (PsaB and PsaF) have a similar pattern of relative abundance and are located in the lumen.

The pattern of distribution of PSI proteins in the 44 pM Cd^{2+} treatment suggests that overall, PSI is less abundant per cell during growth and stationary phase and more abundant during death phase, similar to some of the carboxysome-associated proteins. Perhaps the presence of Cd in the quantities supplied in the 44 pM Cd^{2+} treatment blocks, inhibits or reduces the abundance of PSI proteins, leading to the eventual demise of the cell. Perhaps the death of the cells in the Cd treatments or the presence of Cd itself triggers the upregulation of photosynthesis and carbon fixation proteins. The stoichiometry of PSI to PSII in cyanobacteria is usually higher than 1:1, but can vary (Campbell et al., 1998). This idea of the reduction of cellular levels of PSI in response to metal stress is not unique; two strains of freshwater cyanobacteria grown under iron-depleted conditions reduce the cellular levels of PSI and target the phycobilisome for rapid degradation (Ting et al., 2002 and references therein). Both of these effects are observed in this iron-replete Cd-addition experiment. One could argue that an overabundance of Cd apparently displays some characteristics of a cellular iron depletion. In addition, alternative electron sinks and transport upstream of PSI involving O_2 as a major acceptor in *Synechococcus* WH8102 (Bailey et al., 2008) shows that an open ocean marine cyanobacterium could adjust to a changing PSI to PSII ratio, so adjustments in cellular PSI/PSII ratios hinted at by these changes in relative protein abundance is consistent with observations of previous researchers.

Cadmium appears to either be interfering with the regulatory network that controls the production of lumen-associated proteins, or be interfering directly with PSI proteins inside the lumen. If the former were the case, the regulator has not yet been found. If the latter were true, the question of the Cd^{2+} transfer mechanism across the lumen membrane arises.

A rise in relative protein abundances of stromal side PSI proteins with a decrease in pigmentation could be related to regulation. PsaD, PsaC and PsaE proteins after T3 are inversely correlated with the relative abundance of pigments, phycocyanin and allophycocyanin, whereas PsaB and PsaF appear not to be perhaps due to lower abundance (Figure 3.11). The control shows a drop in pigmentation at T4 and the Cd

treatments show a drop in pigmentation at T5, with corresponding rises in relative protein abundances of PsaD, PsaC and PsaE.

Three of the PSI proteins (PsaD, PsaC and PsaE) have a similar pattern of relative abundance and are located outside the thylakoid membrane. Proteins located in the thylakoid membrane, PsaB and PsaF, have a similar pattern of relative abundance and are located on the lumen side of the thylakoid membrane (Figure 3.11). The Mn-containing oxygen evolving complex of PSII is also located on the lumen side (Figure 3.10), so either the whole complex containing the manganese is assembled in the lumen, or the protein and the Mn are transported to the lumen separately and assembled. The transport of Cd^{2+} with Mn^{2+} systems across the outer membrane of eukaryotic diatoms has been observed (Sunda and Huntsman, 2000), related evidence for possible interactions of Cd^{2+} and Mn^{2+}. Related evidence for the direct interference of Cd on photosynthetic apparatus comes from a study with spinach. Cd and other heavy metals can directly replace for metals in the photosynthetic apparatus, thereby affecting photosynthesis (Sujak et al., 2005). The number of copper plastocyanins can decrease, which causes a decrease in turnover of the cytochrome b_6f electron complex, affecting the electron transfer path to PSI (Sujak et al., 2005).

Ferredoxin and ATP synthase

Electrons are transferred from photosystem I to ferredoxin and used by ATP synthase to make adenine triphosphate (ATP). Three ferredoxins: ferredoxin-NADP reductase, a possible ferredoxin (2Fe-2S), and ferredoxin-thioredoxin reductase catalytic chain and three subunits of ATP synthase were more than two-fold differentially abundant between the control and at least one of the Cd treatments at at least one of the timepoints (Figure 3.12).

Ferredoxin-NADP reductase was more abundant in the control than both of the Cd treatments during early stationary (T2) (Figure 3.12, Table II.2). It was more abundant in the control than the 44 pM Cd^{2+} treatment during very late stationary/death (T5) (Figure 3.12, Table 3.4). Ferredoxin NADP reductase was more abundant in both the Cd treatments than the control during late stationary (T4) (Table II.5).

A possible ferredoxin (2Fe-2S) was more abundant in the control and the 4.4 pM Cd^{2+} treatment than the 44 pM Cd^{2+} treatment during exponential growth (T1) (Figure 3.12, Table 3.2). It was more abundant in the control than both the Cd treatments during late stationary (T4) (Figure 3.12, Table II.6). It was more abundant in the 44 pM Cd^{2+} than either the control or 4.4 pM Cd^{2+} during very late stationary/death (T5) (Figure 3.12, Table 3.4). The relative protein abundance distribution this possible ferredoxin (2Fe-2S) is very similar to that of carboxysome-associated proteins, suggesting similar regulation (Figure 3.13).

A ferredoxin-thioredoxin reductase catalytic chain protein was more abundant in the control and the 4.4 pM Cd^{2+} treatment than the 44 pM Cd^{2+} treatment during early stationary (T2) (Figure 3.12, Table II.2). It was more abundant in the control than both of the Cd treatments during late stationary (T4) (Figure 3.12, Table II.6). This pattern suggests that the catalytic chain was inhibited by 44 pM Cd^{2+} during growth phase and the inhibition by 4.4 pM Cd^{2+} came later, perhaps after enough Cd built up inside the cells.

ATP synthase subunit A was more abundant in the 4.4 pM Cd^{2+} treatment than the 44 pM Cd^{2+} treatment during exponential growth (T1) (Figure 3.12). It was more abundant in the control than both of the Cd treatments during early and late stationary (T2 and T4) (Figure 3.12, Tables II.2, II.6). It was more abundant in both Cd treatments than the control during very late stationary/death (T5) (Figure 3.12, Table 3.3).

ATP synthase subunit B was more abundant in the control and the 4.4 pM Cd^{2+} treatment than the 44 pM Cd^{2+} treatment during exponential growth (T1) (Figure 3.12, Table 3.2). It was more abundant in the control than both of the Cd treatments during early and late stationary (T2 and T4) (Figure 3.12, Tables II.2, II.6). It was more abundant in the 44 pM Cd^{2+} treatment than the control during very late stationary/death (T5) (Figure 3.12, Table 3.3).

ATP synthase subunit C was more abundant in the control and the 4.4 pM Cd^{2+} treatment than the 44 pM Cd^{2+} treatment during exponential growth (T1) (Figure 3.12, Table 3.2). It was more abundant in the control than both of the Cd treatments during

early and late stationary (T2 and T4) (Figure 3.12, Tables II.2, II.6). ATP synthase is a protein complex comprised of multiple subunits responsible for the synthesis of ATP. In the control, ATP synthase is relatively constant to slightly decreasing T1-T3, highly abundant in T4 and not very abundant in T5. Overall, it appears that ATP synthase is less abundant in the 44 pM Cd^{2+} treatments, suggesting inhibition by Cd. As with the ferredoxin-thioredoxin reductase catalytic chain, inhibition in the 4.4 pM Cd^{2+} treatment occurred later in the experiment as inhibition in the 44 pM Cd^{2+}, suggesting inhibition after Cd buildup in the cells.

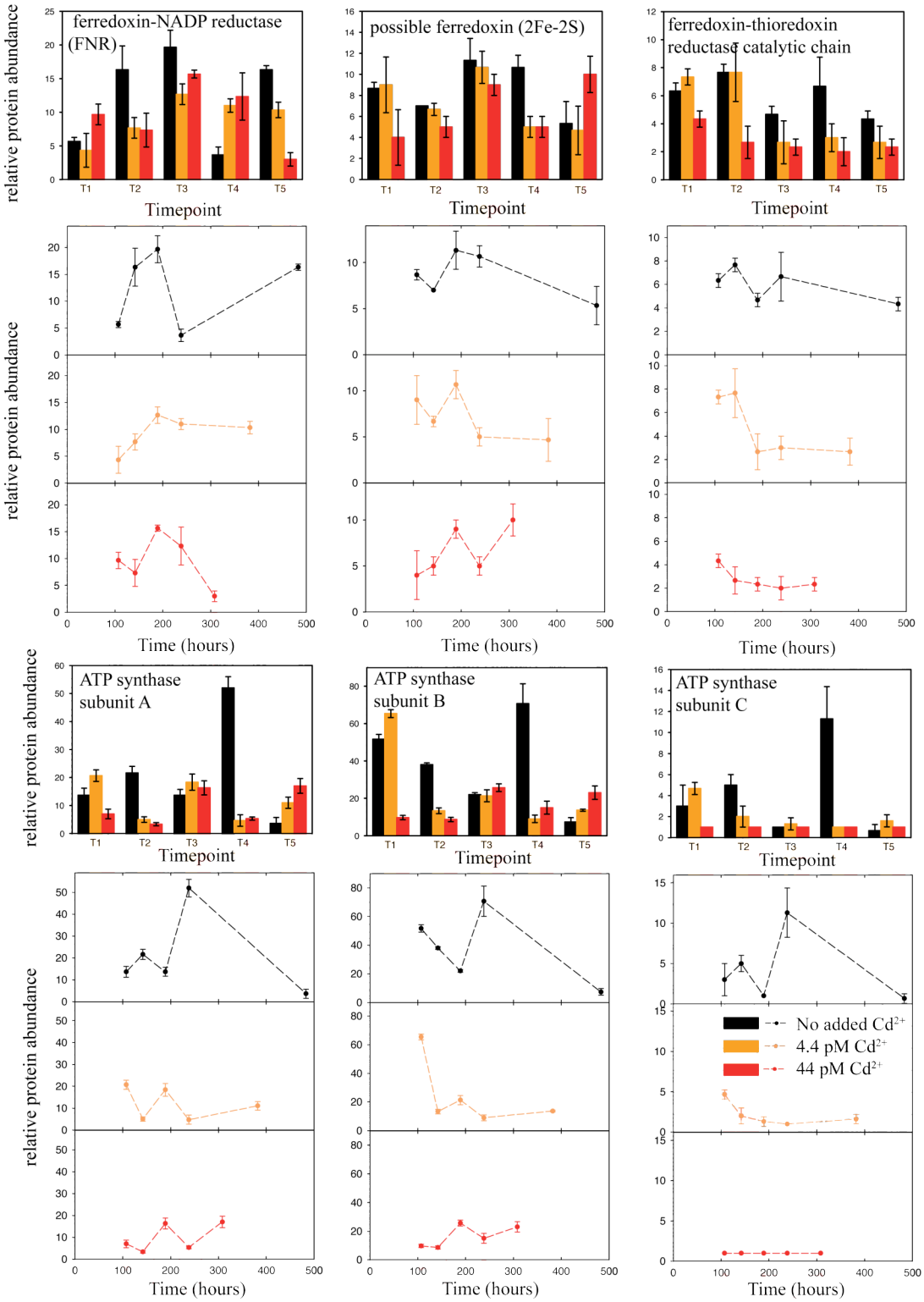

Figure 3.12: Relative protein abundances of photosynthetic proteins, ferredoxin and ATP synthase, that have a two-fold or greater differential abundance between a Cd^{2+} and the no added Cd^{2+} treatment at at least one timepoint. Error bars represent one standard deviation of triplicate injections.

During stationary phase from T3 to T4 in a Zn-deprived culture with no Cd^{2+} added, there was a temporary decrease of phycocyanin (Figure 3.9, Table II.5) and PSII protein (Figure 3.10) abundances with a concurrent increase in PSI protein abundances (Figure 3.11), carboxysome-associated proteins (Figure 3.13), and ATP synthase (Figure 3.12) suggesting that the PSI/PSII ratio increased with a concurrent increase in the production of ATP and carboxysome-associated carbon fixation. There was an unexpected decrease in the phycocyanin relative abundance in the control treatment during late stationary phase (T4) (Figure 3.9). Phycocyanin spectral counts drop from ~600 at T3 to ~200 at T4 and spike back up to ~600 at T5. This sample was colored yellow when extracted as opposed to the usual blue from phycocyanin, consistent with the lowered phycocyanin relative abundances. It is tempting to dismiss this control sample as an outlier, but three lines of evidence support the idea that it is not an outlier, but rather associated with a minor cell death incident: 1) There is an factor of 1.9 decrease in cell number from T3 to T4 suggesting cell death, 2) cluster analysis of the global protein data group the T4 no added Cd treatment with T5 Cd treatments, which were experiencing cell death, and 3) many of the relative abundance distributions of other proteins make sense in their overall distributions i.e. they do not have unexpected spectral counts at T4. Proteins with spectral count distributions consistent with the rest of the timepoints are: possible ferredoxin (Figure 3.12); ferredoxin-thioredoxin reductase catalytic chain (Figure 3.12); ribulose 1,5 bisphosphate carboxylase (Figure 3.13); S-adenosylmethionine synthetase (Figure 3.16); rehydrin (Figure 3.17) and superoxide dismutase (Figure 3.17), among others. Proteins with abundances that decrease dramatically with phycocyanin in the no added Cd at T4 are: allophycocyanin (Figure 3.9); ferredoxin-NADP reductase (Figure 3.12); malate oxidoreductase (Figure 3.14); aspartate aminotransferase (Figure 3.14); glyceraldehydes-3-phosphate dehydrogenase (Figure 3.14); transketolase (Figure 3.14); phosphoglycerate kinase (Figure 3.14); arylsulfatase (Figure 3.15) and cysteine synthase A (Figure 3.16), among others. Proteins with abundances that increased dramatically opposite the drop in phycocyanin in the control at T4 are: PSII Mn-stabilizing polypeptide (Figure 3.10), PSI reaction center

subunit II (PsaD) (Figure 3.11), PSI reaction center subunit IV (PsaE) (Figure 3.11), PSI reaction center subunit VII (PsaC) (Figure 3.11), three subunits of ATP synthase (Figure 3.12), carboxysome shell protein and peptide (Figure 3.13), possible CcmK (Figure 3.13), ribulose 5-phosphate isomerase (Figure 3.14), among others. This suggests a change in regulation of these groups of proteins, perhaps triggered by cell death.

During the transition from stationary phase to death phase (T3-T5) in a Zn-deprived culture with 44 pM Cd^{2+} added, similar to the control, there was a decrease of phycocyanin (Figure 3.9) and PSII proteins (Figure 3.10) with a concurrent increase in PSI (Figure 3.11) and carboxysome-associated proteins (Figure 3.13). Unlike the control, the abundance of ATP synthase remained low throughout the time course for this treatment (Figure 3.12). Many, but not all of the same proteins change in similar ways to the control from T3 to T4. The protein abundances that drop dramatically with the phycocyanin in Cd and the control are: allophycocyanin (Figure 3.9), ferredoxin-NADP reductase (Figure 3.12), malate oxidoreductase (Figure 3.14), aspartate aminotransferase (Figure 3.14), transketolase (Figure 3.14), arylsulfatase (Figure 3.15), and cysteine synthase A (Figure 3.16). The protein abundances that drop dramatically with the phycocyanin in 44 pM Cd^{2+} and not in the control are: ribulose phosphate 3-epimerase (Figure 3.14), ribulose 1,5 bisphosphate carboxylase (Figure 3.13), triose phosphate isomerase (Figure 3.14), putative arylsulfatase (Figure 3.15), S-adenosylmethionine synthetase (Figure 3.16), 5' methylthioadenosine phosphorylase, and superoxide dismutase (Figure 3.17) among others. This suggests a similar downregulation of these proteins with cell death, but additional downregulation with Cd.

The protein abundances that increase dramatically opposite the drop in pigmentation are also found to have the same pattern in the control: photosystem II Mn-stabilizing polypeptide (Figure 3.10), chloroplast membrane-associated 30kD protein-like (Figure 3.10), PSI reaction center subunit II (Figure 3.11), PSI reaction center subunit IV (psaE) (Figure 3.11), PSI reaction center subunit VII (PsaC) (Figure 3.11), carboxysome shell protein (Figure 3.13), carboxysome shell peptide (Figure 3.13), possible CcmK (Figure 3.13), among others. This supports the idea of a similar upregulation in these

proteins with cell death. In summary, during stationary phase in a Zn-deprived culture with 44 pM Cd^{2+} added, there is a decrease of PSII pigmentation with a concurrent increase in PSI and carboxysome-associated proteins, but the abundance of ATP synthase remains low throughout the time course for this treatment. This suggests that similar to the control, ribulose 1,5 bisphosphate carboxylase levels are low, the PSI/PSII ratio increases with a concurrent increase in attempted carboxysome-associated carbon fixation, but contrary to the control, the ATP production could be limited because of the lower abundance of ATP synthase. Direct measurements of ATP were not made, but limited ATP production by the light driven electron flow could cause a cascade of negative effects, including decrease in active transport of HCO_3^- into the cell cytosol, which could provoke an increase in quantity of carboxysomes in order to produce the same amount of carbon dioxide for ribulose 1,5 bisphosphate carboxylase to fix (Figure 3.13). If carbonic anhydrase were detectable, one might also expect this relative abundance of this enzyme to increase. A decrease in ATP production may decrease the active transport of nitrate and phosphate. This could link Cd to the nutrient phosphate, but also nitrate and carbon. Ribulose 1,5 bisphosphate carboxylase did not appear to respond to the dramatic decrease in phycocyanin observed in the control at T4; it had steadily decreased in relative abundance since T2. Ribulose 1,5 bisphosphate carboxylase was also decreased in abundance in the 44 pM Cd^{2+} treatment from T3 to T5, however, similar to the control this decrease did not appear to be related to the decline in phycocyanin.

Carbon fixation - carboxysome associated

The products of the light reactions of photosynthesis and CO_2 are used in carbon fixation. Cyanobacteria can concentrate CO_2 using a carbon concentrating mechanism involving the cell membrane and conversion to HCO_3^-. The HCO_3^- is taken into the carboxysome where carbonic anhydrase converts it back to CO_2. Carboxysomes are polyhedral crystalline structures found in cyanobacteria. In literature older then fifty years, they used to be referred to as polyhedral bodies, but in the 70's they were discovered to be structures related to photosynthesis (Yeates et al., 2008). Structural

studies of the carboxysome shell itself suggest that it controls metabolite flow into and out of the carboxysome (Kerfeld, 2005). The high density of ribulose 1,5 bisphosphate carboxylase concentrated in the carboxysome combines a molecule of CO_2 with a molecule of ribulose 1,5 bisphosphate and water to form two molecules of glycerate-3-phosphate, or PGA. Ribulose 1,5 bisphosphate carboxylase is the most abundant protein in the world (Ellis, 1979) and accounts for 70% of the carboxysome by weight, with the main shell proteins accounting for 17% of the carboxysome (Yeats et al., 2008). Although we did not detect a carbonic anhydrase, we observed four carboxysome-associated proteins more than two-fold differentially abundant between the control and at least one of the Cd treatments at one of the timepoints: a possible carbon concentrating mechanism protein, the carboxysome shell protein, the carboxysome shell peptide and the small subunit of ribulose 1,5 bisphosphate carboxylase (Figure 3.13). As with PSI proteins, some of the most dramatic differences in relative protein abundance between the treatments are observed in these carboxysome-associated proteins.

The possible carbon concentrating mechanism protein (CcmK), carboxysome shell peptide and carboxysome shell protein showed similar relative abundances distributions with one difference (Figure 3.13). These proteins were more abundant in the control and 4.4 pM Cd^{2+} than the 44 pM Cd^{2+} treatment during exponential growth (T1) (Figure 3.13, Table 3.2). They were more abundant in the control than both of the Cd treatments during late stationary (T4) (Figure 3.13, Table II.6). During very late stationary/death (T5), however, the possible CcmK and carboxysome shell peptide proteins were more abundant in the 44 pM Cd^{2+} than either the control or 4.4 pM Cd^{2+}, whereas the carboxysome shell protein was more abundant in both of the Cd treatments relative to the control (Figure 3.13, Table 3.3).

The small subunit of ribulose 1,5 bisphosphate carboxylase (rubisco), the enzyme with a Mg^{2+} cofactor that catalyzes the first step of the Calvin cycle, was more abundant in both of the Cd treatments relative to the control during mid-stationary (T3) (Figure 3.13, Table II.3). It was more abundant during growth, early and mid-stationary (T1, T2, T3) than late stationary and very late stationary/death (T4, T5) (Figure 3.13).

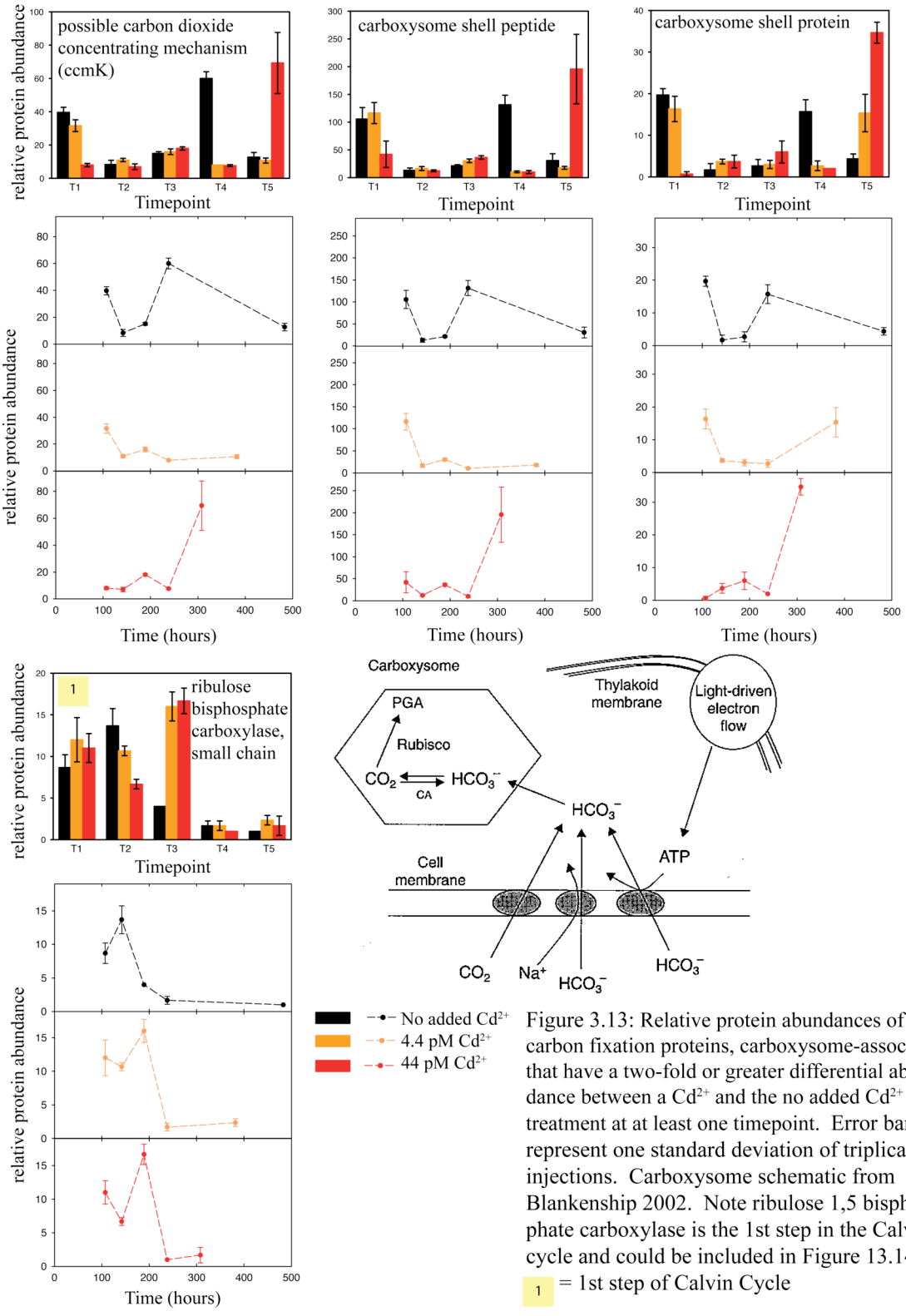

Figure 3.13: Relative protein abundances of carbon fixation proteins, carboxysome-associated, that have a two-fold or greater differential abundance between a Cd^{2+} and the no added Cd^{2+} treatment at at least one timepoint. Error bars represent one standard deviation of triplicate injections. Carboxysome schematic from Blankenship 2002. Note ribulose 1,5 bisphosphate carboxylase is the 1st step in the Calvin cycle and could be included in Figure 13.14.

1 = 1st step of Calvin Cycle

As with PSI proteins, some of the most dramatic differences in relative protein abundance between the treatments are observed in these carboxysome-associated proteins (Figure 3.13, Tables 3.2, II.2, II.3, II.6, 3.3). We see other parts of the carboxysome, the shell protein, the shell peptides, and the small subunit of rubisco. We do not detect the large subunit of rubisco, or carbonic anhydrase.

The small subunit of ribulose 1,5 bisphosphate carboxylase was highly abundant during mid-stationary phase (T3) in both of the Cd treatments, whereas it had already begun to drop in the control treatments. A higher abundance of this protein could indicate more function, or more presence with lack of function.

The greater abundance of the small subunit of rubisco during exponential growth, early, and mid-stationary (T1, T2, T3) than late stationary and very late stationary/death (T4, T5) (Figure 3.13) suggests that the conversion of carbon dioxide to PGA is more active during exponential growth phase. At T3, when rubisco and arylsulfatase relative abundances spike and the chlorophyll/phycoerythrin ratios start to change for the Cd treatments, rubisco is decreasing in the control treatment.

The similar distribution of the possible carbon concentrating mechanism (CcmK), carboxysome shell peptide, and carboxysome shell protein indicates that these three proteins could be transcriptionally related.

Because the only known nutritive use of Cd so far has been in a carbonic anhydrase in the diatom *T. weissflogii*, the detection of carbonic anhydrases is desirable (see future directions). *Synechococcus* WH5701 has an annotated carbonic anhydrase, a possible carbonic anhydrase, a carbonic anhydrase-like protein, and carboxysome shell polypeptide, the latter with high similarities to β-carbonic anhydrases.

Carbon fixation - Calvin cycle proteins

The products of the light reactions of photosynthesis, along with CO_2 are used in carbon fixation, the Calvin cycle. Six proteins involved in the Calvin cycle, a 12 step enzymatic process, were more than two-fold differentially abundant between the control and at least one of the Cd treatments during one of the growth phases (Figure 13.14). These 6 proteins are the aforementioned small subunit of rubisco (Step 1),

phosphoglycerate kinase (Step 2), glyceraldehyde-3-phosphate dehydrogenase ($NADP^+$; phosphorylating) (Step 3), triosephosphate isomerase (Step 4), transketolase (Steps 7 and 10), ribose 5-phosphate isomerase (Step 12) (Figure 13.14). Three other proteins involved in carbon fixation were also differentially abundant. These proteins are malate oxidoreductase, aspartate aminotransferase, and ribulose-phosphate-3-epimerase.

Phosphoglycerate kinase, step 2 of the Calvin cycle, catalyzes the reaction of glycerate-3-phosphate (PGA), and ATP to 1,3 bisphosphoglycerate (BPG) and ADP. It was more abundant in the control than both of the Cd treatments during early stationary and very late stationary/death (T2 and T5) (Figure 13.14, Tables II.2, 3.4).

Glyceraldehyde-3-phosphate dehydrogenase ($NADP^+$; phosphorylating), step 3 of the Calvin cycle, catalyzes the reaction of BPG and NADPH to glyceraldehyde-3-phosphate (GAP) and $NADP^+$. It was more abundant in the 44 pM Cd^{2+} than the control and 4.4 pM Cd^{2+} treatments during exponential growth (T1) (Figure 13.14, Table 3.1). It was more abundant in the control than both of the Cd treatments during mid-stationary (T3) (Figure 13.14, Table II.4). During very late stationary/death (T5), it was more abundant in the control than the 4.4 pM Cd^{2+} treatment (Figure 13.14, Table 3.4).

Triosephosphate isomerase, step 4 of the Calvin cycle catalyzes the reaction of GAP to dihydroxyacetone phosphate (DHAP). It is more abundant in the control than the 44 pM Cd^{2+} treatment during late stationary/death (T5) (Figure 13.14, Table 3.4).

Transketolase, steps 7 and 10 of the Calvin cycle, catalyzes the reaction of fructose 6-phosphate (F6P) and GAP to erythrose 4-phosphate (E4P) and xyulose 5-phosphate (X5P) in step 7 and the reaction of sedoheptulose 7-bisphosphate (S7P) and GAP to ribose 5-phosphate (R5P) and X5P in step 10. Transketolase is more abundant in the 44 pM Cd^{2+} treatment than the control during exponential growth (T1) (Figure 13.14, Table 3.1). It is more abundant in both Cd treatments than the control during late stationary (T4) (Figure 13.14, Table II.5). It is more abundant in the control than both Cd treatments during very late stationary/death (T5) (Figure 13.14, Table 3.4).

Ribose 5-phosphate isomerase, step 12 of the Calvin cycle, catalyzes the reaction of R5P to ribulose 5-phosphate (Ru5P). It is more abundant in the control than both Cd

treatments during late stationary (T4) (Figure 13.14, Table II.6). It is more abundant in the control and the 4.4 pM Cd^{2+} treatment than the 44 pM Cd^{2+} treatment during very late stationary/death (T5) (Figure 13.14, Table 3.4).

Malate oxidoreductase is more abundant in the 44 pM Cd^{2+} treatment than the control and the 4.4 pM Cd^{2+} treatment during growth (T1) (Figure 13.14, Table 3.1). It is more abundant in both Cd treatments than the control during late stationary (T4) (Figure 13.14, Table II.5). During very late stationary/death (T5), however, it is more abundant in the control than both Cd treatments (Figure 13.14 and Table 3.4).

As well as being involved in carbon fixation, aspartate aminotransferase is also involved in amino acid metabolism, including cysteine. Like malate oxidoreductase, it is more abundant in the 44 pM Cd^{2+} treatment than the control and the 4.4 pM Cd^{2+} treatment during exponential growth (T1) (Figure 13.14, Table 3.1) and is more abundant in both Cd treatments than the control during late stationary (T4) (Figure 13.14, Table II.5). During very late stationary/death (T5), however, unlike malate oxidoreductase, it is more abundant in both the control and the 4.4 pM Cd^{2+} treatment than the 44 pM Cd^{2+}treatment (Figure 13.14, Table 3.4).

Ribulose-phosphate-3-epimerase catalyzes the reaction of R5P into X5P. It is more abundant in the control than the 4.4 pM Cd^{2+} treatment during exponential growth phase (T1) (Figure 13.14, Table 3.2). It is more abundant in the control than the 44 pM Cd^{2+} during very late stationary/death (T5) (Figure 13.14, Table 3.4).

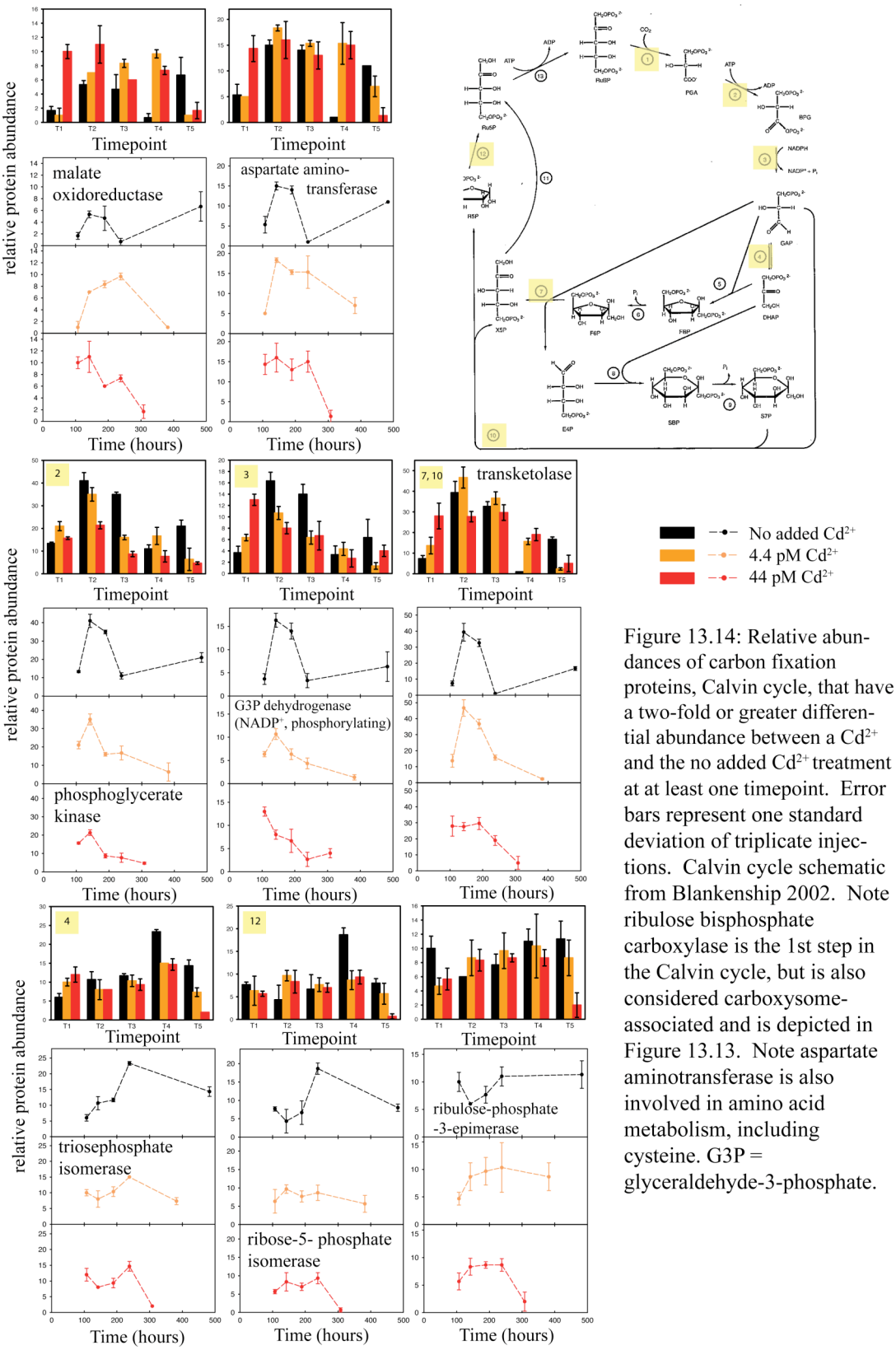

Figure 13.14: Relative abundances of carbon fixation proteins, Calvin cycle, that have a two-fold or greater differential abundance between a Cd^{2+} and the no added Cd^{2+} treatment at at least one timepoint. Error bars represent one standard deviation of triplicate injections. Calvin cycle schematic from Blankenship 2002. Note ribulose bisphosphate carboxylase is the 1st step in the Calvin cycle, but is also considered carboxysome-associated and is depicted in Figure 13.13. Note aspartate aminotransferase is also involved in amino acid metabolism, including cysteine. G3P = glyceraldehyde-3-phosphate.

Many of these proteins have relative abundance distributions opposite that of the carboxysome-associated proteins (Figures 3.13, 3.14). The Calvin cycle is affected by Cd: 6 of the 12 enzymes involved in the Calvin cycle and three other proteins were more than two-fold differentially abundant between the control and at least one of the Cd treatments at one of the time points (Figure 3.14).

Five proteins show a similar distribution pattern with 3 of the 6 Calvin cycle enzymes along with two of the other proteins; they are phosphoglycerate kinase (Step 2), glyceraldehyde-3-phosphate dehydrogenase ($NADP^+$; phosphorylating) (Step 3), transketolase (Steps 7 and 10), malate oxidoreductase, and aspartate aminotransferase (Figure 3.14). Three more proteins have similar distributions to one another: triosephosphate isomerase (Step 4), ribose 5-phosphate isomerase and ribulose phosphate 3-epimerase (Figure 3.14). Rubisco has a unique distribution among the 9 proteins, most resembling the 5 proteins with a similar distribution pattern (Figure 3.13). Overall, many of the Calvin cycle enzymes are affected in a similar way, suggesting similar regulation.

Arylsulfatases

Two proteins involved in steroid and lipid biosynthesis, an arylsulfatase and a putative arylsulfatase, showed dramatic differential abundances throughout this experiment. These arylsulfatases were more than two-fold differentially abundant between the control and at least one of the Cd treatments at three of the timepoints (Figure 3.15). At least one of these proteins was differentially abundant at every timepoint.

The arylsulfatase was more abundant in both Cd treatments than the control during exponential growth (T1) (Figure 3.15, Table 3.1). It was more abundant in the control and 4.4 pM Cd^{2+} treatment than the 44 pM Cd^{2+} treatment during early stationary (T2) (Figure 3.15, Table II.2). During very late stationary/death (T5), however, it was more abundant in the control than the Cd treatments (Figure 3.15, Table 3.4).

The putative arylsulfatase showed a distribution similar to the arylsulfatase in that it was more abundant in both Cd treatments than the control during exponential growth (T1), although unlike the arylsulfatase it was also twice as abundant in the 44 pM Cd^{2+} as

the 4.4 pM Cd^{2+} (Figure 3.15, Table 3.1). Unlike the arylsulfatase, the putative arylsulfatase was more abundant in both Cd treatments than the control during mid-stationary (T3) (Figure 3.15, Table II.3). Like the arylsulfatase, as the experiment progressed through the last two stationary phases, the protein was more abundant in the control compared to the two Cd treatments. For the putative arylsulfatase, this occurred in late stationary (T4) (Figure 3.15, Table II.6), compared to the arylsulfatase in which the greater abundance in the control than the Cd treatment occurred in very late stationary/death (T5).

Combining the relative abundances of the arylsulfatases, the same overall trends remain with greater abundance in the Cd treatments than the control during exponential growth (T1) (Figure 3.15 and Table 3.1), in the control and 4.4 pM Cd^{2+} treatment than the 44 pM Cd^{2+} treatment during early stationary (T2) (Figure 3.15 and Table II.2), in both Cd treatments than the control during mid-stationary (T3) (Figure 3.15 and Table II.3) and in the control than both Cd treatments during very late stationary/death (T5) (Figure 3.15 and Table 3.4).

Sulfur metabolism is linked with lipid and steroid biosynthesis. The involvement of arylsulfatases in steroid and lipid biosynthesis is directly related to sulfur metabolism. Arylsulfatases remove sulfate groups from carbohydrates and other compounds. In *Chlamydomonas reinhardtii* the presence of arylsulfatases implies sulfur starvation (Zhang et al., 2004). We see an over abundance of arylsulfatases in the Cd treatments relative to the control during exponential growth (T1). This could imply that the Cd treatments are procuring sulfur from sulfate esters. The extra sulfur could be used to synthesize cysteine, which can be used to make glutathione, other small thiols and possibly metallothionein, all of which could bind Cd. Sulfate, cysteine, and other components of the cysteine biosynthesis pathway have been shown to repress arylsulfatase formation in different ways in different bacteria, suggesting regulation of this enzyme (Fitzgerald, 1976 and references therein). This supports the hypothesis that Cd is being bound by cysteine or other thiols comprised of cysteine, causing a shortage, activating the formation of arylsulfatases to produce more cysteine. In a different study,

the arylsulfatase from *Helix pomatia*, a snail, was activated by Cd^{2+}in solution; the authors suggested the recovery of sulfate for the ensuing processing of Cd (Tokheim et al., 2005).

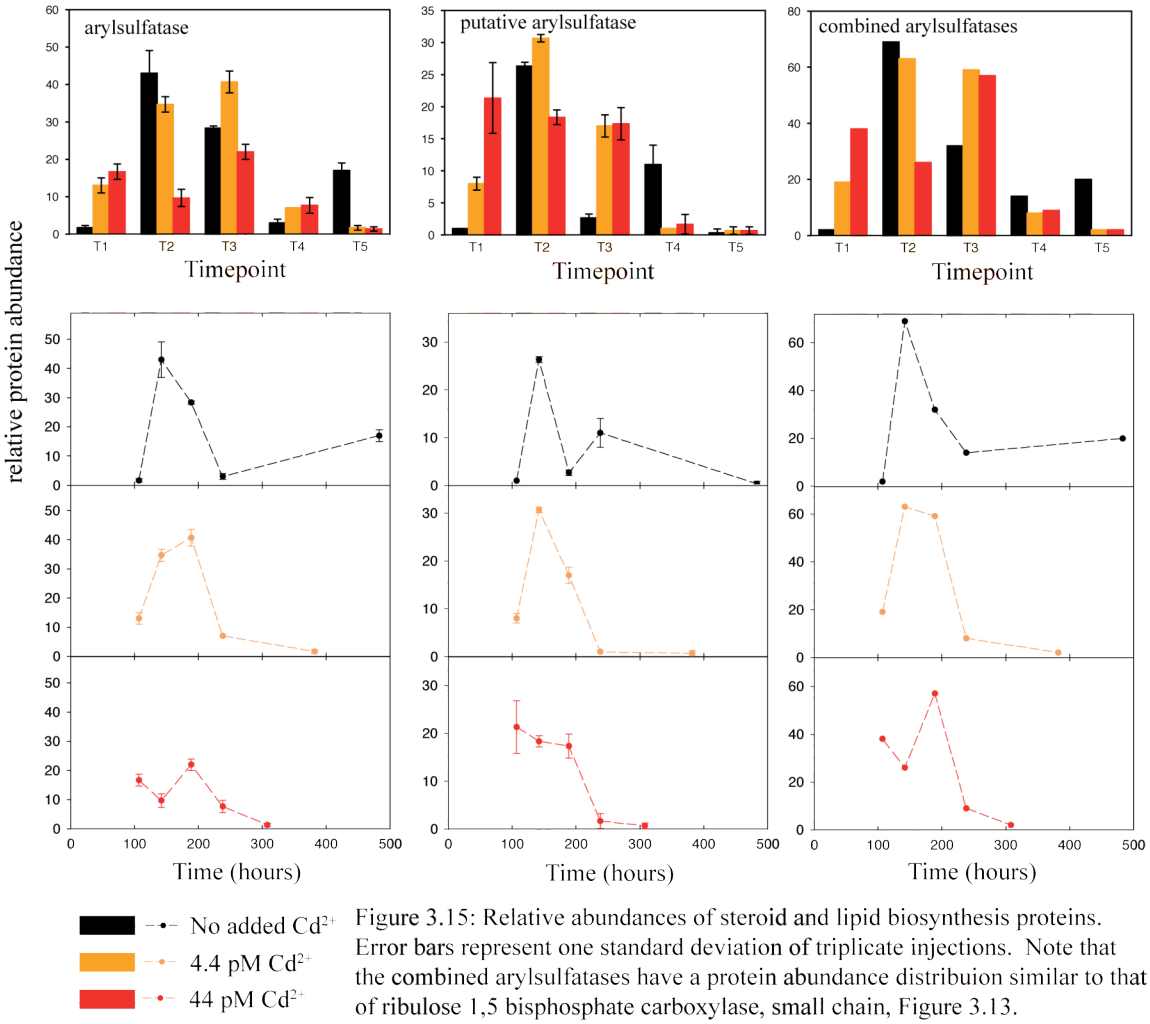

Figure 3.15: Relative abundances of steroid and lipid biosynthesis proteins. Error bars represent one standard deviation of triplicate injections. Note that the combined arylsulfatases have a protein abundance distribuion similar to that of ribulose 1,5 bisphosphate carboxylase, small chain, Figure 3.13.

In humans, arylsulfatases are found in lysosomes in the brain. A deficiency of arylsulfatases causes lysosomal storage disease, a disorder that affects the myelin sheath around nerve cells and results in the accumulation of sulfatide, which in turn affects trafficking homeostasis. The presence of sulfatases is the earliest sign of Alzheimers disease, metachromatic leukodystrophy. In cyanobacteria, we noticed a higher mortality rate in treatments with added Cd, and the differences in arylsulfatases relative abundances were among the most notable. The Cd treatments have more arylsulfatases in exponential growth phase and the control had a high abundance of them during stationary

phase, perhaps indicating sulfur starvation or some stationary phase process. The presence of arylsulfatases observed in this experiment could be a sign of cellular death and destruction in cyanobacteria (see future directions). The increased exposure to Cd could result in the induction of apoptosis by an as yet unknown mechanism. This mechanism could be related to Zn, the observed disturbance in carbon metabolism, the observed disturbance in sulfur metabolism, or perhaps an interference with calcium (Ca). Cd and Ca have similar atomic radii (Ca^{2+}-1.06 A compared to Cd^{2+} -1.03 A, Goldschmidt, 1964). In mammalian cells, calcium is associated with apoptosis, but these pathways are poorly understood and undocumented in cyanobacteria.

The arylsulfatase and putative arylsulfatase showed dramatic differential protein abundances throughout this experiment. These arylsulfatases were more than two-fold differentially abundant between the control and at least one of the Cd treatments at three of the time points (Figure 3.15). At least one of these proteins was differentially abundant at every time point.

Judging by the combined arylsulfatase relative protein abundance distributions in the control, arylsulfatases are not abundant during growth, become abundant upon the transition to stationary phase, and decrease to a steady level of moderate abundance (Figure 3.15). Abundances in the Cd treatments do not follow this distribution, both having greater abundances than the control during growth and low abundances during death phase (T5) (Figure 3.15, Tables 3.1, II.2, II.3, II.6, 3.4). The 4.4 pM Cd^{2+} treatment mimics the control in the drastic increase of arylsulfatase upon the transition to stationary phase, but unlike the control the 4.4 pM Cd^{2+} treatment maintains arylsulfatase abundance through mid-stationary phase (T3) before dropping to late stationary phase (T4) low abundances. The 44 pM Cd^{2+} has moderately high abundances during growth phase, unlike the control and 4.4 pM Cd^{2+} treatment and does not spike in the transition to stationary phase (T2), but does spike during mid-stationary (T3), then declines rapidly. This pattern suggests that arylsulfatases are important in the transition to stationary phase and cells require some level of arylsulfatases throughout stationary phase. The transition to stationary phases may involve changes in many aspects of cellular metabolism,

perhaps including protein synthesis, cellular growth, rearrangement of lipids and degradation of phycobilisomes. Cd disrupts this pattern presumably by interfering in cysteine metabolism. Also, in a possible link to carbon metabolism, the combined arylsulfatase protein distributions actually look similar to that of the small subunit of 1,5 ribulose bisphosphate carboxylase.

It is interesting to note that the scavenging of phosphorus can occur in WH5701. Sulfolipids can be used instead of phospholipids under conditions of phosphate limitation (Van Mooy et al., 2006). The cultures in this experiment are phosphate replete, so one might not expect there to be sulfolipids. Sulfolipids in this experiment, then, would probably not be the substrate for arylsulfatases. The substrate for the arylsulfatases is unknown. We do observe that in the presence of Cd, there is a faster decline in relative abundance of pigments, which contain thioether linkages. Perhaps thioether linkages are a source of organic sulfur substrate for arylsulfatases.

Sulfur and cysteine metabolism

Five proteins involved in sulfur and/or cysteine metabolism were $\geq$ two-fold differentially abundant between the control and at least one of the Cd treatments (Figure 3.16). These proteins are aspartate aminotransferase (already presented in Figure 3.14, carbon fixation - Calvin cycle and others), cysteine synthase A, S-adenosylmethionine synthetase, 5' methylthioadenosine phosphorylase and glutamate synthetase type III.

Cysteine synthase catalyzes the reaction of O^3-acetyl-L-serine and hydrogen sulfide to form L-cysteine and acetate. It was more abundant in both Cd treatments than the control during late stationary phase (T4) (Figure 3.16, Table II.5). It was more abundant in the control than the 44 pM Cd^{2+} treatment during very late stationary/death (T5) (Figure 3.16, Table 3.4).

S-adenosylmethionine synthetase catalyzes the reaction of methionine, ATP and water to S-adenosylmethionine, phosphate and diphosphate. It was more abundant in the 44 pM Cd^{2+} treatment than the control during exponential growth (T1) (Figure 3.16, Table 3.1). During very late stationary/death (T5), however, it was more abundant in the control than the Cd treatments (Figure 3.16, Table 3.4).

5' methylthioadenosine phosphorylase was more abundant in the 4.4 pM Cd^{2+} than the control during mid-stationary (T3) (Figure 3.16, Table II.3). It was more abundant in both of the Cd treatments than the control during late stationary (T4) (Figure 3.16, Table II.5). During very late stationary/death (T5), however, it was more abundant in the control than the Cd treatments (Figure 3.16 and Table 3.4).

Glutamate synthetase type III uses ATP to catalyze the reaction of NH_3 and glutamate to form glutamine, hence it is also important in nitrogen metabolism. It was more abundant in the 44 pM Cd^{2+} treatment than the control during exponential growth (T1) (Figure 3.16, Table 3.1). It was more abundant in the control than the 44 pM Cd^{2+} treatment during early stationary (T2) (Figure 3.16, Table II.2). It was more abundant in the control and the 4.4 pM Cd^{2+} than the 44 pM Cd^{2+} treatment during mid-stationary (T3) (Figure 3.16, Table II.4). It was more abundant in both Cd treatments than the control and in addition was more abundant in the 4.4 pM Cd^{2+} than the 44 pM Cd^{2+} treatment during late stationary (T4) (Figure 3.16, Table II.5). During very late stationary/death (T5) it was more abundant in the control than the Cd treatments and was more abundant in the 44 pM Cd^{2+} than the 4.4 pM Cd^{2+} treatment (Figure 3.16, Table 3.4).

In addition to the arylsulfatase and putative arylsulfatase, 5 proteins involved in sulfur and/or cysteine metabolism were $\geq$ two-fold differentially abundant between the control and at least one of the Cd treatments during at least one of the growth phases (Figure 3.16, Tables 3.1, II.2, II.3, II.5, 3.4). These proteins are cysteine synthase A, S-adenosylmethionine synthetase, 5' methylthioadenosine phosphorylase, and glutamate synthetase type III. Cd appears to affect sulfur and cysteine metabolism. Low molecular weight thiols and metallothioneins are known to bind metals. In this experiment, metallothioneins were detected when protein tolerances were lowered, but in small amounts. Quantification using a triple quadrupole mass spectrometer would allow quantification of this protein. In a repeat experiment, particulate and dissolved total and reduced thiols were measured by HPLC by Tristan Kading. During late log/early stationary phase (judging by fluorescence data) in only the 44 pM Cd^{2+} treatment, a pool

of circa 1 to 10 nM particulate total glutathione is present, presumably oxidized glutathione. These data support an alteration in sulfur and cysteine metabolism in the presence of Cd^{2+}.

Glutathione is a tri-peptide containing the amino acids glutamate, cysteine and glycine. If the 44 pM Cd^{2+} treatment produced a high amount of glutathione, it would have needed greater amount of glutamate and glycine in addition to cysteine, which would result in increased need for nitrogen. Glutamate is also the structural base for δ-aminolevulinic acid, which becomes porphobilinogen. As discussed in the chlorophyll biosynthesis section (Figure 3.8) increased relative abundances of glutamate-1-semialdehyde transferase and δ-aminolevulinic acid dehydratase could imply that this pathway was more active in the high Cd treatment, which would require greater quantities of glutamate. Increased abundances of arylsulfatases as discussed (Figure 3.15) could imply a greater need for sulfur, which could be used to make cysteine. There is also a polar amino acid transport system substrate-binding protein, WH5701_11799 that is more than two-fold greater in abundance in the Cd treatments during exponential growth phase (T1) (Table 3.1). Glycine and cysteine are polar amino acids. Also, it is interesting to note that low levels of cysteine were measured in the media of a repeat experiment and these levels were highest in the control (Kading and Cox et al., unpublished data). Taken together with the upregulated amino acid transporter, the cells may be importing cysteine. In addition, aspartate aminotransferase, involved in the Calvin cycle and also amino acid synthesis was more abundant in the high Cd treatment than the control (Figure 3.14, Table 3.1). All of these data are consistent with the idea that the cells are making sulfur compounds, in this case glutathione, to perhaps ameliorate exposure to chronic Cd^{2+}.

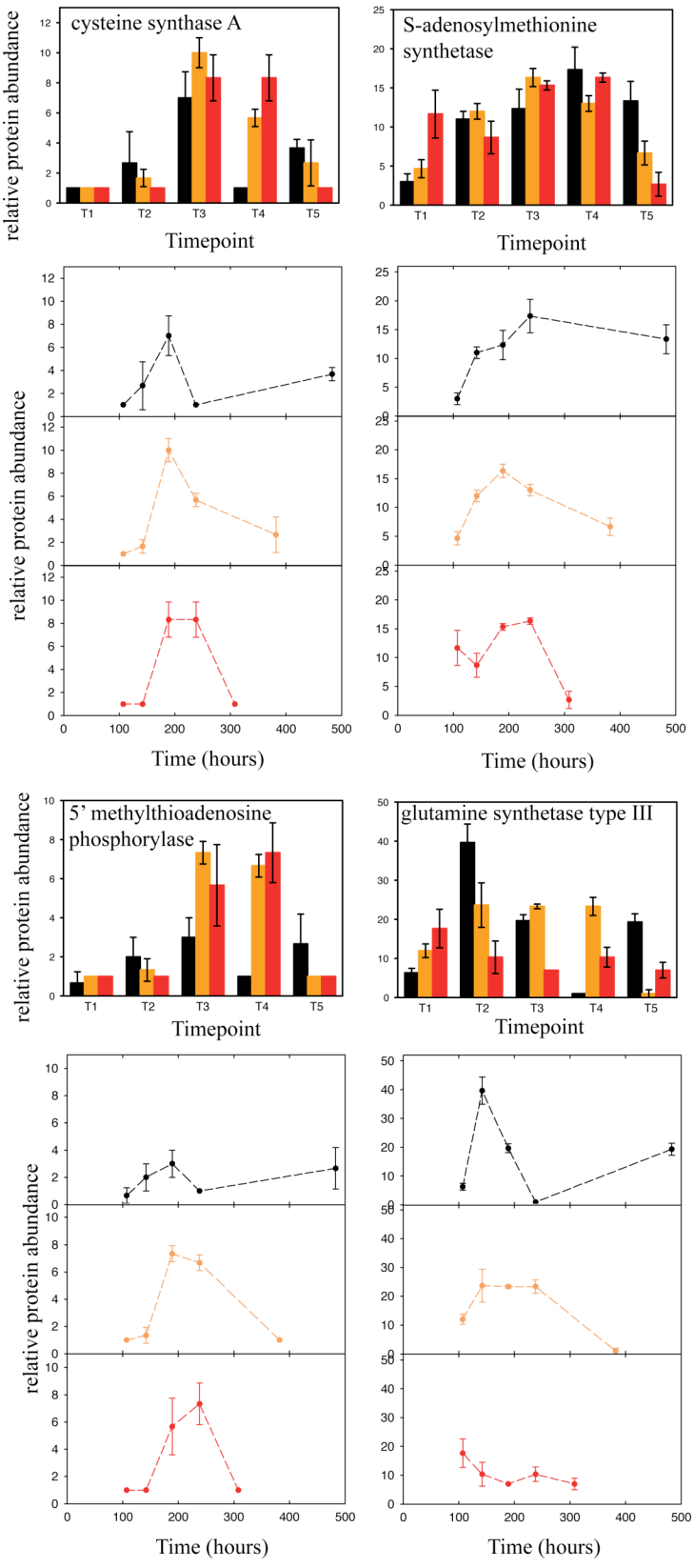

Figure 3.16: Relative abundances of proteins involved in sulfur and/or cysteine metabolism. Error bars represent one standard deviation of triplicate injections. Note aspartate aminotransferase in Figure 3.14 (carbon fixation, Calvin cycle) is involved in amino acid metabolism, cysteine in particular.

Oxidative stress

Four proteins involved in oxidative stress were ≥ two-fold differentially abundant between the control and at least one of the Cd treatments (Figure 3.17, Table 3.1, II.5, 3.3, 3.4). These proteins are rehydrin, superoxide dismutase, a putative DNA protection during starvation or oxidative stress transcription regulator protein, and a fungal/archaeal/bacterial haem catalase/peroxidase. Rehydrin is more abundant in the control than the 4.4 pM Cd^{2+} during late stationary (T4) (Figure 3.17 and Table II.2). Superoxide dismutase is more abundant in the control than the 44 pM Cd^{2+} treatment during very late stationary/death (T5) (Figure 3.17 and Table 3.4). Superoxide dismutase may require Cu/Zn in eukaryotic organisms and Fe, Mn, or Ni in prokaryotic organisms. The putative DNA protection during starvation or oxidative stress transcription regulator protein is more abundant in the 4.4 pM Cd^{2+} than either the control or 44 pM Cd^{2+} treatment during very late stationary/death (T5) (Figure 3.17 and Table 3.3). The fungal/archaeal/bacterial haem catalase/peroxidase is more abundant in both of the Cd treatments than the control during late stationary (T4) (Figure 3.17 and Table II.5). Cd^{2+} appears to affect the relative protein abundances of proteins involved in oxidative stress, but not in as extreme a fashion as proteins involved in carbon or sulfur metabolism.

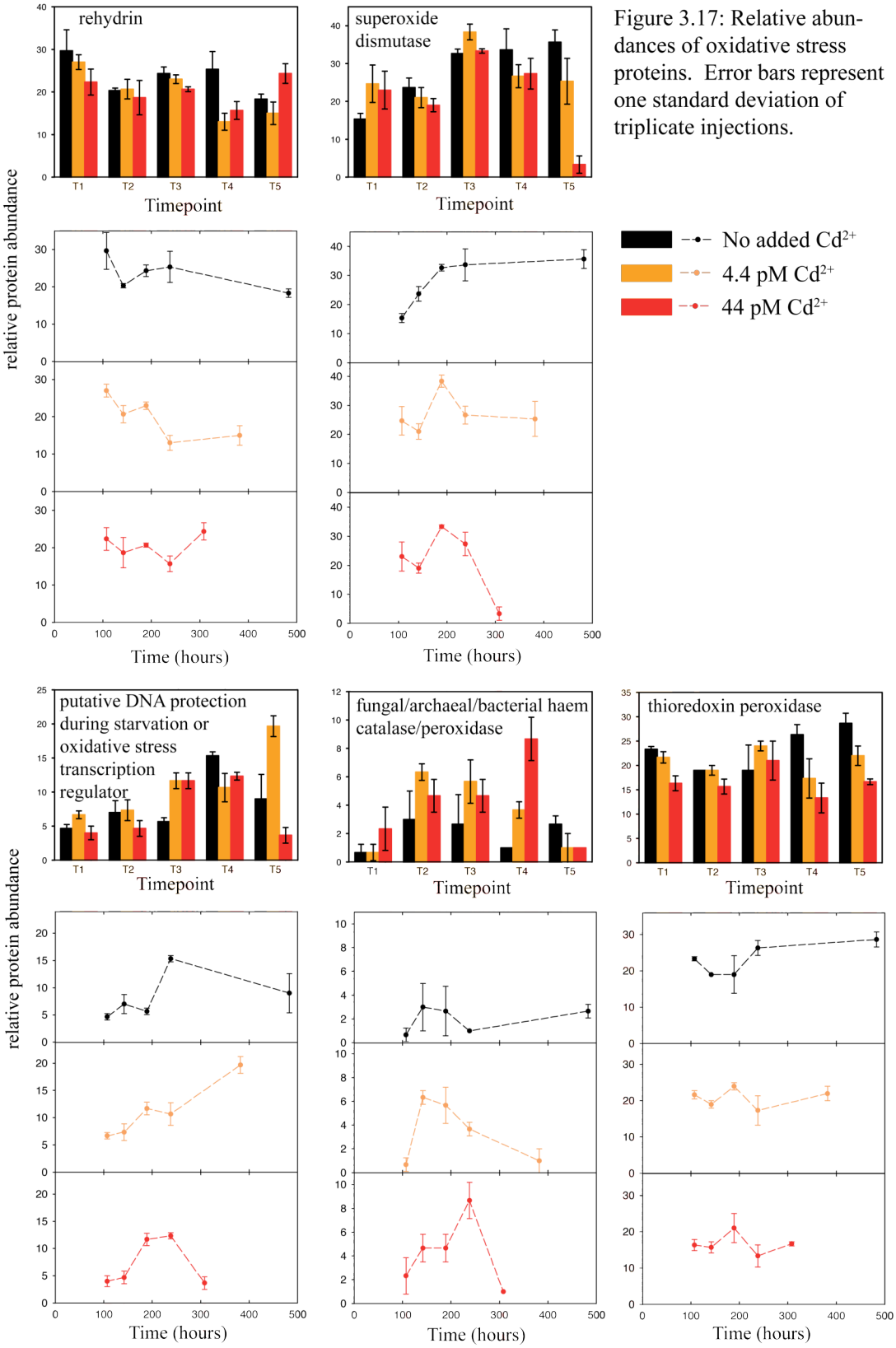

Figure 3.17: Relative abundances of oxidative stress proteins. Error bars represent one standard deviation of triplicate injections.

Genetic information processing protein/protein synthesis

There are many proteins involved in genetic information processing that were ≥ two-fold differentially abundant between the control and at least one of the Cd treatments (Figure 3.5, 3.18). A few of them are depicted here including 50S ribosomal protein L2, 30S ribosomal protein S4, polyribonucleotide nucleotidyltransferase, elongation factor EF-2, and possible protein phosphatase 2C.

The ribosomal proteins 50S L2 and 30S S4, involved in protein synthesis, are more abundant in the Cd treatments during growth (T1) (Figure 3.18, Table 3.1). This suggests the presence of Cd^{2+} causes an upregulation in the synthesis of these proteins and also implies that more protein synthesis is occurring in the Cd^{2+} treatments than the control during growth phase. The greater abundance of ribosomal proteins in the Cd treatments relative to the control during T1 could perhaps be due to the triggering of a cell death pathway or the earlier entrance of the Cd treatments into a metabolic state resembling stationary phase.

The polyribonucleotide nucleotidyltransferase is more abundant in the 44 pM Cd^{2+} treatment than the control during growth and mid-stationary (T1, T3) (Figure 3.18, Tables 3.1, II.3). Elongation factor EF-2 is more abundant in the 44 pM Cd^{2+} treatment than the control during growth (T1) (Figure 3.18, Table 3.1). It is more abundant in the 4.4 pM Cd^{2+} treatment than the control during late stationary (T4) (Figure 3.18, Table II.5). It is more abundant in the control than both Cd treatments in very late stationary/death (T5) (Figure 3.18, Table 3.4). The possible protein phosphatase 2C is more abundant in the control and the 4.4 pM Cd^{2+} treatment than the 44 pM Cd^{2+} treatment during growth (T1) (Figure 3.18, Table 3.2). It is more abundant in the control than both Cd treatments during late stationary (T4) (Figure 3.18, Table II.6). It is more abundant in the 44 pM Cd^{2+} treatment than the control and the 4.4 pM Cd^{2+} treatment during very late stationary/death (T5) (Figure 3.18, Table 3.3).

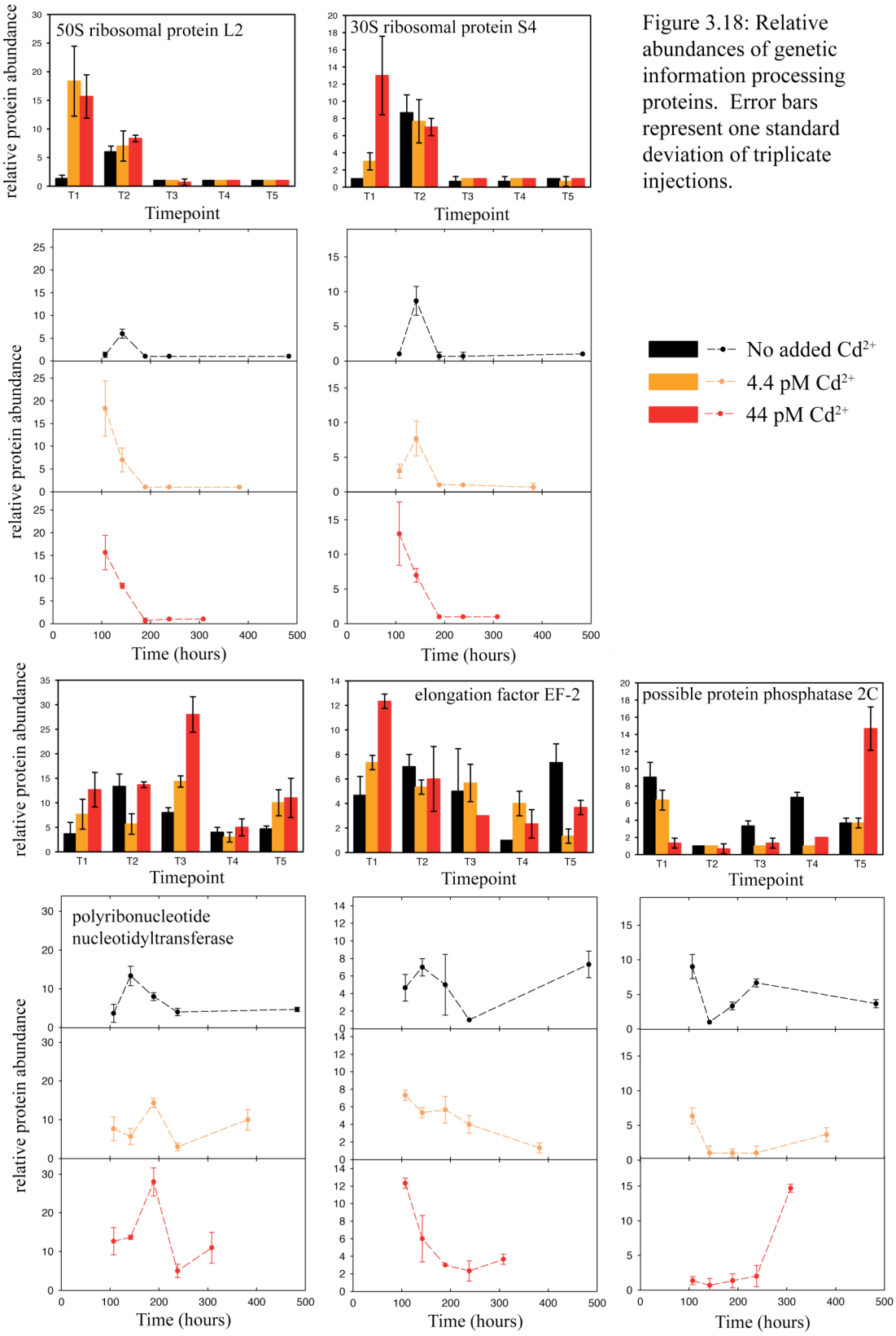

Figure 3.18: Relative abundances of genetic information processing proteins. Error bars represent one standard deviation of triplicate injections.

Other proteins

Many other proteins were ≥ two-fold differentially abundant between the control and at least one of the Cd treatments (Figures 3.19 and 3.20). A few of them are depicted here including chaperonin GroEL, co-chaperonin GroES, nuclear transport factor 2, and a extracellular binding protein (Figure 3.19). Note that GroEL is not differentially abundant, it is shown to compare to GroES. Both of these proteins are thought to help fold ribulose-1,5-bisphosphate carboxylase/oxygenase (Goloubinoff et al., 1989). The other proteins depicted are related to ABC transport, including a ABC-type nitrate/nitrite transport system substrate binding protein, ABC transporter substrate binding protein phosphate and a putative iron ABC transporter substrate binding protein (Figure 3.20).

During very late stationary/death (T5) a putative iron transporter is more abundant in the control and 4.4 pM Cd^{2+} than the 44 pM Cd^{2+} treatment (Figure 3.20, Table 3.4). The fact that this protein becomes more abundant in the control and 4.4 pM Cd^{2+} as stationary phase progresses suggests that iron becomes scarce as it is utilized by the cells in these two treatments. This is similar to superoxide dismutase, which also increases steadily throughout the course of the experiment in the control, suggesting greater oxidative stress as the experiment progressed. Four possible hypotheses to explain this are: 1) The cells in 44 pM Cd^{2+} treatment are already dead or dying during T5 and do not need iron at that point, 2) the cells in the 44 pM Cd^{2+} treatment are more limited for something else during T5 and that limitation takes precedence over iron acquisition, 3) Cd is directly replacing iron somehow, and 4) Cd is triggering a sensor or somehow interfering with cell signaling so the mechanism indicates that the cells have an adequate iron supply. Hypothesis 1 may be less likely because the 4.4 pM Cd^{2+} treatment has a similar amount of cells, in fact less cells, and has a similar rate of degradation of phycobilisome pigmentation during death phase suggesting that the cells in the 4.4 pM Cd^{2+} are also dead and dying, yet it has the putative iron transporter in a high abundance. Assuming that the presence of this transporter is indicative of iron stress or need, this would leave us with the question, why do the cells in the 44 pM Cd^{2+} not appear to need iron when cells are exposed to higher levels of Cd, but do appear to need iron when

exposed to low levels of Cd. This would imply that between the 4.4 and 44 pM Cd^{2+} there is a threshold concentration over which the cells need iron. Hypothesis 2 is plausible, but again it is unlikely that cells in the 44 pM Cd^{2+} would be limited for an element that is not limiting in the 4.4 pM Cd^{2+} treatment. Hypothesis 3 is unlikely because it does not share the redox chemistry of iron, and likely would not function properly as a substitute. In addition, when WH5701 was grown on media with no added iron and no added iron plus 44 pM Cd^{2+} and monitored physiologically, these two treatments both barely grew (data not shown). This implies that Cd cannot nutritionally substitute for iron in this organism, as expected. This leaves us with hypothesis 4, that Cd is triggering a sensor or somehow interfering with cell signaling so the mechanism indicates that the cells have an adequate iron supply.

It is also interesting to note that proteins involved in heavy metal efflux are detected, an expected response to increased exposure of heavy metals, but the spectral counts are low. The heavy metal efflux pump would need to be quantified using labeled peptides and a triple quadrupole mass spectrometer.

Co-chaperonin GroES is involved in protein folding, particularly rubisco (Golourbinoff et al., 1989). During growth phase, there are similar amounts of protein among all of the treatments (Figure 3.19). During death phase, 44 pM Cd^{2+} has approximately five times more than either 4.4 pM Cd^{2+} or the control. This is just like many of the carboxysome-associated proteins (Figure 3.13), suggesting similar regulation.

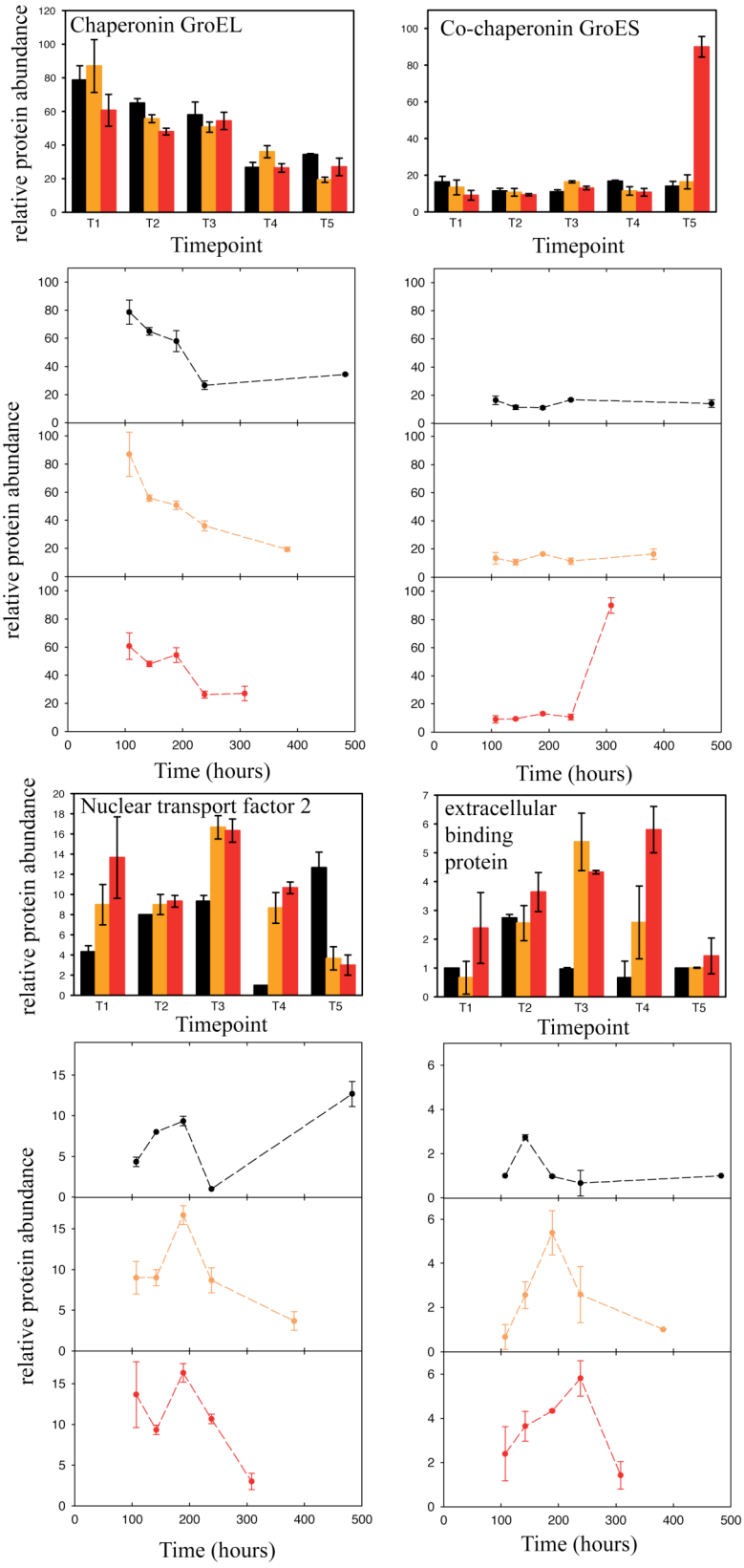

Figure 3.19: Relative abundances of other notable proteins. Error bars represent one standard deviation of triplicate injections. GroEL and GroES are involved in protein folding, especially rubisco.

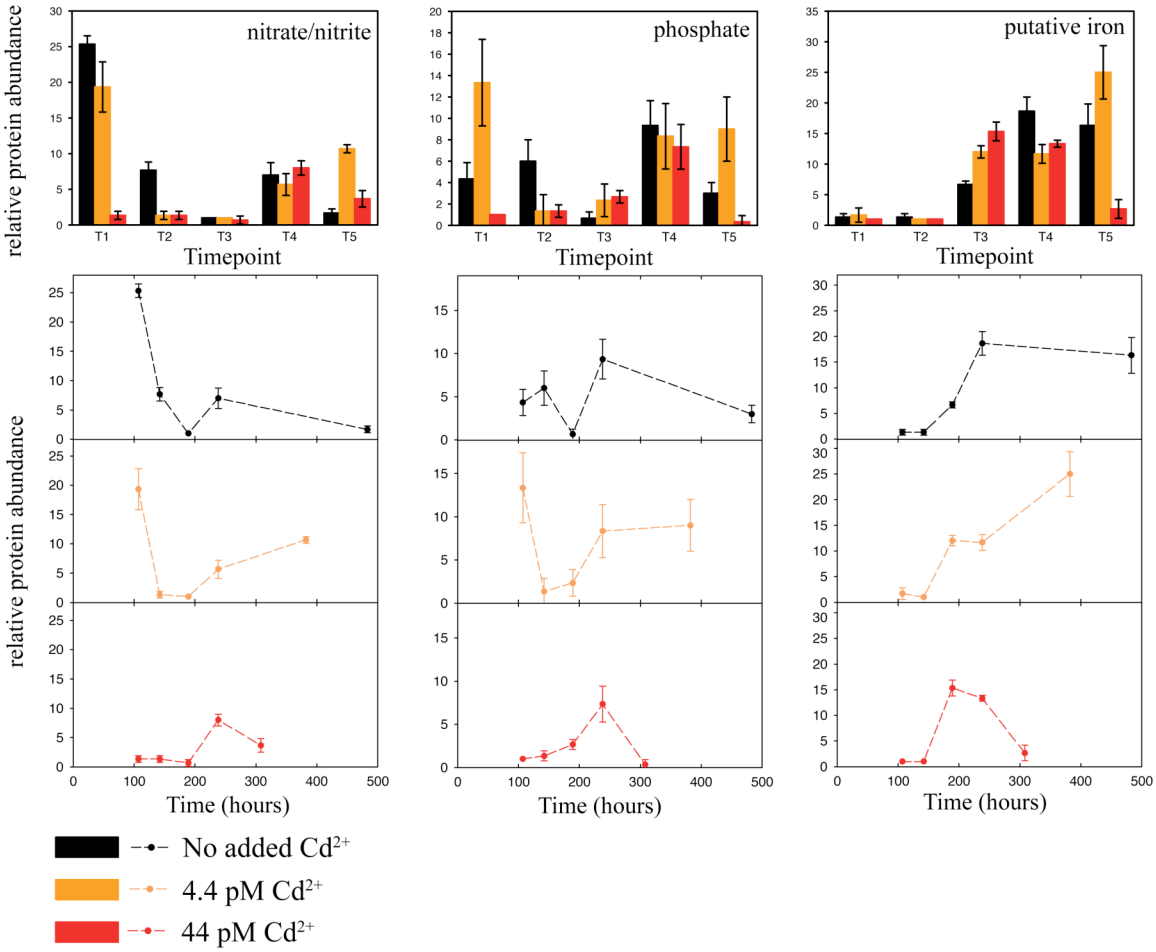

Figure 3.20: Relative abundances of other notable proteins, ABC transport substrate binding proteins. Error bars represent one standard deviation of triplicate injections.

Hypothetical proteins

There are many hypothetical proteins that were ≥ two-fold differentially abundant between the control and at least one of the Cd treatments (Figure 3.21). A few of them are depicted here. The overabundance of three hypothetical proteins in stationary phase relative to exponential phase suggests the function of the hypothetical proteins may have something to do with stationary phase metabolism. One might expect this, because most researchers target their efforts towards understanding growth phase, and as a consequence stationary phase and cellular death are less well-studied in cyanobacteria. Just as there are many Cd^{2+} induced genes and proteins in plant and animal cells that have unknown functions (Deckert, 2005), so we observed some hypothetical proteins that appear to be related to Cd stress. Nucleotide BLAST searches on these eight proteins revealed similarities of two proteins to cyanobacterial hypothetical proteins (WH5701_14806 and WH5701_12034), a cyanobacterial pentapeptide protein (WH5701_07396), a hypothetical protein in *Nitrobacter hamburgensis* X14 (WH5701_09740), a Na^{+}/alanine symporter (WH5701_10100) and three which did not show high similarity to any sequenced DNA (WH5701_04880, WH5701_09875, WH5701_08389).

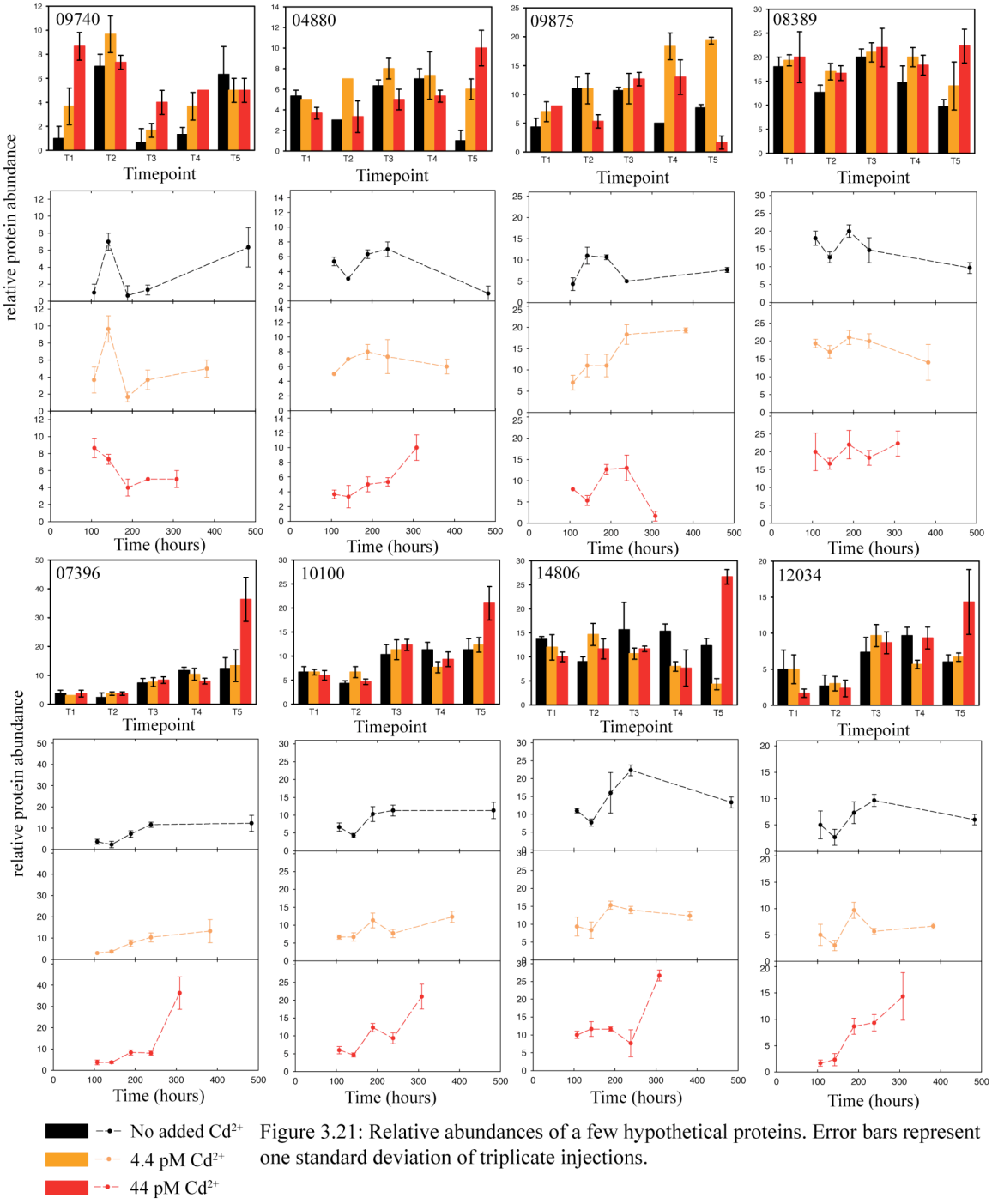

Figure 3.21: Relative abundances of a few hypothetical proteins. Error bars represent one standard deviation of triplicate injections.

Proteomic Data - Overall trends throughout growth of cultures

Considering the dataset as a progression from exponential growth phase through death phase, and how the addition of Cd^{2+} affects the growth phases, the no added Cd^{2+} treatment is the control. Because there is no Zn^{2+} added to the media during this

experiment, it could be considered Zn-deprived. General trends consistent with the change in cell lifestyle from exponential growth to stationary phase in the control treatment are observed in proteins involved in protein synthesis, photosynthesis, oxidative stress, chlorophyll *a* biosynthesis, sulfur metabolism and iron metabolism. Comparing the trends in relative abundances of proteins present in the Cd^{2+} treatments to the trends observed in the no added Cd^{2+} treatment shows that the presence of Cd^{2+} affects the relative abundances of proteins involved in these processes.

The relative protein abundances in the control show the presence of ribosomal proteins during early stationary phase (T2) (Figure 3.18) and not as much in other phases. This is consistent with greater protein synthesis during the transition from growth phase to stationary phase, as the cells cycle into stationary phase. One of the most striking differences with the addition of Cd^{2+} is the higher relative abundance of ribosomal proteins in the Cd^{2+} treatments compared to the no added Cd^{2+} during exponential growth (T1) (Figure 3.5 - Group 1, Figures 3.7, 3.18 , Table 3.1). This suggests that the presence of Cd^{2+} is causing the upregulation of ribosomal proteins by an unknown mechanism that could perhaps be related to Zn. Despite similar physiological characteristics among the three treatments during growth phase of relative fluorescence and growth rates, the greater relative abundance of ribosomal proteins could result in increased protein synthesis in the Cd^{2+} treatments compared to the control during growth phase. During early stationary phase, however, the ribosomal protein relative abundances are relatively similar in the Cd^{2+} and the control treatments. The greater relative abundance of ribosomal proteins in the Cd^{2+} treatments during growth phase (T1) and the similar amounts of ribosomal proteins present in all treatments during early stationary phase (T2) could indicate an early triggering of stationary phase proteins in the Cd treatments relative to the control.

The presence of four photosystem II and I proteins, psbC, photosystem II chlorophyll binding protein, psaB and psaF (Figures 3.10 and 3.11) during growth (T1) and early stationary phase (T2) and not during the remainder of stationary phase (T3-T5) is consistent with cells growing, dividing and photosynthesizing during growth and early

stationary phase and being less active during stationary phase. Culture bottles during growth phase often have gas bubbles adhering to the sides and do not during stationary phase (observations not shown), consistent with the idea of greater photosynthetic activity during growth phase. In terms of the effects of Cd^{2+} on the relative abundances of four photosystem II and I proteins, psbC, photosystem II chlorophyll binding protein, psaB, and psaF (Figures 3.10 and 3.11) that were present in the no added Cd^{2+} treatment during T1 and T2, these four proteins were present in the 4.4 pM Cd^{2+} treatment greater than or equal to six spectral counts during only T1 and never greater than 1 spectral count for the 44 pM Cd^{2+} treatment. This suggests that 44 pM Cd^{2+} negatively affects the presence of these proteins, perhaps impairing the process of photosynthesis and leading to a premature death of the culture. This is despite the physiological similarity of the cultures during growth (T1).

The relative abundance of superoxide dismutase increases from growth through mid-stationary phase (T1-T3) and remains constant throughout the rest of stationary phase (T4 and T5) (Figure 3.17). This suggests that the culture experienced increasing oxidative stress from T1-T3, the amount of oxidative stress perhaps remaining constant for the remainder of stationary phase (T4 and T5). The effects of Cd^{2+} on superoxide dismutase are less clear. The relative abundance of superoxide dismutase in both Cd^{2+} treatments was similar to the control during growth (T1) and early stationary phase (T2) and highest during mid-stationary phase (T3). Unlike the control, in which the relative abundance remained constant, the relative abundance of superoxide dismutase decreased for late stationary (T4) and death phase (T5). This suggests that Cd^{2+} affects the level of oxidative stress in the cells, or the signaling inside the cells that recognizes oxidative stress. Perhaps these differences in superoxide dismutase relative abundances reflect the earlier and faster death of the cultures with added Cd^{2+}.

The five detected proteins involved in the biosynthesis of chlorophyll *a* overall had greater abundances during early stationary phase (T2), otherwise were of lower abundance (Figure 3.8). Cd^{2+} affects the relative abundances of proteins involved in the chlorophyll *a* biosynthesis pathway, as discussed above (see chlorophyll biosynthesis).

An arylsulfatase and a putative arylsulfatase were not abundant during exponential growth (T1) and were the most abundant during early stationary phase (T2) suggesting a shifting of sulfur metabolism into stationary phase (Figure 3.15). Cd^{2+} affects these proteins, also as discussed above (see arylsulfatases). A putative iron ABC transport substrate binding protein was more abundant during mid-stationary to very late stationary (T3-T5) (Figure 3.20). This could suggest increasing iron stress throughout the life of the culture, as discussed above (see other proteins). Overall, the regulation of photosynthesis and cell death may be correlated and related to the presence of metals, especially Zn.

Synechococcus WH5701 compared to Chlamydomonas reinhardtii cadmium response

The comparison of the proteome response of this marine unicellular photosynthetic cyanobacterium, *Synechococcus* WH5701 (this study) with the freshwater unicellular photosynthetic algae, *Chlamydomonas reinhardtii* (Gillet et al., 2006) shows that these organisms react quite differently to chronic Cd stress. Although there are three orders of magnitude more total Cd added to *Chlamydomonas reinhardtii* than *Synechococcus* WH5701 and the toxicity thresholds are quite different in these two organisms, the comparison yields useful insight.

Cells exposed to 150 μM Cd in *Chlamydomonas reinhardtii* showed a decrease in abundance of the large and small subunits of ribulose-1,5-bisphosphate carboxylase/oxygenase as well as other enzymes utilized in photosynthesis, the Calvin cycle and chlorophyll biosynthesis (Gillet et al., 2006). During growth phase, we detected the small subunit of ribulose-1,5-bisphosphate carboxylase/oxygenase, but saw no relative change. We observed an increase, not a decrease in chlorophyll biosynthesis proteins. Similar to *C. reinhardtii* we observed a decrease in PSI proteins and carbon fixation related proteins. Also decreased in abundance in *C. reinhardtii* were proteins involved in fatty acid, amino acid, and protein biosynthesis (Gillet et al., 2006). Contrary to *C. reinhardtii* we observed an increase in proteins related to amino acid and protein biosynthesis in WH5701. We did observe decreased abundance of some hypothetical proteins, although their functions remain unknown.

Proteins more abundant with the presence of 150 μM Cd in *Chlamydomonas*

reinhardtii were those involved in glutathione synthesis, ATP metabolism, oxidative stress, and protein folding (Gillet et al., 2006). Most of the Cd sensitive proteins were regulated through thioredoxin and glutaredoxin, two major cellular thiol redox systems (Gillet et al., 2006). Of the 26 proteins less abundant by at least a factor of 1.5 in the presence of Cd in *C. reinhardtii*, we could identify 13 of these proteins during exponential growth in WH5701, 11 with spectral counts of at least four. Of these 11 proteins, Cd^{2+} in WH5701 did not affect 5 and 6 were actually more abundant in Cd^{2+} treatments by at least a factor of 1.5. Of the 16 proteins more abundant by at least a factor of 1.5, excluding ATP synthase subunits in the presence of Cd in *C. reinhardtii*, we could identify 5 proteins in exponential growth in WH5701, only 2 with spectral counts of at least 4. Of these two proteins, glutathione S-transferase was not affected by Cd in WH5701 and inorganic pyrophosphatase was also more abundant in Cd treatments by a factor of 1.2 and 1.6 for 4.4 and 44 pM Cd^{2+}, respectively. Various ATP synthase subunits were more abundant in *C. reinhardtii* with the addition of Cd. Unlike in *C. reinhardtii*, 6 various subunits of ATP synthase observed in WH5701, with spectral counts of at least four, Cd caused a decrease in abundance in the 44 pM Cd^{2+} treatment and a slight increase in the 4.4 pM Cd^{2+} treatment for four of the subunits. The remaining two subunits of ATP synthase remained the same as the control at the 4.4 pM Cd^{2+} treatment and decreased with the 44 pM Cd^{2+}.

Synechococcus WH5701 comparison to a marine bacterium stationary phase response

Sowell et al., 2008 studied the proteome response of the marine bacterium *Candidatus Pelagibacter ubique* to stationary phase. They found that this organism increases the abundance of a few proteins that contribute to cellular homeostasis rather than remodeling the entire proteome upon adaptation to stationary phase (Sowell et al., 2008). The proteins that increased in abundance were OsmC and thioredoxin reductase (these two proteins may decrease oxidative damage), molecular chaperones, enzymes involved in methionine and cysteine biosynthesis, proteins involved in rho-dependent transcription termination and the signal transduction enzyme CheY-FisH (Sowell et al., 2008). Similarly, in stationary phase compared to exponential, we observed an increase

in superoxide dismutase (Figure 3.17), which mitigates oxidative damage and S-adenosylmethionine synthetase, a protein involved in methionine and cysteine biosynthesis (Figure 3.16).

Environmental Relevance of Results

This experiment was performed on cell cultures with environmentally relevant concentrations of trace metals. The concentrations of NO_3^- (1.1 mM) and PO_4^{3-} (65 μM), however, were higher than those normally measured in the environment, deliberately in order to not limit the cells for these major nutrients, and to produce high densities of cells for protein analysis in a reasonable amount of time using a reasonable amount of oligotrophic seawater.

Death of phytoplankton in the sea is generally attributed to grazing or predation (Walsh, 1983), so the laboratory study of stationary and death phase can perhaps be considered to have been neglected. More recently, the presence of proteases coincident with cell death in cultures of diatoms suggested the importance of cell death processes to cycling of organic matter in aquatic ecosystems (Berges and Falkowski, 1998). Programmed cell death has been documented in several phytoplankton species, including the dinoflagellete, *Peridinium gatunense*, in which an excreted thiol protease is thought to coordinate cell death in culture and in blooms in the environment (Vardi et al., 2007).

As oceans change *Synechococcus* WH5701 could be an important cyanobacterial strain due to its robustness (variable salinity and nutrient tolerances). As of now, naturally-occurring chronic Cd stress to cyanobacteria could really only have the chance to be observed in upwelling regions and maybe some coastal, and as it is the presence of Zn and organic ligands in upwelling regions would serve to buffer the toxicity of Cd in most instances. In general, the presence of complex microbial communities probably would alleviate most potential for Cd stress, due to differential uptake, adsorption to surfaces, and complexation with ligands. Higher dissolved Cd concentration can sometimes be observed in oligotrophic waters (Noble et al., unpublished data).

CONCLUSIONS

In conclusion, in the absence of added Zn, chronic Cd^{2+} exposure has a major impact on the metabolism of WH5701, as evidenced by dramatic changes in the relative protein abundances. Changes are evidenced in proteins involved in chlorophyll *a* biosynthesis, photosynthesis (phycobilisome, photosystem II, photosystem I), carbon fixation (carboxysome, Calvin cycle, others), steroid and lipid biosynthesis, sulfur and/or cysteine metabolism, oxidative stress, genetic information processing and others, suggesting that Cd^{2+} affects the fundamental functioning of the cell. Changes in hypothetical proteins are also evinced. Physiological measurements during growth phase show little difference between Cd^{2+} treatments and the control, yet based on changes in protein relative abundances, cells are affected by chronic Cd^{2+} stress. Chronic Cd^{2+} increases the abundance of arylsulfatases, which have been noted to increase in cells that are experiencing sulfur starvation, and other proteins involved in the making of cysteine, an amino acid involved in thiols, metallothioneins and sulfur metabolism. In addition, measurement of particulate glutathione, a low molecular weight thiol, in a repeat experiment showed a large quantity of this metabolite in the high Cd^{2+} treatment.

Relative protein abundances also yielded insights into the observed physiological changes in the Cd^{2+} treatments during stationary and death phases. Changes in relative abundances of chlorophyll biosynthesis proteins may help explain the increase in chlorophyll *a* maximum observed in the Cd treatments. The strong effect of Cd on cellular metabolism may help explain the early death in the Cd treatments compared to the control. The physiological effects of increased maximum chlorophyll *a* fluorescence and faster mortality with the addition of picomolar free Cd^{2+} were not observed when picomolar free Zn^{2+} was present in the media. This suggests that the presence of Zn^{2+} alleviated Cd^{2+} toxicity and Cd^{2+} may have been affecting Zn^{2+} systems when Zn^{2+} was absent.

Comparison of the reaction of WH5701 to chronic Cd stress in an eukaryotic algae *C. reinhardtii* showed both similarities and differences in terms of changes in relative protein abundances. Some proteins changed in abundance in a similar way,

including similar decreases in PSI proteins and carbon fixation related proteins. Overall however, these two unicellular photosynthetic organisms reacted differently to chronic Cd stress: WH5701 was observed to have an increase in chlorophyll a, amino acid and protein biosynthesis proteins, whereas *C. reinhardtii* showed a decrease in proteins of these biosynthesis functions.

This study also examined the change in the proteome from exponential growth throughout stationary phase documenting the decrease in the relative abundances of ribosomal proteins, among others and increase in superoxide dismutase, among others from exponential throughout stationary phase. In addition, this study also identified many hypothetical proteins of unknown function, which change in abundance from growth to stationary phase and with Cd stress. This gives insight into the possible function of these proteins for future investigation.

These experiments were performed in continuous light with replete macronutrients, and although NO_3^- and PO_4^{3-} concentrations were higher than those found in the environment, clues about the functioning of cyanobacteria in the greater ocean ecosystem can be gleaned. Our results indicate that cyanobacteria are versatile and can survive in changing environmental conditions by adjusting their cellular functioning as discerned by analyzing differences in their relative protein abundances. In the ocean, free-floating cyanobacteria existing in the mixed layer may be exposed to different light, nutrient, and metal concentrations, as well as a changing microbial consortium.

FUTURE DIRECTIONS

The physiological effects of increased maximum chlorophyll *a* fluorescence of Cd^{2+} treatments above the control and the faster death rates disappear with the presence of Zn^{2+} added to the media. To see whether the presence of Zn^{2+} buffers Cd^{2+} toxicity on a cellular level, this experiment could be performed with Zn^{2+} added to the media. Perhaps the carboxysome proteins would not be affected by 44 pM Cd^{2+} as they were in this experiment without Zn^{2+} in the media.

Intriguing is the possibility that Cd^{2+} triggers apoptosis. There are no annotated

caspases in WH5701. All possible caspases could be easily cataloged and blasted against the WH5701 genome at the nucleotide level. Any hits could be added to our WH5701 database and see if we detected those proteins.

Despite the detection of many carboxysome protein components, no carbonic anhydrases were detected. Since the only known nutritive use of Cd is in a carbonic anhydrase of *T. weissflogii* (Lane and Morel, 2000; Lane et al., 2005; Park et al., 2007; Xu et al., 2008), detection of this protein is desirable. As a simple first pass, the carbonic anhydrase might be in a different protein fraction. During protein extraction, after resuspension of the harvested cell pellet in one 100 μM ammonium bicarbonate, sonication and centrifugation, only about half of the supernatant was acetone precipitated. The remainder of the supernatant was evaporated by speed vacuum, stored overnight at -80^{o}C and then extracted and digested with the acetone-precipitated samples. This means that this additional protein fraction is safely in the -80^{o}C, ready for mass spectrometric global proteomic analysis.

The further investigation of PSII/PSI ratios and how these systems are regulated would be interesting because it is flexible. PSII core protein D2 was detected at the highest count of 3. A putative PSII reaction center Psb28 at the highest count of 18 and PSII complex extrinsic protein PsuB at the highest count of 42 were detected. Both of these have the greatest abundance during the 44 pM Cd^{2+} death phase T5. This suggests that Cd interferes with regulation at T5 in high Cd. A similar pattern is observed in a few carboxysome proteins, PSI proteins, among others. These two PSII proteins do not show an increase in relative protein abundance in the no added Cd treatment during the decrease in cell counts observed from T3 to T4.

Also of note is the relationship observed in Figure 4.4d between dose of Cd and the ratio of chlorophyll *a*/phycoerythrin fluorescence. It can be used as a biosenser for Cd at concentrations as low as 0.44 pM Cd^{2+} (data not shown), except that it does not hold in the presence of Zn, rendering its practicality moot. Note that there are fluorescence-based biosensors for Zn that utilize carbonic anhydrase (see work of Richard B. Thompson).

Acknowledgements

I would like to thank the members of the Saito Lab: Dawn Moran, Abigail Noble, Tyler Goepfert and Erin Bertrand. Thank you to John Waterbury and Freddie Valois for the WH5701, use of lab space, and discussion. Thank you to Tristan Kading for discussion and thiol measurements and Tracey Mincer for discussion.

References

Altschul, S. F., Madden, T. L., Schaffer, A. A., Zhang, J., Zhang, Z., Miller, W. and Lipman, D. J. 1997. Gapped BLAST and PSI-BLAST: a new generation of protein database search programs. *Nucleic Acids Research* 25: 3389-3402.

Bailey, S., Melis, A., Mackey, K. R. M., Cardol, P., Finazzi, G., van Dijken G., Berg, G. M., Arrigo, K., Shrager, J., Grossman, A. 2008. Alternative photosynthetic electron flow to oxygen in marine *Synechococcus*. *Biochimica et Biophysica Acta-Bioenergetics* 1777 (3): 269-276.

Berges, J. A. and Falkowski, P.G. 1998. Physiological stress and cell death in marine phytoplankton: Induction of proteases in response to nitrogen or light limitation. *Limnology and Oceanography* 43(1): 129-135.

Beutler, M. 2003. Spectral fluorescence of chlorophyll and phycobilins as an in-situ tool of phytoplankton analysis - models, algorithms and instruments. Christian-Albrechts-Universität, phD-Thesis.

Blankenship, R. E. 2002. *Molecular Mechanisms of Photosynthesis*. Oxford: Blackwell Science.

Campbell, D., Hurry, V., Clarke, A. K., Gustafsson, P. and Öquist, G. 1998. Chlorophyll fluorescence analysis of cyanobacterial photosynthesis and acclimation. *Microbiology Molecular Biology Reviews* 62: 667-683.

Deckert, J. 2005. Cadmium toxicity in plants: Is there any analogy to its carcinogenic effect in mammalian cells? *Biometals* 18: 475-481.

Duncan, K.E.R., Ngu, T.T., Chan, J., Salgado, M.T., Merrifield, M.E. and Stillman, M.J. 2006. Peptide folding, metal-binding mechanisms, and binding site structures in metallothioneins. *Experimental Biology and Medicine* 231: 1488-1499.

Dupont, C.L. and Ahner, B. 2005. Effects of copper, cadmium, and zinc on the production and exudation of thiols by *Emiliania huxleyi*. *Limnology and Oceanography* 50(2):508-515.

Dupont C.L., Yang S., Palenik B., Bourne, PE. 2006. Modern proteomes contain putative imprints of ancient shifts in trace metal geochemistry. *Proceedings of the National Academy of Sciences* 103 (47): 17822-17827.

Dupont, C.L., Moffett, J.W., Bidigare R.R. and Ahner, B.A. 2006. Distributions of dissolved and particulate biogenic thiols in the subartic Pacific Ocean. *Deep Sea Research Part I: Oceanographic Research Papers* 53(12): 1961-1974.

Eisen, M.B., Spellman, P.T., Brown, P.O. and Bostein, D. 1998. Cluster analysis and display of genome-wide expression patterns. *PNAS* 95(25): 14863-14868.

Ellis, J.R. 1979. The most abundant protein in the world. *Trends in Biochemical Sciences* 4(11): 241-244.

Everroad, C., Six, C., Partensky, F., Thomas, J. C., Holtzendorff, J. and Wood, A. M. 2006. Biochemical bases of type IV chromatic adaptation in marine *Synechococcus* spp. *Journal of Bacteriology* 188 (9): 3345-3356.

Fitzgerald, J. W. 1976. Sulfate ester formation and hydrolysis: a potentially important yet often ignored aspect of the sulfur cycle of aerobic soils. *Bacteriological Reviews* 40 (3): 698-721.

Fuller, N.J., Marie, D., Partensky, F., Vaulot, D., Post, A.F. and Scanlan, D. J. 2003. Clade-specific 16S Ribosomal DNA oligonucleotides reveal the predominance of a single marine *Synechococcus* clade in a stratified water column in the Red Sea. *Applied and Environmental Microbiology* 69: 2430-2443.

Gillet, S., Decottignies, P., Chardonnet, S. and Le Maréchal, P. 2006. Cadmium response and redoxin targets in Chlamydomonas reinhardtii: a proteomic approach. *Photosynthesis Research* 89: 201–211.

Goldschmidt, V.M. 1954. edited by Alex Muir. Geochemistry. Oxford at Clarendon Press.

Goloubinoff, P., Christeller, J.T., Gatenby, A.A. and Lorimer, G.H 1989. Reconstitution of active dimeric ribulose bisphosphate carboxylase from an unfoleded state depends on two chaperonin proteins and Mg-ATP. *Nature* 342: 884-889.

Haverkamp, T., Schouten, D., Doeleman, M., Wollenzien U., Huisman, J. and Stal, L. J. 2009. Colorful microdiversity of *Synechococcus* strains (picocyanobacteria) isolated from the Baltic Sea. The ISME Journal 3: 397–408.

Kerfeld, C. A., Sawaya, M. R., Tanaka, S., Nguyen, C. V., Phillips, M., Beeby, M. and Yeates, T.O. 2005. Protein structures forming the shell of primitive bacterial organelles. *Science* 309 (5736): 936-938.

Küpper, H., Küpper, F. and Spiller, M. 1996. Environmental relevance of heavy metal-substituted chlorophylls using the example of water plants. *Journal of Experimental Botany* 47: 259-266.

Küpper, H., Küpper, F. and Spiller, M. 1998. In situ detection of heavy metal substituted chlorophylls in water plants. *Photosynthesis Research* 58: 123–133.

Lane, T.W. and Morel, F.M.M. 2000. A biological function for cadmium in marine diatoms. *Proceedings of the National Academy of Sciences* 97: 4627-4631.

Lane, T.W., Saito, M.A., George, G.N., Pickering, I.J., Prince, R.C. 2005. A cadmium enzyme from a marine diatom. *Nature* 435: 42.

MacColl, R. 1998. Cyanobacterial phycobilisomes. *Journal of Structural Biology* 124: 311-334.

Margoshes, M. and Vallee, B.L. 1957. A cadmium protein from equine kidney cortex. *Journal of the American Chemical Society* 79: 4813-4814.

Martell, A.E. and Smith, R. M. 1993. NIST Critical Stability Constants of Metal Complexes Database.

Martelli, A. E. Rousselet, Dycke, C., Bouron, A. and Moulis, J.-M. 2006. Cadmium toxicity in animal cells by interference with essential metals. *Biochimie* 88 (11):1807-1814.

Morel, F.M.M., Milligan, A.J., and Saito, M.A. 2004. Marine Bioinorganic Chemistry: The Role of Trace Metals in the Oceanic Cycles of Major Nutrients. Treatise on Geochemistry Volume 6 The Oceans and Marine Geochemistry. eds. Henry Elderfield. H.D. Holland and K.K. Turekian. 6.05 113-143.

Mullineaux, C,W. 1999. The thylakoid membranes of cyanobacteria: structure dynamics and function. *Australian Journal of Plant Physiology* 26: 671-677.

Okamura, M. Y., Paddock, M. L., Graige, M. S., and Feher, G. 2000. Proton and electron transfer in bacterial reaction centers. *Biochimica et Biophysica Acta-Bioenergetics*. 1458 (1): 148-163.

Palenik, B. 2001. Chromatic adaptation in marine *Synechococcus* strains. *Applied and Environmental Microbiology* 67(2): 991-994.

Palmiter, R.D. 1998. The elusive function of metallothioneins. *PNAS* 95: 8428-8430.

Park, H., Song, B. and Morel, F. M. M. 2007. Diversity of the cadmium-containing carbonic anhydrase in marine diatoms and natural waters. *Environmental Microbiology* 9(2): 403-413.

Peng, J., Elias, J. E., Thoreen, C. C., Licklider, L. J. and Gygi, S. P. 2003. Evaluation of multidimensional chromatography coupled with tandem mass spectrometry (LC/LC-MS/MS) for large-scale protein analysis: The Yeast Proteome. *Journal of Proteome Research* 2: 43-50.

Saito, M., Moffett, J.W., Chisholm, S.W., and Waterbury, J.B. 2002. Cobalt limitation and uptake in *Prochlorococcus*. *Limnology and Oceanography* 47(6): 1629-1636.

Saito, M.A., Sigman, D.M., Morel, F.M.M. 2003. The bioinorganic chemistry of the ancient ocean: the co-evolution of cyanobacterial metal requirements and biogeochemical cycles at the Archean-Proterozoic boundary? *Inorganica Chimica Acta* 356:308-318.

Scanlan, D.J. 2003. Physiological diversity and niche adaptation in marine *Synechococcus*. *Advances in Microbial Physiology* 47: 1-64.

Schubert, W.D., Klukas, O., Krauss, N., Saenger, W., Fromme, P. and Witt, H.T. 1997. Photosystem I of *Synechococcus elongatus* at 4 A resolution: comprehensive structure analysis. *Journal of Molecular Biology* 272 (5): 741-769.

Semeniuk, D.M., Cullen, J.T., Johnson, W.K., Gagnon, K., Ruth, T.J. and Maldonado, M.T. 2009. Plankton copper requirements and uptake in the subarctic Northeast Pacific Ocean. *Deep Sea Research I* 56, 1130-1142.

Silver, S., and M. Wauderhaug, 1992. Gene regulation of plasmid- and chromosome-determined inorganic ion transport in bacteria. *Microbiological Reviews*. 56:195-264.

Six, C., Finkel, Z. V., Irwin, A. J., Campbell, D. A. 2007. Light variability illuminates niche-partitioning among marine picocyanobacteria. *PLoS ONE* 2(12): e1341. doi:10.1371/journal.pone.0001341.

Sowell, S. M., Norbeck, A. D., Lipton, M. S., Nicora, C. D., Callister, S. J., Smith, R. D., Barofsky, D. F., and Giovannoni, S. J. 2008. Proteomic analysis of stationary phase in the marine bacterium "*Candidatus Pelagibacter ubique*". *Applied and Environmental Microbiology* 74 (13): 4091–4100.

Sujak, A. 2005. Interaction between cadmium, zinc and silver-substituted platocyanin and cytochrome b_6f complex-heavy metals toxicity towards photosynthetic apparatus. *Acta*

Physiologiae Plantarum 27(1):61-69.

Sunda, W.G. 1988. Trace metal interactions with marine phytoplankton. *Biology and Oceanography* 6: 411-442.

Sunda, W.G., and Huntsman, S.A. 2000. Effect of Zn, Mn, and Fe on Cd accumulation in phytoplankton: Implications for oceanic Cd cycling. *Limnology and Oceanography* 45(7): 1501-1516.

Sunda, W.G. and Huntsman, S.A.1995. Cobalt and zinc interreplacement in marine phytoplankton: biological and geochemical implications. *Limnology and Oceanography* 40(8): 1404-1417.

Sunda, W.G., and Hunstman, S.A.1998. Control of Cd concentrations in a coastal diatom by interactions among free ionic Cd, Zn, and Mn in seawater. *Environmental Science and Technology* 32: 2961-2968.

Tang, D., Hung, C., Warnken, K. W. and Santschi, P. H. 2000. The distribution of biogenic thiols in surface waters of Galveston Bay. *Limnology and Oceanography* 45(6): 1289–1297.

Ting, C.S., Rocap, G., King, J. and Chisholm, S.W. 2002. Cyanobacterial photosynthesis in the oceans: the origins and significance of divergent light-harvesting strategies. *Trends in Microbiology* 10 (3): 134-142.

Tokheim, A. M., Spannaus-Martin, D. J., and Martin, B.L. 2005. Evidence for the Cd^{2+} activation of the aryl sulfatase from *helix pomatia*. *BioMetals* 18: 537–540.

Vallee, B.L. and Ulmer, D.D.1972. Biochemical effects of mercury, cadmium and lead. *Annual Review of Biochemistry* **41**: 91-128.

Van Mooy, B. A.S. 2006. Rocap, G., Fredricks, H. F., Evans, C.T. and Devol, A. H. 2006. Sulfolipids dramatically decrease phosphorus demand by picocyanobacteria in oligotrophic marine environments. *PNAS* 103 (23): 8607-8612.

Vardi, A., Eisenstadt, D., Murik, O., Berman-Frank, I., Zohary, T., Levine, A. and Kaplan, A. 2007. Synchronization of cell death in a dinoflagellate population is mediated by an excreted thiol protease. *Environmental Microbiology* 9(2): 360–369.

Wakao, N., Yokoi, N., Isoyama, N., Hiraishi, A., Shimada, K., Kobayashi, M., Kise, H., Iwaki, M., Itoh, S. and Takaichi, S. 1996. Discovery of natural photosynthesis using Zn-containing bacteriochlorophyll in an aerobic bacterium *Acidiphilium rubrum*. *Plant and Cell Physiology* 37 (6): 889-893.

Waldron, K. J., Rutherford, J. C., Ford, D. and Robinson, N.J. 2009. Metalloproteins and metal sensing. *Nature* 460: 823-830.

Xu, Y., Feng, L., Jeffrey, P. D., Shi, Y. and Morel, F. M. M. 2008. Structure and metal exchange in the cadmium carbonic anhydrase of marine diatoms. *Nature* 452: 56-61.

Yeates, T. O, Kerfeld, C. A., Heinhorst, S., Cannon, G.C. and Shively, J. M. 2008. Protein-based organelles in bacteria: carboxysomes and related microcompartments. *Nature Reviews Microbiology* 6: 681-691.

Zhang, B., VerBerkmoes, N. C., Langston, M.A., Uberbacher, E., Hettich, R. L. and Samatova, N. F. 2006. Detecting differential and correlated protein expression in label-free shotgun proteomics. *Journal of Proteome Research* 5(11): 2909–2918.

Zhang, Z., Shrager, J., Jain, M., Chang, C., Vallon, O. and Grossman, A. R. 2004. Insights into the survival of *Chlamydomonas reinhardtii* during sulfur starvation based on microarray analysis of gene expression. *Eukaryotic Cell* 3(5): 1331-1348.

Chapter 4

Oceanic *Synechococcus* WH8102 physiological and proteomic response to acute cadmium addition under zinc deficient and low phosphate conditions

Abstract

Synechococcus sp. WH 8102 is a motile marine cyanobacterium isolated originally from the Sargasso Sea. It is adapted to the open ocean with lower trace metal availability and low variability in irradiance with deep mixed layer depths relative to coastal waters. To test the response of this organism to free cadmium (Cd), generally considered a toxin, four cultures were grown in a matrix of high and low zinc (Zn) and phosphate (PO_4^{3-}) and were acutely exposed to 4.4 pM free Cd^{2+} during mid-log phase and harvested after 24 h. Cell number, relative chlorophyll *a* and phycoerythrin fluorescence were monitored throughout growth phase, where Zn and PO_4^{3-} had little effect on growth rates, but in the final 24 h of the experiment three effects were noticed: 1) low PO_4^{3-} treatments showed increased instantaneous growth rates relative to high PO_4^{3-} treatments, 2) the Zn-high PO_4^{3-} treatment appeared to enter stationary phase, and 3) Cd increased growth rates even more in the both the low PO_4^{3-} and Zn treatments. Global proteomic analysis of relative protein abundance revealed that: 1) Zn appeared to be vital to the PO_4^{3-} response in this organism, 2) Cd caused more proteomic changes at low PO_4^{3-}, and 3) in the presence of both replete PO_4^{3-} and acute Cd the proteome was almost indifferent to the presence of Zn. Comparison to a literature transcriptome study of PO_4^{3-} stress in this organism grown in a media containing Zn by Tetu et al., 2009 showed a similar PO_4^{3-} response in the presence of Zn, including the greater relative abundance of SYNW2391 alkaline phosphatase, SYNW1018 ABC phosphate binding protein (PstS) and other proteins. In the absence of Zn in this experiment, however, the PO_4^{3-} response is remarkably different. In addition, SYNW0359 bacterial metallothionein (SmtA) appears correlated with PO_4^{3-} stress-associated proteins.

INTRODUCTION

Synechococcus WH8102 is a well-studied isolate of cyanobacteria, belonging to the marine cyanobacterial subcluster 5.1, MC-A group. It was originally isolated from the Sargasso Sea and the fully sequenced genome is available (Palenik et al., 2003). The MC-A group is thought to be the dominant *Synechococcus* group within the euphotic zone of open ocean and coastal waters (Fuller et al., 2003 and references therein). Previous culture studies of this organism showed that at low zinc (Zn) concentrations cadmium (Cd) lowered growth rates, whereas this was not observed at higher Zn concentrations (Saito et al., 2003).

As discussed in Chapter 1 on pages 15-16, Cd and Zn have nutrient-like distributions in the ocean, implying that Cd and Zn are taken up by microorganisms in the surface water and remineralized at depth. Zn is vitally important to the proper functionality of many enzymes, an essential metal in living organisms, whereas Cd is not.

These metals may have different roles in different environments. Zn is considered a nutrient in the open ocean. Zn availability, for instance, may influence phytoplankton diversity in the Ross Sea (Saito et al., 2010). In cyanobacteria, the Zn requirements are very low, consistent with the idea that cyanobacteria may have evolved in a sulfidic ancient ocean (Saito et al., 2003). There are almost no studies of Zn handling mechanisms in marine cyanobacteria (Blindauer, 2008). In terms of Cd, it has been noticed that the dissolved Cd:PO_4^{3-} ratios are lower in the surface waters of Fe-limited regions, implying preferential removal of Cd relative to PO_4^{3-} in Fe-limited waters (Cullen, 2006; Lane et al., 2009, references therein).

As stated, dissolved Cd and PO_4^{3-} are correlated in the ocean, but Zn and phosphorus could be colimiting in some areas of the ocean. Phosphorus is an essential nutrient, utilized in the cell for purposes ranging from the backbone of DNA to the energy currency of a cell, adenine triphosphate, ATP. It is typically found at low micromolar concentrations in the ocean and is limiting in some regions. It composes some 2-4% dry weight of cells and is considered by some to be the 'staff of life' (Karl, 2000). Considering Zn and phosphorus together, they are thought to exhibit Type III

biochemically dependent colimitation, i.e. the uptake of one nutrient, phosphorus, is dependent upon adequate nutrition with regard to the other, Zn (Saito et al, 2008). Based on extrapolation of experimentation with the coccolithophore, *Emiliania huxleyi*, Zn and phosphorus colimitation could occur in highly oligotrophic regions such as the Sargasso Sea (Shaked et al., 2006).

In this paper, the physiological and proteomic responses of the open ocean *Synechococcus* WH8102 to acute Cd exposure under varying chronic Zn and PO_4^{3-} concentrations was examined. Physiological results indicated that all treatments had similar growth rates throughout the first 10 days of the experiment until Cd addition, but in the last 24 hours of the experiment, low PO_4^{3-} treatments showed increased instantaneous growth rates relative to high PO_4^{3-} treatments. Also, the acute addition of Cd increased instantaneous growth rates further above those in both the low PO_4^{3-} and Zn treatments. Global proteomic results showed a response to lowered PO_4^{3-} in the presence of Zn similar to previous transcriptome studies, including a greater relative abundance of an SYNW2391 alkaline phosphatase (phoA), a protein thought to require Zn as a cofactor, and a SYNW1019 ABC phosphate binding protein (PstS). In the absence of Zn with low PO_4^{3-}, these proteins were not as abundant, and the proteome was quite different, suggesting a different PO_4^{3-} response under these conditions. SYNW0359 bacterial metallothionein (SmtA), involved in Zn handling, showed a similar relative protein abundance response pattern to the alkaline phosphatase and ABC phosphate binding protein (PstS).

METHODS

Culturing and protein extraction

Axenic cultures of *Synechococcus* sp. WH 8102 obtained from J. Waterbury (Woods Hole Oceanographic Institution) and maintained in a modified PRO-TM media as described in Chapter 3 on pages 75-76. The deplete Zn^{2+} condition had no Zn added whereas replete had Zn added to a total concentration of 10 nM, with the free concentrations based on a previous study estimated to be tens of picomolar Zn^{2+}. Low

PO_4^{3-} cultures had 1 µM PO_4^{3-} added, whereas high had 65 µM PO_4^{3-}. Acute Cd treatments had Cd added to a total concentration of 10 nM $CdCl_2$, with the free concentration estimated to be 4.4 pM Cd^{2+} and blanks estimated as described in Chapter 3 on page 76. Cultures were grown in either 28 mL polycarbonate tubes or 500 mL polycarbonate bottles under 30 µmol photons (µEinstein) $m^{-2}s^{-1}$ continuous white light. At mid-log phase, the four cultures were split and one of each spiked with 4.4 pM Cd^{2+}. The 8 resulting cultures were harvested 24 hours later (Figure 4.1). Culture growth was monitored by a combination of chlorophyll *a* and phycoerythrin fluorescence and cell counting by microscopy. All plasticware was cleaned as described in Chapter 3 on page 76. Growth rates were calculated from the natural log of *in vivo* relative chlorophyll *a* fluorescence (n = 5). For protein samples, approximately 200 mL of culture were harvested and processed as described in Chapter 3 on pages 76-77.

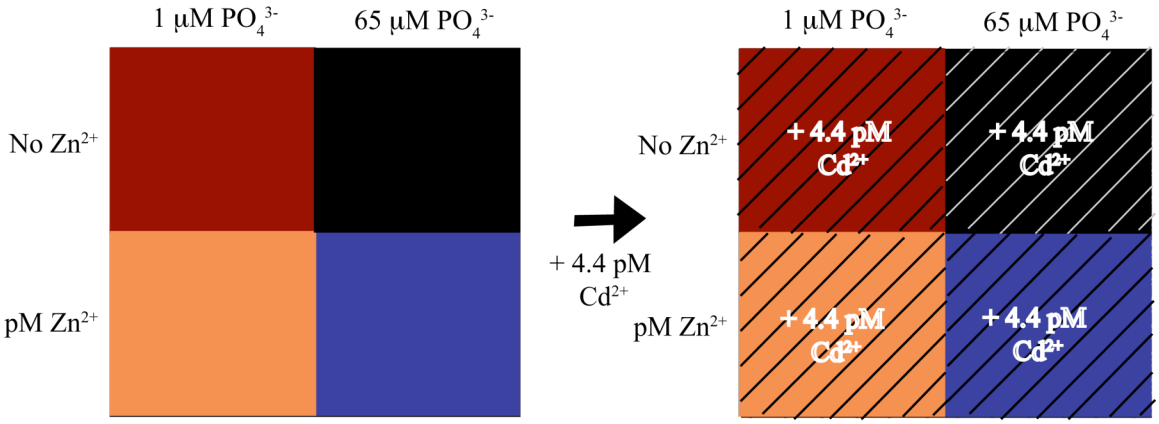

Figure 4.1: Experimental Design. Four experimental treatments with variable Zn and PO_4^{3-} concentrations (No Zn^{2+} 65 µM PO_4^{3-}, pM Zn^{2+} 65 µM PO_4^{3-}, No Zn^{2+} 1 µM PO_4^{3-}, pM Zn^{2+} 1 µM PO_4^{3-}) were grown to mid-log phase, split evenly and 4.4 pM Cd^{2+} added acutely to one of the splits of each treatment.

Liquid Chromatography-Mass Spectrometry (LC-MS)

The digests were analyzed by LC-MS using a Paradigm MS4 HPLC system with reverse phase chromatography, Thermo LTQ ion trap mass spectrometer and Microhm ADVANCE source (2 µL/min flow rate, 345 min runs, 150 mm column, 40 µL injections, water ACN gradient). Each digest was injected three times for a total of 24 mass spectrometry runs, only two digests from each treatment were analyzed. Mass

spectra were processed by SEQUEST and PeptideProphet with a fragment tolerance of 1.0 Da (monoisotopic), parent tolerance of 2.0 Da (monoisotopic, fixed modification of +57 on C (carbamidomethyl), variable modification of +16 on M (oxidation) and a maximum of 2 missed trypsin cleavages using a database including reversed proteins and common contaminants.

Spectral counts of 16 files were compiled in Scaffold 3 with a peptide false discovery rate of 1.9%, minimum peptide and protein tolerances of 95 and 99%, respectively with a minimum of 2 peptides (Peng et al., 2003; Zhang et al., 2006). A spectral count is the number of times a particular peptide from a protein is sampled during an MS/MS experiment and is indicative of protein relative abundance. Protein functions were assigned by using the Kyoto Encyclopedia of Genes and Genomes (KEGG) unless otherwise noted.

RESULTS

Physiological Data

WH8102 was grown under the four variable Zn and PO_4^{3-} conditions, Zn-high PO_4^{3-}, Zn-low PO_4^{3-}, no Zn-high PO_4^{3-}, and no Zn-low PO_4^{3-} (Figure 4.1). The response to acute 4.4 pM Cd stress was monitored by the relative fluorescence of phycoerythrin and chlorophyll *a* in vivo and by cell counts every other day over the course of the 11 day experiment and four times in the last 24 hours of the experiment (Figures 4.2, 4.3). These growth curves revealed four main observations: 1) the growth rates as calculated up until the Cd addition were similar (Figure 4.4a), 2) the Zn-high PO_4^{3-} treatment appeared to enter stationary phase (Figures 4.3,4.4b), 3) the low PO_4^{3-} treatments showed increased instantaneous growth rates relative to the high PO_4^{3-} during the final 24 hours of the experiment (Figure 4.4b), and 4) Cd addition increased instantaneous growth rates further above the low PO_4^{3-} and Zn treatments (Figure 4.4b). The final cell numbers at harvest were similar for most of the treatments, but showed slightly elevated cell numbers for two treatments, the low PO_4^{3-}, Cd added both with and without added Zn (Figure 4.5).

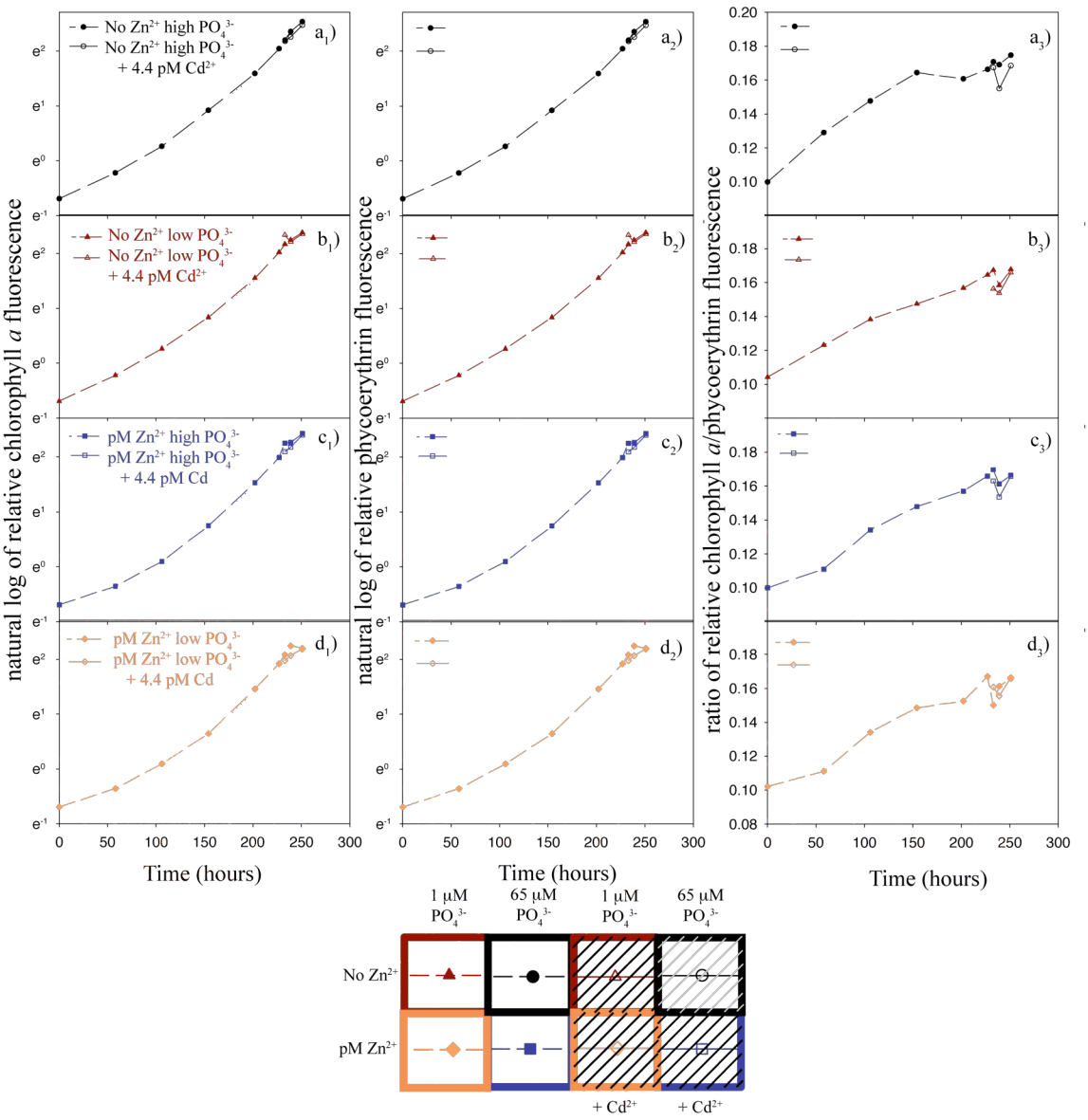

Figure 4.2: Physiological data. The natural log of relative chlorophyll *a* fluorescence (Column 1), natural log of phycoerythrin fluorescence (Column 2) and ratio of chlorophyll a/phycoerythrin (Column 3) vs. time for all eight experimental conditions. a) no Zn^{2+} added 65 µM PO_4^{3-} with and without + 4.4 pM Cd^{2+}, b) no Zn^{2+} added 1 µM PO_4^{3-} with and without + 4.4 pM Cd^{2+}, c) Zn^{2+} added 65 µM PO_4^{3-} with and without + 4.4 pM Cd^{2+}, d) Zn^{2+} added 1 µM PO_4^{3-} with and without + 4.4 pM Cd^{2+}. Protein samples analyzed and discussed in the text were from the last timepoint depicted.

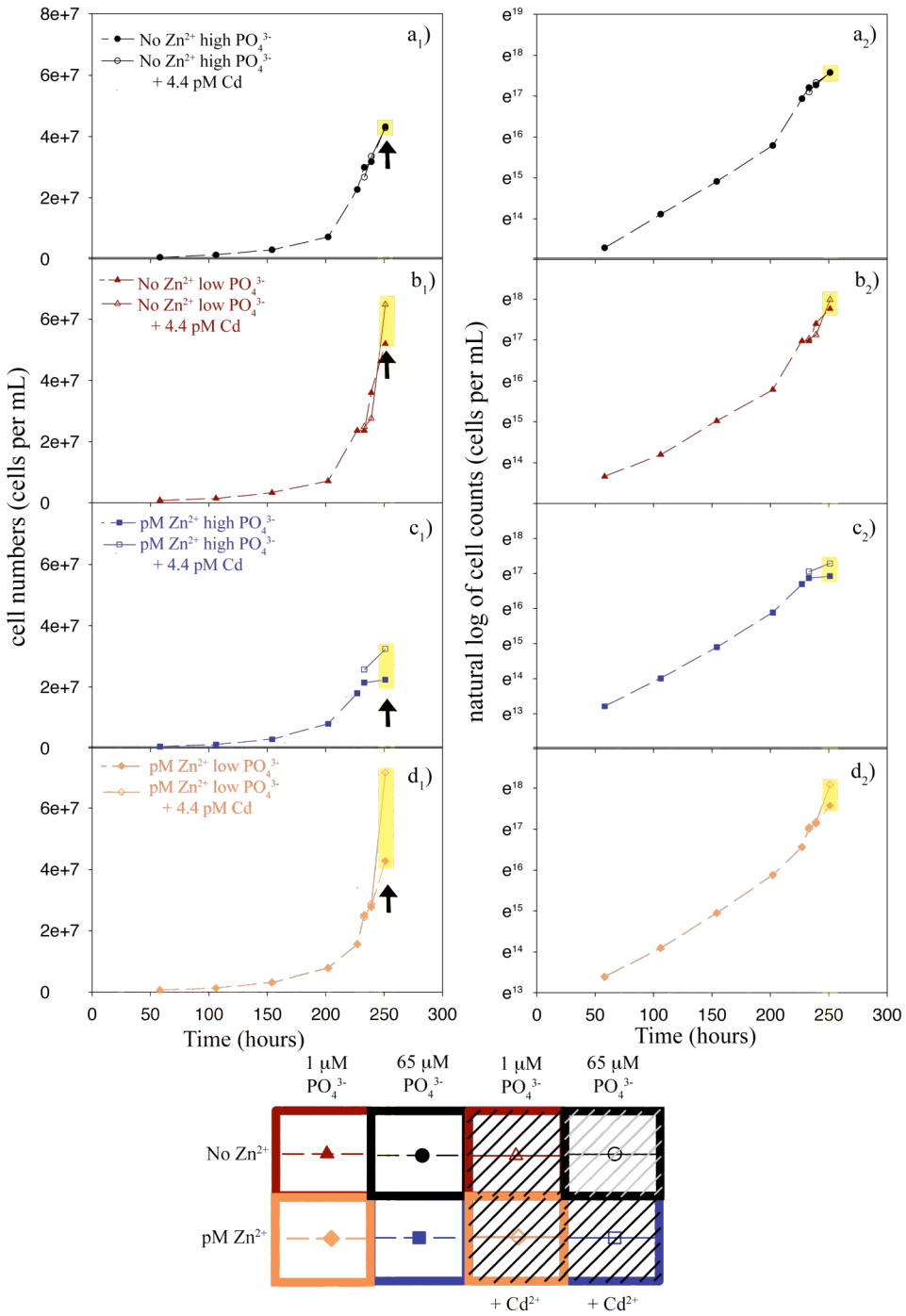

Figure 4.3: Cell numbers (Column 1) and natural log of cell numbers (Column 2) vs. time for all eight experimental conditions. a) no Zn^{2+} added high PO_4^{3-} with and without + 4.4 pM Cd^{2+}, b) no Zn^{2+} added low PO_4^{3-} with and without + 4.4 pM Cd^{2+}, c) Zn^{2+} added high PO_4^{3-} with and without + 4.4 pM Cd^{2+}, d) Zn^{2+} added low PO_4^{3-} with and without + 4.4 pM Cd^{2+}. Yellow highlights and arrow indicate protein samples analyzed and discussed in the text. Note that phycoerythrin fluorescence in the low PO_4^{3-} treatments appear (Figure 4.2) to level off as cell numbers reveal that cells are still experiencing exponential growth (Figure 4.3). Final cell numbers are higher in low than high phosphate (Figure 4.5).

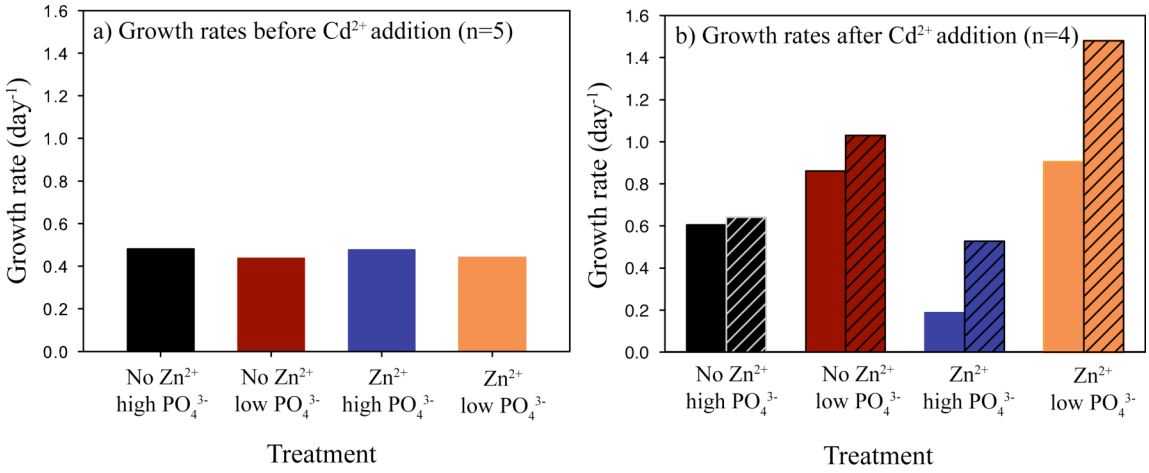

Figure 4.4: a) Growth rates. b) Growth rates in the twenty-four hours after cadmium addition until harvest.

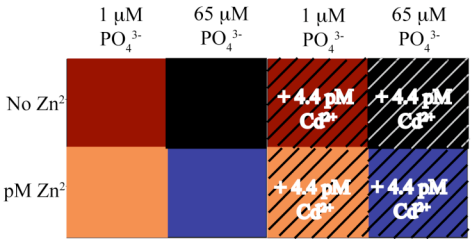

Figure 4.5: Final cell counts at harvest. Error bars represent 10% of value.

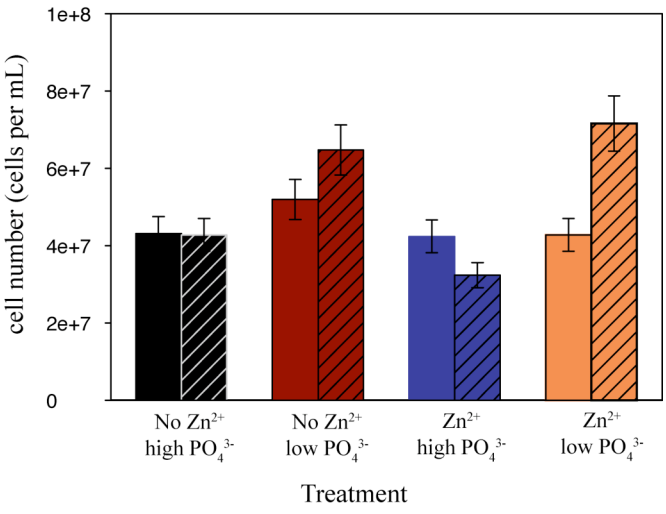

The ratios of chlorophyll *a* fluorescence per cell, phycoerythrin fluorescence per cell and ratios of relative chlorophyll *a* fluorescence to phycoerythrin fluorescence per cell showed deviations during the last 31 hours of the experiment (Figure 4.6). The Zn-high PO_4^{3-} treatment had the highest ratio for all three of these ratios. This implies directly that there is more chlorophyll *a* fluorescence, less phycoerythrin fluorescence, or fewer cells than other treatments or a combination of these factors. Given that the cell abundances in the Zn-high PO_4^{3-} treatment are similar to the Zn-low PO_4^{3-}, no Zn-high PO_4^{3-} and no Zn-high PO_4^{3-} + Cd treatments (Figure 4.5), this implies a difference in the relative fluorescence ratio among these treatments. These similar cell abundances suggest that: 1) the addition of Cd without Zn in the medium does not make a difference in the relative chlorophyll *a*/ phycoerythrin ratios per cell, 2) at a constant added Zn concentration, low PO_4^{3-} causes more of a decrease in the chlorophyll *a* /phycoerythrin ratio than high PO_4^{3-} and 3) at high PO_4^{3-} the absence of Zn causes more of a decrease in the chlorophyll *a*/ phycoerythrin ratio.

Considering treatments with different final cell counts, one notices that in the presence of Zn at both 1 and 65 μM PO_4^{3-}, Cd causes a greater decrease in chlorophyll *a*/ phycoerythrin fluorescence. This implies that in the presence of Zn, Cd causes 1) a decrease in chlorophyll *a*, 2) increase in phycoerythrin, 3) increase in number of cells, or 4) a combination of these factors. Figure 4.5 shows an increase in the number of cells in the Zn treatment with Cd addition at 1, but not 65 μM PO_4^{3-}.

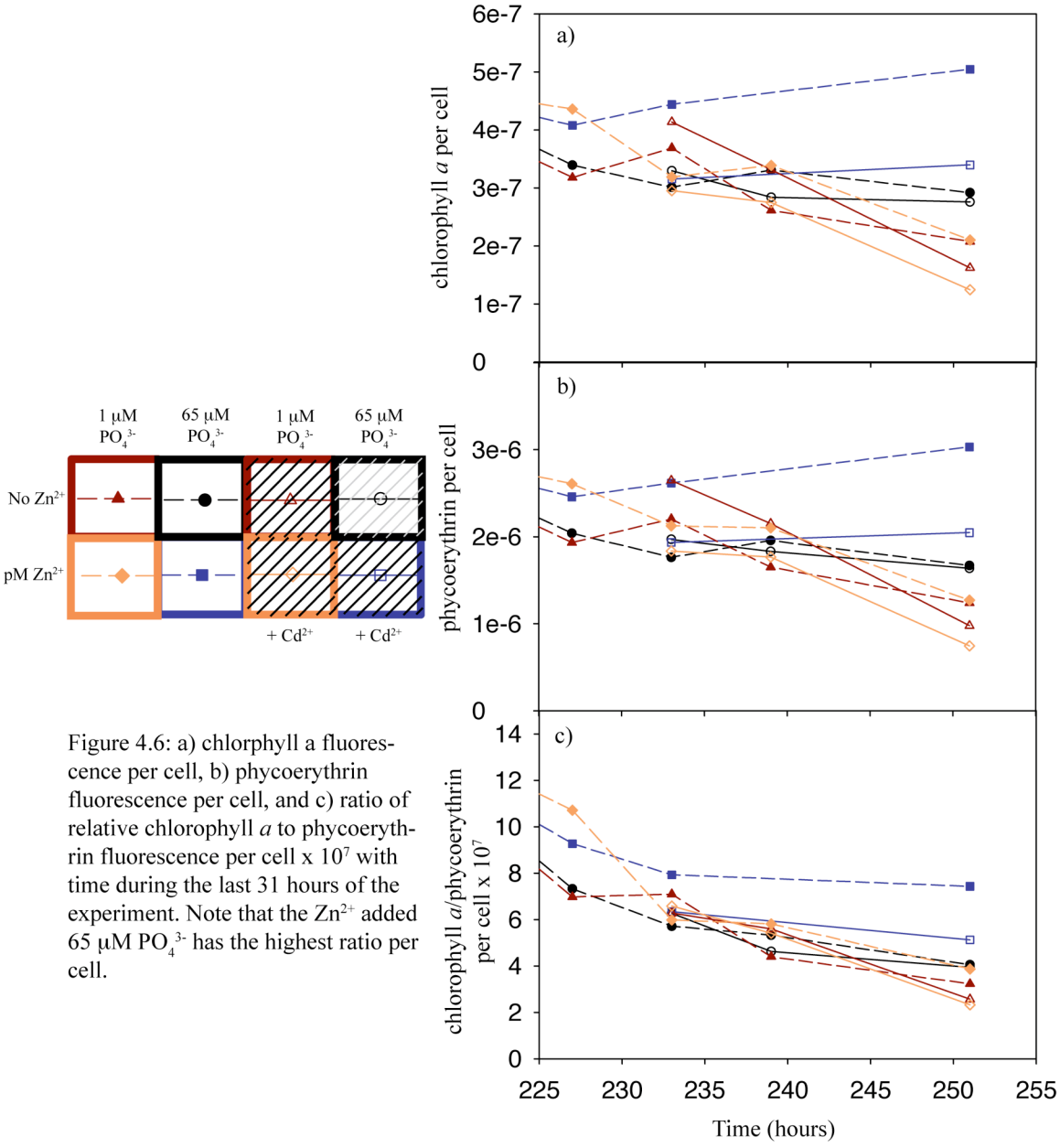

Figure 4.6: a) chlorophyll a fluorescence per cell, b) phycoerythrin fluorescence per cell, and c) ratio of relative chlorophyll *a* to phycoerythrin fluorescence per cell x 10^7 with time during the last 31 hours of the experiment. Note that the Zn^{2+} added 65 µM PO_4^{3-} has the highest ratio per cell.

Global Proteomic Data

Analysis resulted in the identification of 594 proteins from 62,264 mass spectra over 16 injections (8 treatments injected in duplicate). In Scaffold 3, using filters of 95% peptide minimum confidence level, 99.9% protein minimum confidence level and a minimum of 2 peptides resulted in a 1.9% peptide false discovery rate (Peng et al., 2003, Zhang et al., 2006). This experiment identified 23.6% of the 2519 possible proteins present in the genome of WH8102. Using a more stringent filter, analysis resulted in the identification of 420 proteins from 60,388 mass spectra using 95% peptide minimum confidence level, 99.9% minimum confidence level and a minimum of 3 peptides. This resulted in a 0.9% peptide false discovery rate (Peng et al., 2003, Zhang et al., 2006). Using these more stringent conditions, 16.8% of the 2519 possible proteins present in the genome of WH8102 were identified. Seventy-one proteins showed differences in protein abundances in at least two treatments using a minimum difference of 7 spectral counts and a threshold of 7 spectral counts, based on technical replicates of each of the 8 treatments. Cluster analysis (Eisen et al., 1998) reveals most prominently phosphate-stress effects (Figure 4.7).

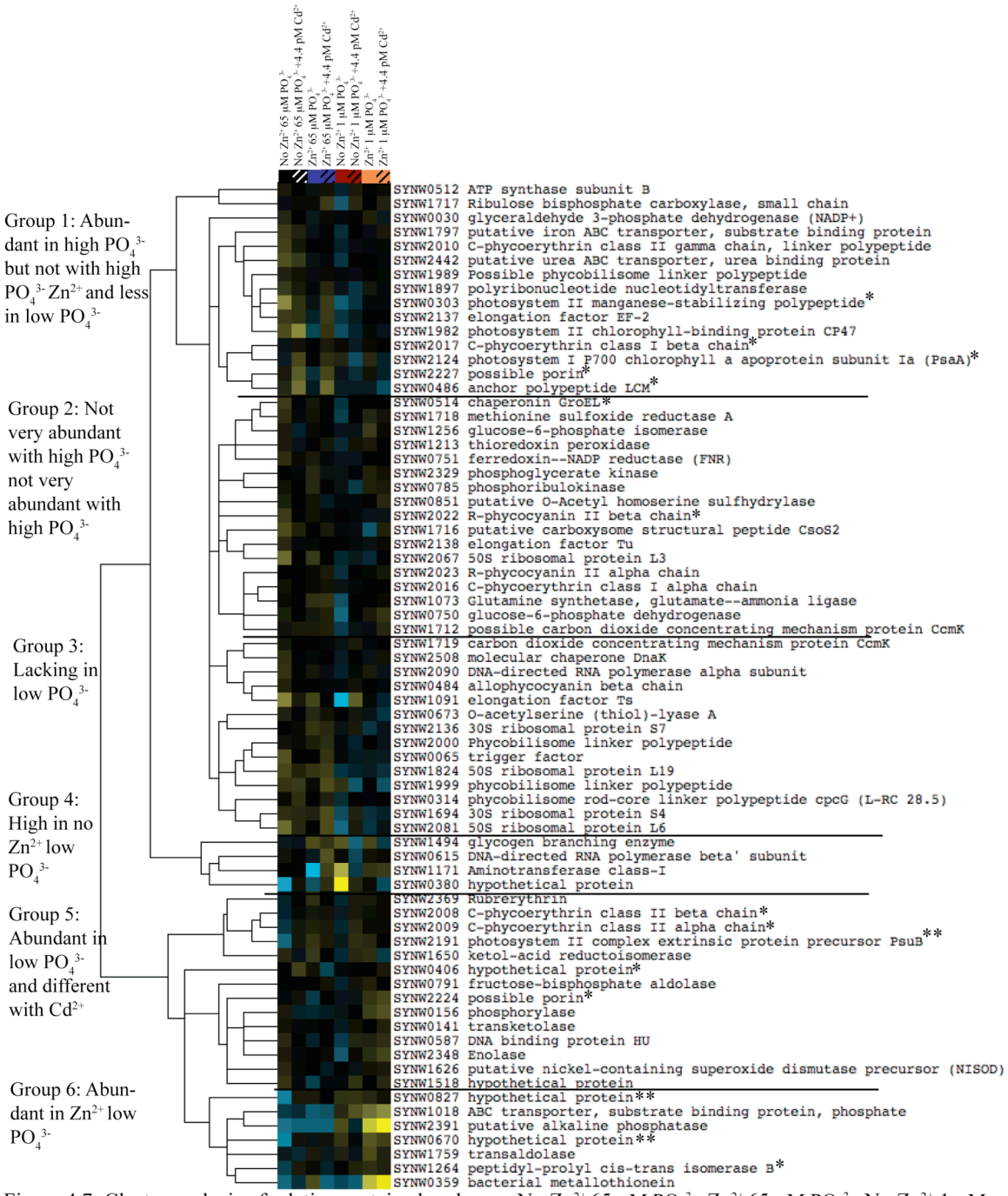

Figure 4.7: Cluster analysis of relative protein abundance. No Zn^{2+} 65 µM PO_4^{3-}, Zn^{2+} 65 µM PO_4^{3-}, No Zn^{2+} 1 µM PO_4^{3-}, Zn^{2+} 1 µM PO_4^{3-} and these four chronic treatments with 4.4 pM Cd^{2+} acutely added. Four low, 1 µM PO_4^{3-} on the right and replete, 65 µM PO_4^{3-} on the left. There are 71 proteins. Proteins are averages of duplicates have at least 7 counts and are different by a value of 7. Data are log transformed, centered, clustered by Kendall's Tau, centroid linkage. Yellow = more abundant, Blue = less abundant, * = statistically different by Fisher's Exact Test between the No Zn^{2+} 65 µM PO_4^3 and the No Zn^{2+} 65 µM PO_4^3 + 4.4 pM Cd^{2+} ** = differentially abundant by two-fold or greater and statistically different by Fisher's Exact Test between the No Zn^{2+} 65 µM PO_4^3 and the No Zn^{2+} 65 µM PO_4^3 + 4.4 pM Cd^{2+}.

Pairwise analyses between experimental treatments reveal most noticeably the effects of PO_4^{3-} stress, but also lesser Cd and Zn effects (Figure 4.8). There are 28 ways to pair 8 treatments, only 12 are considered here, querying what happens to the proteome when two conditions are held constant and the third is varied. Among the 16 pairwise comparisons not discussed here, one could query, for example, if Cd could replace Zn at low PO_4^{3-} (compare no Zn-low PO_4^{3-} to no Zn-low PO_4^{3-} + Cd). Proteins are considered differentially abundant here if the average spectral count value of one of the pairs is equal to or greater than five and the pair of proteins are different by two-fold or more. Use of Fisher's Exact Test (Zhang et al., 2006) confirms that most proteins are different in abundance using these stringencies, excepting a few proteins with five spectral counts. The two-fold or more differentially abundant proteins with low spectral counts remain in the tables, but are considered tenuous in analysis. The results of Fisher's Exact Test also conclude that more proteins are statistically different in abundance than the $\geq$ two-fold analysis alone. This is because a smaller fold difference in a greater value is statistically different, thus proteins with higher spectral counts that are different by less than two-fold are differentially abundant (Compare Tables 4.4 and 4.5).

In these pairwise proteome comparisons, three observations can be made: 1) the no Zn-low PO_4^{3-} treatment had the greatest number of proteins $\geq$ two-fold different in abundance (Compare Figure 4.8a, b and c), 2) Cd addition caused a greater change in the number of $\geq$ two-fold different in abundance in the absence of Zn (Figure 4.8b), and 3) the acute addition of Cd under both low and high PO_4^{3-} conditions had fewer proteins of $\geq$ two-fold different in abundance in the presence or absence of Zn (Figure 4.8c). The combination of no Zn-low PO_4^{3-} (red) had the greatest number of proteins (55 in Figure 4.8a, 32 in Figure 4.8b and 31 in Figure 4.8c) differentially abundant compared to any other treatment. For comparison, the no Zn-high PO_4^{3-} treatment had the number of proteins different as 55 in Figure 4.8a, 10 in Figure 4.8b and 16 in Figure 4.8c. The presence of Zn caused a smaller change in the total number of proteins $\geq$ two-fold different in abundance when Cd was added acutely (compare 42 with no added Zn, both high and low PO_4^{3-} to 11 proteins in the presence of Zn, both high and low PO_4^{3-}; Figure

4.8b). Cadmium addition under low and high PO_4^{3-} conditions caused fewer proteins to be differentially abundant in the presence or absence of Zn, perhaps hinting that Cd alleviates Zn deprivation (Figure 4.8c).

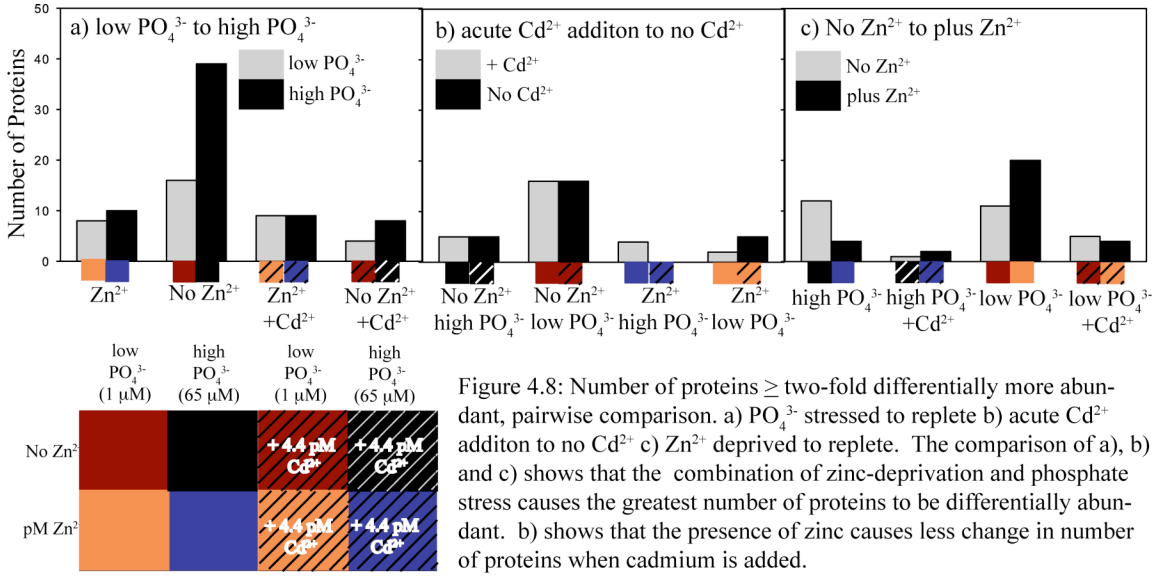

Figure 4.8: Number of proteins ≥ two-fold differentially more abundant, pairwise comparison. a) PO_4^{3-} stressed to replete b) acute Cd^{2+} additon to no Cd^{2+} c) Zn^{2+} deprived to replete. The comparison of a), b) and c) shows that the combination of zinc-deprivation and phosphate stress causes the greatest number of proteins to be differentially abundant. b) shows that the presence of zinc causes less change in number of proteins when cadmium is added.

The influence of phosphate (pairwise comparisons)

As noted by cluster analysis in Figure 4.7 and the number of proteins differentially abundant in Figure 4.8, PO_4^{3-} appeared to cause the most difference in this multivariate Cd-Zn-PO_4^{3-} matrix experiment. In the Zn added, 1 compared to 65 µM PO_4^{3-} treatments, 18 proteins were two-fold or more differentially abundant with a spectral count of at least five (Table 4.1). Eight proteins were more abundant in the 1 µM PO_4^{3-} treatment, including 6 proteins also found to be differentially expressed as transcripts in a microarray experiment by Tetu et al. (2009) (starred in Table 4.1). These 6 proteins are SYNW2391 putative alkaline phosphatase, SYNW1018 ABC transporter, substrate binding protein, phosphate (PstS), SYNW0953 cell-surface protein required for swimming motility (SwmB), SYNW0085 cell-surface protein required for swimming motility (SwmA), SYNW0700 glyceraldehyde-3-phosphate dehydrogenase and SYNW224 possible porin. Also of note is SYNW0359 bacterial metallothionein. See Figure 4.9 for relative abundances of SYNW0359, SYNW2391 and SYNW1018. Ten proteins were more abundant in the 65 µM PO_4^{3-} treatments, including 6 ribosomal proteins one of which was found to be downregulated as a transcript in the Tetu et al.

(2009) analysis, SYNW2082 50S ribosomal protein L18.

Table 4.1: WH8102 proteins that are two-fold or greater differentially abundant in the Zn^{2+} 1 µM PO_4^{3-} (low PO_4^{3-}) vs. Zn^{2+} 65 µM PO_4^{3-} (high PO_4^{3-}).

SYNW ID	Function	Protein	Zn^{2+} 1 µM PO_4^{3-} counts	Zn^{2+} 65 µM PO_4^{3-} counts	Zn^{2+} 1 µM PO_4^{3-}/ Zn^{2+} 65 µM PO_4^{3-} fold change
2391*	U,P	putative alkaline phosphatase	8.1±0.8	1.0±0.0	+8.1
1018*	ABC,P	ABC transporter, substrate-binding protein, phosphate (PstS)	76.9±1.3	19.2±2.4	+4.0
1661	ukn	hypothetical protein	5.2±2.1	1.4±0.7	+3.7
0953*	Mo	cell-surface protein required for swimming motility (swmB)	5.2±0.6	1.4±0.7	+3.7
0359	U,Zn	bacterial metallothionein (SmtA)	7.1±3.2	3.3±0.6	+2.2
0085*	Mo	cell-surface protein required for swimming motility (swmA)	9.0±0.8	4.2±0.6	+2.1
0799*	M,E,C	glyceraldehyde-3-phosphate dehydrogenase (gap3)	2.4±0.6	0.5±0.7	+4.7
2224*	U,Om	possible porin (som)	61.2±1.7	29.4±2.6	+2.1
1773	M,Nu,Pu,A	adenylosuccinate synthetase (purA, adeK)	1.4±0.7	7.5±0.1	-5.2
0814	M,Nu,Pu	adenine phosphoribosyltransferase	1.0±0.0	5.1±0.8	-5.1
2500	M,Cb,TCA E,C	aconitate hydratase (acnB)	2.8±0.0	7.5±0.1	-2.6
2069	GI,T	50S ribosomal protein L23 (rpl23,rplW)	3.8±1.3	8.9±0.5	-2.3
2068	GI,T	50S ribosomal protein L4 (rpl4,rplD)	4.3±2.1	9.3±0.2	-2.2
2079	GI,T	50S ribosomal protein L5 (rpl5,rplE)	5.2±1.9	10.7±0.4	-2.1
1716	C	putative carboxysome structural peptide (CsoS2)	6.6±0.1	13.1±1.6	-2.0
2136	GI,T	30S ribosomal protein S7 (rps7,rpsG)	8.1±0.5	15.9±1.0	-2.0
2083	GI,T	30S ribosomal protein S5 (rps5,rpsE)	5.2 ±0.8	10.3±0.2	-2.0
2082**	GI,T	50S ribosomal protein L18 (rpl18,rplR)	3.3±0.6	6.5±2.5	-2.0

Arranged in highest to lowest fold change Zn-low PO_4^{3-} (1 µM PO_4^{3-}) then Zn-high PO_4^{3-} (65 µM PO_4^{3-}). + = fold greater than Zn-high PO_4^{3-}, - = fold less than Zn-high PO_4^{3-}, * = Corresponding transcript identitfied in Tetu et al. 2009 as strongly upregulated under early P-stress (5 µM PO_4^{3-}), * * = Corresponding transcript identitfied in Tetu et al. 2009 as strongly downregulated under early P-stress (5µM PO_4^{3-}).
U = unclassified, P = phosphorus metabolism, ABC = ABC transporter, ukn = unknown, Mo = motility, Zn = zinc metabolism, M = metabolism, E= energy metabolism, C = carbon fixation, Om = outer membrane protein, Nu=nucleic acid metabolism, Pu = purine metabolism, A = amino acid metabolism, Cb = carbohydrate metabolism, TCA = citrate cycle, GI = genetic information processing, T = translation.

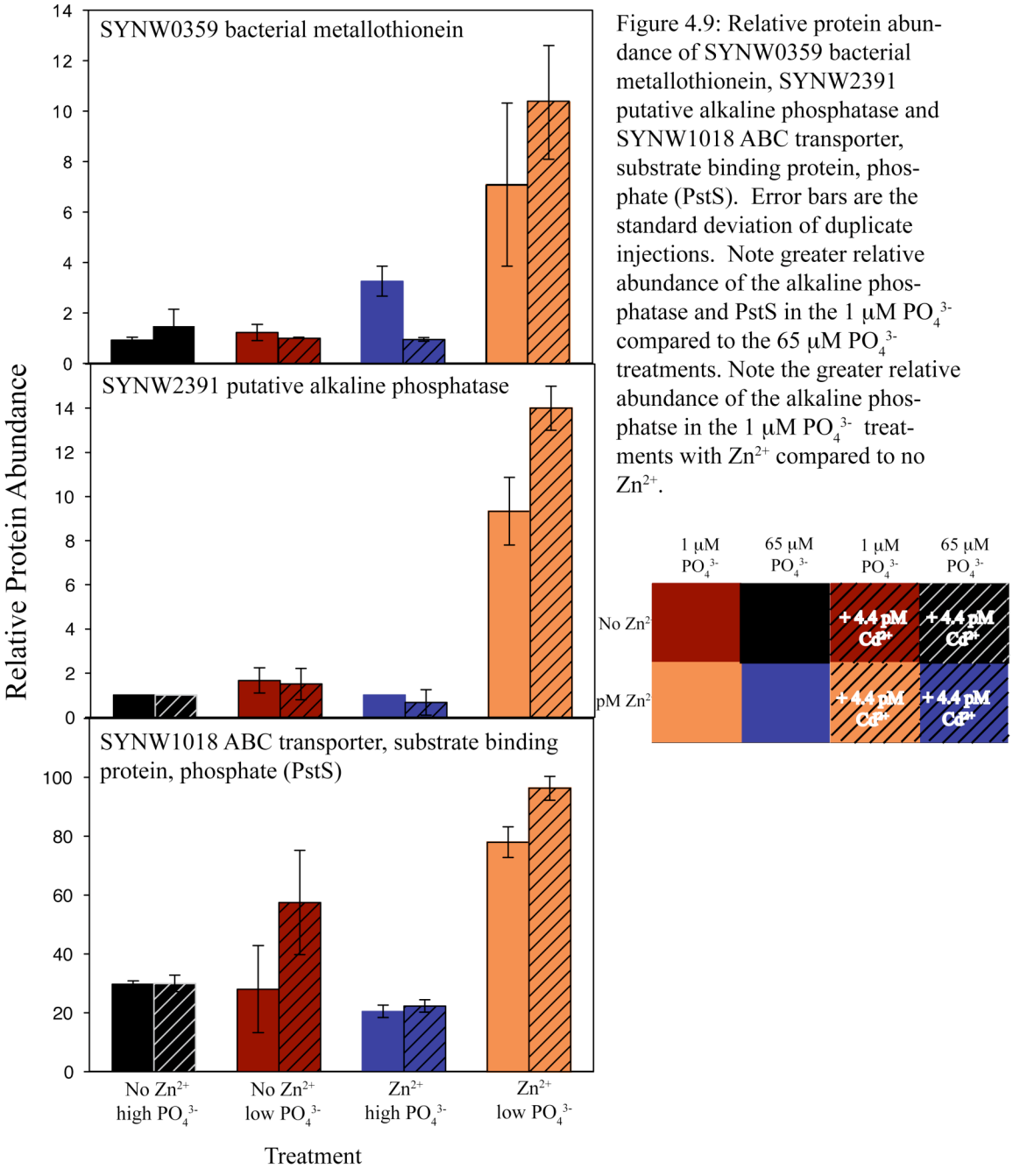

Figure 4.9: Relative protein abundance of SYNW0359 bacterial metallothionein, SYNW2391 putative alkaline phosphatase and SYNW1018 ABC transporter, substrate binding protein, phosphate (PstS). Error bars are the standard deviation of duplicate injections. Note greater relative abundance of the alkaline phosphatase and PstS in the 1 µM PO_4^{3-} compared to the 65 µM PO_4^{3-} treatments. Note the greater relative abundance of the alkaline phosphatse in the 1 µM PO_4^{3-} treatments with Zn^{2+} compared to no Zn^{2+}.

Seven proteins were strongly upregulated transcripts in the Tetu et al., 2009 microarray experiment that were not two-fold or greater differentially abundant in this experiment (Table 4.2). One of these was close, however: SYNW0156 phosphorylase, 1.9-fold greater in the 1 µM PO_4^{3-} treatment.

Table 4.2: WH8102 proteins that are strongly upregulated (≥ two-fold) under early P-stress according to transcript analysis in Tetu et al. 2009, but not ≥ two-fold more abundant according to our global proteomic analysis, **1 µM PO_4^{3-} Zn^{2+}** (low PO_4^{3-}) than the **65 µM PO_4^{3-} Zn^{2+}** (high PO_4^{3-}).

SYNW ID	Function	Protein	Zn^{2+} 1 µM PO_4^{3-} counts	Zn^{2+} 65 µM PO_4^{3-} counts	**Zn^{2+} 1 µM PO_4^{3-}/ Zn^{2+} 65 µM PO_4^{3-}** fold change
1815	ABC,P	ABC transporter, substrate binding protein, phosphate (PstS)	5.2±0.8	6.6±1.4	-1.3
0156	M, Ss	phosphorylase	36.6±5.3	20.0±4.9	+1.9
0406	Ukn	hypothetical protein	13.8±2.2	14.9±1.0	-1.1
1119	M,Pt,G	6-phosphogluconate dehydrogenase	6.6±0.1	4.1±1.2	+1.6
1213	U,GI	thioredoxin peroxidase	34.6±0.1	30.8±1.9	+1.1
2508	GI	molecular chaperone DnaK2, heat shock protein hsp70-2	19.4±1.7	23.4±0.5	-1.2
0160	Ukn	conserved hypothetical protein	7.6±1.2	4.7±0.1	+1.6

ABC = ABC transporter, P = phosphate metabolism, M = metabolism, Ss = sugar and starch metabolism, Ukn = unknown, Pt = pentose phosphate pathway, G = glutathione metabolism, U = unclassified, G I= genetic information prrocessing

In the no Zn-1 µM PO_4^{3-} compared to no Zn-65 µM PO_4^{3-}, 55 proteins were two-fold or more differentially abundant with a spectral count of at least five (Table 4.3). Sixteen proteins were more abundant in the 1 PO_4^{3-} treatment, including five hypothetical proteins and two proteins involved in photosynthesis. No proteins showed abundances similar to gene expression in Tetu et al., 2009. Thirty-nine proteins were more abundant in the 65 µM PO_4^{3-} treatments, including 12 involved in genetic information processing, two involved in the biosynthesis of chlorophyll and two hypothetical proteins.

Table 4.3: WH8102 proteins that are two-fold or more differentially abundant in the **no Zn^{2+} 1 µM PO_4^{3-}** vs. **no Zn^{2+} 65 µM PO_4^{3-}**.

SYNW ID	Function	Protein	No Zn^{2+} 1 µM PO_4^{3-} counts	No Zn^{2+} 65 µM PO_4^{3-} counts	**No Zn^{2+} 1 µM PO_4^{3-} / No Zn^{2+} 65 µM PO_4^{3-}** fold change
0380	Ukn	hypothetical protein	13.5±4.7	0.4±0.6	+31.0
0727	GI,Re	DNA gyrase subunit A (gyrA)	5.9±2.2	0.9±0.0	+6.9
0235	M,Cb, As	phosphoglucomutase/phosphomannomutase family protein	5.7±0.1	0.9±0.1	+6.2
1610	Rg	putative bifuntional enzyme: tRNA methyl-transferase; 2-C-methyl-D-erythritol 2,4-cyclodiphosphate synthase	5.0±0.9	0.9±0.1	+5.3
1090	GI,T	30S ribosomal protein S2 (rps2,rpsB)	7.4±0.2	1.7±0.0	+4.3
1145	Ukn	hypothetical protein	5.2±3.2	1.3±0.6	+4.0
0670	Ukn	hypothetical protein	8.6±4.2	2.2±1.9	+4.0
0278	M,Nu,Py	deoxycytidine triphosphate deaminase (dcd)	8.1±0.9	2.1±0.7	+3.8
0827	Ukn	hypothetical protein	12.9±2.3	3.4±0.1	+3.8
0340	Ukn	hypothetical protein	7.4±0.2	2.1±0.7	+3.5
1171	M,A,GI,T	aminotransferase class-I (aspC)	7.6±2.5	2.6±0.1	+3.0
0402	M,L	possible acyl carrier protein	5.0±0.9	2.1±0.5	+2.3
1852	M,L	3-oxoacyl-[acyl carrier protein] reductase (fabG)	5.9±2.2	2.6±0.1	+2.3
0144	PS	photosystem I subunit VII (psaC)	10.2±4.1	4.7±1.9	+2.2
0535	PS	ferredoxin (petF4)	12.7±4.7	6.0±0.1	+2.1
1936	ABC, S	putative sulfate transporter	5.2±3.2	2.6±2.5	+2.0
1091	GI	elongation factor Ts (tsf)	0.9±1.3	10.2±1.5	-11.0
1816	Ukn	hypothetical protein	0.7±1.0	6.8±1.0	-9.4
0303	PS	photosystem II manganese-stabilizing polypeptide (psbO)	7.4±0.2	35.7±7.5	-4.8
1495	M,V,Po,chl	uroporphyrinogen decarboxylase (hemE)	1.7±0.3	7.7±2.6	-4.6
2139	GI,T	30S ribosomal protein S10 (rps10, rpsJ)	1.2±0.3	5.5±1.7	-4.5
2081	GI,T	50S ribosomal protein L6 (rpl6,rplF)	2.4±0.7	10.2±2.1	-4.3
0852	Ukn	hypothetical protein	1.7±0.3	5.5±0.5	-3.3
2069	GI,T	50S ribosomal protein L23 (rpl23,rplW)	2.6±1.6	8.5±1.0	-3.3
2500	M,Cb,TCA E,C	aconitate hydratase (acnB)	1.7±0.3	5.1±1.3	-3.1
2356	GI,T	aspartyl/glutamyl-tRNA amidotransferase subunit B (gatB)	2.4±0.7	7.3±2.0	-3.0
1933	M,V,Po,chl	δ-aminolevulinic acid dehydratase (hemB)	2.4±0.7	7.2±1.6	-3.0
1025	M,A	putative anthranilate synthase component II (trpD/G)	3.1±1.8	9.0±0.8	-2.9
2074	GI,T	50S ribosomal protein L16 (rpl16,rplP)	2.4±0.7	6.8±2.2	-2.8
0045	U,M	soluble hydrogenase small subunit (DHSS)	2.6±1.6	7.2±2.8	-2.8
1982	PS	photosystem II chlorophyll-binding protein CP47 (psbB)	4.8±1.5	13.2±2.1	-2.8
0032	GI	putative cyclophilin-type peptidyl-prolyl cis-trans isomerase	2.2±3.1	6.0±0.1	-2.7

Table 4.3 (continued, page 2 of 2):

SYNW ID	Function	Protein	No Zn^{2+} 1 µM PO_4^{3-} counts	No Zn^{2+} 65 µM PO_4^{3-} counts	No Zn^{2+} 1 µM PO_4^{3-} / No Zn^{2+} 65 µM PO_4^{3-} fold change
0033	GI,T	elongation factor P (efp)	2.4±0.7	6.4±2.8	-2.7
0750	M,Cb,G	glucose-6-phosphate dehydrogenase (zwf)	4.0±0.4	10.7±2.1	-2.6
0462	Ei,Si	nitrogen regulatory protein P-II (glnB)	2.6±1.6	6.8±1.0	-2.6
0819	M,A	dihydrodipicolinate reductase (dapB)	2.7±2.4	6.8±1.0	-2.5
2067	GI,T	50S ribosomal protein L3 (rpl3,rplC)	4.9±5.5	12.0±3.9	-2.5
2082	GI,T	50S ribosomal protein L18 (rpl18,rplR)	3.1±1.8	7.7±0.2	-2.5
2442	ABC,Si	putative urea ABC transporter, urea binding protein (urtA1)	24.1±5.0	55.9±4.5	-2.3
1815	ABC,P	ABC transporter, substrate binding protein, phosphate (PstS)	4.0±0.4	9.4±1.0	-2.3
1694	GI,T	30S ribosomal protein S4 (rps4,prsD)	4.1±4.4	9.4±0.2	-2.3
2348	M,Cb,E,GI	enolase (eno)	7.0±4.5	15.7±2.6	-2.3
1824	GI,T	50S ribosomal protein L19 (rpl19)	6.6±1.2	14.5±0.4	-2.2
0687	M,Nu,Py	putative thioredoxin reductase	2.4±0.7	5.1±1.3	-2.1
2246	Ei	two-component response regulator (rpaB)	5.7±0.1	11.9±2.1	-2.1
2137	GI,T	elongation factor EF-2 (fusA)	12.1±1.3	25.1±1.2	-2.1
1835	PS	photosystem I reaction center subunit III (PsaF)	3.3±0.6	6.9±2.6	-2.1
1718	C	ribulose bisphosphate carboxylase, large chain (rbcL,cbbL)	38.2±11.7	78.7±9.4	-2.1
0405	M,Nu,Pu,A	fumarate lyase: adenylosuccinate lyase (purB)	3.1±1.8	6.4±0.8	-2.1
1617	GI,T	30S ribosomal protein S16 (rps16,rpsP)	4.8±1.5	9.8±2.1	-2.1
2487	ABC, Ei	putative cyanate ABC transporter	5.5±2.5	11.1±2.7	-2.0
0514	GI,F	chaperonin (GroEL)	55.8±15.5	112.0±0.1	-2.0
0613	U,GI,T	DNA-directed RNA polymerase beta subunit (rpoB)	4.0±0.4	8.1±1.6	-2.0
2068	GI,T	50S ribosomal protein L4 (rpl4,rplD)	5.6±6.5	11.1±1.5	-2.0
1073	M,E,N,A	glutamine synthetase, glutamate--ammonia ligase (glnA)	20.0±4.5	39.6±1.6	-2.0

Arranged in highest to lowest fold change Zn-high PO_4^{3-}, than Zn-low PO_4^{3-}. + = fold greater thanZn-high PO_4^{3-}, - = fold less than Zn-high PO_4^{3-}. Ukn = unknown, GI = genetic information processing, Re = DNA replication and repair, M = metabolism, Cb = carbohydrate metabolism, As = amino sugar metabolism, Rg = regulatory function, T = translation, Nu = nucleic acid metabolism, Py = pyrimidine metabolism, A = amino acid metabolism, L = lipid metabolism, PS = photosynthesis, ABC = ABC transporter, S = sulfur metabolism, V = vitamin metabolism, Po = porphryin metabolism, chl = chlorophyll metabolism, TCA = citrate cycle, E = energy metabolism, C = carbon fixation, G = glutathione metabolism, Ei = environmental information processing, Si = signalling, P = phosphorus metabolism, F = protein folding, Pu = purine biosynthesis, N = nitrogen metabolism

In the Zn + 4.4 pM Cd^{2+}, low compared to high PO_4^{3-} treatments, 17 proteins were two-fold or more differentially abundant with a spectral count of at least five (Table III.1). Nine proteins were more abundant in the Zn-low PO_4^{3-} + Cd treatment, including five proteins also found to be differentially expressed as genes in a microarray experiment by Tetu et al., 2009 (starred in Table III.1). These five proteins are

SYNW2391 putative alkaline phosphatase, SYNW1018 ABC transporter, substrate binding protein, phosphate (PstS), SYNW0953 cell-surface protein required for swimming motility (SwmB), and SYNW0156 phosphorylase. Eight proteins were more abundant in the Zn-high PO_4^{3-} + Cd treatment, including three related to the phycobilisomes and two ribosomal proteins.

In the no Zn + 4.4 pM Cd^{2+}, low compared to high PO_4^{3-} treatments, 12 proteins were two-fold or more differentially abundant with a spectral count of at least five (Table III.2). Four proteins were more abundant in the no Zn-low PO_4^{3-} + 4.4 pM Cd^{2+} treatment, including two proteins also found to be differentially expressed as genes in a microarray experiment by Tetu et al., 2009. These two proteins are SYNW0953 cell-surface protein required for swimming motility (SwmB) and SYNW1018 ABC transporter, substrate binding protein, phosphate (PstS). Eight proteins were more abundant in the no Zn-high PO_4^{3-} + 4.4 pM Cd^{2+} treatment, including six involved in photosynthesis (two phycobilisome, three Photosystem II and one Photosystem I proteins).

The influence of cadmium (pairwise comparisons)

Cd effects can be discerned by examining pair-wise protein comparisons (Figure 4.8b). In the no Zn-high PO_4^{3-} + 4.4 pM Cd^{2+} compared to no Cd added treatments, 10 proteins were two-fold or more differentially abundant with a spectral count of at least five (Table 4.4). Five proteins were more abundant in the no Zn-high PO_4^{3-} + 4.4 pM Cd^{2+} treatment, including three unknown proteins, one involved in photosystem II and one involved in the biosynthesis of riboflavin (Vitamin B2) (Figure 4.10). Five proteins were more abundant in the no Zn-high PO_4^{3-} no added Cd^{2+} treatment (Figure 4.11).

Table 4.4:WH8102 proteins that are ≥ two-fold differentially abundant in the no Zn^{2+} 65 μM PO_4^{3-} + 4.4 pM Cd^{2+} vs. the no Zn^{2+} 65 μM PO_4^{3-}.

SYNW ID	Function	Protein	No Zn^{2+} 65 μM PO_4^{3-} + 4.4 pM Cd^{2+} counts	No Zn^{2+} 65 μM PO_4^{3-} counts	No Zn^{2+} 65 μM PO_4^{3-} + 4.4 pM Cd^{2+}/ No Zn^{2+} 65 μM PO_4^{3-} fold change	Fisher Test P-value
0908	Ukn	hypothetical protein	6.2±0.5	1.3+0.6	+4.9	95% (0.01)
0670	Ukn	hypothetical protein	7.2+0.4	2.2+1.9	+3.3	95% (0.0048)
0827	Ukn	hypothetical protein	11.0+2.4	3.4+0.1	+3.2	95% (0.0016)
2191	PS	photosytem II complex extrinsic protein precursor (psuB)	13.8+0.2	5.5+1.7	+2.5	95% (0.0016)
0082	M,V,R	riboflavin synthase subunit beta (ribH)	8.6+2.4	4.3+0.1	+2.0	95% (0.047)
1118	M,Cb	glucose-1-phosphate adenylyltransferase (agp,glgC)	1.5+0.7	5.5+0.5	-3.6	95% (0.019)
0405	M,Nu,Pu,A	fumarate lyase: adenylo-succinate lyase (purB)	1.9+0.1	6.4+0.8	-3.4	95% (0.041)
2139	GI,T	30S ribosomal protein S10 (rps10,rpsJ)	1.9+0.1	5.5+1.7	-2.9	0% (0.09)
1953	Ukn,L	putative glycerol kinase	2.4+2.1	5.6+2.0	-2.3	0% (0.15)
2500	M,Cb,TCA E,C	aconitate hydratase (acnB)	2.4+0.7	5.1+1.3	-2.1	0% (0.21)

Arranged in highest to lowest fold change 4.4 pM Cd^{2+} vs. control (no Zn and no added Cd). + = fold greater than control, - = fold less than control, Ukn = unknown, PS = photosynthesis, M = metabolism, V = vitamin metabolism, R = riboflavin metabolsim, Cb = carbohydrate metabolism, Nu = nucleic acid metabolism, Pu = purine metabolism, A = amino acid metabolism, GI = genentic information processing, T = translation, L = lipid metabolism,TCA = citrate cycle, E = energy metabolism, C = carbon fixation, in this case reductive glyoxylate cycle.

In addition to proteins being considered differentially abundant by a two-fold or greater differential abundance, there is Fisher's Exact Test as explained earlier in this section. Applying Fisher's Exact Test results in 13 more proteins being labeled significantly differential in abundance, in addition to the 7 in Table 3.1 (Table 4.5). Ten proteins are statistically more abundant in the no Zn-65 μM PO_4^{3-} + 4.4 pM Cd^{2+}, of which five are involved in photosynthesis (Figure 4.10). Three are statistically more abundant in the no Zn-65 μM PO_4^{3-} no added Cd^{2+} (Figure 4.11). Seven of these 13 are involved in photosynthesis.

Table 4.5: Additional WH8102 proteins that are differentially abundant in the acute no Zn^{2+} 65 μM PO_4^{3-} + 4.4 pM Cd^{2+} vs. the no Zn^{2+} 65 μM PO_4^{3-} according to Fisher's Exact Test.

SYNW ID	Function	Protein	No Zn^{2+} 65 μM PO_4^{3-} + 4.4 pM Cd^{2+} counts	No Zn^{2+} 65 μM PO_4^{3-} counts	No Zn^{2+} 65 μM PO_4^{3-} + 4.4 pM Cd^{2+}/ No Zn^{2+} 65 μM PO_4^{3-} fold change	Fisher Test P-value
0486	PS	anchor polypeptide L_{CM} (apcE)	16+2.5	10+2.1	+1.6	95% (0.035)
0406	Ukn	hypothetical protein	20+1.3	13 +4.6	+1.5	95% (0.034)
2022	PS	R-phycocyanin II beta chain (rpcB)	91+9.3	121.8+0.7	-1.3	95% (0.032)
2224	U,Om	possible porin (som)	51+12.4	42+2.3	+1.2	95% (0.025)
2124	PS	photosystem I P700 chlorophyll *a* apoprotein subunit Ia (psaA)	15+1.2	8+2.0	+1.8	95% (0.01)
0303	PS	photosystem II manganese-stabilizing polypeptide (psbO)	20.1+0.6	35.7+7.5	-1.7	95% (0.0094)
2227	U, Om	possible porin (som)	31+7.7	21+4.8	+1.4	95% (0.0090)
0514	GI,F	chaperonin GroEL (groEL)	77+1.1	112.0+0.1	-1.4	95% (0.0079)
1264	U, F	peptidyl-prolyl cis-trans isomerase B	18+2.8	9.4+0.2	+1.9	95% (0.0067)
2017	PS	C-phycoerythrin class I beta chain (cpeB)	74.0+0.3	59+5.1	+1.2	95% (0.0032)
2369	U,Fo	rubrerythrin	57+5.6	43 +2.9	+1.3	95% (0.0031)
2008	PS	C-phycoerythrin class II beta chain (mpeB)	410+6.5	296+19	+1.2	95% (1.5E-17)
2009	PS	C-phycoerythrin class II alpha chain (mpeA)	346+25	210+23	+1.7	95% (1.4E-25)

Arranged in order of decreasing P-value. + = fold greater than control, - = fold less than control, PS = photosynthesis, Ukn = unknown, U = unclassified, Om = outer membrane protein, GI = genentic information processing, F = folding, Fo = possible ferroxidase activity

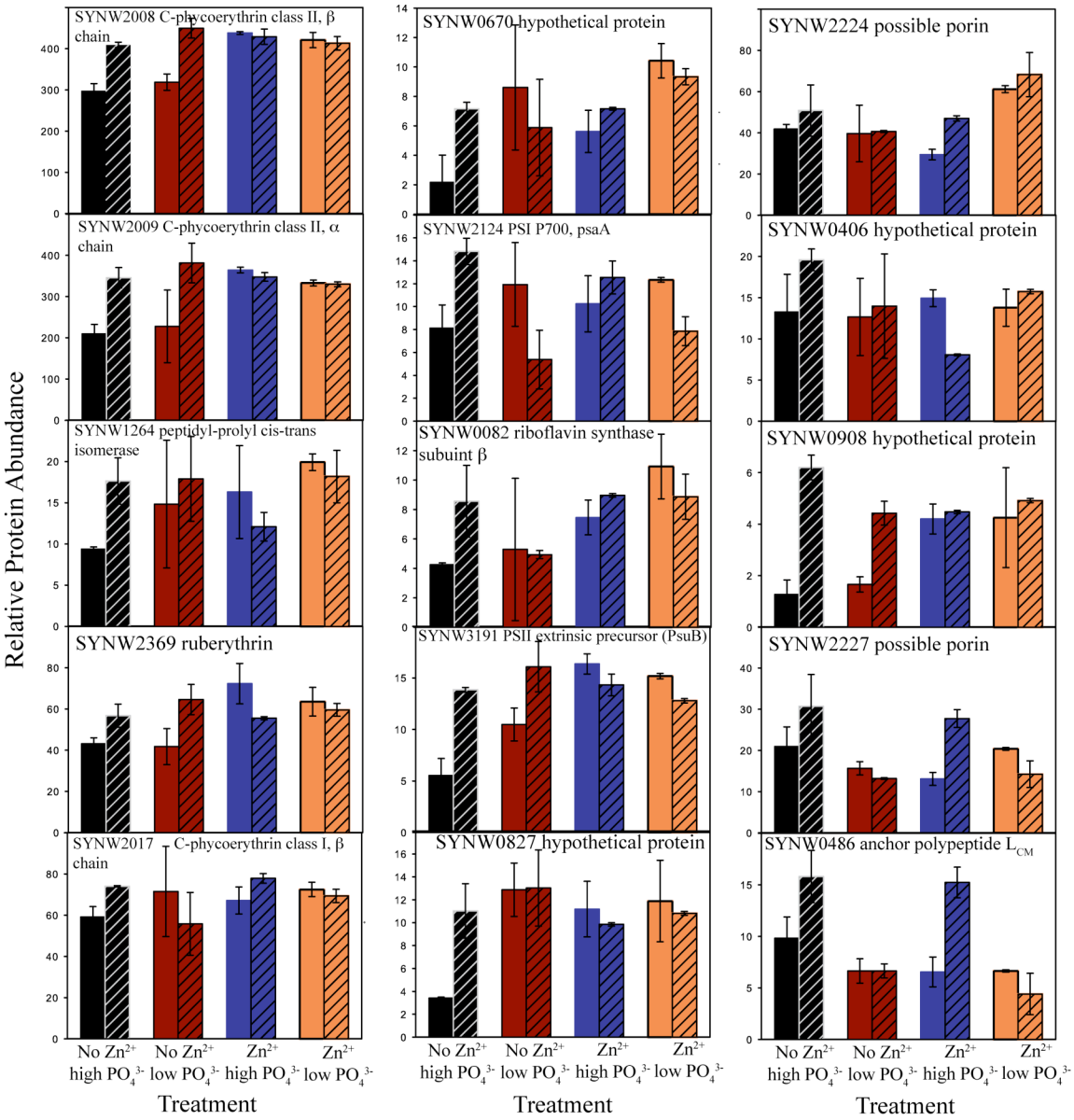

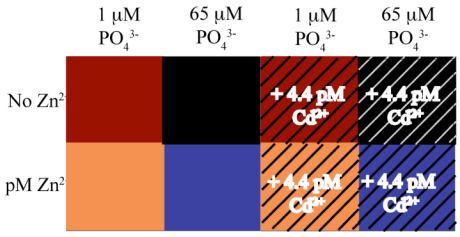

Figure 4.10: Relative protein abundance of proteins ≥ two-fold greater in abundance and/or statistically different by Fisher's Exact Test in the no Zn^{2+} added 65 μM PO_4^{3-} + 4.4 pM Cd^{2+} compared to the no Zn^{2+} added 65 μM PO_4^{3-} treatments. Error bars are the standard deviation of duplicate injections.

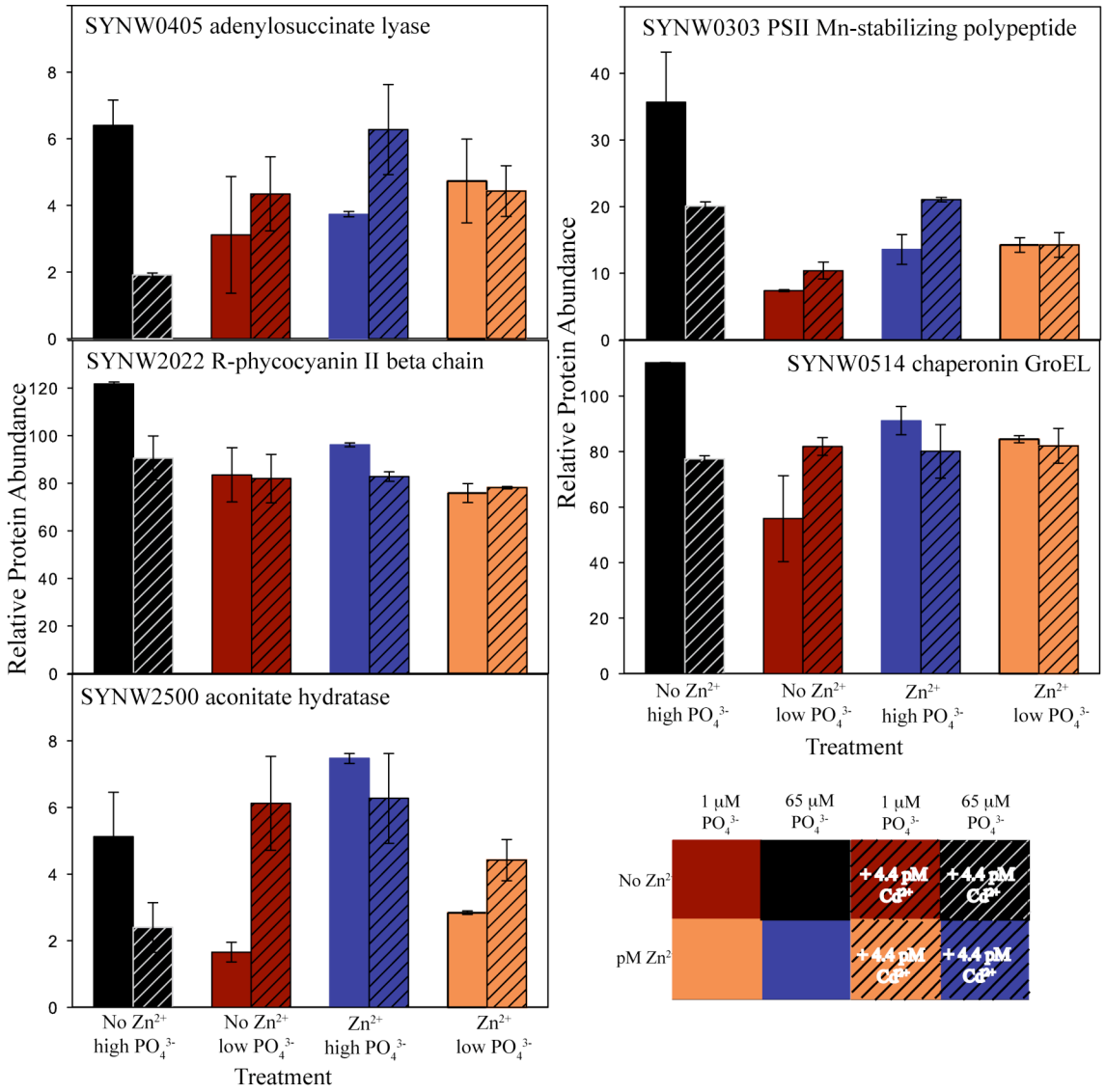

Figure 4.11: Relative protein abundance of proteins more than two-fold less abundant and/or statistically different by Fisher's Exact Test in the no Zn^{2+} added 65 µM PO_4^{3-} + 4.4 pM Cd^{2+} compared to the no Zn^{2+} added 65 µM PO_4^{3-} treatments. Error bars are the standard deviation of duplicate injections.

In the Zn-high PO_4^{3-} + 4.4 pM Cd^{2+} compared to no Cd^{2+} added treatments, four proteins were two-fold or more differentially abundant with a spectral count of at least five (Table III.3). All four proteins were more abundant in the Zn-high PO_4^{3-} + 4.4 pM Cd^{2+} treatment, three of the four are involved in photosynthesis and one SYNW2227 possible porin, unknown function, probably outer membrane protein.

In the no Zn-low PO_4^{3-} + 4.4 pM Cd^{2+} compared to no Cd^{2+} added treatments, 32

proteins were two-fold or more differentially abundant with a spectral count of at least five (Table III.4). Sixteen proteins were more abundant in the no Zn-low PO_4^{3-} + 4.4 pM Cd^{2+} treatment, including three ribosomal proteins, a protein involved in chlorophyll biosynthesis and one protein involved in photosynthesis. Sixteen proteins were more abundant in the no Zn-low PO_4^{3-} no added Cd^{2+} treatment, including three hypothetical proteins, a protein involved in chlorophyll biosynthesis and two proteins involved in photosynthesis.

In the Zn-low PO_4^{3-} + 4.4 pM Cd^{2+} compared to no Cd^{2+} added treatments, seven proteins were two-fold or more differentially abundant with a spectral count of at least five (Table III.5). Two proteins were more abundant in the Zn-low PO_4^{3-} + 4.4 pM Cd^{2+} treatment, SYNW1933 δ-aminolevulinic acid dehydratase, which is in the biosynthetic pathway for chlorophyll and SYNW1716 putative carboxysome structural peptide (CsoS2), presumably useful for carbon fixation. Five proteins were more abundant in the Zn-low PO_4^{3-} no added Cd^{2+} treatment, including one hypothetical protein, a protein involved in lipid metabolism, a protein involved in purine metabolism, a protein involved in carbohydrate metabolism and a protein involved in amino acid metabolism.

The influence of zinc (pairwise comparisons)

Zn effects can be discerned by examining pair-wise protein comparisons (Figure 4.8). In the high PO_4^{3-} treatments comparing no Zn to Zn added (Figure 4.1 - black to blue), 16 proteins were two-fold or more differentially abundant with a spectral count of at least five (Table III.6). Twelve proteins were more abundant in the no Zn-high PO_4^{3-} treatment, including three proteins involved in photosynthesis (SYNW0303 photosystem II manganese-stabilizing polypeptide, SYNW1982 photosystem II chlorophyll-binding protein CP47 and SYNW1835 photosystem I reaction center subunit III (PsaF)), two hypothetical proteins, SYNW1933 δ-aminolevulinic acid dehydratase involved in chlorophyll biosynthesis and SYNW0085 cell surface protein required for swimming motility (SwmA). Four proteins were more abundant in the Zn-high PO_4^{3-} treatment, including SYNW0670 hypothetical protein, SYNW2191 photosystem II complex extrinsic protein precursor (PsuB) and SYNW2310 glutaredoxin.

In low PO_4^{3-} treatments comparing no Zn to Zn added (Figure 4.1 - red to orange), 31 proteins were two-fold or more differentially abundant with a spectral count of at least five (Table III.7). Eleven proteins were more abundant in the no Zn-low PO_4^{3-} treatment, including three hypothetical proteins, two ribosomal proteins, and one protein involved in photosynthesis. Twenty proteins were more abundant in the Zn-low PO_4^{3-} treatment, including SYNW0259 bacterial metallothionein, SYNW2391 putative alkaline phosphatase, SYNW0953 cell surface protein required for swimming mobility (SwmB), three hypothetical proteins (SYNW0128, SYNW0160 and SYNW1661), one protein involved in chlorophyll biosynthesis, SYNW1065 putative photosystem II reaction center (psb28), SYNW1717 ribulose bisphosphate carboxylase small chain and SYNW0082 riboflavin (Vitamin B2) synthase subunit beta.

In the high PO_4^{3-} + acute 4.4 pM Cd^{2+} comparing no Zn to Zn added (Figure 4.1 - black/hatched to blue/hatched), three proteins were two-fold or more differentially abundant with a spectral count of at least five (Table III.8). One protein was more abundant in the no Zn-high PO_4^{3-} + 4.4 pM Cd^{2+} treatment, SYNW0406 hypothetical protein. Two proteins were more abundant in the Zn-high PO_4^{3-} + 4.4 pM Cd^{2+} treatment, SYNW0405 adenylosuccinate lyase, involved in purine and amino acid metabolism and SYNW2500 aconitate hydratase, involved in carbohydrate metabolism, TCA cycle, glyoxylate and dicarboxylate metabolism and energy metabolism, reductive carboxylate cycle.

In the low PO_4^{3-} + acute 4.4 pM Cd^{2+} comparing no Zn to Zn added (Figure 4.1 - red/hatched to orange/hatched), 9 proteins were two-fold or more differentially abundant with a spectral count of at least five (Table III.9). Five proteins were more abundant in the no Zn-low PO_4^{3-} + 4.4 pM Cd^{2+} treatment, including SYNW1815 ABC transporter, substrate binding protein, phosphate. Four proteins were more abundant in the Zn-low PO_4^{3-} + 4.4 pM Cd^{2+} treatment, including SYNW0359 bacterial metallothionein and SYNW2391 putative alkaline phosphatase (Figure 4.9).

Cadmium-zinc interactions at high phosphate (pairwise comparison)

This pairwise comparison is not part of the 12 pairwise comparisons. It queries if

the relative protein abundances look similar if Cd is present instead of Zn at high PO_4^{3-} (Figure 4.1 - black/hatched to blue). In the no Zn-high PO_4^{3-} + 4.4 pM Cd^{2+} compared to Zn-high PO_4^{3-} treatments, 8 proteins were two-fold or more differentially abundant with a spectral count of at least five (Table III.10). Seven proteins were more abundant in the no Zn-high PO_4^{3-} + 4.4 pM Cd^{2+}, including four proteins involved in photosynthesis, SYNW0085 cell surface protein required for swimming motility (SwmA) and SYNW2227 possible porin, unknown function, outer membrane associated. SYNW2500 aconitate hydratase, involved in carbohydrate metabolism, TCA cycle, glyoxylate and dicarboxylate metabolism and energy metabolism, reductive carboxylate cycle was more abundant in the Zn-high PO_4^{3-} treatment.

DISCUSSION

Phosphate stress and limitation in *Synechococcus* WH8102 has been much studied in recent years by many different methods, including computational prediction (Su et al., 2003; Su et al., 2007), physiological experimentation (Moore et al., 2005), and microarray analyses (Tetu et al., 2009, Ostrowski et al., 2010). Phosphate stress and limitation has also been studied in *Prochlorococcus* by microarray (Martiny et al., 2006). PCR-based field assays of picocyanobacteial phnD, phosphonate-binding protein of ABC-type phosphonate transporter (SYNW1169) showed a depth-dependent pattern of expression which followed gradients of P-availability (Ilikchyan et al., 2009) and the phnD from the cyanobacterium, *Trichodesmium erythraeum*, was found to be differentially expressed in field populations in the North Atlantic (Dyhrman et al., 2006). Previous experiments revealed an interaction between the addition of Cd and the greater relative abundance of phosphate stress proteins (Cox et al., unpublished data) and this interaction was further explored in this study. Because of the role of Zn in the metalloenzyme alkaline phosphatase, involved in acquisition of phosphate from organophosphate, the influences of Zn on the potential interfering metal, Cd were probed. The present study combines physiological experimentation with global proteomic analyses to study the interactions of phosphorus, Zn, and Cd in *Synechococcus* WH8102.

Physiological Data

Cd may have a hormetic effect in this experiment and the mechanism, albeit unknown, could be in the interaction with Zn. A hormetic response is defined as low dose stimulation, although different concentrations of Cd, both lower and higher would need to be added to get a full hormetic curve, defined as stimulation at low dosages with toxicity at higher dosages (Calabrese, 2005). The instantaneous growth rates in the Zn treatments, both 1 and 65 μM PO_4^{3-}, during the last 24 hours of the experiment show an increase in instantaneous growth rates by factors of ~2 and 1.7 respectively with 4.4 pM Cd^{2+} addition relative to the no Cd added (Figure 4.4b). In contrast, there is hardly an increase in instantaneous growth rates in the no Zn treatments, both 1 and 65 μM PO_4^{3-} with the addition of Cd relative to the no Cd added, increase by factors of ~1.2 and ~1.1, respectively (Figure 4.4b). This may be described as a hormetic response (Calabrese, 2005). The growth of *Chlorella*, an eukaryotic algae, is stimulated by low concentrations of Cd and inhibited by higher concentrations (Vallee and Ulmer, 1972). Perhaps the response is favorable due to displacement of Zn by Cd and subsequent nutritive use of Zn. Metallothionein is one possible 'Zn buffer' (Frausto da Silva and Williams, 1991) and in mammals upon cadmium and copper loading, metallothionein has been know to release Zn (Zhang et al., 2003. Alternatively, perhaps the Cd is directly having a nutritive effect or a regulatory effect inducing cell division. Using this data set, one cannot distinguish between Cd having a nutritive effect because of its interactions with Zn or because of Cd alone.

Relative chlorophyll *a* and phycoerythrin fluorescence are adequate to monitor cell growth, but they do not accurately show when a culture enters stationary phase. Growth rates calculated using phycoerythrin fluorescence, for example, yielded similar results to actual growth rates in that the four initial treatments had almost identical growth rates (Figure III.2a, 4.4a). Instantaneous growth rates calculated by phycoerythrin fluorescence in the last 24 hours of the experiment, however, indicated that the 1 μM PO_4^{3-} treatments entered stationary phase (Figure III.2b). Actual growth rates, calculated using cell numbers, demonstrated that the Zn added low phosphate treatments

entered stationary phase during the last 24 hours of the experiment (Figure 4.4b). This disparity in growth phase does suggest that at 1 μM PO_4^{3-}, during mid-late exponential growth, phycoerythrin perhaps is not being produced even though the cells continue to divide.

Global Proteomic Data

Tetu et al. (2009) performed a transcriptome analysis of PO_4^{3-} limited and replete cultures in *Synechococcus* WH8102, as previously mentioned in the results section. In that experiment, *Synechococcus* WH8102 was grown in SN medium (Waterbury and Willey, 1988) or artificial seawater with PO_4^{3-} concentrations varying from 5 to 87 μM, 5 μM being P-stressed and 87 μM being P-replete. In this experiment, *Synechococcus* WH8102 was grown in modified Pro-TM medium at a four concentrations: no PO_4^{3-} added, 1, 5, and 65 μM PO_4^{3-}, finding the cultures to be P-stressed at 1 μM PO_4^{3-} (Figure III.1). The global proteomic analyses reported in this chapter, therefore, were from cultures grown at 1 and 65 μM PO_4^{3-}, low and high PO_4^{3-}, respectively. Thirty-six percent of the transcripts that Tetu et al. (2009) reported upregulated (36 total transcripts) under PO_4^{3-} stress in this experiment (13 proteins). Fifteen percent of the total (6 proteins) were found to be $\geq$ two-fold more abundant in the low PO_4^{3-} treatment.

The transcriptome response reported by Tetu et al. (2009) is similar to the proteome response in this experiment. Of the 36 transcripts deemed strongly upregulated by $\geq$ two-fold under early P-stress in the transcriptome study, 13 of these transcripts were identified as proteins in this experiment (Figure 4.12). Of the 13 proteins observed, 6 were $\geq$ two-fold more abundant, including SYNW2391 alkaline phosphatase, SYNW1018 ABC transporter substrate binding protein phosphate (PstS), SYNW0953 cell surface protein required for swimming motility (SwmB), SYNW0799 glyceraldehyde-3-phosphate dehydrogenase and SYNW2224 possible porin (Table 4.1, Figure 4.1 - orange and blue, Figure 4.12 - pink, upper right quadrant), and 7 showed minor changes in abundance, including SYNW1815 ABC transporter substrate binding protein phosphate, SYNW0156 phosphorylase, SYNW0406 hypothetical protein, SYNW1119 6-phosphogluconate dehydrogenase, SYNW1213 thioredoxin peroxidase

and SYNW2508 molecular chaperone DnaK2, heat shock protein hasp 70-2, and SYNW0160 conserved hypothetical protein (Table 4.2, , Figure 4.12 - black, lower right quadrant). SYNW0156 phosphorylase was close to being ≥ two-fold more abundant, it was more abundant in the low PO_4^{3-} compared to the high PO_4^{3-} by a factor of 1.9. Two more proteins were identified that were ≥ two-fold more abundant that were absent from the Tetu list of ≥ two-fold upregulated transcripts, SYNW1982 photosystem II chlorophyll-binding protein CP47 and SYNW1147 ribonucleotide reductase (Class II) (Table 4.1). Of the 23 transcripts observed strongly downregulated (≥ two-fold less) by Tetu et al. (2009) only 3 were identified as proteins, SYNW2340 50S ribosomal protein L7/L12, SYNW2030 conserved hypothetical protein, and SYNW2082 50S ribosomal protein L18, only SYNW2082 50S ribosomal protein L18 was ≥ two-fold less in abundance. One might expect less overlap in the protein data from down-regulated transcripts because less protein would presumably be made, reflecting the lower proteome coverage relative to the transcriptome. It is interesting to note that four of these phosphate acquisition genes, in addition to others, increased in expression in a microarray experiment when WH8102 was grown with *Vibrio parahaemolyticus*, a model heterotroph (Tai et al., 2009). This information, combined with results from previous protein experiments in which these phosphate acquisition genes were more abundant with acute Cd addition in WH8102 stationary phase cultures (Cox et al., unpublished data), suggests that the phosphate response may ultimately be triggered by many factors.

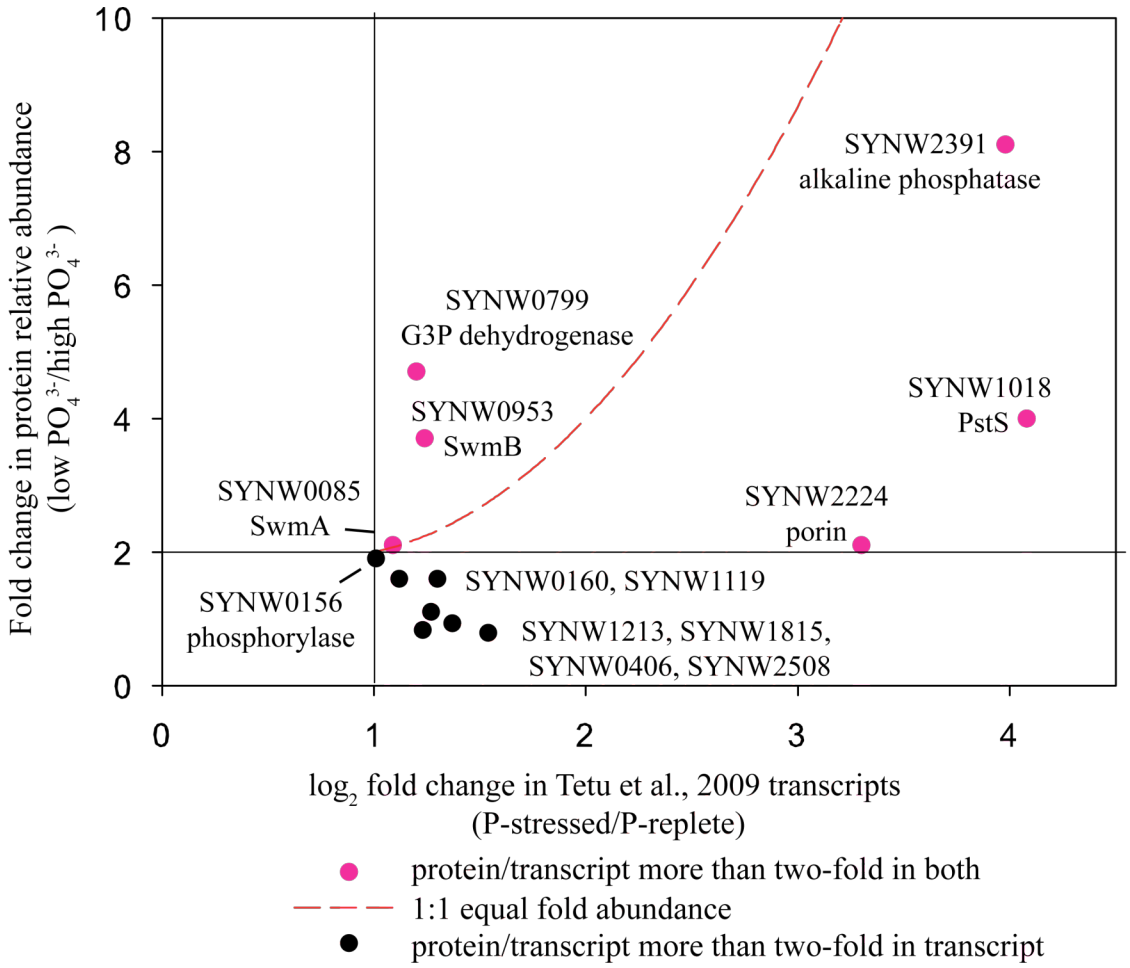

Figure 4.12: Fold change in protein relative abundance (this experiment) as ratio of low phosphate to high phosphate vs. Log_2 fold change in gene relative abundance (Tetu et al., 2009) as ratio of P-stressed to P-replete. Pink dots represent protein/transcripts more than two-fold abundant in both protein and transcript data. Black dots represent protein/transcripts more than two-fold abundant in transcript data. Red dashed line indicates a 1:1 equal fold abundance. SYNW0160 - conserved hypothetical protein, SYNW1119 - 6-phosphogluconate dehydrogenase, SYNW1213 - thioredoxin peroxidase, SYNW1815 - ABC transporter, substrate binding protein, phosphate, SYNW0406 - hypothetical protein, SYNW2508 - molecular chaperone DnaK2, heat shock protein hsp 70-2. See Tables 4.1 and 4.2.

None of the 16 proteins that were ≥ two-fold more abundant in the Zn-low PO_4^{3-} compared to Zn-high PO_4^{3-} matched the 55 proteins that were ≥ two-fold more abundant in the no Zn-low PO_4^{3-} compared to no Zn-high PO_4^{3-} (Table 4.3, Figure 4.1 - red and black, see also Figure 4.9). In addition, none of the 36 transcripts strongly upregulated under P-stress in the Tetu et al. transcriptome experiment matched the 55 proteins that

were ≥ two-fold more abundant in the no Zn-low PO_4^{3-} compared to no Zn-high PO_4^{3-}. If a figure such as Figure 4.12 were to be made, it would be blank. These observations show that the proteome response to low PO_4^{3-} in the absence of Zn is very different than in the presence of Zn. This could suggest that Zn is somehow vital to the functioning of the P-stress response in this organism, perhaps as a cofactor in SYNW2391 putative alkaline phosphatase, or in the signaling mechanism.

Alkaline phosphatases

There are four genes in the genome of WH8102 that are annotated as alkaline phosphatases, SYNW0120 putative alkaline phosphatase-like protein, SYNW0196 putative alkaline phosphatase, SYNW2390 putative alkaline phosphatase/5' nucleotidase, and SNW2391 putative alkaline phosphatase (phoA). In addition, SYNW1799 is an alkaline phosphatase (phoX) (Kathuria and Martiny, 2010). Alkaline phosphatases are variable in their cellular location and associated metal ions. Two alkaline phosphatases purified from different strains of *Vibrio cholerae*, a gamma-proteobacteria, both acted on a variety of organic phosphate esters, but showed different levels of reactivation upon addition of Na^+, K^+ and Mg^{2+} ions (Roy et al., 1982). Alkaline phosphatases (phoA) are thought to be located in the periplasm and are activated by Zn and magnesium, whereas other alkaline phosphatases (phoX, phoD) are activated by calcium ions (Luo et al., 2009). A recent survey of the metagenomic databases concluded that phoX appeared to be more widespread in the ocean than phoA (Sebastian and Ammerman, 2009). There are also other types of alkaline phosphatases in cyanobacteria. The freshwater cyanobacterium *Synechococcus* 7942 contains a phoV in addition to phoA (Wagner et al., 1995). PhoV had a broad substrate specificity for phosphomonoesters, required Zn^{2+} for activity and was inhibited by phosphate, but it was inhibited by Mn^{2+} (Wagner et al., 1995). Recent experimentation on SYNW1799 phoX overexpressed in *E. coli* have shown enhanced enzyme activity in the presence of calcium, leading the authors to conclude that bacterial lineages with the presence of phoX in the genome may not be subject to Zn-P colimitation (Kathuria and Martiny, 2010).

In this experiment, we detect SYNW2391 and SYNW1799, but not SYNW0120,

SYNW2390 or SYN0196 in the proteome. SYNW2391 alkaline phosphatase (phoA) is depicted in Figure 4.9, but SYNW1799 alkaline phosphatase (phoX) is only detected by a few counts, making quantitative comparison difficult. Perhaps it is important that we did not detect high amounts of this protein at low phosphate in the absence of Zn, which is what one might expect from a phoX that does not presumably require Zn.

Metallothionein in* Synechococcus *WH8102

As discussed in Chapter 1 on pages 21-22, metallothioneins are small, approximately 56 amino acid residue proteins with a high percentage of cysteine residues that are involved in chelating metals such as zinc, cadmium, copper, silver, mercury, and arsenic (Duncan et al., 2006). Their exact function is elusive but metallothioneins may function as 1) metal resistance proteins for detoxifying zinc, cadmium and copper; 2) reservoirs for the storage of excess Zn and/or copper than can be mobilized under metal limiting conditions; 3) metal chaperones that deliver Zn to Zn-dependent proteins; and/or 4) antioxidants that scavenge oxygen radicals (Palmiter, 1998). In these data, metallothionein relative protein abundances look similar to the relative protein abundances of PO_4^{3-} stress proteins (Figure 4.9) and in combination with previous proteome experiments, in which metallothionein was detectable only when Zn or Cd was present in the medium (Cox et al., unpublished data), many questions arise: 1) Is metallothionein related to PO_4^{3-} stress? 2) Does it supply the alkaline phosphatase with Zn, acting as a metal reservoir? or 3) is it somehow involved in Zn signaling and/or the PO_4^{3-} stress signaling mechanism?

Metallothionein abundance appeared to show a dependence on growth phase of the culture, with metallothionein being more abundant with the addition of Cd and Zn in stationary phase. The cells in this experiment were harvested during growth phase and metallothionein did not show relative protein abundances in this experiment as expected. Consistent with previous experiments, it is present when there is Zn in the medium as opposed to no Zn added, however, it did not increase with acute Cd stress, no matter the Zn concentration unlike in previous experiments (Cox et al., unpublished data). In previous experiments at 65 μM PO_4^{3-} (high phosphate), with Zn and no Zn added and

with and without Cd addition, cultures were in stationary phase at time of harvest. Metallothionein protein abundance was higher in the Cd treatments and also in the Zn treatments (Cox et al., unpublished data). In this experiment, which was expanded to include a low PO_4^{3-} treatment, contrary to the previous experiments, metallothionein did not appear to be more abundant in the presence of Zn in general, rather metallothionein was high in the Zn added, low PO_4^{3-} treatment and had a similar relative protein abundance distribution to P-stress proteins (Figure 4.9). More quantitative analyses using a triple quadrupole mass spectrometer would be useful to constrain metallothionein change in WH8102.

The influence of phosphate (pairwise discussion)

As noted by the ordering of the heat map in Figure 4.7 and the number of proteins differentially abundant in Figure 4.8, phosphate appeared to cause the most difference in this multivariate Cd-Zn-phosphate interaction experiment. We used the Zn added treatments to compare to the Tetu et al, 2009 microarray experiment because their media would have Zn present. We saw 6 of the 9 proteins more abundant as the same proteins differentially expressed in the Tetu et al., 2009 microarray experiment. When Zn was not added, 16 proteins were more abundant but none of them were the same as the Tetu et al., 2009 experiment (Table 4.3). This suggests that Zn is integral to the phosphate response in this cyanobacterium.

Proteins more abundant in the high phosphate compared to the low phosphate in the absence of Zn (Table 4.3) suggests that phosphate may be related to the abundance of ribosomal proteins and it is similar, but not exactly the same with or without Zn. Twelve proteins that were $\geq$ two-fold more abundant with high phosphate in the absence of Zn were involved in genetic information processing, including ten ribosomal proteins, which are involved in protein synthesis. Comparing the high to the low phosphate in the presence of Zn, six ribosomal proteins were $\geq$ two-fold more abundant, three of which were the same proteins as in the no Zn added treatments (Table 4.1). Note that the tables compare low phosphate to high phosphate.

In the Zn added + 4.4 pM Cd^{2+} low compared to high phosphate treatments

(Figure 4.1 - orange/hatched to blue/hatched), 9 proteins were more abundant in the low phosphate treatment (Table III.1). Of these, five proteins were also found to be ≥ two-fold differentially abundant with phosphate in the Zn treatments without Cd (Table 4.1). Five were expressed as transcripts in a microarray experiment by Tetu et al., 2009 (Table 4.1). These five proteins similar to Zn treatments without Cd were SYNW2391 putative alkaline phosphatase, SYNW1018 ABC transporter, substrate binding protein, phosphate (PstS), SYNW0953 cell-surface protein required for swimming motility (SwmB), and SYNW0359 bacterial metallothionein. Four of the 5 proteins were the same as those found in Tetu et al., 2009, with SYNW0359 bacterial metallothionein present instead of SYNW0156 phosphorylase. One of the four proteins that was differentially abundant with phosphate with Zn added and acute Cd and not Zn alone was SYNW1533 probable glutathione reductase (NADPH); glutathione may be involved in the intracellular binding of Cd (Table III.1). Eight proteins were more abundant in the Zn added + 4.4 pM Cd^{2+} high phosphate treatment compared to the Zn added + 4.4 pM Cd^{2+} low phosphate treatment, including three related to the phycobilisomes and two ribosomal proteins, implying perhaps the interference of Cd in photosynthesis (Table III.1).

In the no Zn added + 4.4 pM Cd^{2+} low compared to high phosphate treatments (Figure 4.1 - red/hatched to black/hatched), there were four proteins more abundant in the low phosphate treatment, including two proteins also found to be differentially expressed as genes in the Tetu et al., 2009 microarray experiment (Table III.2). These two proteins are SYNW0953 cell-surface protein required for swimming motility (SwmB) and SYNW1018 ABC transporter, substrate binding protein, phosphate (PstS). Because these two proteins were not observed as being differentially abundant in the absence of added Zn, perhaps the acute addition of Cd stimulated the presence of these proteins. Eight proteins were more abundant in the no Zn added + 4.4 pM Cd^{2+} high phosphate treatment, including six involved in photosynthesis (two phycobilisome, three Photosystem II and one Photosystem I proteins) (Table II.2). In the absence of added Zn, organisms are more vulnerable to Cd (See Chapter 3), in this case perhaps the process of photosynthesis becomes more vulnerable to Cd with no added Zn and low phosphate

concentrations.

The influence of cadmium (pairwise discussion)

Cd effects can be discerned by examining pairwise protein comparisons (Figure 4.8). In the no Zn added high phosphate + 4.4 pM Cd^{2+} compared to no Cd added treatments (Figure 4.1 - black and black/hatched), five proteins were more abundant in the Cd treatment, including three unknown proteins, one involved in photosystem II and one involved in the biosynthesis of riboflavin (Vitamin B2) (Figure 4.10). Perhaps these unknown proteins are involved in Cd handling in the absence of Zn, because they are not differentially abundant in the treatments with Zn in the medium. Five proteins were more abundant in the no Zn added, high phosphate no added Cd^{2+} treatment, two of which are involved in carbohydrate metabolism (Figure 4.11). Ten additional proteins were found to be significantly different by Fisher's Exact Test, five of which are involved in photosynthesis (Figure 4.10). Three more proteins are statistically more abundant in the no Zn added high phosphate no added Cd^{2+}, two of which are involved in photosynthesis (Figure 4.11). Perhaps Cd in the absence of Zn affects the photosynthetic apparatus.

The number of proteins differentially abundant with acute Cd addition decreases with Zn in the media (Figure 4.8b). Only four proteins were $\geq$ two-fold more abundant in the Zn-high PO_4^{3-} + 4.4 pM Cd^{2+} compared to no Cd^{2+} added treatments, three of the four are involved in photosynthesis and one SYNW2227 possible porin (som), unknown function, probably outer membrane protein (Table III.3). This porin appears to be more abundant with acute Cd addition, but only at 65 μM PO_4^{3-} concentrations.

In the no Zn-low PO_4^{3-} + 4.4 pM Cd^{2+} compared to no Cd added treatments (Figure 4.1 - red and red/hatched), 16 proteins were more abundant in the no Zn + Cd treatment, including three ribosomal proteins, a protein involved in chlorophyll biosynthesis and one protein involved in photosynthesis (Table III.4). Sixteen proteins were more abundant in the no Zn-high PO_4^{3-} no added Cd treatment, including three hypothetical proteins, a protein involved in chlorophyll biosynthesis and two proteins involved in photosynthesis. Compared to only 10 proteins differentially abundant in total at no Zn-high PO_4^{3-} (Figure 4.8b, Table 4.4), Cd appears to affect the proteome more at

low PO_4^{3-} in terms of the greater number of proteins differentially abundant.

The number of proteins differentially abundant with acute Cd addition decreased with Zn in the media at low PO_4^{3-} (Table III.5). In the Zn-low PO_4^{3-} + 4.4 pM Cd^{2+} compared to no Cd^{2+} added treatments, two proteins were more abundant in the Zn-low PO_4^{3-} + 4.4 pM Cd^{2+} treatment, SYNW1933 δ-aminolevulinic acid dehydratase, which is in the biosynthetic pathway for chlorophyll and SYNW1716 putative carboxysome structural peptide (CsoS2), presumably useful for carbon fixation. Five proteins were more abundant in the Zn-low PO_4^{3-} no added Cd^{2+} treatment, including one hypothetical protein, a protein involved in lipid metabolism, a protein involved in purine metabolism, a protein involved in carbohydrate metabolism and a protein involved in amino acid metabolism. The acute addition of Cd decreased the relative protein abundance of metabolic proteins.

The influence of zinc (pairwise comparison)

Zn effects can be discerned by examining pairwise protein comparisons (Figure 4.8). In the no Zn-high PO_4^{3-} compared to Zn-high PO_4^{3-} treatments (Figure 4.1 - black and blue), 11 proteins were more abundant in the no Zn-high PO_4^{3-} treatment, including three proteins involved in photosynthesis (SYNW0303 photosystem II manganese-stabilizing polypeptide, SYNW1982 photosystem II chlorophyll-binding protein CP47 and SYNW1835 photosystem I reaction center subunit III (PsaF)), two hypothetical proteins, SYNW1933 δ-aminolevulinic acid dehydratase involved in chlorophyll biosynthesis and SYNW0085 cell surface protein required for swimming motility (SwmA) (Table III.6). The photosystem II binding proteins are curious, especially SYNW1982 photosystem II chlorophyll-binding protein CP47, which is similarly abundant in the no Zn-high PO_4^{3-} as the Zn-high PO_4^{3-} + 4.4 pM Cd^{2+} treatments, both about two-fold greater than Zn-high PO_4^{3-}. Perhaps this has to do with the Zn-high PO_4^{3-} entering stationary phase at the time of harvest. Four proteins were more abundant in the Zn-high PO_4^{3-} treatment, including SYNW0670 hypothetical protein, SYNW2191 photosystem II complex extrinsic protein precursor (PsuB) and SYNW2310 glutaredoxin.

In the no Zn-low PO_4^{3-} compared to Zn-low PO_4^{3-} treatments (Figure 4.1- red and

orange), 11 proteins were more abundant in the no Zn-low PO_4^{3-} treatment, including three hypothetical proteins (SYNW0380, SYNW1145 and SYNW0340), two ribosomal proteins and one protein involved in photosynthesis (Table III.7). Because we observed such a response to lower PO_4^{3-} concentrations in treatments with Zn present, one might expect a response to phosphate in the absence of Zn. Thus, since there is no obvious known PO_4^{3-} response observed in the fold-change protein abundance data, perhaps the hypothetical proteins could be involved in PO_4^{3-} response in the absence of Zn. This could be considered an example of proteome plasticity. Twenty proteins were more abundant in the Zn-low PO_4^{3-} treatment, including SYNW0259 bacterial metallothionein, SYNW2391 putative alkaline phosphatase, SYNW0953 cell surface protein required for swimming mobility (SwmB), three hypothetical proteins (SYNW0128, SYNW0160 and SYNW1661), one protein involved in chlorophyll biosynthesis, SYNW1065 putative photosystem II reaction center (psb28), SYNW1717 ribulose bisphosphate carboxylase small chain and SYNW0082 riboflavin (Vitamin B2) synthase subunit beta. These proteins corroborate the ideas that the presence of Zn affects the PO_4^{3-} response and the presence of metallothionein is correlated with the presence of Zn.

In the no Zn-high PO_4^{3-} + 4.4 pM Cd^{2+} compared to Zn-high PO_4^{3-} + 4.4 pM Cd^{2+} treatments (Figure 4.1 - black/hatched and blue/hatched), SYNW0406 hypothetical protein was more abundant in the absence of Zn (Table III.8). Two proteins were more abundant with added Zn, SYNW0405 adenylosuccinate lyase, involved in purine and amino acid metabolism and SYNW2500 aconitate hydratase, involved in carbohydrate metabolism, TCA cycle, glyoxylate and dicarboxylate metabolism and energy metabolism, reductive carboxylate cycle (Table II.8). This suggests that in the presence of high PO_4^{3-} and acute Cd the proteome is not strongly affected by the presence or absence of Zn.

When Zn was modulated at low PO_4^{3-} with the addition of Cd (no Zn-low PO_4^{3-} + 4.4 pM Cd^{2+} compared to Zn-low PO_4^{3-} + 4.4 pM Cd^{2+}) (Figure 4.1 - red/hatched and orange/hatched), five proteins were more abundant in the no Zn-low PO_4^{3-} + 4.4 pM Cd^{2+} treatment, including SYNW1815 ABC transporter, substrate binding protein, phosphate

(PstS) (Table III.9). Four proteins were more abundant in the Zn-low PO_4^{3-} + 4.4 pM Cd^{2+} treatment, including SYNW0359 bacterial metallothionein, SYNW2391 putative alkaline phosphatase and SYNW1533 probable glutathione reductase (NADH) (Table III.9, see also Figure 4.9). The greater abundance of metallothionein and alkaline phosphatase in the Zn treatment is consistent with Zn being involved with these proteins. Because Cd is known to induce the production of metallothioneins in many systems, the metallothionein was expected to be higher in both of these treatments, as opposed to just the Zn treatment. This may be because of the low spectral counts detected. Further quantification of this protein would be desirable.

Cadmium-zinc interactions (pairwise discussion)

Holding PO_4^{3-} constant, the comparison of the no Zn-high PO_4^{3-} + 4.4 pM Cd^{2+} to Zn-high PO_4^{3-} treatments (Figure 4.1 - blue and black/hatched) will expose Zn replacement by Cd or Cd sensitivity in the absence of Zn if such occur. Seven proteins were more abundant in the no Zn-high PO_4^{3-} + 4.4 pM Cd^{2+}, including four proteins involved in photosynthesis, SYNW0085 cell surface protein required for swimming motility (SwmA) and SYNW2227 possible porin, unknown function, outer membrane associated (Table III.10). SYNW2500 aconitate hydratase, involved in carbohydrate metabolism, TCA cycle, glyoxylate and dicarboxylate metabolism and energy metabolism, reductive carboxylate cycle was more abundant in the Zn-high PO_4^{3-} treatment (Table III.10). Perhaps the lower abundances of photosynthesis proteins is reflective of the Zn-high PO_4^{3-} treatment entering stationary phase shortly before harvest. Perhaps WH8102 is more sensitive to acute Cd addition in the absence of added Zn. This would be similar to the sensitivity of WH5701 in Chapter 3 to chronic Cd exposure and consistent with previous experiments in which growth rates of WH8102 were decreased with added Cd and low Zn (Saito et al., 2003).

Other proteins of note

Photosystem II D1 proteins

The function and evolution of the psbA gene family in marine *Synechococcus* was investigated fairly recently with marine *Synechococcus* WH7803 as a case study

(Garczarek et al., 2008). Basically, the D1 protein of photosystem II is encoded by a family of genes, up to six different genes in as observed in 11 marine cyanobacterial genomes. In each of these genomes, only one of is the D1:1 isoform and the rest are D1:2 isoforms; in freshwater cyanobacteria D1:2 isoforms are exchanged for D1:1 isoforms in response to stress, thereby altering photosystem II photochemistry (Garczarek et al., 2008). *Synechococcus* WH8102 has four psaB genes, one D1:1 and three D1:2. We only detected the D1:1 isoform, at an average low of 2.1 and average high of 4.9 spectral counts. The fact that we only detected the D1:1 isoform suggests that these cultures are not experiencing stress to cause them to use the D1:2 isoform, implies that the D1:2 isoform is below our detection limit, or could mean that the D1:2 isoform does not have a measurable tryptic peptide.

ATP-Binding Cassette Systems

ABC binding cassette systems use the energy of hydrolysis of ATP to transport a substance across a membrane, as well as being involved in cellular processes and their regulation (Bu et al., 2009). Their reliance on phosphate in ATP makes these systems important to phosphorus cycling. Molecules can be transported into (metals, phosphate, phosphonates, etc) or outside of a cell (heavy metals, drugs, peptides, etc.). In a recent study, the genome of WH8102 was shown to have 41 ABC systems, the highest of the marine *Synechococcus* genomes included in the analysis (Bu et al., 2009). Note that WH5701 was not included in their analysis. Nineteen ABC systems were common to all 10 marine *Synechococcus* and 12 *Prochlorococcus* genomes analyzed, including the import systems of cobalt uptake (CBY), metals, predicted substrate-manganese (MET), phosphonates and phosphates (PHN), oligopeptides and Ni (OPN) and mineral and organic, predicted substrates-phosphate and iron (III) (MOI) , and various export systems of drugs, peptides and lipids (DPL) (Bu et al., 2009).

The cyanobase database (website) has 90 genes annotated as ATP-cassette binding systems. We detected 20 of these genes as proteins, 22%. They are listed here with their substrate: SYNW0193 multidrug, SYNW0217 ATP-binding component, SYNW0320 ATP-binding component, SYNW0840 amino acids, SYNW0843 amino

acids, *SYNW1018 phosphate (PstS), SYNW1112 ATP-binding component, SYNW1169 phosphonate, SYNW1286 possibly phosphate, SYNW1415 nitrate-like, SYNW1541 multidrug, *SYNW1815 phosphate (PstS), *SYNW1797 iron (futA, sfuA, idiA), SYNW1917 glycine betaine, SYNW2175 ATP-binding component, SYNW2325 oligopeptides, *SYNW2442 urea, SYNW2485 cyanate, *SYNW2487 cyanate and SYNW2522 exinuclease (uvrA). Note that the five ABC system components that were overall most abundant in terms of spectral counts (starred) are involved with the essential elements phosphorus, iron and nitrogen. PstS is also seen upregulated in *Prochlorococcus* under P-stress (Martiny et al., 2006).

Polyphosphate

The fine structure of cyanobacteria has been of interest for many years (Lang, 1968). Granules had been noticed that differed in size and abundance with amount of PO_4^{3-} in the medium and age or developmental stage of cell, bigger and more granules present with more PO_4^{3-} and the older the cell (Lang, 1968). Although dissolved PO_4^{3-} concentrations in the oceans are rarely more than 2 μM, many marine *Synechococcus* have the genes related to polyphosphate metabolism, *Synechococcus* WH8102 and *Synechococcus* WH5701 included. Because phosphorus is such a vital element to life and marine cyanobacteria are not exposed to high PO_4^{3-} concentrations in the environment, this suggests that the polyphosphate metabolism may be vestigial or alternatively, laterally transferred. Although we may not expect to observe polyphosphates in cyanobacteria gathered directly from the ocean, we expect to see polyphosphates in cultures grown with excess phosphate.

Polyphosphate is proposed to interact with Cd. *Chlamydomonas acidophila*, a eukaryotic algae, dramatically changes its cellular structure in the presence of 10 and 20 μM Cd, causing the degradation of polyphosphate and increased short-chain and orthophosphates in the vacuole (Nishikawa et al., 2003). Other researchers have reported the presence of Cd deposits in vacuoles of *Saccharomyses cerevisiae*, baker's yeast, with corresponding high quantities of phosphorus by electron microscopy (Volesky et al., 1992). In the unicellular cyanobacterium *Anacystis nidulans* R2, cells with a large

polyphosphate reserve showed a greater tolerance to 0.02 ppm Cd than cells with a small polyphosphate reserve (Keyhani et al., 1996). They propose that a decrease in polyphosphate reserves results in fewer sites for Cd chelation and thus a higher intracellular concentration of metals (Keyhani et al., 1996). This led one of the authors to later propose that although in many microorganisms polyphosphate is correlated with heavy metal tolerance, the ability to degrade orthophosphate may result in the binding of metals to orthophosphate and the removal of the resulting metal phosphates by the inorganic phosphate transport system (Keasling, 1997). A recent study by Zeng and Wang 2009 found that elevated cellular phosphate concentrations increased the short-term uptake of Cd and Zn in the freshwater cyanobacterium, *Microcystis aeruginosa*. They propose that polyphosphate bodies may have served as a metal sink to sequester/detoxify the Cd and Zn (Zeng and Wang, 2009).

Polyphosphates are relevant to phosphorus cycling in the ocean. In a fairly recent study of a site in a Pacific fjord off of Vancouver Island, British Columbia with surface water total dissolved phosphate concentrations of 0.5 μM, ~11% of the total dissolved phosphorus pool, 7% of total phosphorus in surface water biomass and 7% of total phosphorus in sinking material was polyphosphate (Diaz et al., 2008). These data and other supporting evidence led the authors to conclude that diatom-derived polyphosphates play a critical role in the formation of calcium phosphate minerals observed in marine sediments worldwide (Diaz et al., 2008).

Two important enzymes in the metabolism of polyphosphate were observed at low spectral counts in this experiment SYNW1846 putative exopolyphosphatase (ppx), which removes a phosphate from polyphosphate, and SYNW2495 polyphosphate kinase (ppk), which forms polyphosphate using ATP, but not at a high enough abundance for comparative analysis. SYNW2270 predicted inorganic polyphosphate/ATP NAD^+ kinase was not detected. These proteins have potential for future research. Direct measurement of polyphosphate alongside proteomic analysis would yield valuable information about the interaction of Cd and polyphosphate.

The physiological response to Cd addition may be nutritive at low PO_4^{3-} and added Zn

The instantaneous (24 hour) growth rates and higher cell counts in the added Zn low phosphate with added Cd would imply that Cd is acting like a nutrient. Perhaps this is by the direct use of Cd as a nutrient or the release of an intracellular pool of Zn due to Cd exposure (Figure 4.4b, 4.5). This nutritive effect of Cd was not observed in any of the other treatments.

Biochemical branch point - insertion of a metal ion - heme to chlorophyll

The insertion of a metal ion into protoporphyrin IX determines the biochemical fate of the molecule. It is a branch point in the biochemical pathway of heme proteins, including phycobilins and chlorophyll. If an iron atom is inserted by ferrochelatase, the molecule is destined to be a heme or biliverdin. If a Mg is inserted by Mg-chelatase, the molecule is destined to be chlorophyll. Mg-chelatase uses energy from the hydrolysis of ATP to insert a Mg^{2+} ion into porphyrin (Reid and Hunter, 2002). Branch-point enzymes such as these are tightly regulated according to the prevailing metabolic conditions (Walker and Willows, 1997). As was mentioned in Chapter 3, Cd has been known to substitute for Mg in chlorophylls in higher plants (Küpper et al., 1998). Cd could substitute into a porphyrin without enzymatic catalysis. There is the potential for Cd to affect these enzymes. There are five annotated genes for chelatases in WH8102: SYNW0213 protoporphyrin IX Mg-chelatase subunit (chlD), SYNW0327 Mg-chelatase family protein, SYNW0716 protoporphyrin IX Mg-chelatase subunit (chlI), SYNW0820 protoporphyrin IX Mg-chelatase subunit (chlH) (cyanobase, NCBI annotates as cobaltochelatase) and SYNW1747 ferrochelatase. We detect three of these at low spectral counts in this experiment, SYNW0213 protoporphyrin IX Mg-chelatase subunit (chlD), SYNW0820 protoporphyrin IX Mg-chelatase subunit (chlH) (cyanobase, NCBI annotates as cobaltochelatase) and SYNW0716 protoporphyrin IX Mg-chelatase subunit (chlI). Quantitative studies of these enzymes could be applied for further study.

Vitamin D

The response of a culture to acute Cd addition could be akin to a culture exposed to intense light. The vitamin D family (Vitamin D_2 and D_3) comprises fat soluble

secosteroids. Vertebrates require the active form ($1,25(OH)_2D_3$) to be physiologically functional in terms of calcium and bone metabolism (Holick, 1989). Provitamin D (ergosterol) is produced in fungi, plants, animals, phytoplankton, and zooplankton (Holick, 1989). Vitamin D has been relatively little studied in the ocean. A study documents the production of previtamin D_2 (ergosterol) in cultures of *Emiliania huxleyi* and proposes that the provitamin D and family of compounds evolved as natural sunscreens to absorb damaging UV radiation (Holick et al., 1982). Two additional ideas as to the functionality of vitamin D are photodegradation as a photochemical signal directly correlating to amount of UV exposure in an organism and the opening of ergosterol ring in the cell membrane upon UV exposure resulting in membrane permeability to allow cations such as calcium into a cell (Holick, 2003). In mammalian systems, vitamin D is thought to be a hormonal link between Zn^{2+} and Ca^{2+} (da Silva and Williams, 1991). In these systems, vitamin D controls the expression of calbindin, a protein involved in Ca^{2+} transport and metallothionein, a proposed Zn 'buffer' (da Silva and Williams, 1991). Vitamin D was also observed to stimulate Ca and PO_4^{3-} uptake across the brush border boundary in chick intestines by increasing the V_{max} of these carrier-mediated processes (Matsumoto and Rasmussen, 1982). Perhaps vitamin D is partially regulating the presence of metallothionein in cyanobacteria. Metallothionein is more abundant when Zn is added (Figure 4.9) and in a different experiment with 8102, harvested in stationary phase, acute Cd addition correlated with increased metallothionein abundance, whether or not Zn was added. Very little is known about Vitamin D in cyanobacteria. One Vitamin D receptor in a *Prochlorococcus* genome is annotated.

CONCLUSIONS

In conclusion, the physiologic response of *Synechococcus* WH8102 to acute 4.4 pM free Cd^{2+} under four varying Zn and PO_4^{3-} treatments (Zn-high PO_4^{3-}, no Zn-low PO_4^{3-}, no Zn-high PO_4^{3-}, and no Zn-low PO_4^{3-}) revealed during the last 24 hours of the experiment relative to the high PO_4^{3-} conditions: 1) increased growth rates under low PO_4^{3-} conditions and 2) even greater increased growth rates with Cd addition under low

PO_4^{3-} and Zn conditions. The proteomic response revealed differential abundances of PO_4^{3-} stress proteins comparing low to high PO_4^{3-} conditions and differential protein abundances with chronic Zn and acute Cd. Considering the proteomic data, it appears that Zn is vital to the PO_4^{3-} response in this organism because 1) Cd causes more proteomic changes at low PO_4^{3-} and 2) in the presence of high PO_4^{3-} and acute Cd the proteome is relatively indifferent to the presence of Zn. These findings are consistent with the ideas that Zn is beneficial for the functioning of alkaline phosphatase and other proteins involved in PO_4^{3-} acquisition, and at environmentally relevant PO_4^{3-} concentrations the presence of Zn and Cd make a difference in the physiology and proteome of cells, perhaps by influencing regulation.

Comparison of proteomic data to literature transcriptome analyses shows a similar response of many important P-stress related proteins (putative alkaline phosphatase, periplasmic ABC phosphate binding protein (PstS), motility-related proteins (SwmA and SwmB), and possible porin), but also shows other proteins that did not respond in the microarray study, bacterial metallothionein (SmtA), as well as proteins that did respond in the microarray study and not this one, thioredoxin peroxidase. These data suggest that there is a fair amount of consistency between the transcriptome and proteome under P-stress. Taken together with the fact that the treatments without Zn showed a different proteomic reaction to phosphorus stress, the presence of Zn appears important to the phosphorus metabolism of this open ocean cyanobacterium.

FUTURE RESEARCH

Quantitative analyses by triple quadrupole of metallothioneins, alkaline phosphatases, polyphosphates and chelatases would yield useful information. Unfortunately, the peptides needed for the quantification of this particular metallothionein are unable to be produced using current commercially available methods, probably because of the high number of cysteine residues.

A repeat experiment with analysis of protein across late growth phase into stationary phase would be advantageous because physiologically and proteomically,

much changes across this late-log to stationary phase transition. Time course experiments have not been performed thus far with *Synechococcus* WH8102 and detail across this transition would be revealing. A time course experiment with chronic Cd exposure could be performed and compared to *Synechococcus* WH5701, yielding a comparison of chronic exposure from a coastal to an open ocean cyanobacterium.

In addition, the microarray is available for WH8102. It would be possible to collect for transcriptome analyses at the some time and compare gene expression with protein abundance directly. Also, genetic manipulations of WH8102 are possible to perform if one was interested in detailed gene functionality (Brahamsha, 1996).

REFERENCES

Blindauer, C.A. 2008a. Zinc-handling in cyanobacteria: An update. *Chemistry and Biodiversity* 5: 1990- 2013.

Blindauer, C.A. 2008b. Metallothioneins with unusual residues: Histidines as modulators of zinc affinity and reactivity. *Journal of Inorganic Biochemistry* 102: 507-521.

Boyle, E.A., Sclater, F. and Edmond, J.M. 1976. On the marine geochemistry of cadmium. *Nature* 263: 42-44.

Boyle, E.A. 1988. Cadmium: chemical tracer of deepwater paleoceanography. *Paleoceanography* 3:471-489.

Brahamsha, B. 1996. A genetic manipulation system for oceanic cyanobacteria of the genus *Synechococcus*. *Applied and Environmental Microbiology* 62: 1747-1751.

Brand, L.E., Sunda, W.G. and Guillard, R.R.L. 1986. Reduction of marine phytoplankton reproduction rates by copper and cadmium. *Journal of Experimental Marine Biology and Ecology* 96: 225-250.

Bruland, K. W. 1980. Oceanographic distributions of cadmium, zinc, nickel, and copper in the North Pacific. *Earth and Planetary Science Letters* 47: 176-198.

Bruland, K.W. 1989. Complexation of zinc by natural organic ligands in the central North Pacific. *Limnology and Oceanography* 34: 269-285.

Bu, L., Xiao, J., Lu, L., Xu, G., Li, J., Zhao, F., Li, X. and Wu, J. 2009. The repertoire and evolution of ATP-binding cassette systems in *Synechococcus* and *Prochlorococcus*. *Journal of Molecular Evolution* 69 (4): 300-310.

Cullen, J. 2006. On the nonlinear relationship between dissolved cadmium and phosphate in the modern global ocean: Could chronic iron limitation of phytoplankton growth cause the kink? *Limnology and Oceanography*: 51(3): 1369–1380.

Diaz, J., Ingall, E., Benitez-Nelson, C., Paterson, D., de Jonge, M. D., McNulty I. and Brandes, J.A. 2008. Marine polyphosphate: A key player in geologic phosphorus sequestration. *Science* 320: 652-655.

Duncan, K.E.R., Ngu, T.T., Chan, J., Salgado, M.T., Merrifield, M.E. and Stillman, M.J. 2006. Peptide folding, metal-binding mechanisms, and binding site structures in metallothioneins. *Experimental Biology and Medicine* 231: 1488-1499.

Eisen, M.B., Spellman, P.T., Brown, P.O., and Bostein, D. 1998. Cluster analysis and display of genome-wide expression patterns. *PNAS* 95(25): 14863-14868.

Frausto da Silva, J.R.R. and Williams, R.J.P. 1991. The Biological Chemistry of the Elements: The Inorganic Chemistry of Life. Oxford University Press.

Fuller, N.J., Marie, D., Partensky, F., Vaulot, D., Post, A.F. and Scanlan, D. J. 2003. Clade-specific 16S ribosomal DNA oligonucleotides reveal the predominance of a single marine *Synechococcus* clade in a stratified water column in the Red Sea. *Applied and Environmental Microbiology* 69: 2430-2443.

Garczarek, L., Dufresne, A., Blot, N., Cockshutt, A. M., Peyrat, A., Campbell, D.A., Joubin, L. and Six, C. 2008. Function and evolution of the psbA gene family in marine *Synechococcus*: *Synechococcus* sp. WH7803 as a case study. *The ISME Journal* 2: 937–953.

Holick, M.F. 1989. Phylogenetic and evolutionary aspects of vitamin D from phytoplankton to humans. In: Schreibman P, Pang M, editors. Vertebrate endocrinology: Fundamentals and biomedical implications. San Diego: Academic Press.Vertebrate Endocrinology pp 7-43.

Holick, M. F. 2003. Vitamin D: A millenium perspective. *Journal of Cellular Biochemistry* 88 (2): 296-307.

Holick, M.F., Holick, S.A. and Guilliard, R.L. 1982. On the origin and metabolism of Vitamin D in the sea. In: Oguro C, Pang P, editors. Comparative endocrinology and calcium regulation. Tokyo: Sci Soc Press pp. 85-91.

Frausto da Silva, J.R.R. and Williams, R.J.P. 1991. The Biological Chemistry of the Elements: The Inorganic Chemistry of Life. Oxford University Press.

Karl, D.M. 2000. Phosphorus, the staff of life. *Nature* 406: 31-32.

Kathuria, S. and Martiny, A. C. 2010. Prevalence of a calcium-based alkaline phosphatase associated with the marine cyanobacterium *Prochlorococcus* and other ocean bacteria. *Environmental Microbiology* doi:10.1111/j.1462-2920.2010.02310.x.

Keasling, J.D. 1997. Regulation of intracellular toxic metals and other cations by hydrolysis of polyphosphate. *Annals of the New York Academy of Sciences* 829:242-249.

Keyhani, S., Lopez, J. L., Clark, D. S. and Keasling, J.D. 1996. Intracellular polyphosphate content and cadmium tolerance in *Anacystis nidulans* R2. *Microbios* 88:105-114.

Küpper, H., Küpper, F. and Spiller, M. 1998. In situ detection of heavy metal substituted chlorophylls in water plants. *Photosynthesis Research* 58: 123–133.

Ilikchyan, I. N., McKay, R. M., Zehr, J. P., Dyhrman, S. T., and Bullerjahn, G.S. 2009. Detection and expression of the phosphonate transporter gene phnD in marine and freshwater picocyanobacteria. *Environmental Microbiology* 11(5): 1314-24.

Lane, E.S., Semeniuk, D. M., Strzepek, R. F., Cullen, J.T., and Maldonado, M. T. 2009. Effects of iron limitation on intracellular cadmium of cultured phytoplankton: Implications for surface dissolved cadmium to phosphate ratios. *Marine Chemistry* 115: 55-162.

Lane, T.W. and Morel, F.M.M. 2000. A biological function for cadmium in marine diatoms. *Proceedings of the National Academy of Sciences* 97: 4627-4631.

Lang, N.J. 1968. The fine structure of blue-green algae. *Annual Review of Microbiology* 22:15-46.

Lee, J.G. and Morel, F.M.M. 1995. Replacement of zinc by cadmium in marine phytoplankton. *Marine Ecology Progress Series* 127:305-309.

Lee, JG., Roberts, S.B. and Morel, F.M.M. 1995. Cadmium: a nutrient for the marine diatom *Thalassioria weissflogii*. *Limnology and Oceanography* 40:1056-1063.

Luo, H., Benner, R., Long, R. A. and Hu J. 2009. Subcellular localization of marine bacterial alkaline phosphatases. *PNAS* 106: 21219-21223.

Martiny, A.C, Coleman, M. L. and Chisholm, S.W. 2006. Phosphate acquisition genes in *Prochlorococcus* ecotypes: Evidence for genome-wide adaptation. *PNAS* 103(33): 12552-12557.

Martelli, A. E. Rousselet, Dycke, C., Bouron, A. and Moulis, J.-M. 2006. Cadmium toxicity in animal cells by interference with essential metals. *Biochimie* 88 (11):1807-1814.

Matsumoto, T. and Rasmussen, H. 1982. Mechanism of acation of 1,25(OH)2D3 on chick intestinal calcium and phosphate transport. In: Oguro C, Pang P, editors. Comparative endocrinology and calcium regulation. Tokyo: Sci Soc Press pp. 85-91.

Moore, L. R., Ostrowski, M., D.J. Scanlan, D. J., Feren, K. and Sweetsir, T. 2005. Ecotypic variation in phosphorus-acquisition mechanisms within marine picocyanobacteria. *Aquatic Microbial Ecology* 39: 257–269

Morel, F.M.M., Milligan, A.J. and Saito, M.A. 2003. Marine bioinorganic chemistry: The role of trace metals in the oceanic cycles of major nutrients. Treatise on Geochemistry Volume 6 The Oceans and Marine Geochemistry. eds. Henry Elderfield. H.D. Holland and K.K. Turekian. 6.05: 113-143.

Nishikawa, K., Yamakoshi, Y., Uemura, I. and Tominaga, N. 2003. Ultrastructural changes in *Chlamydomonas acidophila* (Chlorophyta) induced by heavy metals and polyphosphate metabolism. *FEMS Microbiology Ecology*: 44(2):253-259.

Okamura, M. Y., Paddock, M. L., Graige, M. S., and Feher, G. 2000. Proton and electron transfer in bacterial reaction centers. *Biochimica et Biophysica Acta-Bioenergetics* 1458 (1): 148-163.

Ostrowski, M., Mazard, S., Tetu, S. G., Phillippy, K., Johnson, A., Palenik, B., Paulsen, I. T. and Scanlan, D. J. 2010. PtrA is required for coordinate regulation of gene expression during phosphate stress in a marine *Synechococcus*. *The ISME Journal* 4: 908–921.

Palenik, B., Ren, Q., Dupont, C.L., Myers, G.S., Heidelberg, J.F., Badger, J.H., Madupu, R., Nelson, W.C., Brinkac, L.M., Dodson, R.J., Durkin, A.S., Daugherty, S.C., Sullivan, S.A., Khouri, H., Mohamoud, Y., Halpin, R. and Paulsen, I.T. 2006. Genome sequence of *Synechococcus* CC9311: Insights into adaptation to a coastal environment. *PNAS*: 103(36): 13555-13559.

Palmiter, R.D. 1998. The elusive function of metallothioneins. *PNAS* 95: 8428-8430.

Park, H., Song, B. and Morel, F. M. M. 2007. Diversity of the cadmium-containing carbonic anhydrase in marine diatoms and natural waters. *Environmental Microbiology* 9(2): 403-413.

Payne, C.D. and Price, N.M 1999. Effects of cadmium toxicity on growth and elemental composition of marine phytoplankton. *Journal of Phycology* 35:293-302.

Peng, J., Elias, J. E., Thoreen, C. C., Licklider, L. J. and Gygi, S. P. 2003. Evaluation of multidimensional chromatography coupled with tandem mass spectrometry (LC/LC-MS/MS) for large-scale protein analysis: The yeast proteome. *Journal of Proteome Research* 2: 43-50.

Price, N.M. and Morel, F.M.M. 1990. Cadmium and cobalt substitution for zinc in a marine diatom. *Nature* 344:658-660.

Reid, J.D. and Hunter, C.N. 2002. Current understanding of the function of magnesium chelatase. *Biochemical Society Transactions* 30: 643–645.

Rocap, G., Distel, D.L., Waterbury, J.B. and Chisholm, S.W. 2002. Resolution of *Prochlorococcus* and *Synechococcus* ecotypes by using 16S-23S ribosomal DNA internal transcribed spacer sequences. *Applied and Environmental Microbiology* 68(3):1180-1191.

Saito, M.A., Sigman, D.M. and Morel, F.M.M. 2003. The bioinorganic chemistry of the ancient ocean: the co-evolution of cyanobacterial metal requirements and biogeochemical cycles at the Archean-Proterozoic boundary? *Inorganica Chimica Acta* 356:308-318.

Saito, M.A, Goepfert, T.J. and Ritt, J. 2008. Some thoughts on the concept of colimitation: Three definitions and the importance of bioavailability. *Limnology and Oceanography* 53(1): 276–290.

Saito, M. A., Goepfert, T. J., Noble, A. E., Bertrand, E. M., Sedwick, P. N. and DiTullio, G. R. 2010. A seasonal study of dissolved cobalt in the Ross Sea, Antarctica: micronutrient behavior, absence of scavenging, and relationships with Zn, Cd, and P. *Biogeosciences* 7: 4059-4082.

Sebastian, M. and Ammerman, J. W. 2009. The alkaline phosphatase PhoX is more widely distributed in marine bacteria than the classical PhoA. *The ISME Journal* 3: 563-572.

Shaked, Y., Xu, K., Leblanc, K. and Morel, F. M. M. 2006. Zinc availability and alkaline phosphatase activity in *Emiliania huxleyi*: Implications for Zn-P co-limitation in the ocean. *Limnology and Oceanography* 51: 299–309.

Su, Z., Dam, P., Chen, X., Olman, V., Jiang, T., Palenik, B. and Xu, Y. 2003. Computational Inference of Regulatory Pathways in Microbes: an Application to Phosphorus Assimilation Pathways in *Synechococcus* sp. WH8102. *Genome Informatics* 14: 3-13.

Su, Z., Olman, V. and Xu, Y. 2007. Computational prediction of Pho regulons in cyanobacteria. *BMC Genomics* 8:156.

Sunda, W.G. and Huntsman, S.A. 2000. Effect of Zn, Mn, and Fe on Cd accumulation in phytoplankton: Implications for oceanic Cd cycling. *Limnology and Oceanography* 45(7): 1501-1516.

Tai, V., Paulsen, I.T., Phillippy, K., Johnson, D.A. and Palenik, B. 2009. Whole-genome microarray analyses of *Synechococcus-Vibrio* Interactions. *Environmental Microbiology* 11(10): 2698 - 2709.

Tetu, S. G., Brahamsha, B., Johnson, D. A., Tai, V., Phillippy, K., Palenik, B. and Paulsen, I. T. 2009. Microarray analysis of phosphate regulation in the marine cyanobacterium *Synechococcus* sp. WH8102. *ISME Journal* 3: 835-849.

Vallee, B.L. and Ulmer, D.D.1972. Biochemical effects of mercury, cadmium and lead. *Annual Review of Biochemistry* **41**: 91-128.

Volesky, B., May, H. and Holan Z.R. 1993. Cadmium biosorption by *Saccharomyces cerevisiae*. *Biotechnology and Bioengineering* 41: 826-829.

Walker, C.J. and Willows, R. D.. 1997. Mechanism and regulation of Mg-chelatase. *Biochemical Journal* 327: 321–333.

Waterbury, J. B. and Willey, J.M. 1988. Isolation and growth of marine planktonic cyanobacteria. *Methods in Enzymology* 167: 100-105.

Xu, Y., Feng, L., Jeffrey, P. D., Shi, Y. and Morel, F. M. M. 2008. Structure and metal exchange in the cadmium carbonic anhydrase of marine diatoms. *Nature* 452: 56-61.

Zeng, J. and Wang, W. 2009. The importance of cellular phosphorus in controlling the uptake and toxicity of cadmium and zinc in *Microcystis aeruginosa*, A freshwater cyanobacterium. *Environmental Toxicology and Chemistry* 28(8): 1618–1626.

Zhang, B., VerBerkmoes, N. C., Langston, M.A., Uberbacher, E., Hettich, R. L. and Samatova, N. F. 2006. Detecting differential and correlated protein expression in label-free shotgun proteomics. *Journal of Proteome Research* 5(11): 2909–2918.

Zhang, B., Georgiev, O., Hagmann, M., Günes, Ç., Cramer, M., Faller, P., Vasák, M. and Schaffner, W. 2003. Activity of metal-responsive transcription factor 1 by toxic heavy metals and H_2O_2 in vitro is modulated by metallothionein. *Molecular and Cellular Biology* 23 (23): 8471-8485.

Chapter 5: Conclusions

In summary, the combination of uptake field studies on natural phytoplankton assemblages and laboratory proteomic and physiological experiments on cyanobacterial isolates have yielded much information about the interactions of cadmium, zinc, and phosphorus in the ocean and in marine *Synechococcus*. Environmentally relevant concentrations of total dissolved Cd in the ocean range from lower than pM in shallow water to around 1 nM in deeper waters and EDTA-buffered culture media experiments were performed with free concentrations in this range.

Enriched stable isotope uptake field studies using picomolar additions of ^{110}Cd in the Costa Rica Upwelling dome showed that the intermediate abundance enriched Cd stable isotope tracer method appears to function as long as the total dissolved natural Cd present is below ~200 pM. Overall, uptake of ^{110}Cd occurs in waters shallower than 40m, the uptake rate of ^{110}Cd correlates positively with chlorophyll *a* concentrations, ^{110}Cd uptake increases with time, a single 24-hour time point seems adequate to measure ^{110}Cd uptake rates in environmental samples at sea, preexisting particulate Cd must be considered especially in high biomass regions, calculated upwelling flux of Cd is roughly equivalent to uptake flux into the particulate fraction inside the dome, and stations inside the dome do not show a decrease in chlorophyll *a* concentrations with added Cd up to 5 nM whereas stations outside the dome do.

The physiological and proteomic effects of two levels of chronic Cd exposure (4.4 and 44 pM Cd^{2+}) over the life cycle of a little-studied coastal cyanobacterium representative of the natural population in the Baltic Sea, *Synechococcus* WH5701, revealed that cells exposed to Cd under Zn deficiency appear to be physiologically robust during exponential growth phase, showing no difference in growth rates or fluorescence, but their proteome was quite different compared to cultures with no added Cd. The proteome of exponential cultures with Cd added showed differences in relative abundances of proteins involved in chlorophyll *a* biosynthesis, photosynthesis, carbon fixation, steroid and lipid biosynthesis, sulfur and cysteine metabolism, and genetic information processing suggesting a great metabolic impact. During stationary phase,

chronic Cd exposure caused an increase in relative chlorophyll *a* fluorescence and faster mortality rates. The proteome changed during exponential phase and throughout stationary phase. This is the first detailed proteomic study over the life cycle of *Synechococcus* and of chronic Cd exposure under Zn deficiency. It also showed that Cd may be used to indicate where Zn is important in a cell.

The interactions of acute Cd (4.4 pM free Cd^{2+}) exposure under a matrix of Zn deficient (no added Zn^{2+}) and Zn replete (tens of picomolar free Zn^{2+}), low PO_4^{3-} (1 μM) and high PO_4^{3-} (65 μM) conditions in the well-studied open-ocean cyanobacterium, *Synechococcus* WH8102, revealed a number of physiological and proteomic results. Low PO_4^{3-} cultures had higher growth rates during the last 24 hours of the experiment than the high PO_4^{3-} and had even higher growth rates with the addition of Cd in both the low PO_4^{3-} and Zn added treatments. The proteomic response to low PO_4^{3-} was different under Zn deficient and Zn replete conditions, which suggests that the presence of Zn is vital to the response of the organism to different PO_4^{3-} concentrations and provides an example of proteome plasticity. The acute addition of Cd caused more changes in protein response at low PO_4^{3-} than high PO_4^{3-} conditions, which may indicate a connection between Cd and P. Comparisons with literature transcriptome analyses of PO_4^{3-} stress in this organism showed similar increases in relative abundance of PO_4^{3-} stress response proteins including PstS (a phosphate binding protein) and an alkaline phosphatase (access of organic phosphate), which shows consistency in the two approaches. One bacterial metallothionein (SmtA) also appeared to be correlated with proteins present under low PO_4^{3-} conditions.

These studies also raised questions about the meaning of toxicity. As discussed in Chapter 2 on page 39, toxicity can be considered the deleterious effects of a substance to an organism. Toxicity itself refers to the degree of being poisonous, or degree of harmful effects produced by a substance in an organism. Toxic effects can range from decreased performance to death. In field experiments described in Chapter 2, toxicity was considered to be decreased performance of bottled phytoplankton assemblages in terms of decreased chlorophyll *a* concentrations relative to a control treatment. Although the

phytoplankton assemblages did not die (using chlorophyll *a* concentrations as a proxy for biomass), they were negatively affected. In laboratory experiments described in Chapter 3, the decreased performance of cultures exposed to chronic Cd as evinced by greater than or equal to two-fold differences in protein abundances was observed followed by the earlier death of these cultures. The effect was dose-dependent, with the higher Cd treatment dying faster than the lower Cd treatment. Most studies that only focus on growth phase or only measure cell abundances coupled with fluorescence measurements would miss the toxicity of Cd observed in Chapter 3. These results support the idea that chronic exposure of organisms to small amounts of a toxin may take time for the deleterious effects to be observed, and that global proteomics may serve as a tool to identify toxic effects.

Overall, this work has yielded many insights into the interactions of Cd, Zn and P and set the stage for future research in the laboratory and in the field. It has shown that Cd affects many cellular processes and that there are interactions between Cd, Zn and P. The global proteomic analyses allowed observation of changes in relative protein abundances among different treatments even when growth rates and fluorescence measurements were similar giving a detailed view of the reactions of cells to changing environmental conditions and suggesting proteome plasticity. Global proteomic methods applied to cyanobacterial and other systems in the future will also be useful for elucidating mechanisms of hormetic response. The relationships of metals to proteins will be vital to understanding the interactions observed between these elements and organisms in the environment.

Appendix I: Supplementary Data to Chapter 2

Table I.1: Costa Rica Upwelling Dome station locations

Station	Latitude (° N)	Longitude (° W)	Local date '05
5	8.4750	89.9969	July 18
7	10.0035	90.0026	July 19
11	8.6864	87.4922	July 22
13	9.5025	92.3287	July 24
14	9.9983	96.4955	July 26
15	9.9835	96.9808	July 27
17	2.0417	97.0512	July 29

See Figure 2.1.

Table I.2: Station 11 particulate cadmium uptake, cyanobacterial cell numbers and chlorophyll *a*

Depth (m)	Cd_{Tot} (pM)	Cd Uptake Rate (pmol L^{-1} d^{-1})	chl *a* (µg L^{-1})	chl *a* 2µm -10µm (µg L^{-1})	chl *a* >10µm (µg L^{-1})	chl *a* <2µm (µg L^{-1})	*Prochlorococcus* (cells mL^{-1})	*Synechococcus* (cells mL^{-1})
8	0	2.8±0.14	0.510	0.150	0.126	0.173	$2.50x10^5$	$3.47x10^5$
15	30	1.3±0.09	0.548	0.182	0.062	0.269	$2.63x10^5$	$3.61x10^5$
30	78	0.43±0.02	0.448	0.114	0.027	0.218	$1.10x10^5$	$1.02x10^5$
50	185	nd	0.178	0.038	0.024	0.148	$2.55x10^4$	$5.94x10^3$
80	399	nd	nm	nm	nm	nm	$4.28x10^3$	$3.96x10^2$
100	551	nd	nm	nm	nm	nm	405	531

See Figure 2.4. nd = non-detectable, nm = not measured.

Table I.3: Station 17 particulate cadmium uptake, cyanobacterial cell numbers and chlorophyll *a*

Depth (m)	Cd_{Tot} (pM)	Cd Uptake Rate (pmol L^{-1} d^{-1})	chl *a* (µg L^{-1})	chl *a* 2µm -10µm (µg L^{-1})	chl *a* >10µm (µg L^{-1})	chl *a* <2µm (µg L^{-1})	*Prochlorococcus* (cells mL^{-1})	*Synechococcus* (cells mL^{-1})
8	0	1.23±0.09	0.183	0.069	0.033	0.078	$1.05x10^5$	$2.45x10^4$
15	0	1.92±0.14	0.198	0.067*	0.041*	0.092*	$1.15x10^5$	$2.85x10^4$
30	66	0.96±0.06	nm	0.062*	0.043*	0.163*	$4.46x10^4$	$3.36x10^4$
80	161	0.26±0.02	nm	0.013	0.003	0.036	$2.37x10^4$	46
100	267	nd	nd	nm	nm	nm	nm	nm
310	317	0.40±0.03	nm	nm	nm	nm	nm	nm
350	nm	0.059±0.004+	nm	nm	nm	nm	nm	nm
400	715	nd	nd	nm	nm	nm	nm	nm
460	754	nd	nd	nm	nm	nm	nm	nm
650	844	nd	nd	nm	nm	nm	nm	nm

See Figure 2.5. nd = non-detectable. nm = not measured. Data marked with an * are values in rows actually measured at 25 and 47 m depth, respectively. Data marked with an + indicate a Cd uptake rate calculated without accounting for total dissolved cadmium. Data points plotted in Figure 2.8f represent the correct depth.

Table I.4: Station 11 Cadmium isotope ratios

Depth (m)	$^{114}Cd/^{110}Cd$	$^{114}Cd/^{111}Cd$	$^{111}Cd/^{110}Cd$	Blank $^{114}Cd/^{110}Cd$	Blank $^{114}Cd/^{111}Cd$	Blank $^{111}Cd/^{110}Cd$
8	0.230±0.020	1.907±0.160	0.120±0.011	2.139	2.146	0.997
15	0.424±0.058	1.947±0.237	0.218±0.026	2.244	2.140	1.049
30	0.675±0.068	2.095±0.235	0.322±0.035	2.349	2.235	1.051
50	1.163±0.128	1.501±0.191	0.775±0.069	2.369	2.313	1.024
80	2.188±0.213	1.372±0.210	1.596±0.103	2.634	2.414	1.091
100	nd	nd*	3.715±0.120	2.431	2.038	1.193

nd = non-detectable. See Figure 2.6. * = had 0.088 as error

Table I.5: Station 11 Time-course experiment isotope ratios

Time (hr)	$^{114}Cd/^{110}Cd$	$^{114}Cd/^{111}Cd$	$^{111}Cd/^{110}Cd$
3	0.310±0.031	2.078±0.213	0.149±0.013
6	0.288±0.034	2.092±0.281	0.138±0.015
24	0.110±0.011	1.778±0.169	0.062±0.005
30	0.090±0.009	1.629±0.151	0.055±0.005

See Figure 2.7.

Table I.6: Time-course experiment

Station	Time (days)	^{110}Cd Uptake Rate (pmol L^{-1} d^{-1})
5	0.125	0.97
5	1.000	0.47
5	2.000	1.7
7	0.125	3.36
7	0.250	3.54
7	1.000	6.33
7	2.000	10.86
11	0.125	2.3
11	0.250	2.6
11	1.000	7.5
11	1.250	5.5
13	0.125	4.64
13	0.250	5.13
13	0.500	2.56
13	1.000	12.2
15	0.250	0.06
15	0.500	0.16
15	0.750	0.14
15	1.000	0.27
17	0.125	0.72
17	0.250	0.69
17	0.542	1.84
17	1.000	2.9

See Figure 2.8. Note that these data are not corrected for preexisting particulate cadmium.

Appendix II: Supplementary Data to Chapter 3

Table II.1: WH5701 proteins during early stationary phase (T2) that are more abundant in the Cd^{2+} treatments than the control by ≥ two-fold.

WH5701 ID	KEGG Function	Protein	4.4 pM Cd^{2+} abundance relative to control	44 pM Cd^{2+} abundance relative to control
05830	U,GI	putative ribonuclease D	+3.4	+4.5
03624	M	GDP-mannose pyrophosphorylase	+1.9	+3.9
09149	C	malate oxidoreductase	+1.4	+2.5
15471	C	ribose 5-phosphate isomerase	+2.3	+2.3
15156	Ukn	hypothetical protein	+2.6	+2.2
01855	Ukn	hypothetical protein	+2.5	+2.2
10470	En,ABC	extracellular solute-binding protein, family 3	+4.1	+1.4
04880	Ukn	hypothetical protein	+2.2	+1.3
15186	M	putative aminopeptidase P	+2.3	+1.3
02904	Ukn	hypothetical protein	+2.1	+1.9
03504	M,Cb,N	formamidase	+2.1	+1.7

Arranged in highest to lowest fold change, 44 pM Cd^{2+}, then 4.4 pM Cd^{2+}. + = fold greater than control, - = fold less than control, U = unclassified, GI = genetic information processing, M = metabolism, C = CO_2 fixation, Ukn = unknown, En = environmental sensing, ABC = membrane transport ABC type, Cb = carbohydrate metabolism, N = nitrogen

Table II.2: WH5701 proteins during early stationary phase (T2) that are two-fold or more less abundant in the Cd^{2+} treatments than the control.

WH5701 ID	KEGG Function	Protein	4.4 pM Cd^{2+} abundance relative to control	44 pM Cd^{2+} abundance relative to control
01585	PS	photosystem I subunit VII	-3.7	-20
05480	PS	photosystem I core protein (psaB)	-11.2	-16
11384	Chl	photochlorophyllide oxidoreductase	-5.9	-8.3
08839	M,Cb	acetate--CoA ligase	-5.9	-8.3
14421	PS	photosynthetic II protein (psbC)	-6.7	-6.7
06000	PS	photosystem II chlorphyll binding protein	-4.6	-5.6
04930	GI,T	aspartyl/glutamyl-tRNA amidotransferase subunit B	-4.9	-5.5
15241	PS	ATP synthase subunit A	-4.2	-5.0
08459	GI,T	glutamyl-tRNA (Gln) amidotransferase subunit A	-4.4	-4.8
04715	N,ABC	ABC-type nitrate/nitrite transport system substrate-binding protein	-4.0	-5.8
02614	P,ABC	ABC transporter, substrate binding protein, phosphate	-4.4	-3.8
04620	St,L	arylsulfatase	-1.2	-3.7
06176	PS	photosystem I reaction center subunit IV	-2.0	-3.6
15121	PS	ATP synthase subunit B	-2.7	-3.5
08944	M,N, A,S	glutamine synthethase type III	-1.6	-3.3
01470	M,A, V	serine hydroxymethyltransferase	-2.0	-3.3
05815	Chl	coproporphyrinogen III oxidase	-2.7	-2.9
05565	GI,T	30S ribosomal protein S11	-2.5	-2.7
12533	Chl	uroporphyrinogen decarboxylase	-3.4	-2.6
15851	PS	ferredoxin-thioredoxin reductase catalytic chain	-1.0	-2.5
05050	GI,T	transcription antitermination protein NusG	-2.7	-2.4
15626	U	putative membrane protein	-1.1	-2.2
07386	M,Nu,A	possible cytosine deaminase	+1.1	-2.2
13850	Ukn	hypothetical protein	-1.4	-2.2
12538	M,Cb	glycogen branching enzyme	-1.6	-2.2
01005	M,N	ferredoxin-dependent glutamate synthase, Fd-GOGAT	+1.1	-2.0
05060	GI,T	50S ribosomal protein L1	-2.0	-2.0
05910	PS	phycobilisome linker polypeptide	-1.1	-2.0
05610	GI,T	30S ribosomal protein S8	-6.0	-2.0
15451	U,GI	DNA-directed RNA polymerase beta subunit	-2.6	-2.0
05590	GI,T	50S ribosomal protein L15	-2.6	-2.0
01150	PS	photosystem Il Mn-stabilizing protein	-2.5	-1.7

Table II.2 (continued, page 2 of 2):

WH5701 ID	KEGG Function	Protein	4.4 pM Cd^{2+} abundance relative to control	44 pM Cd^{2+} abundance relative to control
05600	GI,T	50S ribosomal protein L18	-2.3	-1.2
06556	M,N,GI	polyribonucleotide nucleotidyltransferase	-2.1	+1.2
05570	GI,T	30S ribosomal protein S13	-2.1	-1.6
10210	PS	ferredoxin--NADP reductase (FNR)	-2.0	-1.9

Arranged in highest to lowest fold change, 44 pM Cd^{2+}, then 4.4 pM Cd^{2+}. + = fold greater than control, - = fold less than control, PS = photosynthesis, Chl = chlorophyll biosynthesis, M = metabolism, Cb = carbohydrate metabolism, GI = genetic information processing, T = translation, N = nitrogen metabolism, ABC = membrane transport - ABC type, P = phosphorus metabolism, St = steroid hormone synthesis, L = lipid biosynthesis, A = amino acid metabolism, S = sulfur metabolism, V = vitamin metabolism, U = unclassified, Nu = nucleic acid metabolism, Ukn = unknown

Table II.3: WH5701 proteins during mid-stationary phase (T3) that are more abundant in the Cd^{2+} treatments compared to the control by ≥ two-fold.

WH5701 ID	KEGG Function	Protein	4.4 pM Cd^{2+} abundance relative to control	44 pM Cd^{2+} abundance relative to control
02239	St,L	putative arylsulfatase	+5.9	+6.2
03654	M	glycogen/starch/alpha-gulcan phosphorylase	+4.7	+6.2
15451	U,GI	DNA-directed RNA polymerase beta subunit	+2.6	+4.2
15441	U,GI	DNA-directed RNA polymerase beta' subunit	+2.6	+4.1
03604	M	glycogen/starch/alpha-gulcan phosphorylase	+6.0	+4.1
11344	M,C	ribulose 1,5 bisphosphate carboxylase small chain	+3.7	+4.0
01860	Ukn	hypothetical protein	+2.2	+3.9
11349	U, GI	methionine sulfoxide reductase A	+2.8	+3.6
07844	Ukn	hypothetical protein	+2.6	+3.6
05030	M	enolase	+2.8	+3.5
10470	En, ABC	extracellular solute-binding protein family 3	+1.4	+3.4
06556	M,Nu,GI	polyribonucleotide nucleotidyl-transferase	+1.7	+3.3
03504	M,Cb,N	formamidase	+3.5	+3.1
13100	M,A,Ly	diaminopimelate epimerase	+3.8	+2.9
04700	N	ferredoxin-nitrite reductase	+2.7	+2.9
05815	M,Chl	coproporphyrinogen III oxidase	+3.3	+2.5
01585	PS	photosystem I subunit VII	+1.3	+2.5
11924	U, T	ribosome releasing factor	+2.1	+2.4
12134	En,ABC U,Fe	putative iron ABC transporter substate binding protein	+1.7	+2.2
13035	M,A	branched-chain amno acid aminotransferase	+1.9	+2.1
11339	C	carboxysome shell protein	+1.0	+2.1
01855	Ukn	hypothetical protein	-1.1	+2.0
08744	U	zinc-containing alcohol dehydrogenase superfamily	+5.5	+4.5
13575	M,E,N,A En	glutamine synthetase, glutamate ammonia ligase	+4.5	+5.8
14556	M,Nu,V	stationary-phase survival protein SurE	+4.1	+2.6
15671	U,GI	methionine sulfoxide reductase B	+2.8	+2.1
12533	M,Chl	uroporphyrinogen decarboxylase	+2.6	+1.8
12538	M,Cb	glycogen branching enzyme	+2.5	+1.8
13175	M, A,Cy, Met	5'-methylthioadenosine phosphorylase	+2.3	+1.6

Arranged in highest to lowest fold change, 44 pM Cd^{2+}, then 4.4 pM Cd^{2+}. + = fold greater than control, - = fold less than control, St = steroid hormone synthesis, L = lipid biosynthesis, M = metabolism, U = unclassified, GI = genetic information processing, C = CO_2 fixation, Ukn = unknown, En = environmental sensing, ABC = membrane transport ABC type, Nu = nucleic acid metabolsim, Cb = carbohydrate metabolism, N = nitrogen, A = amino acid metabolism, Ly = lysine synthesis, Chl = chlorophyll biosynthesis, PS = photosynthesis, T = translation, V = vitamin metabolism, Cy = cysteine metabolism, Met = methionine synthesis

Table II.4: WH5701 proteins during mid-stationary phase (T3) that are two-fold or more less abundant in the Cd^{2+} than the control treatments.

WH5701 ID	KEGG Function	Protein	4.4 pM Cd^{2+} abundance relative to control	44 pM Cd^{2+} abundance relative to control
15341	M, Nu, PB,A	adenylosuccinate lyase	-6.8	-4.8
05145	M,Cb,E,C	phosphoglycerate kinase	-2.3	-4.2
14591	Ukn	hypothetical protein	-2.2	-3.1
08944	M,N,A,S	glutamine synthetase type III	+1.1	-2.9
05910	PS	phycobilisome linker polypeptide	-2.0	-2.9
12014	M,Nu,PB	adenylosuccinate synthetase	-1.1	-2.7
05360	GI	glutaredoxin	-1.2	-2.4
07799	(GI)	60 kD chaperonin 2, GroEL-like 2	-2.4	-2.3
02844	M,E,C	glyceraldehyde 3-phosphate dehydrogenase (NADP+; phosphorylating)	-2.2	-2.2
05580	M,Nu,PB	adenylate kinase	-2.8	-1.3
05050	GI,T	transcription antitermination protein, NusG	-2.6	-1.7
03029	U,GI	trigger factor	-2.4	-1.7
15281	PS	anchor polypeptide LCM	-2.3	-1.3
04735	(En,Si)	predicted HTH of cAMP family transcirptional regulator	-2.1	-1.1

Arranged in highest to lowest fold change: 44 pM Cd^{2+} then 4.4 pM Cd^{2+}. + = fold greater than control, - = fold less than control, PB = purine biosynthesis, M = metabolism, E = energy metabolism, C = CO_2 fixation, Ukn = unknown, N = nitrogen, A = amino acid metabolism, S = sulfur metabolism, PS = photosynthesis, Nu = nucleic acid metabolsim, GI = genetic information processing, T = translation, U = unclassified, En = environmental sensing, Si = signaling.

Table II.5: WH5701 proteins during late stationary phase (T4) that are more abundant in at least one of the Cd^{2+} treatments compared to the control by ≥ two-fold.

WH5701 ID	KEGG Function	Protein	4.4 pM Cd^{2+} abundance relative to control	44 pM Cd^{2+} abundance relative to control
01780	TCA	isocitrate dehydrogenase	+47	+68
01529	M, Nu, V	phosphoribosylaminoimidazole carboxamide formyltrans-ferase/IMP cyclohydrolase	+21.7	+16.3
10070	Po,Chl	glutamate-1-semialdehyde aminotransferase	+16.2	+15.7
07161	O	fungal/archaeal/bacterial haem catalase/peroxidase	+6.2	+14.6
10130	Ukn	hypothetical protein	+10.0	+14.0
01085	M,C,A	aspartate aminotransferase	+14.4	+13.8
01595	M,L	3-oxoacyl-(acyl-carrier-protein) synthase II	+10.8	+13.0
13175	M,A,Cy,Met	5'-methylthioadenosine phosphorylase	+11.1	+12.0
09149	C	malate oxidoreductase	+14.5	+10.7
11524	S,Cy,Se	cysteine synthase A	+13.4	+10.2
02719	M,Nu,GI,Rr	DNA polymerase III subunit beta (dnaN)	+9.4	+10.1
08944	M,N,A,S	glutamine synthethase type III	+22.9	+9.8
04010	U,S	nuclear transport factor 2	+8.2	+9.8
08839	M,Cb	acetate--CoA ligase	+6.7	+9.3
01600	M,E,C,An	transketolase	+7.5	+9.0
08744	U	zinc-containing alcohol dehydrogenasease superfamily protein	+3.9	+8.7
03474	S,Cy,Se	cysteine synthase	+5.6	+8.4
09500	M,A	3-isopropylmalate dehydrogenase (leuB)	+7.2	+8.0
07326	M,Pp	ATP-dependent Clp protease proteolytic subunit	+5.6	+7.6
09495	M,E,C	phosphoribulokinase (prkB)	+6.1	+7.5
12533	Chl	uroporphyrinogen decarbosylase	+5.3	+7.3
02359	Ukn	hypothetical protein	+3.6	+7.1
15736	Ukn	hypothetical protein	+1.4	+6.9
12493	E	ATPase	+6.1	+6.9
07844	Ukn	hypothetical protein	+3.0	+6.9
07171	U,N	drgA protein	+4.8	+6.9
00625	U,GI	putative glutathione S-transferase	+6.0	+6.8
03604	M	glycogen/starch/alpha-glucan phosphorylase	+4.5	+6.4
13345	M,Pp	ATP-dependent Clp protease proteolytic subunit	+2.7	+6.1
02854	GI,D	putative cyclophilin-type peptidyl-prolyl cis-trans isomerase	+1.9	+5.8
05580	M,Nu,PB	adenylate kinase	+5.6	+5.8
05830	U,GI	putative ribonuclease D	+4.5	+5.8

Table II.5 (continued page 2 of 3)

WH5701 ID	KEGG Function	Protein	4.4 pM Cd^{2+} abundance relative to control	44 pM Cd^{2+} abundance relative to control
15626	U	putative membrane protein	+5.8	+5.5
09635	U,GI	putative glutathione S-transferase	+3.3	+5.4
04700	PS	ferredoxin--NADP reductase (FNR)	+2.5	+5.2
15671	U	methionine sulfoxide reductase B	+2.5	+5.2
08459	GI,T	glutamyl-tRNA (Gln) amido-transferase subunit A	+5.8	+5.0
10110	M,A,Nu	carbamoyl-phosphate synthase large subunit	+4.5	+4.2
15926	M,Cb,Nu	phosphoglucomutase (pgm)	+2.4	+4.1
05130	ukn	hypothetical protein	+2.4	+3.9
08064	PB	inositol-5-monophosphate dehydrogenase	+4.1	+3.9
01205	M,E,C,Cb	phosphoenolpyruvate carboxylase (ppc)	+3.2	+3.7
14781	ukn	hypothetical protein	+2.8	+3.6
07386	M,Nu,A	possible cytosine deaminase	-1.4	+3.6
09740	ukn	hypothetical protein	+2.6	+3.5
00960	M,A	tryptophan synthase subunit beta	+1.6	+3.5
15771	GI,T	translation initiation factor IF-2B subunit alpha	+2.8	+3.3
15141	M,Pt	penicillin-binding protein (pbp)	+1.1	+3.2
13170	GI,D	cyclophilin-type peptidyl-prolyl cis-trans isomerase	+4.0	+3.0
10210	PS	ferredoxin-NADP reductase (FNR)	+2.6	+2.8
07316	M,A,V	acetohydroxy acid isomeroreductase	+2.1	+2.8
12029	ukn	hypothetical protein	+1.9	+2.8
10235	ukn	hypothetical protein	+3.0	+2.8
04930	GI,T	aspartyl/glutamyl-tRNA amido-transferase subunit B	+2.6	+2.6
11384	chl	protochlorophyllide oxidoreductase	+2.1	+2.6
15291	PS	allophycocyanin, beta subunit	+2.4	+2.5
05900	PS	phycocyanin beta subunit	+2.6	+2.5
09875	ukn	hypothetical protein	+3.5	+2.4
04620	St,L	arylsulfatase	+2.2	+2.4
15286	PS	phycocyanin alpha chain	+2.2	+2.4
10105	ukn	hypothetical protein	+2.2	+2.3
10599	PS	phycocyanin beta subunit	+2.5	+2.3
09835	ukn	hypothetical protein	+2.1	+2.3
12958	PS	allophycocyanin alpha-B chain	+1.6	+2.2
05895	PS	phycocyanin, alpha subunit	+2.1	+2.1
13580	PS	phycobilisome core component-allophycocyanin beta-18 subunit	+1.8	+2.1
01470	M,A,V	serine hydroxymethyltransferase	+1.4	+2.1
15186	M	putative aminopeptidase P	+20	+12

Table II.5 (continued page 3 of 3)

WH5701 ID	KEGG Function	Protein	4.4 pM Cd^{2+} abundance relative to control	44 pM Cd^{2+} abundance relative to control
03881	M,A,GI	aspartyl-tRNA synthetase	+17.8	+9.9
01855	ukn	hypothetical protein	+15.2	+9.6
12593	M	putative oligopeptidase A	+6.3	+4.7
14991	ukn	hypothetical protein	+5.2	+2.7
08464	GI,T	glutamyl-tRNA (Gln) amido-transferase A subunit	+5.0	+1.8
13795	ukn	hypothetical protein	+4.4	-1.1
13335	D	ATP-dependent protease-like protein (ftsH)	+2.5	+2.0
15541	ukn	hypothetical protein	+2.3	+1.2

Arranged in highest to lowest fold change, 44 pM Cd^{2+} followed by 4.4 pM Cd^{2+}. + = fold greater than control, - = fold less than control, TCA = TCA cycle, M = metabolism, Nu = nucleic acid metabolism, V = vitamin metabolism, Po = porphyrin biosynthesis, chl = chlorophyll biosynthesis, O = oxidiave stress, ukn = unknown, C = CO_2 fixation, A = amino acid metabolism, L = lipid biosynthesis, Cy = cysteine metabolism, Met = methionine synthesis, S = sulfur metabolism, Se = selenoaminoacid synthesis, GI = genetic information processing, Rr = replication and repair, N = nitrogen metabolism, U = unclassified, Cb = carbohydrate metabolism, E = energy metabolism, An = ansamycin metabolism, Pp = peptidase, D = cell division, PS = photosynthesis, PB = purine biosynthesis, T = translation, Pt = peptidoglycan biosynthesis, St = steroid hormone synthesis.

Table II.6: WH5701 proteins during late stationary phase (T4) that are two-fold or more less abundant in at least one of the Cd^{2+} treatments compared to the control.

WH5701 ID	KEGG Function	Protein	4.4 pM Cd^{2+} abundance relative to control	44 pM Cd^{2+} abundance relative to control
11354	C	carboxysome shell peptide	-13.4	-14.2
13075	Ukn	hypothetical protein	-9.0	-14.1
15236	PS	ATP synthase subunit C	-13.2	-13.3
15241	PS	ATP synthase subunit A	-11.9	-10.6
15886	Ukn	hypothetical protein	-7.1	-9.7
11349	U	methionine sulfoxide reductase A	-13.3	-9.5
00710	U, Om	possible porin (som)	-8.7	-8.7
11319	C	possible carbon dioxide concentrating mechanism protein (CcmK)	-8.0	-8.5
11919	M,Nu	uridylate kinase (pyrH)	-3.3	-8.4
01585	PS	photosystem I reaction center subunit VII	-15.6	-7.8
02239	St, L	putative arylsulfatase	-17.8	-7.3
11339	C	carboxysome shell protein	-6.3	-7.2
08594	Ukn	hypothetical protein	-1.3	-7.1
14966	GI,T	50S ribosomal protein L27	-10.1	-6.6
00585	Ukn	hypothetical protein	-2.0	-6.3
13035	BA	branched-chain amino acid aminotransferase	-10.9	-5.5
07426	M	dihydrolipoamide dehydrogenase	-5.3	-5.4
15591	Chl	delta-aminolevuliic acid dehydratase (hemB)	-7.2	-5.1
15121	PS	ATP synthase subunit B	-8.0	-5.1
05655	GI,T	30S ribosomal protein S19	-7.6	-5.1
09520	Ukn	hypothetical protein	-4.9	-5.0
05215		nicotinate-nucleotide pyrophosphatase	-5.0	-4.9
09565	Ukn	hypothetical protein	-8.2	-4.8
06176	PS	photosystem I reaction center subunit IV	-5.3	-4.5
00820	U,GI	putative RNA-binding protein (RRM domain)	-3.2	-4.2
13585	M,E,A	serine:pyruvate/alanine: glyoxylate aminotransferase (spt,agt)	-5.3	-4.0
15661	GI,Rr	chromosome segregation protein (smc)	-5.8	-4.0
07771	M,Cb	N-acetylmannosamine-6-phosphate 2-epimerase (nanEK)	-2.9	-4.0
15961	U	possible protein phosphatase 2C	-7.5	-3.6
05030	M	enolase	-3.8	-3.6
00705	U,Om	possible porin (som)	-1.7	-3.6

Table II.6 (continued 2 of 3)

WH5701 ID	KEGG Function	Protein	4.4 pM Cd^{2+} abundance relative to control	44 pM Cd^{2+} abundance relative to control
15851	PS	ferredoxin-thioredoxin reductase catalytic chain	-2.3	-3.6
02654	Ukn	hypothetical protein	-4.6	-3.4
14481	GI,T	30S ribosomal protein S16	-3.3	-3.3
05860	Ukn	hypothetical protein	-3.6	-3.2
12094	M,E,Op	putative inorganic pyrophosphatase	-4.3	-2.9
01210	GI,T	glutamyl-tRNA (Gln) amido-transferase subunit C	-2.4	-2.9
05795	PS	photosystem I reaction center subunit II (psaD)	-4.9	-2.8
02864	M,Cb,L	acetyl-CoA carboxylase, biotin carboxyl carrier protein	-3.5	-2.8
02634	GI,T	30S ribosomal protein S6	-3.1	-2.8
13185	Ukn	hypothetical protein	-3.6	-2.6
12518	M	cytochrome c, class IC: cytochrome c, class I	-1.7	-2.6
07651	PS	chloroplast membrane associated 30 kD protein-like	-3.3	-2.6
02005	U,M,A	glycine cleavage system H protein (gcvH)	-2.4	-2.5
03459	Ukn	hypothetical protein	-3.3	-2.5
03654	M	glycogen/starch/alpha-glucan phosphorylase	-5.4	-2.5
14881	M,G	leucyl aminopeptidase	-2.3	-2.4
08229	Ukn	hypothetical protein	-3.0	-2.4
01105	Ukn	hypothetical protein	-3.4	-2.4
09725	Ukn	hypothetical protein	-2.0	-2.4
15176	Ukn	hypothetical protein	-2.5	-2.3
05360	GI,F	glutaredoxin	-1.8	-2.3
11984	M,PS	possible ferredoxin (2Fe-2S)	-2.3	-2.3
06581	U,N	NifU-like protein	-2.1	-2.3
15471	M	ribose 5-phosphate isomerase	-2.3	-2.2
14806	Ukn	hypothetical protein	-2.0	-2.2
01965	U	rubrerythrin	-2.6	-2.2
13470	Ukn	hypothetical protein	-1.8	-2.2
12873	U,GI,F,G	thioredoxin peroxidase	-1.6	-2.1
06721	Ukn	hypothetical protein	-2.0	-2.1
14866	Ukn	hypothetical protein	-1.7	-2.1
02264	Ukn	hypothetical protein	-2.5	-2.0
02929	U,M	soluble hydrogenase small subunit (DHSS)	-2.2	-2.0
11474	Ukn	hypothetical protein	-1.2	-2.0
00840	Ukn	hypothetical protein	-3.5	-1.6
02714	M,A,V	threonine synthase	-3.0	-1.8

Table II.6 (continued 3 of 3)

WH5701 ID	KEGG Function	Protein	4.4 pM Cd^{2+} abundance relative to control	44 pM Cd^{2+} abundance relative to control
08824	U,GI,F	putative bacterioferritin comigratory (BCP) protein	-2.9	-1.3
10549	Ukn	hypothetical protein	-2.8	-1.4
05450	GI	two component transcriptional regulator, LuxR family protein	-2.4	-1.3
02030	GI,T	50S ribosomal protein L9	-2.4	-1.4
14556	M,Nu,V	stationary-phase survival protein (surE)	-2.4	-2.0
15506	GI,T	translation initiation factor IF-2 (infB)	-2.3	-1.4
14296	Ukn	hypothetical protein	-2.2	-1.3
00735	Ukn	hypothetical protein	-2.1	-1.8
03039	M,A,Ly	dihydrodipicolinate synthase (dapA)	-2.1	-2.0
11499	M,V,Po,chl	ferritin (ftn)	-2.1	-1.6
16006	Ukn,O	rehydrin	-2.1	-1.7
11924	GI,T	ribosome releasing factor	-2.0	-1.0
13085	Ukn	hypothetical protein	-2.0	-1.9

Arranged in highest to lowest fold change, 44 pM Cd^{2+}, then 4.4 pM Cd^{2+}. + = fold greater than control, - = fold less than control, C = CO_2 fixation, Ukn = unknown, PS = photosynthesis, U = unclassified, Om = outer membrane protein, M = metabolism, Nu = nucleic acid metabolism, St = steroid hormone synthesis, L = lipid biosynthesis, GI = genetic information processing, T = translation, BA = branched chain amino asid metabolism, chl = chlorophyll biosynthesis, E = energy metabolism, A = amino acid metabolism, Rr = replication and repair, Cb = carbohydrate metabolism, Op = oxidative phosphorylation, F = protein folding, N = nitrogen metabolism, G = glutathione metabolism, V = vitamin metabolism, Ly=lysine synthesis, Po = porphyrin biosynthesis, O = oxidative stress.

Appendix III: Supplementary Data to Chapter 4

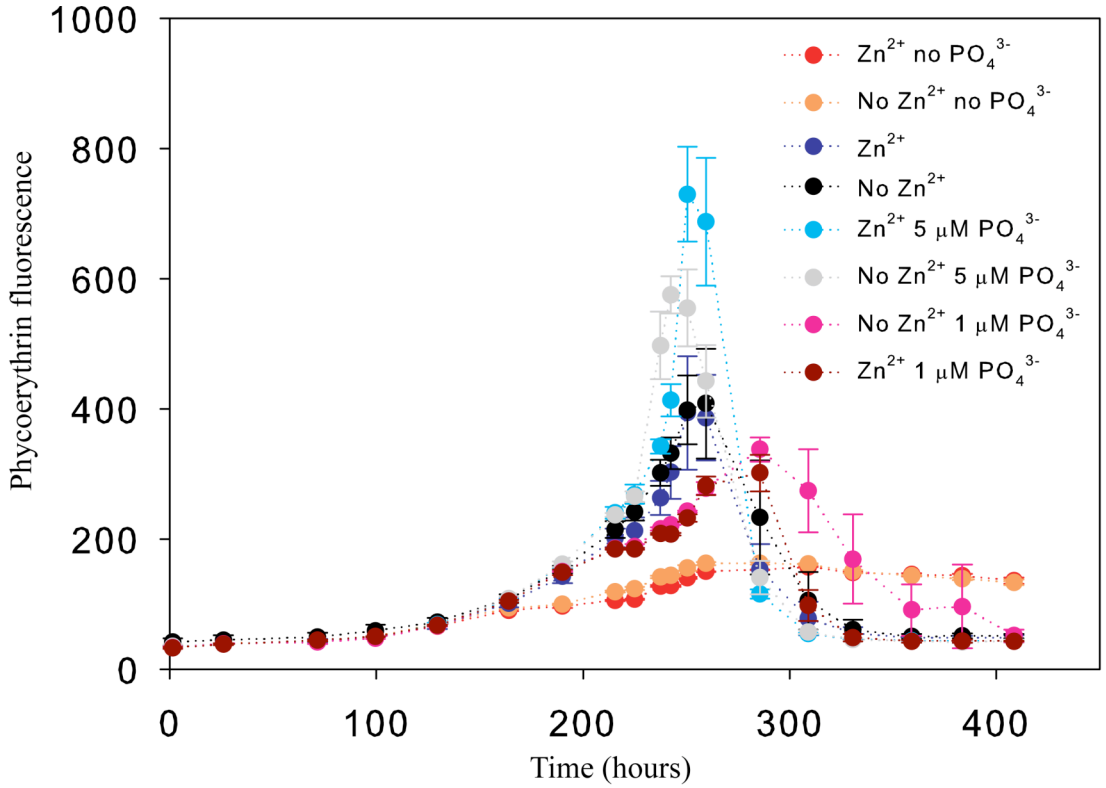

Figure III.1: Phycoerythrin fluorescence vs. time, chronic PO_4^{3-} limitation reconaissance study. Error bars are one standard deviation of triplicate 28 mL tubes. Note that no PO_4^{3-} added treatmnts, both with and without Zn^{2+} appear to have a stationary phase. 1 µM PO_4^{3-} treatments appear to have a brief stationary phase and then enter death phase, the Zn^{2+} dying faster than the no added Zn^{2+}. The 5 µM PO_4^{3-} treatements fluoresced to a greater maximum than the 65 µM PO_4^{3-}. This phenomenen is thus far unexplained and was not observed in a concurrent 500 mL experiment (four treatments, 1 and 65 µM PO_4^{3-} with and without Zn^{2+}).

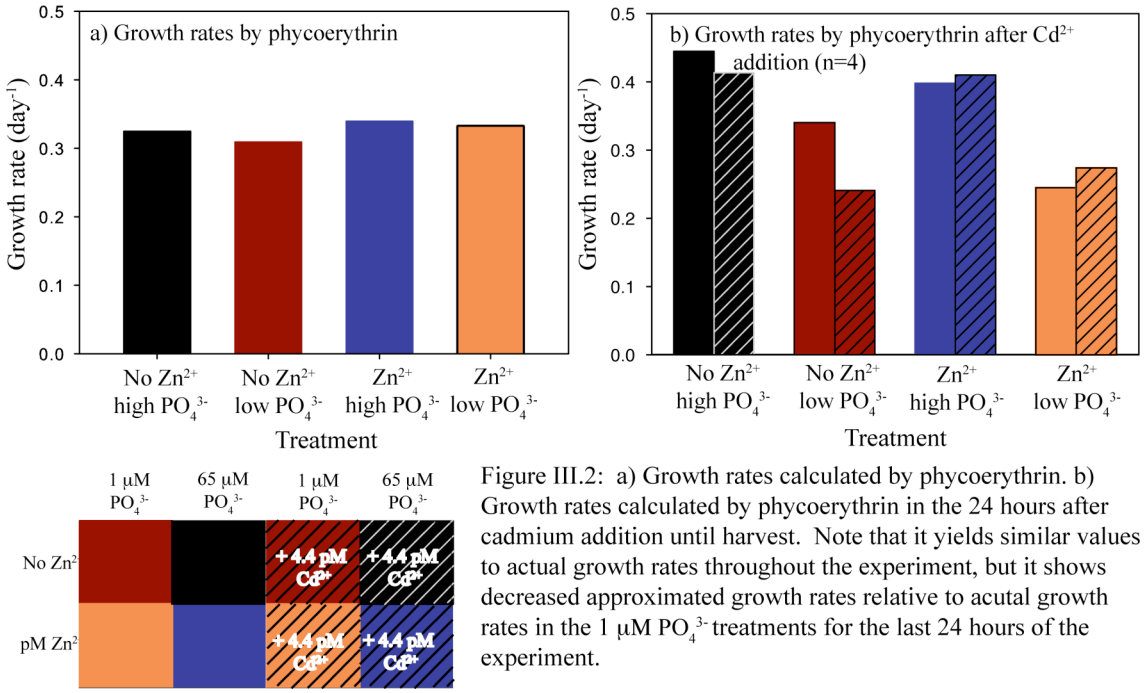

Figure III.2: a) Growth rates calculated by phycoerythrin. b) Growth rates calculated by phycoerythrin in the 24 hours after cadmium addition until harvest. Note that it yields similar values to actual growth rates throughout the experiment, but it shows decreased approximated growth rates relative to acutal growth rates in the 1 µM PO_4^{3-} treatments for the last 24 hours of the experiment.

Table III.1: WH8102 proteins that are ≥ two-fold differentially abundant in the Zn^{2+} 1 μM PO_4^{3-} + 4.4 pM Cd^{2+} vs. Zn^{2+} 65 μM PO_4^{3-} + 4.4 pM Cd^{2+}.

SYNW ID	KEGG Function	Protein	Zn^{2+} 1 μM PO_4^{3-} + 4.4 pM Cd^{2+} counts	Zn^{2+} 65 μM PO_4^{3-} + 4.4 pM Cd^{2+} counts	Zn^{2+} 1 μM PO_4^{3-} + 4.4 pM Cd^{2+}/ Zn^{2+} 65 μM PO_4^{3-} + 4.4 pM Cd^{2+} fold change
2391	U, P	putative alkaline phosphatase	13.8±1.6	1.0±0.0	+13.8
1661	ukn	hypothetical protein	5.4±2.2	0.4±0.6	+12.2
0359	U, Zn	bacterial metallothionein (smtA)	10.3±2.3	1.0±0.1	+10.9
1018	ABC, P	ABC transporter, substrate binding protein, phosphate (PstS)	94.4±4.0	21.0±0.9	+4.5
0953	ukn	hypothetical protein	8.3±3.3	2.2±0.7	+3.7
1533	M,A,G	probable glutathione reductase (NADPH)	6.4±0.6	2.7±2.5	+2.4
1123	M,A,V	dihydroxy-acid dehydratase	5.4±2.2	2.7±1.3	+2.0
0156	M,Ss	phosphorylase	41.3±0.7	21.0±0.3	+2.0
0406	ukn	hypothetical protein	15.7±0.3	8.1±0.1	+2.0
1773	M,Nu, Pu,A	adenylosuccinate synthetase	1.0±0.0	6.7±0.5	-6.7
2378	GI,T	50S ribosomal protein L9	1.5±0.7	6.7±0.7	-4.5
0486	PS	anchor polypeptide L_{CM}	4.4±2.0	15.2±1.5	-3.5
1999	PS	phycobilisome linker polypeptide	4.4±2.2	13.0±0.8	-2.9
0613	U,GI,T	DNA-directed RNA polymerase β subunit	4.4±2.2	9.8±3.7	-2.2
1494	M,Cb	glycogen branching enzyme	3.9±0.1	8.1±0.1	-2.0
1824	GI,T	50S ribosomal protein L19	6.9±1.3	13.9±0.8	-2.0
2001	PS	possible phycobilisome linker polypeptide	3.0±0.0	5.8±0.7	-2.0

Arranged in highest to lowest fold change Zn-low PO_4^{3-} Cd then Zn-high PO_4^{3-} Cd, + = fold greater than Zn-high PO_4^{3-} Cd, - = fold less thanZn-high PO_4^{3-} Cd, U = unclassified, P = phosphorus metabolism, ukn = unknown, Zn = zinc metabolism, ABC = ABC transporter,M=metabolism, A = amino acid metabolism, G = glutathione metabolism, V = vitamin metabolism, Ss = sugar and starch metabolism, Nu = nucleic acid metabolism, Pu = purine metabolism, A = amino acid metabolsim, GI = genetic information processing, T = translation, Cb = carbohydrate metabolism.

Table III.2: WH8102 proteins that are ≥ two-fold differentially abundant in the no Zn^{2+} 1 μM PO_4^{3-} + 4.4 pM Cd^{2+} vs. no Zn^{2+} 65 μM PO_4^{3-} + 4.4 pM Cd^{2+}.

SYNW ID	Function	Protein	No Zn^{2+} 1 μM PO_4^{3-} + 4.4 pM Cd^{2+} counts	No Zn^{2+} 65 μM PO_4^{3-} + 4.4 pM Cd^{2+} counts	No Zn^{2+} 1 μM PO_4^{3-} + 4.4 pM Cd^{2+}/ No Zn^{2+} 65 μM PO_4^{3-} + 4.4 pM Cd^{2+} fold change
2500	M,Cb, TCA E,C	aconitate hydratase (acnB)	6.1±1.4	2.4±0.7	+2.6
0402	M,L	possible acyl carrier protein	6.0±0.1	2.4±0.6	+2.5
0953	Mo	cell surface protein required for swimming motility (swmB)	6.2±3.0	2.8±2.6	+2.2
1018	ABC, P	ABC transporter, substrate binding protein, phosphate (PstS)	62.6±13.0	28.7±3.6	+2.2
1982	PS	photosystem II chlorophyll-binding protein CP47 (psbB)	6.6±0.9	20.1±0.7	-3.1
2124	PS	photosystem I P700 chlorophyll a apoprotein subunit Ia (PsaA)	5.4±2.6	14.8±1.2	-2.8
1999	PS	phycobilisome linker polypeptide (cpeC)	4.3±2.7	11.5±1.7	-2.7
0486	PS	anchor polypeptide L_{CM} (apcE)	6.6±0.7	15.8±2.5	-2.4
0677	PS	photosystem II D2 protein (psbD1)	2.2±0.2	5.2±1.9	-2.4
2227	U, Om	possible porin (som)	13.2±0.2	30.7±7.7	-2.3
0676	PS	photosystem II chlorophyll-binding protein CP43 (psbC)	5.5±0.6	11.4±1.0	-2.1
0613	U, GI,T	DNA-directed RNA polymerase β subunit (rpoB)	3.8±2.0	7.6±0.2	-2.0

Arranged in highest to lowest fold change no Zn-low PO_4^{3-} Cd then no Zn-high PO_4^{3-} Cd, + = fold greater than no Zn-high PO_4^{3-} Cd, - = fold less than no Zn-high PO_4^{3-} Cd. M = metabolism, Cb = carbohydrate metabolism, TCA = citrate cycle, L = lipid metabolism, Mo = motility, ABC = ABC transporter, P = phosphorus metabolism, PS = photosynthesis, U = unclassified, Om = outer membrane protein , GI = genetic information processing, T = translation.

Table III.3: WH8102 proteins that are two-fold or more differentially abundant in the Zn^{2+} 65 μM PO_4^{3-} + 4.4 pM Cd^{2+} vs. Zn^{2+} 65 μM PO_4^{3-}.

SYNW ID	Function	Protein	Zn^{2+} 65 μM PO_4^{3-} + 4.4 pM Cd^{2+} counts	Zn^{2+} 65 μM PO_4^{3-} counts	Zn^{2+} 65 μM PO_4^{3-} + 4.4 pM Cd^{2+}/ Zn^{2+} 65 μM PO_4^{3-} fold change
0486	PS	anchor polypeptide L_{CM} (apcE)	15.2±1.5	6.6±1.4	+2.3
1982	PS	photosystem II chlorophyll-binding protein CP47 (psbB)	11.7±2.7	5.1±3.2	+2.3
2227	U, Om	possible porin (som)	27.7±2.1	13.1±1.6	+2.1
1835	PS	photosystem I reaction center subunit III (psaF)	5.8±0.6	2.8±1.4	+2.1

Arranged in highest to lowest fold change Zn 4.4 pM Cd^{2+}. + = fold greater than Zn, - = fold less than Zn. PS = photosynthesis, U = unclassified, Om = outer membrane protein.

Table III.4: WH8102 proteins that are ≥ two-fold differentially abundant in the no Zn^{2+} 1 μM PO_4^{3-} + 4.4 pM Cd^{2+} vs. the no Zn^{2+} 1 μM PO_4^{3-}.

SYNW ID	Function	Protein	No Zn^{2+} 1 μM PO_4^{3-} + 4.4 pM Cd^{2+} counts	No Zn^{2+} 1 μM PO_4^{3-} counts	No Zn^{2+} 1 μM PO_4^{3-} + 4.4 pM Cd^{2+}/ No Zn^{2+} 1 μM PO_4^{3-} fold change
1091	GI,T	elongation factor Ts (tsf)	7.8±2.4	0.9±1.3	+8.4
0166	M, Cb,TCA	isocitrate dehydrogenase (icd)	5.1±2.9	0.7±1.0	+7.0
1495	M,V,Po, chl	uroporphyrinogen decarboxylase (hemE)	7.1±1.6	1.7±0.3	+4.3
0953	Mo	cell surface protein required for swimming motility (SwmB)	6.2±3.0	1.7±0.3	+3.7
2500	M,Cb,TCA E,C	aconitate hydratase (acnB)	6.1±1.4	1.7±0.3	+3.7
1025	M,A	putative anthranilate synthase component II (TrpD/G)	9.2±2.9	3.1±1.8	+3.0
2081	GI, T	50S ribosomal protein L6 (rpl6, rplF)	6.2±3.0	2.4±0.7	+2.6
0023	GI,F	putative heat shock protein (GrpE)	9.5±3.3	3.8±2.8	+2.5
0819	M,A	dihydrodipicolinate reductase (dapB)	6.6±0.7	2.7±2.4	+2.5
1717	C	ribulose bisphosphate carboxylase, small chain (rbcS,cbbS)	15.8±2.2	6.4±1.2	+2.5
1065	PS	putative photosystem II reaction center (psb28)	8.6±3.8	3.6±5.1	+2.4
0750	M,Cb,G	glucose-6-phosphate dehydrogenase (zwf)	9.0±4.0	4.0±0.4	+2.2
1694	GI,T	30S ribosomal protein S4 (rps4,rpsD)	8.9±0.9	4.1±4.4	+2.1
2348	M,Cb,E,GI	enolase (eno)	14.9±0.8	7.0±4.5	+2.1
2069	GI,T	50S ribosomal protein L23 (rpl23,rplW)	5.5±1.0	2.6±1.6	+2.1
0259	M,E,A,V	serine hydroxymethyltransferase (glyA)	10.4±1.3	5.1±7.2	+2.0
1936	ABC,S	putative sulfate transporter	0.6±0.8	5.2±3.2	-8.7
0380	Ukn	hypothetical protein	2.2±0.2	13.5±4.7	-6.1
0235	M,Cb,As	phosphoglucomutase/phosphomanno-mutase family protein	1.1±0.1	5.7±0.1	-5.1
1171	M,A,GI,T	aminotransferase class-I (aspC)	1.6±0.6	7.6±2.5	-4.7
1494	M,Cb	glycogen branching enzyme (glgB)	2.7±0.5	10.0±1.8	-3.7
0727	GI,Re	DNA gyrase subunit A (gyrA)	1.6±0.6	5.9±2.2	-3.7
1145	Ukn	hypothetical protein	1.6±0.6	5.2±3.2	-3.2
0278	M,Nu,Py	deoxycytidine triphosphate deaminase (dcd)	2.8±1.1	8.1±0.9	-2.9
1090	GI,T	30S ribosomal protein S2 (rps2,rpsB)	2.7±0.5	7.4±0.2	-2.7
0340	Ukn	hypothetical protein	2.7±0.5	7.4±0.2	-2.7
852	M,L	3-oxoacyl-[acyl carrier protein] reductase (fabG)	2.2±0.2	5.9±2.2	-2.7
1999	PS	phycobilisome linker polypeptide (cpeC)	4.3±2.7	11.0±5.0	-2.6

Table III.4 (continued, page 2 of 2):

SYNW ID	Function	Protein	No Zn^{2+} 1 µM PO_4^{3-} + 4.4 pM Cd^{2+} counts	No Zn^{2+} 1 µM PO_4^{3-} counts	No Zn^{2+} 1 µM PO_4^{3-} + 4.4 pM Cd^{2+}/ No Zn^{2+} 1 µM PO_4^{3-} fold change
1610	Rg	putative bifuntional enzyme: tRNA methyltransferase; 2-C-methyl-D-erythritol 2,4-cyclodiphosphate synthase	2.2±0.2	5.0±0.9	-2.3
2124	PS	photosystem I P700 chlorophyll *a* apoprotein subunit Ia (psaA)	5.4±2.6	11.9±3.7	-2.2
2040	M,V,Po,chl	coproporphyrinogen III oxidase (hemF)	2.7±0.5	5.9±2.2	-2.2
2342	GI,T	50S ribosomal protein L1 (rpl1,rplA)	4.3±1.1	9.0±0.5	-2.1

Arranged in highest to lowest fold change no Zn-low PO_4^{3-} + 4.4 pM Cd^{2+} than no Zn-low PO_4^{3-}. + = fold greater than no Zn-low PO_4^{3-}, - = fold less than no Zn-low PO_4^{3-}, GI = genetic information processing, T = translation, M = metabolism, Cb = carbohydrate metabolism, TCA = citric acid cycle, V = vitamin metabolism, Po = porphryin metabolism, chl = chlorophyll metabolism, Mo = motility, E = enegy metabolism, C = carbon fixation, A = amino acid metabolism, F = folding, G = glutathione metabolism, ABC = ABC transporter, S = sulfur metabolism, Ukn = unknown, As = amino sugar metabolism, Re = DNA replication and repair, Nu = nucleic acid metabolism, Py = pyramidine metabolism, L = lipid metabolism, PS = photosynthesis, Rg = regulation.

Table III.5: WH8102 proteins that are ≥ two-fold differentially abundant in the Zn^{2+} 1 µM PO_4^{3-} + 4.4 pM Cd^{2+} vs. Zn^{2+} 1 µM PO_4^{3-}.

SYNW ID	Function	Protein	Zn^{2+} 1 µM PO_4^{3-} + 4.4 pM Cd^{2+} counts	Zn^{2+} 1 µM PO_4^{3-} counts	Zn^{2+} 1 µM PO_4^{3-} + 4.4 pM Cd^{2+}/ Zn^{2+} 1 µM PO_4^{3-} fold change
1933	M,V,Po, chl	δ-aminolevulinic acid dehydratase	5.9±1.3	1.9±1.4	+3.1
1716	C	putative carboxysome structural peptide (CsoS2)	15.2±1.8	6.6±0.1	+2.3
0304	M,S,Pu,Se	ATP-sulfurylase	2.5±0.7	9.0±0.8	-3.7
0160	Ukn	hypothetical protein	3.0±0.0	7.6±1.2	-2.6
1953	Ukn, L	putative glycerol kinase	2.5±0.7	5.7±0.1	-2.3
1494	M, Cb	glycogen branching enzyme	3.9±0.1	9.0±1.9	-2.3
1650	(M,A)	ketol-acid reducto-isomerase	7.9±1.3	15.7±0.4	-2.0

Arranged in highest to lowest fold change Zn-low PO_4^{3-} + 4.4 pM Cd^{2+} than Zn-low PO_4^{3-}. + = fold greater than Zn-low PO_4^{3-}, - = fold less than Zn-low PO_4^{3-}, M = metabolism, V = vitamin metabolism, Po = porphyrin metabolism, chl = chlorophyll metabolism, C = carbon fixation, S = sulfur metabolism, Pu = purine metabolism, Se = selenoamino-acid metabolism, Ukn = unknown, L = lipid metabolism, Cb = carbohydrate metabolism, A = amino acid metabolism.

Table III.6: WH8102 proteins that are ≥ two-fold differentially abundant in the **no Zn^{2+} 65 µM PO_4^{3-}** vs. **Zn^{2+} 65 µM PO_4^{3-}**.

SYNW ID	Function	Protein	No Zn^{2+} 65 µM PO_4^{3-} counts	Zn^{2+} 65 µM PO_4^{3-} counts	**No Zn^{2+} 65 µM PO_4^{3-}/ Zn^{2+} 65 µM PO_4^{3-}** fold change
2139	GI,T	30S ribosomal protein S10	5.5±1.7	1.9±0.0	+3.0
0303	PS	photosystem II manganese-stabilizing polypeptide (psbO)	35.7±7.5	13.6±2.2	+2.6
1982	PS	photosystem II chlorophyll-binding protein CP47(psbB)	13.2±2.1	5.1±3.2	+2.6
0032	GI,T,F	putative cyclophilin-type peptidyl-prolyl cis-trans isomerase	6.0±0.1	2.3±0.6	+2.6
0045	U,M	soluble hydrogenase small subunit (DHSS)	7.2±2.8	2.8±1.4	+2.6
0085	Mo	cell surface protein required for swimming motility (swmA)	10.7±0.9	4.2±0.6	+2.5
1835	PS	photosystem I reaction center subunit III (psaF)	6.9±2.6	2.8±1.4	+2.4
1118	M,Cb,St Su, As	glucose-1-phosphate adenylyltransferase	5.5±0.5	2.3±3.3	+2.4
1933	M,V,Po,chl	δ-aminolevulinic acid dehydratase	7.2±1.6	3.3±0.6	+2.2
0546	GI,T	50S ribosomal protein L27	5.1±1.1	2.3±0.6	+2.2
1518	ukn	hypothetical protein	19.2±0.1	8.9±0.5	+2.2
0827	ukn	hypothetical protein	3.4±0.1	11.2±2.4	-3.3
0278	M,Nu,Py	deoxycytidine triphosphate deaminase	2.1±0.7	6.5±1.2	-3.1
2191	PS	photosystem II complex extrinsic protein precursor (psuB)	5.5±1.7	16.4±1.0	-3.0
0670	ukn	hypothetical protein	2.2±1.9	5.6±1.4	-2.6
2310	GI,F	glutaredoxin	4.3±0.1	8.4±1.2	-2.0

Arranged in highest to lowest fold change no Zn than Zn. + = fold greater than Zn, - = fold less than Zn, GI = genetic information processing, T = translation, PS = photosynthesis, F = folding, U = unclassified, M = metabolism, Mo = motility, Cb = carbohydrate metabolism, St = starch metabolism, Su = sugar metabolism, As = amino and nucleotide sugar metabolism, V = vitamin metabolism, Po = porphyrin metabolism, chl = chlorophyll metabolism, ukn = unknown, Nu = nucleotide metabolism, Py = pyrimidine metabolism

Table III.7: WH8102 proteins that are ≥ two-fold differentially abundant in the no Zn^{2+} 1 μM PO_4^{3-} vs. the Zn^{2+} 1 μM PO_4^{3-}.

SYNW ID	Function	Protein	No Zn^{2+} 1 μM PO_4^{3-} counts	Zn^{2+} 1 μM PO_4^{3-} counts	No Zn^{2+} 1 μM PO_4^{3-} / Zn^{2+} 1 μM PO_4^{3-} fold change
1090	GI,T	30S ribosomal protein S2	7.4±0.2	0.5±0.7	+15.7
0235	M,Cb,As	phosphoglucomutase/phospho-mannomutase family protein	5.7±0.1	0.5±0.7	+12.1
0380	Ukn	hypothetical protein	13.5±4.7	1.9±0.0	+7.1
0727	GI,Re	DNA gyrase subunit A (gyrA)	5.9±2.2	1.0±0.0	+6.2
1145	Ukn	hypothetical protein	5.2±3.2	1.0±0.0	+5.4
0340	Ukn	hypothetical protein	7.4±0.2	1.9±1.4	+3.9
1610	Rg	putative bifuntional enzyme: tRNA methyltransferase; 2-C-methyl-D-erythritol 2,4-cyclo-diphosphate synthase	5.0±0.9	1.4±0.7	+3.5
1852	M,L	3-oxoacyl-[acyl carrier protein] reductase (fabG)	5.9±2.2	1.9±0.0	+3.1
1171	M,A,GI,T	aminotransferase class-I (aspC)	7.6±2.5	3.3±0.6	+2.3
2001	PS	possible phycobilisome linker polypeptide (cpeE)	7.4±0.2	3.3±0.7	+2.2
2342	GI,T	50S ribosomal protein L1 (rpl1,rplA)	9.0±0.5	4.3±0.7	+2.1
0359	U,Zn	bacterial metallothionein (smtA)	1.2±0.3	7.1±3.2	-5.8
1495	M,V, Po, chl	uroporphyrinogen decarboxylase (hemE)	1.7±0.3	7.6±1.2	-4.6
0953	Mo	cellsurface protein required for swimming motility (SwmB)	1.7±0.3	5.2±0.6	-3.1
2356	GI,T	aspartyl/glutamyl-tRNA amido-transferase subunit B (gatB)	2.4±0.7	7.1±0.6	-3.0
1025	M,A	putative anthranilate synthase component II (trpD/G)	3.1±1.8	8.5±0.1	-2.7
0750	M,Cb,G	glucose-6-phosphate dehydrogenase (zwf)	4.0±0.4	10.4±1.2	-2.6
2348	M,Cb,E,GI	enolase (eno)	7.0±4.5	17.5±1.7	-2.5
1065	PS	putative photosystem II reaction center (Psb28)	3.6±5.1	9.0±0.5	-2.5
2391	U,P	putative alkaline phosphatase	3.3±0.6	8.1±0.8	-2.4
0128	Ukn	hypothetical protein	2.4±0.7	5.7±0.1	-2.4
0033	GI,T	elongation factor P (efp)	2.4±0.7	5.7±1.2	-2.4
0819	M,A	dihydrodipicolinate reductase (dapB)	2.7±2.4	6.2±0.6	-2.3
1119	M,Cb,G	6-phosphogluconate dehydrogenase (gnd)	2.9±4.1	6.6±0.1	-2.3
0160	Ukn	hypothetical protein	3.3±0.6	7.6±1.2	-2.3
1661	Ukn	hypothetical protein	2.4±0.7	5.2±2.1	-2.2
0023	GI,F	putative heat shock protein (GrpE)	3.8±2.8	8.1±0.5	-2.1

Table III.7 (continued, page 2 of 2):

SYNW ID	Function	Protein	No Zn^{2+} 1 µM PO_4^{3-} counts	Zn^{2+} 1 µM PO_4^{3-} counts	No Zn^{2+} 1 µM PO_4^{3-} / Zn^{2+} 1 µM PO_4^{3-} fold change
0082	M,V,R	riboflavin synthase subunit beta (ribH)	5.3±4.8	10.9±2.2	-2.1
0613	U,GI,T	DNA-directed RNA polymerase beta subunit (rpoB)	4.0±0.4	8.1±0.8	-2.0
1717	C	ribulose bisphosphate carboxylase, small chain (rbcS,cbbS)	6.4±1.2	12.8±1.8	-2.0
1533	M,G	probable glutathione reductase (NADPH) (gshR)	3.1±1.8	6.2±0.8	-2.0

Arranged in highest to lowest fold change no Zn-low PO_4^{3-} than Zn-low PO_4^{3-} . + = fold greater than Zn-low PO_4^{3-}, - = fold less than Zn-low PO_4^{3-}. GI = genetic information processing, T = translation, M = metabolism, Cb = carbohydrate metabolism, As = amino sugar metabolism, Ukn = unknown, Re = DNA replication and repair, Rg = regulatory function, L = lipid metbolism, A = amino acid metabolism, U = unclassified, Zn = zinc metabolism, V = vitamin metabolism, Po = porphryin metabolism, chl = chlorophyll metabolism, Mo = motility, G = glutathione metabolism, E = energy metabolism, PS = photosynthesis, P = phosphorus metabolism, R = riboflavin metabolsim, C = carbon fixation.

Table III.8: WH8102 proteins that are ≥ two-fold differentially abundant in the no Zn^{2+} 65 µM PO_4^{3-} + 4.4 pM Cd^{2+} vs. Zn^{2+} 65 µM PO_4^{3-} + 4.4 pM Cd^{2+}.

SYWN ID	Function	Protein	No Zn^{2+} 65 µM PO_4^{3-} + 4.4 pM Cd^{2+} counts	Zn^{2+} 65 µM PO_4^{3-} + 4.4 pM Cd^{2+} counts	No Zn^{2+} 65 µM PO_4^{3-} + 4.4 pM Cd^{2+}/ Zn^{2+} 65 µM PO_4^{3-} + 4.4 pM Cd^{2+} fold change
0406	Ukn	hypothetical protein	19.6±1.3	8.1±0.1	+2.4
0405	M,Nu,Pu,A	fumarate lyase:adenylo-succinate lyase (purB)	1.9±0.1	6.3±1.4	-3.3
2500	M,Cb,TCA,E,C	aconitate hydratase (acnB)	2.4±0.7	6.3±1.4	-2.6

Arranged in highest to lowest fold change no Zn-high PO_4^{3-} Cd han Zn-high PO_4^{3-} Cd. + = fold greater than Zn-high PO_4^{3-} Cd, - = fold less than Zn-high PO_4^{3-} Cd, Ukn = unknown, M = metabolism, Nu = nucleotide metabolsim, Pu = purine metabolism, A = amino acid metabolism, Cb = carbohydrate metabolism, TCA = citrate cycle, E = energy metabolism, C = carbon fixation (in this case reductive carboxylate cycle).

Table III.9: WH8102 proteins that are ≥ two-fold differentially abundant in the no Zn^{2+} 1 μM PO_4^{3-} + 4.4 pM Cd^{2+} vs. Zn^{2+} 1 μM PO_4^{3-} + 4.4 pM Cd^{2+}.

SYNW ID	Function	Protein	No Zn^{2+} 1 μM PO_4^{3-} + 4.4 pM Cd^{2+} counts	Zn^{2+} 1 μM PO_4^{3-} + 4.4 Cd^{2+} counts	No Zn^{2+} 1 μM PO_4^{3-} + 4.4 pM Cd^{2+} / Zn^{2+} 1 μM PO_4^{3-} + 4.4 pM Cd^{2+} fold change
0166	M,Cb,TCA	isocitrate dehydrogenase	5.1±2.9	1.0±0.0	+5.2
0304	M,S,Pu, Se	ATP-sulfurylase	6.0±0.1	2.5±0.7	+2.5
1091	GI	elongation factor Ts	7.8±2.4	3.5±0.7	+2.3
1815	ABC, P	ABC transporter, substrate binding protein, phosphate	7.7±0.8	3.9±1.4	+2.0
1650	(M,A)	ketol-acid reductoisomerase	15.3±1.5	7.9±1.3	+2.0
0359	U, Zn	bacterial metallothionein	1.0±0.0	10.3±2.3	-10.2
2391	U, P	putative alkaline phosphatase	1.6±0.6	13.8±1.6	-8.5
1533	M,A,G	probable glutathione reductase (NADPH)	2.6±2.1	6.4±0.6	-2.4
0033	GI, T	elongation factor P	2.7±0.5	5.4±0.8	-2.0

Arranged in highest to lowest fold change no Zn-low PO_4^{3-} + Cd than Zn-low PO_4^{3-} + Cd. + = fold greater than Zn-low PO_4^{3-} + Cd, - = fold less thanZn-low PO_4^{3-} + Cd, M = metabolism, Cb = carbohydrate metabolism, TCA = citrate cycle, S = sulfur metabolism, Pu = purine metabolism, Se = selenoaminoacid metabolism, GI = genetic information processing, ABC= ABC transporter, P = phosphorus metabolism, A = amino acid metabolism, U = unknown, Zn = zinc metabolism, G = glutathione metabolism, T = translation.

Table III.10: WH8102 proteins that are ≥ two-fold differentially abundant in the no Zn^{2+} 65 μM PO_4^{3-} +4.4 pM Cd^{2+} vs. Zn^{2+} 65 μM PO_4^{3-}.

SYNW ID	Function	Protein	No Zn^{2+} 65 μM PO_4^{3-} + 4.4 pM Cd^{2+} counts	Zn^{2+} 65 μM PO_4^{3-} counts	No Zn^{2+} 65 μM PO_4^{3-} + 4.4 pM Cd^{2+}/ Zn^{2+} 65 μM PO_4^{3-} fold change
1982	PS	photosystem II chlorophyll-binding protein CP47 (psbB)	20.1±0.7	5.1±3.2	+3.9
0677	PS	photosystem II D2 protein (psbD1)	5.2±1.9	1.4±0.6	+3.7
0045	U,M	soluble hydrogenase small subunit (DHSS)	7.6±0.2	2.8±1.4	+2.7
0486	PS	anchor polypeptide L_{CM} (apcE)	15.8±2.5	6.6±1.4	+2.4
2227	U,Om	possible porin (som)	30.7±7.7	13.1±1.6	+2.3
1835	PS	photosystem I reaction center subunit III (psaF)	6.2±0.9	2.8±1.4	+2.2
0085	Mo	cell surface protein required for swimming motility (swmA)	8.6±0.3	4.2±0.6	+2.0
2500	M,Cb,TCA, E,C	aconitate hydratase (acnB)	2.4±0.7	7.5±0.1	-0.3

Arranged in highest to lowest fold change 4.4 pM Cd^{2+} than Zn. + = fold greater than Zn, - = fold less than Zn. PS = photosynthesis, U = unclassified, M = metabolism, Om = outer membrane protein, Mo = motility, Cb = carbohydrate metabolism, TCA = citrate cycle, E = energy metabolism, C = carbon fixation, in this instance reductive carboxylate cycle.